

2016

# A study of the action of risperidone at 5-HT<sub>2A</sub> receptors

Supriya A. Gaitonde

*Virginia Commonwealth University*, [gaitondesa@vcu.edu](mailto:gaitondesa@vcu.edu)

Follow this and additional works at: <http://scholarscompass.vcu.edu/etd>

 Part of the [Medicine and Health Sciences Commons](#)

© The Author

---

Downloaded from

<http://scholarscompass.vcu.edu/etd/4112>

This Dissertation is brought to you for free and open access by the Graduate School at VCU Scholars Compass. It has been accepted for inclusion in Theses and Dissertations by an authorized administrator of VCU Scholars Compass. For more information, please contact [libcompass@vcu.edu](mailto:libcompass@vcu.edu).

© Supriya Gaitonde 2016  
All Rights Reserved

A STUDY OF THE ACTION OF RISPERIDONE AT 5-HT<sub>2A</sub> RECEPTORS

A dissertation submitted in partial fulfillment of the requirements for the degree of Doctor  
of Philosophy at Virginia Commonwealth University.

by

SUPRIYA A. GAITONDE

Bachelor of Pharmaceutical Science, University of Mumbai, India, 2011

Director: DR. MAŁGORZATA DUKAT, PH.D.  
ASSOCIATE PROFESSOR, DEPARTMENT OF MEDICINAL CHEMISTRY

Co-Director: DR. RICHARD A. GLENNON, PH.D.  
PROFESSOR AND CHAIRMAN, DEPARTMENT OF MEDICINAL CHEMISTRY

Virginia Commonwealth University  
Richmond, Virginia  
April 2016

### Acknowledgement

I would like to sincerely thank my advisors, Dr. Małgorzata Dukat and Dr. Richard A. Glennon for their contribution in my life during my years as a graduate student in their laboratory. I will be forever indebted to them for their constant patience and support, especially during my initial years in the lab, and that has gone a long way in helping me both, personally and professionally.

I would like to thank all my lab colleagues who have become good friends over the years: Kavita, Malaika, Urjita, Osama, Farhana, Renata, Umberto, Rachel and Abdelrehman. I will always cherish the time spent in lab, especially lunchtime and the routine walk to Starbucks with Kavita, Malaika and Urjita. I would like to thank them for all the help and support in lab. A special thanks to Dr. Osama Alwassil for his help and guidance with molecular modeling. I would like to thank Dr. Javier González-Maeso for all his help with the radioligand binding data, and also my committee members Dr. Glen E. Kellogg, Dr. Diomedes E. Logothetis and Dr. Dana E. Selley.

I would like to thank my best friends: Amrita, Debolina, Anuya, Neha Gangal, and Manasi for being with me through thick and thin. I want to thank my parents, who have been with me through every step of this journey, and my husband Hitesh, who has been a great support system. This wouldn't have been possible without their constant love, support and encouragement.

## Table of Contents

|   | Page |
|---|------|
| Acknowledgements.....   | ii   |
| List of Tables .....  | viii |
| List of Figures.....  | ix   |
| List of Schemes.....  | xiv  |
| List of Abbreviations .....                                       | xv   |
| Abstract.....   | xxii |
| <br>Chapter   |      |
| I Introduction .....  | 1    |
| II Background .....   | 4    |
| A. Mental health and the world .....                              | 4    |
| 1. Current status of mental health in the world.....              | 4    |
| 2. An overview of antipsychotic therapy in the United States..... | 8    |
| 3. Are antipsychotics helpful in the long run? .....              | 11   |
| 4. Therapeutic strategies and those under development .....       | 13   |
| B. Conditions associated with serotonin imbalance .....           | 19   |
| 1. Psychosis due to 5-HT agonists and/or hallucinogens.....       | 21   |
| 2. Depression .....   | 24   |

|  |    |
|--|----|
| 3. Anxiety disorders.....  | 26 |
| 4. Schizophrenia .....   | 29 |
| a. Symptoms and neuroanatomical changes .....                        | 31 |
| b. The dopamine hypothesis of schizophrenia.....                     | 34 |
| c. The serotonin hypothesis of schizophrenia.....                    | 36 |
| d. The NMDA hypofunction/ glutamate hypothesis.....                  | 38 |
| C. The 5-HT class of receptors .....                                 | 39 |
| 1. 5-HT <sub>2A</sub> receptors and some ligands targeting them..... | 42 |
| 2. The 5-HT <sub>2A</sub> -mGlu <sub>2</sub> heteromer .....         | 44 |
| III Specific aims .....  | 46 |
| IV Approach, results and discussion.....                             | 59 |
| A. Deconstruction of risperidone.....                                | 59 |
| 1. Approach.....   | 59 |
| 2. Results.....  | 64 |
| a. Chemistry .....   | 64 |
| b. Functional activity studies .....                                 | 70 |
| c. Radioligand binding studies.....                                  | 81 |
| 3. Discussion.....   | 84 |
| B. Elaboration of risperidone.....                                   | 87 |
| 1. Approach.....   | 87 |
| 2. Results.....  | 92 |
| a. Chemistry .....   | 92 |

|  |     |
|--|-----|
| b. Functional activity studies .....   | 99  |
| c. Radioligand binding studies.....  | 101 |
| 3. Discussion.....   | 104 |
| C. Molecular modeling studies .....  | 106 |
| 1. Approach.....   | 106 |
| 2. Results and discussion .....  | 110 |
| V Conclusion .....   | 130 |
| VI Experimentals .....   | 137 |
| A. Synthesis .....   | 137 |
| 6-Fluoro-3-(piperidin-4-yl)benz[ <i>d</i> ]isoxazole hydrochloride ( <b>55</b> ) .....   | 138 |
| 4-(4-(6-Fluorobenz[ <i>d</i> ]isoxazol-3-yl)piperidin-1-yl)-1-(piperidin-1-yl)butan-1-one<br>hydrochloride ( <b>56</b> ) .....                 | 138 |
| 6-Fluoro-3-(1-(4-(piperidin-1-yl)butyl)piperidin-4-yl)benz[ <i>d</i> ]isoxazole<br>hydrochloride ( <b>57</b> ) .....                           | 139 |
| 6-Fluoro-3-(1-methylpiperidin-4-yl)benz[ <i>d</i> ]isoxazole hydrochloride ( <b>58</b> ) .....   | 140 |
| (±)4-(4-(6-Fluorobenz[ <i>d</i> ]isoxazol-3-yl)piperidin-1-yl)-1-(3-hydroxypiperidin-1-<br>yl)butan-1-one hydrogen oxalate ( <b>59</b> ) ..... | 141 |
| 3-(Piperidin-4-yl)-1,2-benz[ <i>d</i> ]isoxazole hydrochloride ( <b>60</b> ) .....   | 142 |
| 3-(1-Methylpiperidin-4-yl)benz[ <i>d</i> ]isoxazole hydrochloride ( <b>61</b> ) .....  | 142 |
| 4-Chloro-1-(piperidin-1-yl)butan-1-one ( <b>67</b> ) .....   | 143 |
| (±)4-Chloro-1-(3-hydroxypiperidin-1-yl)butan-1-one ( <b>74</b> ) .....   | 143 |
| 1-Formylpiperidine-4-carboxylic acid ( <b>76</b> ) .....   | 144 |

|  |     |
|--|-----|
| 1-Formylpiperidine-4-carboxylic acid chloride ( <b>77</b> ) .....  | 144 |
| 1-Formyl-4-(2,4-difluorobenzoyl)piperidine ( <b>78</b> ) .....   | 145 |
| 1-Formyl-4-((2,4-difluorophenyl)hydroxyimino)methyl)piperidine ( <b>79</b> ) .....   | 145 |
| 1-Formyl-4-(6-fluorobenz[ <i>d</i> ]isoxazol-3-yl)piperidine ( <b>80</b> ).....  | 146 |
| (2-Fluorophenyl)(1-methylpiperidin-4-yl)methanone ( <b>82</b> ) .....  | 146 |
| Phenyl 4-(benz[ <i>d</i> ]isoxazol-3-yl)piperidine-1-carboxylate ( <b>83</b> ).....  | 147 |
| 3-[2-[4-(6-Fluoro-1,2-benzisoxazol-3-yl)-1-piperidinyl]ethyl]-2,4(1 <i>H</i> ,3 <i>H</i> )-<br>quinazolinedione hydrochloride ( <b>85</b> ).....                                   | 148 |
| 4-(6-Fluoro-[1 <i>H</i> ]-indol-3-yl)-1,2,3,6-tetrahydropyridine hydrogen oxalate ( <b>88</b> ) ...  | 148 |
| 6-Fluoro-3-(piperidin-4-yl)-1 <i>H</i> -indole ( <b>89</b> ).....  | 149 |
| 5-Methoxy-3-(piperidin-4-yl)benz[ <i>d</i> ]isoxazole hydrochloride ( <b>90</b> ).....   | 150 |
| 3-[2-[4-(6-Fluoro[1 <i>H</i> ]indol-3-yl)-1-piperidinyl]ethyl]-6,7,8,9-tetrahydro-2-methyl-<br>4 <i>H</i> -pyrido[1,2- <i>a</i> ]pyrimidin-4-one hydrochloride ( <b>91</b> ) ..... | 150 |
| 3-(2-(1-Piperidinyl)ethyl)-2,4-quinazolinedione hydrochloride ( <b>94</b> ) .....  | 151 |
| 2,3-Dihydro-5 <i>H</i> -oxazolo[2,3- <i>b</i> ]quinazolin-5-one ( <b>95</b> ).....   | 152 |
| 1-Acetylpiperidine-4-carboxylic acid ( <b>97</b> ) .....   | 152 |
| 1-Acetylpiperidine-4-carboxylic acid chloride ( <b>98</b> ) .....  | 153 |
| 1-Acetyl-4-(2-hydroxy-5-methoxybenzoyl)piperidine ( <b>99</b> ) .....  | 153 |
| 1-Acetyl-4-((2-hydroxy-5-methoxyphenyl)hydroxyimino)methyl)piperidine ( <b>100</b> )<br>.....  | 154 |
| 1-Acetyl-4-(5-methoxybenz[ <i>d</i> ]isoxazol-3-yl) hydrochloride ( <b>101</b> ) .....   | 154 |
| B. Molecular modeling .....  | 155 |



|  |     |
|--|-----|
| C. Functional activity studies .....           | 156 |
| a. Calcium imaging epifluorescence assay ..... | 156 |
| b. Electrophysiology studies .....             | 157 |
| D. Radioligand binding studies .....           | 158 |
| Bibliography .....                             | 159 |
| Appendix A .....                               | 187 |
| Vita .....                                     | 191 |

## List of Tables

|  |     |
|--|-----|
| Table 1: Classification of metabotropic glutamate receptors. ....  | 16  |
| Table 2: Classification of 5-HT receptors.....   | 39  |
| Table 3: Binding affinity and functional activity profile of risperidone and its predecessors<br>.....   | 51  |
| Table 4: Biological activity of risperidone and its deconstructed analogs. ....  | 83  |
| Table 5: Biological activity of risperidone, ketanserin and their two hybrids.....   | 103 |
| Table 6: Initial template choices for homology modeling of 5-HT receptors. ....  | 108 |
| Table 7: Site-directed mutagenesis data reported in the literature for the binding affinity of<br>ketanserin.....                                  | 113 |
| Table 8: Risperidone and its deconstructed analogs: Ligands and the models chosen based<br>on the GOLD and HINT scores.....                        | 116 |
| Table 9: Risperidone, ketanserin and their structural hybrids: Ligands and the models<br>chosen based on the GOLD and HINT scores.....             | 123 |
| Table 10: Study of the effect of substituents on the three benzisoxazoles: Ligands and the<br>models chosen based on the GOLD and HINT scores..... | 129 |

## List of Figures

|  |    |
|--|----|
| Figure 1: Examples of antipsychotic agents currently on the market.....  | 5  |
| Figure 2: Structure of iloperidone in relation to risperidone .....  | 14 |
| Figure 3: Structure of lurasidone in relation to ziprasidone .....   | 15 |
| Figure 4: Some agonists and PAMs at mGlu <sub>2</sub> receptor with antipsychotic activity in preclinical and/or clinical studies .....                  | 18 |
| Figure 5: 5-HT and some representatives of classical hallucinogens.....  | 20 |
| Figure 6: NMDA receptor antagonists capable of producing schizophrenia-like symptoms .....   | 23 |
| Figure 7: Antidepressants of the past and of the present .....   | 26 |
| Figure 8: The first antianxiety agents .....   | 27 |
| Figure 9: Antianxiety agents currently prescribed.....   | 29 |
| Figure 10: Neural circuits involved in schizophrenia .....   | 31 |
| Figure 11: The three major symptoms of schizophrenia .....   | 32 |
| Figure 12: The second messenger signal transduction pathway of 5-HT <sub>2A</sub> receptors.....   | 42 |
| Figure 13: Radioligands commonly used to label 5-HT <sub>2A</sub> receptor sites.....  | 44 |
| Figure 14: Overlay of 5-HT <sub>2A</sub> and mGlu <sub>2</sub> receptors in mouse somatosensory cortex (A), and mouse cortical primary culture (B) ..... | 45 |
| Figure 15: Representative structures of 5-HT <sub>2A</sub> antagonists.....  | 47 |

|  |    |
|--|----|
| Figure 16: The development of risperidone from butyrophenones .....  | 48 |
| Figure 17: The ‘halves’ or ‘fragments’ of benperidol and lenperone.....  | 49 |
| Figure 18: The receptor occupancy profile of risperidone (○), clozapine (□) and haloperidol (Δ) at 5-HT <sub>2A</sub> receptors (A), and dopamine D <sub>2</sub> receptors (B).....  | 54 |
| Figure 19: Metabolism of risperidone .....   | 55 |
| Figure 20: Approach to the deconstruction of risperidone/paliperidone .....  | 60 |
| Figure 21: The halves of risperidone and the deconstructed analogs .....   | 61 |
| Figure 22: A comparison of the deconstruction of ketanserin and risperidone .....  | 62 |
| Figure 23: Compounds <b>55</b> (A), <b>56</b> (B), <b>57</b> (C), and <b>58</b> (D) did not generate the calcium signal indicating the intracellular release of calcium.....   | 72 |
| Figure 24: Dose-response curves for risperidone and compounds <b>55-58</b> by the calcium imaging assay.....   | 74 |
| Figure 25: A schematic representation of the measurement of G <sub>αq</sub> -mediated activity at 5-HT <sub>2A</sub> receptors by the TEVC assay .....   | 76 |
| Figure 26: The dose-response curves for inhibitory activity exhibited by risperidone (A), compounds <b>55</b> (A), <b>56</b> (B), <b>57</b> (C), and <b>58</b> (D) .....   | 77 |
| Figure 27: The positive efficacy of compounds <b>55-58</b> (A), and the potential ‘superagonist’ activity of compound <b>57</b> (B).....   | 78 |
| Figure 28: The outward current due to the inward movement of chloride ions and the inward current due to the intracellular release of calcium ions after application of 5-HT (A), and the lack of inward and outward current after the application of the compounds, represented by the <i>N</i> -methyl compound <b>58</b> (B)..... | 79 |

|  |     |
|--|-----|
| Figure 29: The crosstalk in the 5-HT <sub>2A</sub> -mGlu <sub>2</sub> heteromer system exhibited by compound <b>55</b> .....   | 81  |
| Figure 30: Radioligand binding affinity at 5-HT <sub>2A</sub> receptors expressed in HEK293 cells of risperidone (A), compounds <b>55-58</b> (B), (C), (D), (E), respectively .....  | 82  |
| Figure 31: A comparison of the left and right ‘halves’ of ketanserin and risperidone .....   | 88  |
| Figure 32: The structures of risperidone ( <b>3</b> ), ketanserin ( <b>42</b> ) and hybrids <b>84</b> and <b>85</b> .....  | 89  |
| Figure 33: Comparison of the benzisoxazole ring with tetrahydropyridylindole ring .....  | 90  |
| Figure 34: Elaboration of risperidone with constrained tryptamine analogs.....   | 91  |
| Figure 35: The activity of risperidone, paliperidone, ketanserin and compounds <b>84</b> and <b>85</b> in the presence of 5-HT .....   | 100 |
| Figure 36: The positive efficacy shown by ketanserin and compound <b>85</b> .....  | 101 |
| Figure 37: The binding affinity data for risperidone (A), ketanserin (B), compounds <b>84</b> (C), and <b>85</b> (D) .....   | 102 |
| Figure 38: A model of the 5-HT <sub>2A</sub> receptor generated as a part of the current study.<br>.....   | 107 |
| Figure 39: Multiple sequence alignment between 5-HT <sub>2A</sub> and 5-HT <sub>2B</sub> receptors generated by the software CLUSTALX 2.1 .....  | 109 |
| Figure 40: An energy-minimized model from the current study with the binding pocket highlighted along with the residues constituting the binding pocket.....   | 111 |
| Figure 41: An energy-minimized ketanserin-receptor complex (A), interactions of ketanserin (purple) with amino acids forming the binding pocket (B), and hydrophobic residues, depicted as spheres, surrounding ketanserin in the binding pocket (C) ..... | 112 |

|   |     |
|---|-----|
| Figure 42: The two binding modes of ketanserin: our model with the fluorine atom pointing towards TM5 (A), previously reported models with the fluorine atom pointing towards TM5 (B), and pointing towards TM7 (C) .....   | 114 |
| Figure 43: The binding modes of risperidone: our model with the fluorine atom pointing towards TM5 (A), literature model with the fluorine atom pointing towards TM7 (B)...   | 117 |
| Figure 44: The binding orientation of risperidone (magenta), paliperidone (cyan) and their deconstructed analogs <b>55</b> (green), <b>56</b> (orange), <b>57</b> (yellow) and <b>58</b> (teal) at the receptor (A), and their interactions with amino acids in the binding pocket (B)..... | 118 |
| Figure 45: The bifurcated H-bonds by compound <b>55</b> with S242 (TM5) in comparison to risperidone (magenta) (A), and the additional hydrophobic interactions made by compound <b>58</b> (B).....   | 120 |
| Figure 46: The interaction of compound <b>57</b> (yellow) with N363 (TM7) compared to risperidone (magenta) (A), and a comparison of the binding pose of risperidone (magenta) and paliperidone (cyan) (B) .....  | 122 |
| Figure 47: The similar binding pose of risperidone (magenta), ketanserin (purple), compounds <b>84</b> (gold) and <b>85</b> (dark green) at the receptor .....  | 124 |
| Figure 48: A snapshot of the differences in the orientation of the common <i>p</i> -fluorobenzoyl moiety of ketanserin (purple) and compound <b>84</b> (gold) at the receptor .....   | 125 |
| Figure 49: The alignment of the hybrid compounds <b>84</b> (gold) and <b>85</b> (dark green) with risperidone (magenta) (A), differences in the orientation of the common quinazolinedione moiety of ketanserin (purple) and compound <b>85</b> (dark green) at the receptor (B), and the   |     |

perfect alignment of the left halves of risperidone (magenta) and compounds **84** (gold) and **85** (dark green) (C) .....126

Figure 50: Structural comparison for the study of the effect of substituents on the three benzisoxazoles .....127

Figure 51: The binding modes of the three benzisoxazoles, **55** (green), **60** (pink) and **90** (lilac) (A), and the molecular interactions with specific amino acids forming the binding pocket (B)

.....128

Figure 52: The range of efficacies (intrinsic activities) that the quinazolinedione moiety can be a part of. The intrinsic activity (i.a.) assay was measured using either rat tail artery (RTA) or rat jugular vein (RJV).....134

## List of Schemes

|  |    |
|--|----|
| Scheme 1: Synthesis of compounds <b>56</b> and <b>57</b> .....             | 65 |
| Scheme 2: Initial attempts to synthesize compound <b>59</b> .....          | 66 |
| Scheme 3: Synthesis of compound <b>59</b> .....                            | 67 |
| Scheme 4: Synthesis of compounds <b>55</b> and <b>58</b> .....             | 69 |
| Scheme 5: Synthesis of compounds <b>60</b> and <b>61</b> .....             | 70 |
| Scheme 6: Synthesis of compound <b>84</b> .....                            | 93 |
| Scheme 7: Initial attempts to synthesize compound <b>85</b> .....          | 94 |
| Scheme 8: Syntheses of compounds <b>85</b> and <b>94</b> .....             | 96 |
| Scheme 9: Syntheses of compounds <b>88</b> , <b>89</b> and <b>91</b> ..... | 97 |
| Scheme 10: Synthesis of compound <b>90</b> .....                           | 98 |



## List of Abbreviations

|                      |  |
|----------------------|--|
| 5-HT                 | Serotonin  |
| 5-HT <sub>1</sub>    | Serotonin type 1 receptor  |
| 5-HT <sub>2A</sub>   | Serotonin type 2A receptor   |
| 5-HT <sub>2C</sub>   | Serotonin type 2C receptor   |
| 5-HTP                | 5-Hydroxytryptophan  |
| 7-OH                 | 7-Hydroxy  |
| μ                    | Micro  |
| Å                    | Angstrom(s)  |
| ACC                  | Anterior cingulate cortex  |
| Ac <sub>2</sub> O    | Acetic anhydride   |
| ADZ8529              | 7-Methyl-5-(3-(piperazin-1-ylmethyl)-1,2,4-oxadiazol-5-yl)-2-(4-(1-(trifluoromethoxy)benzyl)isoindolin-1-one |
| AMPA                 | α-Amino-3-hydroxy-5-methyl-4-isoxazolepropionic acid   |
| AlCl <sub>3</sub>    | Aluminum chloride  |
| APO                  | Apomorphine  |
| ATP                  | Adenosine 5'-triphosphate  |
| bp                   | Boiling point  |
| BH <sub>3</sub> -THF | A solution of borane-tetrahydrofuran (1 M)   |

|                                      |   |
|--------------------------------------|---|
| BI                                   | Balance index   |
| BINA                                 | Biphenylindanone-A                                    |
| br                                   | Broad (spectral)                                      |
| °C                                   | Degrees Celcius                                       |
| C                                    | Cysteine  |
| C322K                                | Amino acid cysteine at position 322 mutated to lysine |
| cAMP                                 | Cyclic adenosine monophosphate                        |
| cGMP                                 | Cyclic guanosine monophosphate                        |
| CHCl <sub>3</sub>                    | Chloroform  |
| CH <sub>2</sub> Cl <sub>2</sub>      | Dichloromethane                                       |
| ClCH <sub>2</sub> CH <sub>2</sub> Cl | Dichloroethane  |
| (COOH) <sub>2</sub>                  | Oxalic acid   |
| CPZ                                  | Chlorpromazine  |
| D                                    | Aspartate   |
| D <sub>2</sub>                       | Dopamine type 2 receptor                              |
| DAG                                  | Diacylglycerol  |
| DIEA                                 | <i>N,N</i> -Diisopropylethylamine                     |
| DOI                                  | 1-(2,5-methoxy-4-iodophenyl)-2-aminopropane           |
| DOM                                  | 1-(2,5-methoxy-4-methylphenyl)-2-aminopropane         |
| DOPE                                 | Discrete optimized protein energy                     |
| DLFL                                 | Dorsolateral frontal lobe                             |

|                                     |  |
|-------------------------------------|--|
| DMF                                 | <i>N,N</i> -Dimethylformamide  |
| DMSO                                | Dimethyl sulfoxide   |
| DMT                                 | <i>N,N</i> -Dimethyltryptamine   |
| DRN                                 | Dorsal raphe nucleus   |
| DSM-5                               | Diagnostic and Statistical Manual of Mental Disorder-5 <sup>th</sup> Edition |
| <i>E. coli</i>                      | <i>Escherichia coli</i>  |
| ECD                                 | Extracellular domain   |
| ECL                                 | Extracellular loop   |
| ED <sub>50</sub>                    | Median effective dose  |
| EPS                                 | Extrapyramidal side effects  |
| EPSP                                | Excitatory postsynaptic potential  |
| ER                                  | Endoplasmic reticulum  |
| EtOH                                | Absolute ethanol   |
| EtOAc                               | Ethyl acetate  |
| Et <sub>3</sub> N                   | Triethylamine  |
| F                                   | Phenylalanine  |
| G <sub>aq</sub> , G <sub>ai/o</sub> | G-protein subunits   |
| GABA                                | Gamma-aminobutyric acid  |
| Glu-GABA-Glu-DA                     | Glutamate-GABA-Glutamate-Dopamine pathway                                    |
| GlyT-1                              | Glycine transporter type 1   |
| GPCRs                               | G-protein coupled receptors  |

|                                |   |
|--------------------------------|---|
| h                              | Hour(s)   |
| H <sub>1</sub>                 | Histamine type 1 receptor   |
| HCHO                           | Formaldehyde  |
| HCOOH                          | Formic acid   |
| HCl                            | Hydrochloric acid   |
| HEK293                         | Human embryonic kidney cells  |
| HINT                           | Hydropathic INteraction   |
| HK                             | High concentration of K <sup>+</sup>                                  |
| Hz                             | Hertz   |
| IC <sub>50</sub>               | Half maximal inhibitory constant                                      |
| ICD                            | Intracellular domain  |
| <i>i</i> -PrOH                 | Isopropyl alcohol   |
| IR                             | Infrared spectroscopy   |
| GIRK4*                         | G-protein sensitive inwardly-rectifying potassium channel             |
| IP <sub>3</sub>                | Inositol 1,4,5-triphosphate   |
| JNJ-40411818                   | 1-Butyl-3-chloro-4-(4-phenyl-1-piperidinyl)-2(1 <i>H</i> )-pyridinone |
| K                              | Lysine  |
| KI                             | Potassium iodide  |
| <i>K<sub>i</sub></i>           | Inhibitory constant   |
| K <sub>2</sub> CO <sub>3</sub> | Potassium carbonate   |
| L                              | Leucine   |
| LSD                            | Lysergic acid diethylamide  |

|                                      |   |
|--------------------------------------|---|
| LY354740                             | (5 <i>R</i> )-2-Aminobicyclo[3.1.0]hexane-2,6-dicarboxylic acid                             |
| LY379268                             | (1 <i>R</i> )-4-Amino-4-(carboxymethyl)-2-oxabicyclo[3.1.0]hexane-6-carboxylic acid         |
| LY487379                             | <i>N</i> -Benzyl-2,2,2-trifluoro- <i>N</i> -(4-(2-methoxyphenoxy)phenyl)ethan-1-sulfonamide |
| m                                    | Multiplet (spectral)  |
| mGluR                                | Metabotropic glutamate receptor   |
| mGlu <sub>2</sub> /mGlu <sub>3</sub> | Metabotropic glutamate receptors type 2 and 3   |
| mp                                   | Melting point   |
| MAO                                  | Monoamine oxidase   |
| MAOI                                 | Monoamine oxidase inhibitor   |
| MeCN                                 | Acetonitrile  |
| MeOH                                 | Methanol  |
| MHz                                  | Megahertz   |
| MRI                                  | Magnetic resonance imaging  |
| MS                                   | Mass spectroscopy   |
| N                                    | Asparagine  |
| NaH                                  | Sodium hydride  |
| NaOH                                 | Sodium hydroxide  |
| NE                                   | Norepinephrine  |
| NIMH                                 | National Institute of Mental Health   |
| NMDA                                 | <i>N</i> -Methyl-D-aspartate  |
| nM                                   | Nanomolar   |
| NRI                                  | Norepinephrine reuptake inhibitor   |

|                  |  |
|------------------|--|
| OCTs             | Organic cationic transporters  |
| PAM              | Positive allosteric modulator  |
| PCP              | Phencyclidine  |
| Pd/C             | Palladium on carbon  |
| PDE10A           | Phosphodiesterase type 10A   |
| PF-2545920       | 2-[4-(1-(4-Methyl-4-pyridin-4-yl)-1H-pyrazole-3-yl)phenoxy]methylquinolone |
| PIP <sub>2</sub> | Phosphatidylinositol 4,5-bisphosphate                                      |
| PLC              | Phospholipase C  |
| Q                | Glutamine  |
| Qtc              | Heart rate-corrected QT interval   |
| rt               | Room temperature   |
| R                | Arginine   |
| RGS2             | Regulator of G-protein signaling   |
| RU 28253         | 5-Methoxy-3(1,2,5,6-tetrahydropyridin-3-yl)-1H-indole                      |
| RU 24969         | 5-Methoxy-3(1,2,5,6-tetrahydropyridin-4-yl)-1H-indole                      |
| s                | Singlet (spectra)  |
| S                | Serine   |
| SAR              | Structure-activity relationship  |
| SDA              | Serotonin-dopamine antagonists   |
| SERT             | Serotonin transporter  |
| SNRIs            | Serotonin norepinephrine reuptake inhibitors                               |
| SSRIs            | Selective serotonin reuptake inhibitors                                    |

|           |   |
|-----------|---|
| s.c.      | Subcutaneous  |
| TEVC      | Two-electrode voltage clamp   |
| THF       | Tetrahydrofuran   |
| TLC       | Thin layer chromatography   |
| TMD       | Transmembrane domain  |
| TMSCl     | Trimethylsilylchloride  |
| TRY       | Tryptamine  |
| USFDA     | The Food and Drugs Administration   |
| V         | Valine  |
| W         | Tryptophan  |
| WT        | Wild type   |
| WAY-10063 | <i>N</i> -[2-[4-(2-Methoxyphenyl)-1-piperazinyl]ethyl]- <i>N</i> -(2-pyridyl)<br>cyclohexanecarboxamide |
| WHO       | World Health Organization   |
| Y         | Tyrosine  |

## Abstract

### A STUDY OF THE ACTION OF RISPERIDONE AT 5-HT<sub>2A</sub> RECEPTORS

By Supriya A. Gaitonde, Ph.D.

A dissertation submitted in partial fulfillment of the requirements for the degree of Doctor of Philosophy at Virginia Commonwealth University.

Virginia Commonwealth University, 2016

Major Director: Dr. Małgorzata Dukat, Ph.D.  
Associate Professor, Department of Medicinal Chemistry

Co-director: Dr. Richard A. Glennon, Ph.D.  
Professor and Chairman, Department of Medicinal Chemistry

Risperidone is an ‘atypical’ antipsychotic and is approved by the USFDA mainly for the treatment of schizophrenia and symptoms of bipolar disorder. Risperidone (an SDA or serotonin-dopamine antagonist) has ~20-fold higher affinity at 5-HT<sub>2A</sub> receptors over dopamine D<sub>2</sub> receptors, which makes it more efficacious against the negative symptoms of schizophrenia and less liable to causing extrapyramidal side effects than ‘typical’ antipsychotics.

The major goal of the current investigation was to study the structure of risperidone and to identify the minimum structural features required for 5-HT<sub>2A</sub> receptor affinity that retain antagonist action. The structure of risperidone was systematically deconstructed, and



functional activity studies using calcium imaging in HEK293 cells and a two-electrode voltage clamp (TEVC) assay in a *Xenopus laevis* heterologous system were coupled with radioligand binding affinity studies to achieve this goal. The biological studies showed that the entire structure of risperidone was not required for activity or affinity at the receptor, as 6-fluoro-[3-(1-methylpiperidin-4-yl)]benz[*d*]isoxazole was comparable to risperidone in both affinity and activity.

Next, the structure of risperidone was elaborated to determine the importance of its left and right “halves” in its actions. The left and the right halves of risperidone were substituted with those of another antagonist, ketanserin, to give structural hybrids. Biological studies suggested that the right half of risperidone [i.e., the 6-fluoro-(3-piperidin-4-yl)benz[*d*]isoxazole moiety] might be important for affinity.

In order to assess how the biologically-active compounds interact at the receptor, homology models of the human 5-HT<sub>2A</sub> receptor were developed, and docking and Hydropathic INTERaction studies were conducted. Risperidone seemed to form a bifurcated hydrogen bond with S159 (TM3), which ketanserin was unable to form. This interaction might account for high binding affinity at the receptor as it is common to both, risperidone and 3-[2-(4-(6-fluorobenz[*d*]isoxazol-3-yl)piperidin-1-yl)ethyl]-2,4-(1*H*,3*H*)quinazolin-6-one.

With the data currently in hand, we can conclude that the entire structure of risperidone is not required for activity or affinity, and that the right “half” (i.e. the benzisoxazolyl portion) of risperidone might be influencing activity and affinity at 5-HT<sub>2A</sub> receptors.

## **CHAPTER I: INTRODUCTION**

Schizophrenia is a mental disorder currently affecting about 1% of the world's population, and is a leading cause of disability, unemployment and suicide in developed countries.<sup>1</sup> Compared to depression, mania and other psychiatric disorders, the documented origins of schizophrenia are fairly recent (early nineteenth century), although earlier the disorder might have been referred to in general as 'madness'.<sup>2</sup>

A striking property of schizophrenia that distinguishes it from other psychiatric illnesses is the apparent loss of touch with reality. This manifests in the form of paranoid delusions and hallucinations (positive symptoms).<sup>3</sup> Before the advent of antipsychotics, large mental institutions were common and patients were locked up – often lifelong, and their symptoms were suppressed by inducing insulin coma or by the surgical excision of certain sections of the brain.<sup>4</sup> These techniques, though temporarily effective in calming patients, had disastrous repercussions in the long run.

The discovery of chlorpromazine and the subsequent development of the typical antipsychotics was a revolution in psychiatry as they alleviated the positive symptoms of the disorder.<sup>5</sup> These typical antipsychotics were dopamine D<sub>2</sub> receptor antagonists and although effective against the positive symptoms, they were ineffective against the apathy

and anhedonia (negative symptoms) and cognitive deficits associated with the disorder and their predominantly dopaminergic activity led to extrapyramidal side effects such as tremors and rigidity.<sup>5</sup>

The importance of the serotonergic system was realized after certain 5-HT<sub>2A</sub> receptor antagonists such as ritanserin and spiperone exhibited activity against the negative symptoms of schizophrenia.<sup>6</sup> It was established later that an optimum ratio of D<sub>2</sub>/5-HT<sub>2A</sub> receptor affinity (Meltzer's ratio) was necessary for activity against the positive, negative and cognitive symptoms; and a higher Meltzer's ratio correlated with a lower risk of causing extrapyramidal side effects.<sup>7</sup> This led to the development of atypical antipsychotics, which are dual serotonin-dopamine antagonists such as risperidone.

Risperidone had certain structural features that distinguished it from structurally related predecessors such as ketanserin and from its atypical contemporaries such as clozapine. Its high Meltzer's ratio of ~20 led to an ideal D<sub>2</sub>/5-HT<sub>2A</sub> receptor affinity profile such that when about 50% of the D<sub>2</sub> receptors are occupied, nearly all 5-HT<sub>2A</sub> receptors are occupied and this was sufficient for its antipsychotic activity. In addition, it has a gradual occupancy at D<sub>2</sub> receptors, combined with a rapid dissociation rate.<sup>8</sup> Thus, risperidone seemed to possess the perfect features to combat the symptoms of schizophrenia without causing extrapyramidal side effects.

Risperidone has recently demonstrated the ability to crosstalk at the 5-HT<sub>2A</sub>-mGlu<sub>2</sub> receptor heteromer complex, which is a potential novel target for schizophrenia.<sup>9</sup> The purpose of the current investigation is to determine the structural features of risperidone conferring it with its antagonist activity at 5-HT<sub>2A</sub> receptors, with the long-term goal of synthesizing a bivalent ligand capable of targeting the 5-HT<sub>2A</sub>-mGlu<sub>2</sub> receptor heteromer.

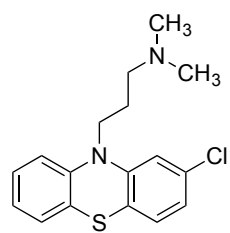
## **CHAPTER II: BACKGROUND**

### **A. MENTAL HEALTH AND THE WORLD**

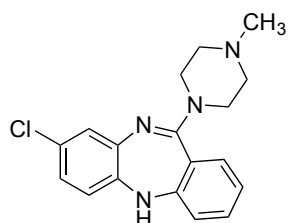
#### **1. Current status of mental health in the world:**

After years of hiding under the garb of ignorance and superstitions, psychiatry finally came to the forefront of health science after Delay and Deniker administered chlorpromazine (thorazine<sup>®</sup>) (CPZ) (1) (Figure 1) to patients at the St. Anne's hospital in Paris in 1952.<sup>4</sup> Psychiatry has come a long way since the days of moral therapy and barbaric methods such as insulin coma, convulsive therapy, and pre-frontal lobotomy.<sup>4</sup> The National Mental Health Act of 1946 and the establishment of the National Institute of Mental Health (NIMH) called for government-sponsored research towards mental illness.<sup>10</sup> There has been progress in every field of psychiatry including development of antipsychotic agents (Figure 1) to combat schizophrenia-like symptoms and antianxiety drugs (initially referred to as minor tranquilizers), to antidepressants (initially called psychic energizers).<sup>4,11</sup>

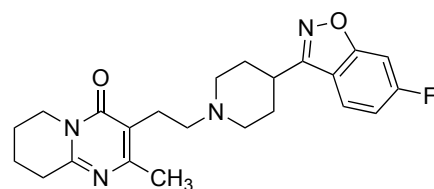
Research of over three quarters of a century has generated a wealth of research articles; blog posts and the media have helped propel mental health into public scrutiny, and communities all over the world are gradually accepting the importance of mental well-being.<sup>10</sup>



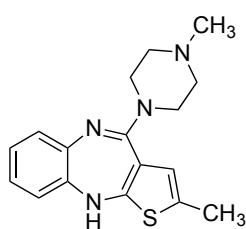
CPZ (1)



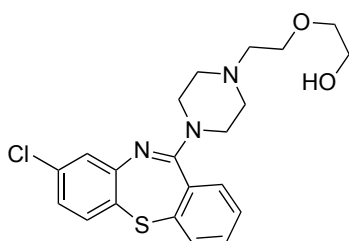
Clozapine (2)



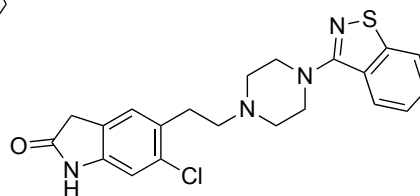
Risperidone (3)



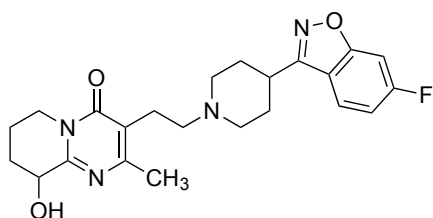
Olanzapine (4)



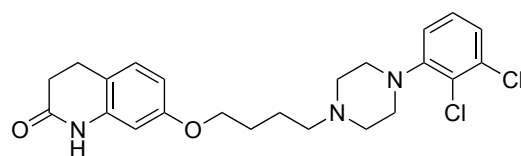
Quetiapine (5)



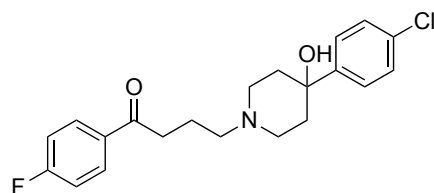
Ziprasidone (6)



Paliperidone (7)



Aripiprazole (8)



Haloperidol (9)

**Figure 1.** Examples of antipsychotic agents currently on the market.<sup>12</sup>

The World Health Organization (WHO) has charted the ‘Comprehensive Mental Health Action Plan 2013-2020’ with the aim of ensuring the worldwide availability of mental health resources, and released the WHO Mental Health Atlas starting from 2001 and

updated in 2005, 2011 and 2014, that measures the progress of member states in realizing the goals of the plan. According to the WHO Mental Health Atlas 2014, out of the 131 responders of the 194 WHO members, about 68% had a mental health policy or a plan for mental health and 51% have a self-contained mental health law.<sup>13</sup>

As per the report there is a huge gap in the conditions existing among the countries based on per capita income. As regards availability of resources, there is a huge gap in low- and high-income countries. The situation is as dire as 1 mental health worker per 100,000 population in low-income countries to more than 50 per 100,000 population in high-income countries.<sup>13,14</sup> This disparity seems to continue even in sources of funding for treatment of mental health conditions and the median mental health expenditure per capita. Government is the main source of funding in 79% of the countries; however, out-of-pocket is also the main source of funding for 18% of the countries, suggesting either a dearth in funds or its unequal distribution.<sup>13</sup> The median mental health expenditure per capita is as low as \$1.53 and \$1.96 for low- and middle-income countries, respectively, and \$58.73 for high-income countries.<sup>13,14</sup>

Over the years there has been a greater focus on community-based mental health services (psychiatric wards in general hospitals) over large mental institutions.<sup>15</sup> These services promote rehabilitation and gradual incorporation of recently discharged, chronically mentally disturbed individuals into society. The intention is to create a support system for the affected people and is also one of the goals of the 'Comprehensive Mental Health

Action Plan 2013-2020'.<sup>13</sup> Accordingly, there has been a steady decline in the number of mental hospitals since 2011 and a pronounced increase (around 60%) in the number of psychiatric wards in general hospitals.<sup>13</sup>

Studies have shown that social acceptance has gone a long way towards the reestablishment of mental health patients.<sup>16</sup> The stigma associated with these disorders, stemming not only from ignorance and indifference but also from intolerance, leads to a vicious circle of discrimination in terms of basic necessities such as treatment, housing, employment, which then leads to a loss of self-esteem, resistance to treatment and relapse, ultimately making it difficult for people to recover.<sup>16,17</sup> Literature suggests that in the United States, about 46% of homeless adults in shelter homes are living with severe mental illness, about 90% of suicidal deaths have a strong background of mental illness and an unbelievably increasing number of people are deemed disabled due to mental diseases every year and most of them are in the prime years of their lives.<sup>18,19</sup> However, there is hope and there are global efforts to reduce misconceptions that people might harbor. The Japanese society of Psychiatry and Neurology recently changed the term for schizophrenia “Seishin-Bunretsu-Byo” which translates to “Split-Mind-Disease” and has replaced it with “Togo-Shitcho-Sho” which means “Integration Disorder.”<sup>17</sup> Programs are being established with the intention of educating the public, protesting against possible discrimination, and promoting direct contact between the people suffering and the public.<sup>16,17</sup> Psychiatry, as a practice, has seen a number of changes in recent times. It has now shifted gears towards clinical neuroscience, attempting to bring the basic etiology and



pathophysiology of the disorders to the forefront, hopefully giving us a better picture of the situation.<sup>20,21</sup>

## **2. An overview of antipsychotic therapy in the United States:**

In the United States, mental disorders exact a huge toll on the economy.<sup>14</sup> The NIMH has estimated that 1 in 4 Americans suffers from some form of mental disorder. Schizophrenia affects about 1%, and bipolar disorder affects about 2.6%, of the adult population in the US.<sup>3</sup> In 2010, schizophrenia alone was responsible for nearly 400,000 hospitalizations.<sup>22</sup>

There are two groups of antipsychotic drugs currently on the market to treat schizophrenia (Figure 1).<sup>23,24</sup> The ‘first generation’ or typical antipsychotics, previously called neuroleptics, targeted dopamine D<sub>2</sub> receptors and are effective against the positive symptoms of schizophrenia, but, inevitably, led to Parkinson-like extrapyramidal side effects (EPS).<sup>5</sup> This class of agents is typified by CPZ (**1**) (Figure 1). The ‘second generation’ or atypical antipsychotics are mostly dual dopamine D<sub>2</sub> and serotonin 5-HT<sub>2A</sub> receptor antagonists and/or inverse agonists effective against the positive as well as negative symptoms and cognitive deficits.<sup>24–26</sup>

The atypical antipsychotics were initially thought of as being devoid of the side effects caused by typical antipsychotics; however, recent studies have shown that long-term use of these agents can also cause motor side effects (due to their high affinity at dopamine D<sub>2</sub> receptors), in addition to metabolic disorders and sexual dysfunction.<sup>27–29</sup>

The 1990s ushered in a new era in the field of antipsychotics with a number of atypical antipsychotic drugs being approved for clinical use.<sup>30</sup> Although mainly indicated for the treatment of schizophrenia, these agents are now gaining importance in the management of other psychiatric conditions such as bipolar disorders and depression as well.<sup>31,32</sup>

Clozapine (**2**) (Clozaril<sup>®</sup>) (Figure 1) was the first atypical antipsychotic drug to be approved for the treatment of schizophrenia.<sup>30</sup> However, it was associated with serious blood conditions such as agranulocytosis, and is currently prescribed only for treatment-resistant schizophrenia with indications of regular monitoring of blood cells.<sup>33–35</sup>

Risperidone (**3**) (Risperdal<sup>®</sup>) (Figure 1) was introduced by Janssen-Cilag in 1993.<sup>24</sup> In addition to monotherapy in schizophrenia, it is now also used as a clozapine-adjunct in clozapine-resistant patients of schizophrenia and schizoaffective disorders.<sup>36</sup> It is, unfortunately, associated with metabolic disorders, weight gain, prolactin elevation, and is contraindicated in patients with dementia-related psychosis.<sup>37</sup>

This was followed by olanzapine (**4**) (Zyprexa<sup>®</sup>) (Figure 1), which was introduced by Eli Lilly in 1996.<sup>23</sup> It appeared to be sparing of agranulocytosis caused by its structural predecessor, clozapine, and there was minimal elevation of prolactin.<sup>38</sup> However, there were reports of transient increases in serum transaminases (indicative of liver damage) and increased appetite that seemed to be of concern.<sup>39,40</sup> Olanzapine is approved for use in the

United States as maintenance therapy for schizophrenia, as an adjunct to fluoxetine in refractory depression, and in bipolar disorder.<sup>41,42</sup> Quetiapine (**5**) (Seroquel®) (Figure 1), was developed by AstraZeneca and was introduced in the United States in 1997.<sup>23</sup> It is in clinical use for the treatment of schizophrenia, bipolar depression, and recently, for generalized anxiety disorder.<sup>43,44</sup> Ziprasidone (**6**) (Geodon®) (Figure 1), was introduced in 2001 and, although significantly helpful against motor and metabolic side effects common with the other atypicals, ziprasidone had a tendency to cause Qtc prolongation leading to cardiac events and, as with risperidone, is contraindicated in dementia-related psychosis.<sup>23</sup>

Paliperidone (**7**) (Invega®) (Figure 1) is a metabolite of risperidone and an antipsychotic agent in its own right.<sup>45</sup> It was approved for clinical use in 2006 and shares most of its side effects with risperidone.<sup>46</sup>

A new class of atypical antipsychotics, termed ‘third generation’ antipsychotics, was introduced in the mid-2000s.<sup>47</sup> Aripiprazole (**8**) (Abilify®) (Figure 1), an example of this class, was ranked the best-selling drug in the United States from the period of October 2013 to September 2014.<sup>48</sup> It differs from the other atypical antipsychotics in being a partial agonist at D<sub>2</sub> receptors – sparing EPS, and a partial agonist (instead of an antagonist) at 5-HT<sub>2C</sub> receptors, thus avoiding the weight gain.<sup>49,50</sup> It is used for the treatment of schizophrenia, bipolar I disorder, depression, and anxiety disorder.<sup>51</sup> Haloperidol (**9**) (Haldol®) (Figure 1) a typical antipsychotic developed in 1958, is still used clinically and accounted for 5% of the market prescriptions in 2011.<sup>23,48</sup>

Despite this clinical progress, there is still a sense of uncertainty in whether long-term use of antipsychotic medications really helps patients regain their independence and, eventually, lead a normal life.<sup>52</sup>

### **3. Are antipsychotics helpful in the long run?**

“Could our drug-based paradigm of care, in some unforeseen way, be fueling this modern day plague?” questions Robert Whitaker in his book ‘Anatomy of an epidemic: Magic bullets, psychiatric drugs and the astonishing rise of mental illness in America’ when examining the growing pandemic of mental illness in the United States despite extensive biomedical facilities and drugs to combat the diseases.<sup>4</sup>

The modern belief of psychiatry is to maintain schizophrenia patients on antipsychotic drugs long after even the acute stage of the illness has been relieved.<sup>52</sup> Treatment of schizophrenia can be divided into three stages: an acute stage of psychosis, usually accompanied by hospitalization, a second stage that includes the next 2-3 years after the initial episode, and thereafter a third stage where active symptoms may or may not persist.<sup>53,54</sup> The question many in the scientific community have raised is whether to keep patients on long-term medication – most of which carry their own plethora of side effects, or to discontinue medication gradually.<sup>52,55</sup> The scientific community is also divided over whether antipsychotics have any efficacy in the long run, or simply make people so dependent that they are unable to resume an unaided life.<sup>4,56,57</sup>

In his book, Whitaker presents case studies of two scenarios: first, of people who have discontinued (mostly stealthily) medication and have made significant progress both personally and professionally, and second, of people who have come so far on the drugs that they seem to be functioning solely due to them. However, people on the drugs, while tolerating the side effects, still wonder what life would have been like while medication-free.<sup>4</sup>

Short-term double-blind studies have provided positive reviews about the effectiveness of antipsychotic use, with some patients even showing remission.<sup>52</sup> However, most of the long-term studies are often a reflection of short-term discontinuation studies of the medication – wherein the first 6-10 months after drug discontinuation, patients either relapse or remain stable. Interestingly, relapse rates are much lower for patients who remain stable during these 6-10 months off-medication.<sup>52</sup>

Long-term longitudinal studies are in contradiction to the positive short-term studies and some studies even question the long-term efficacy of drug treatment.<sup>52,56,57</sup> In a 15-year longitudinal study, Harrow and Jobe<sup>52</sup> reported that only about 40% of schizophrenia patients show one or more periods of recovery. More than 50% of the patients had recurring episodes of psychosis and some had psychotic episodes that were serious enough to affect normal functioning.<sup>57</sup> Another 20-year, multi-follow-up longitudinal study reported that a substantial percentage of schizophrenia patients who were no longer on antipsychotic therapy were psychosis-free, had a lower relapse rate and recovered faster,

suggesting that, perhaps, not all schizophrenia patients need to be on drug-therapy for their entire lives.<sup>56</sup> This shows that while long-term treatment with antipsychotic drugs does not guarantee recovery, the prognosis depends on the individual.<sup>58</sup> The risks (which are numerous and dangerous)-benefit ratio of antipsychotic drug therapy need to be weighed carefully before pharmacotherapeutically dealing with this complicated and multifaceted disorder.<sup>58,59</sup>

#### **4. Therapeutic strategies and those under development:**

Most current efforts are mainly directed towards improving the pharmacokinetics and side-effect profiles of currently marketed antipsychotic drugs.<sup>23,28</sup> While most drugs target dopamine D<sub>2</sub> receptors, with varying degrees of binding affinity and efficacy (with most acting as D<sub>2</sub> antagonists), efforts are being directed towards novel therapeutic targets for antipsychotic therapy.<sup>9,60,61</sup> Some clinically-relevant developments are discussed.

##### **a. Improvements over current antipsychotic drugs:**

The major grievances against currently marketed atypical antipsychotics are their tendency to cause significant weight gain, metabolic disorders, cardiac problems and sedation, among others.<sup>58</sup> These problems might be a result of additional multi-receptor interactions, such as those with 5-HT<sub>2C</sub>, H<sub>1</sub>, M<sub>1</sub>-M<sub>5</sub> and  $\alpha_1$ -adrenoceptors.<sup>23,39</sup> Structural modifications have attempted to achieve selectivity and avoid off-target interactions.

Iloperidone (**10**) (Fanapt<sup>®</sup>) (Figure 2) was approved by the USFDA in 2009 and is structurally related to risperidone (**3**).<sup>23,62</sup> It has low affinity for H<sub>1</sub> histamine and muscarinic receptors, so there is a lower chance of weight gain, sedation and metabolic disorders caused by the older atypical agents.<sup>23</sup> However, its affinity for  $\alpha_1$ -adrenoceptors is sufficient to cause Qtc prolongation. Oral iloperidone is now recommended for the acute treatment of adults with schizophrenia.<sup>55</sup>

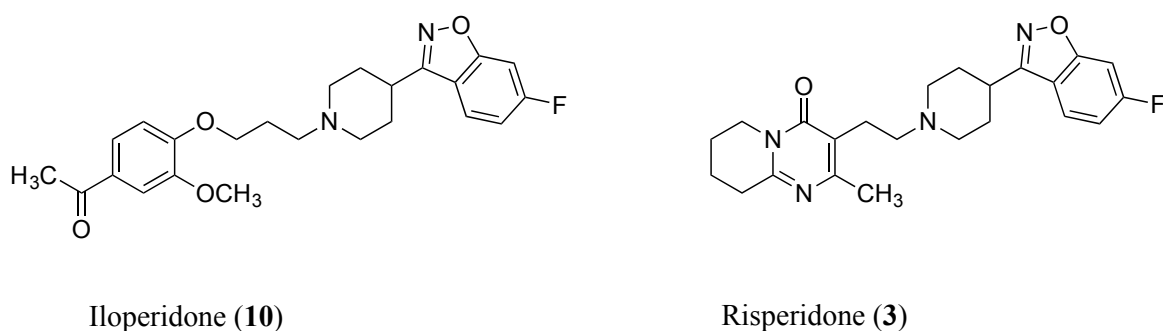
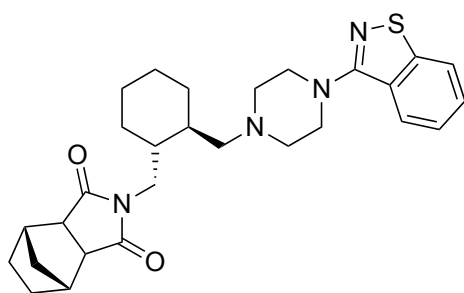
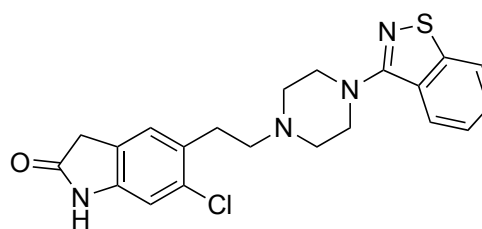


**Figure 2.** Structure of iloperidone in relation to risperidone.<sup>23</sup>

Lurasidone (**11**) (Latuda<sup>®</sup>) (Figure 3) is structurally similar to ziprasidone (**6**) and was approved for the treatment of schizophrenia in 2010.<sup>23,48</sup> Apart from 5-HT<sub>2A</sub> and D<sub>2</sub> receptors, lurasidone is also a 5-HT<sub>7</sub> receptor antagonist that has been shown to be helpful against the cognitive deficits of schizophrenia.<sup>63</sup> Also, lurasidone has reduced affinity at  $\alpha_1$ -adrenoceptors and 5-HT<sub>2C</sub> receptors, and no affinity at H<sub>1</sub> histamine or M<sub>1</sub> muscarinic receptors leading to an improved cardiovascular profile, and a low liability of weight gain and sedation.<sup>23,63</sup>



Lurasidone (**11**)



Ziprasidone (**6**)

**Figure 3.** Structure of lurasidone in relation to ziprasidone.<sup>23</sup>

Another novel class of compounds that was actually developed in the 1980s but that has only recently been clinically explored is what have been termed ‘dopamine stabilizers.’<sup>64</sup> The clinically approved atypical antipsychotic drug aripiprazole (**8**) (Figure 1) belongs to this class.<sup>49</sup> These compounds are either dopamine partial agonists or antagonists, depending on basal dopaminergic tone, and have the ability to interact with D<sub>2</sub> dopamine receptors just enough to decrease the hyperdopaminergia of schizophrenia without carrying the risk of hypodopaminergia.<sup>49,64</sup> Studies have shown that even after 80% occupation of D<sub>2</sub> receptors, there are minimal chances of EPS.<sup>65</sup> This group of compounds is being extensively researched and some of them have even reached clinical trials.<sup>23</sup>



b. Non-dopaminergic and non-serotonergic targets:

Atypical antipsychotics are effective against the negative symptoms and cognitive deficits of schizophrenia in addition to the positive symptoms but their overall advantage over typical antipsychotics is only modest and they also come with their own side effects.<sup>66</sup> In such scenarios, there is an acute need to explore other therapeutic targets.

i. Glutamatergic drugs: The ‘NMDA hypothesis of schizophrenia’ (which will be discussed later) was established in 1995 based on the observation that NMDA receptor antagonists such as ketamine and phencyclidine (PCP) mimic not only the positive symptoms, shown by amphetamine, but also the negative and cognitive symptoms of schizophrenia.<sup>67</sup> The metabotropic glutamate (mGlu) receptors belong to class C G-protein coupled receptors (GPCRs) and consist of 8 subtypes of which mGlu<sub>2</sub> and mGlu<sub>3</sub> (and recently, mGlu<sub>5</sub>) have been extensively studied with regards to schizophrenia (Table 1).<sup>68</sup>

**Table 1.** Classification of metabotropic glutamate receptors adapted from Swanson et al.<sup>69</sup>

| Family receptor   | Coupling                             | Localization   |
|-------------------|--------------------------------------|--|
| Group 1           |                                      |  |
| mGlu <sub>1</sub> | Excitatory – G <sub>αq</sub> coupled | Postsynaptic at glutamatergic synapses and cerebellar localization in granular cell and parallel fibre layer |
| mGlu <sub>5</sub> | Excitatory – G <sub>αq</sub> coupled | Postsynaptic at glutamatergic synapses, also in glial cells. High expression in forebrain                    |

|                   |  |  |
|-------------------|--|--|
|                   |  | regions such as<br>hippocampus and amygdala  |
| Group II          |  |  |
| mGlu <sub>2</sub> | Inhibitory – G <sub>ai/o</sub> coupled | Largely presynaptic<br>glutamatergic localization,<br>also high expression in<br>forebrain regions such as<br>hippocampus and amygdala |
| mGlu <sub>3</sub> | Inhibitory – G <sub>ai/o</sub> coupled | Largely presynaptic<br>glutamatergic localization,<br>also high expression in<br>forebrain regions such as<br>hippocampus and amygdala |
| Group III         |  |  |
| mGlu <sub>4</sub> | Inhibitory – G <sub>ai/o</sub> coupled | Both pre- (cerebellar parallel<br>fibres) and postsynaptic<br>localization   |
| mGlu <sub>6</sub> | Inhibitory – G <sub>ai/o</sub> coupled | Expression confirmed only<br>in retinal bipolar ON cells.  |
| mGlu <sub>7</sub> | Inhibitory – G <sub>ai/o</sub> coupled | Only presynaptic inhibitory<br>mGlu localized to active<br>zone of synapses  |
| mGlu <sub>8</sub> | Inhibitory – G <sub>ai/o</sub> coupled | Largely presynaptic<br>glutamatergic localization,<br>also high expression in<br>forebrain regions such as<br>hippocampus and amygdala |

Evidence from the ability of mGlu<sub>2/3</sub> orthosteric agonists [e.g. LY354740 (**12**) and LY379268 (**13**)] (Figure 4) to inhibit phencyclidine (PCP)-induced positive and negative symptoms led to mGlu<sub>2/3</sub> receptors to be studied as novel targets for drug development.<sup>68</sup> However, since the orthosteric site of GPCRs in general is highly conserved among all the subtypes, it necessitated development of selective agents and, hence, positive allosteric modulators (PAM) of mGlu<sub>2/3</sub> were investigated. A few examples of clinically relevant mGlu<sub>2</sub> PAMs are LY487379 (**14**) (the first identified selective mGlu<sub>2</sub>-selective PAM) (Figure 4), biphenylindanone-A (BINA) (**15**) and JNJ-40411813 (**16**). JNJ-40411813 (**16**) (Addex and Janssen) and ADZ8529 (**17**) (AstraZeneca) (structure undisclosed) have reached clinical trials (Figure 4).<sup>23,68-70</sup>

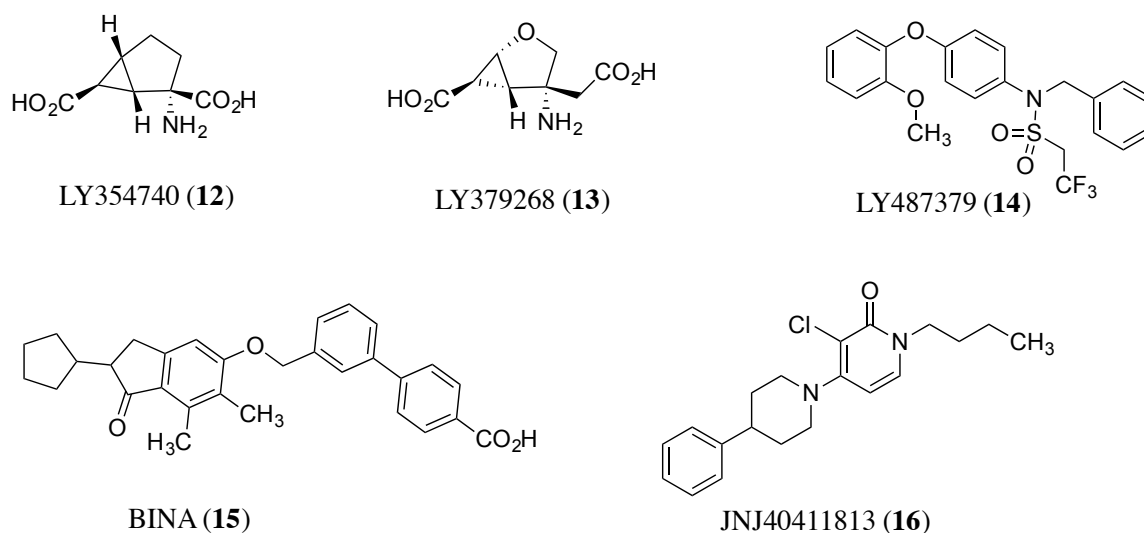


**Figure 4.** Some agonists and PAMs at mGlu<sub>2</sub> receptor with antipsychotic activity in preclinical and/or clinical studies.<sup>23,68</sup>

ii. Phosphodiesterase (PDE) inhibitors: These are inhibitors of the intracellular second messengers 3,5-cyclic adenosine monophosphate (cAMP) and 3,5-cyclic guanosine monophosphate (cGMP). Specifically, inhibitors of the subtype PDE10A, which is located primarily in the brain and the testes in mammals has been extensively studied and PF-2545920 from Pfizer has been identified as a clinical candidate for the treatment of schizophrenia.<sup>23,71</sup>

iii. Glycine transporter inhibitors: Following the NMDA hypothesis, one more avenue being explored to enhance glutamatergic signaling, especially to overcome the negative symptoms of schizophrenia, was to reinforce the effects of the NMDA receptor co-agonist glycine. This was achieved by the inhibition of the glycine transporter-1 (GlyT-1) on glial cells and is being examined clinically.<sup>72</sup>

## **B. CONDITIONS ASSOCIATED WITH SEROTONIN IMBALANCE**

5-Hydroxytryptamine (5-HT) or serotonin (**18**) (Figure 5) was first identified as a vasoconstrictor in mammalian serum in 1948 and was also found in gastric mucosa, and to have an excitatory effect on intestinal smooth muscles.<sup>73,74</sup> Thereafter, its presence in the central nervous system was established in invertebrates, rodents, and eventually in several species of mammals.<sup>73</sup> The effects of modulating 5-HT levels (through activation of 5-HT receptors) by pharmacological agents such as lysergic acid diethylamide (LSD) (**19**) (Figure 5), led to the conclusion that 5-HT plays a key role in behavior.<sup>75,76</sup> It is now known that 5-HT is not only responsible for neuronal development, memory, emotional

processing, depression, anxiety, schizophrenia, appetite, sleep and sexual behavior, but also for platelet aggregation and regulation of smooth muscles of the heart.<sup>77-80</sup>

An increase and decrease of 5-HT can have profound effects on the body and the most evident result is on behavior. A few clinical effects of 5-HT imbalance on behavior are discussed.

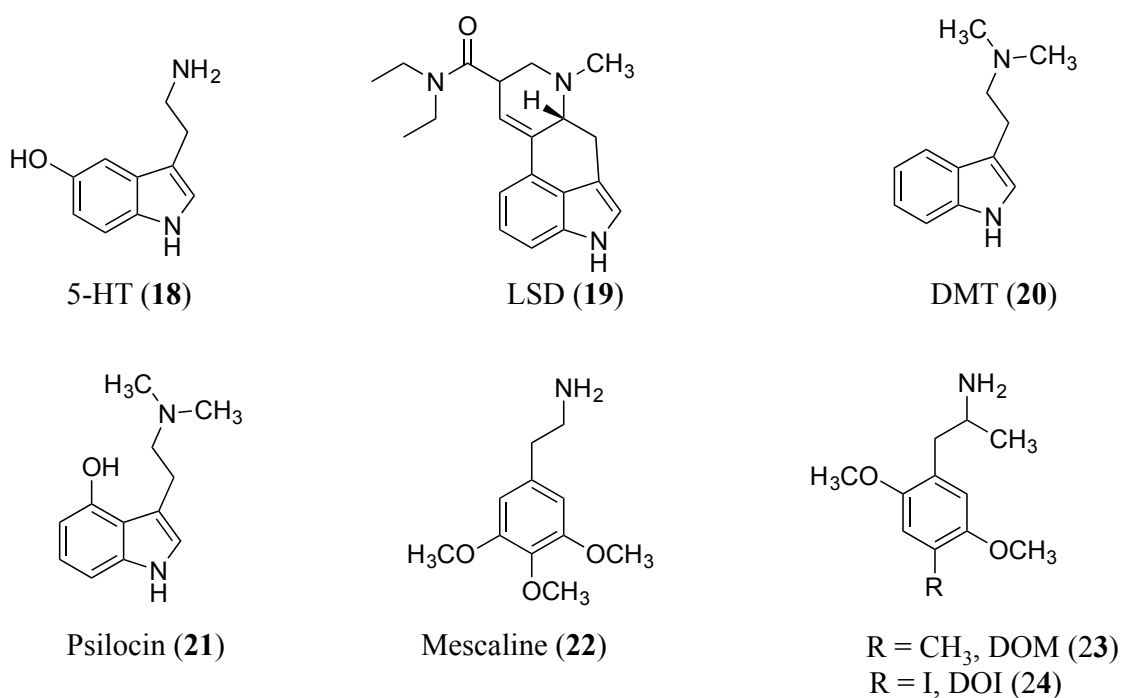


**Figure 5.** 5-HT and representative structures of classical hallucinogens.<sup>81</sup>

### 1. Psychosis due to 5-HT agonists and /or hallucinogens:

In order to pinpoint the origin of the effects he experienced after accidental chemical exposure in his laboratory, Albert Hofmann, a natural products chemist at Sandoz Pharmaceuticals in Basel, Switzerland, had deliberately self-administered 0.25 g of d-lysergic acid diethylamide (LSD) in 1943.<sup>81,82</sup> After a period of 40 minutes, his journal entry reported: “slight giddiness, restlessness, difficulty in concentration, visual disturbances, laughing”.<sup>82</sup> This was followed by a loss of time, disorganized perception of space, dissociation, alternating restlessness and paralysis; and visual deformation that lasted hours after the other symptoms had abated.<sup>82</sup>

Psychosis is an abnormal perception of reality (as described above) and can manifest itself as hallucinations, delusions, altered consciousness, delirium, cognition problems, and in certain cases, even death.<sup>81</sup> Hallucinogens (classical hallucinogens and dissociatives) bring about these changes and are mostly used for their recreational potential, in certain religious experiences (where they are also referred to as *entheogens*), and are now increasingly being studied with respect to psychiatric diseases such as schizophrenia.<sup>81,83</sup>

Classical hallucinogens mainly belong to two main chemical classes: the indolealkylamines and the phenylalkylamines (Figure 5). The indolealkylamines include LSD (**19**), *N,N*-dimethyltryptamine (DMT) (**20**), psilocin (**21**), and the phenylalkylamines include mescaline (**22**), 1-(2,5-dimethoxy-4-methylphenyl)-2-aminopropane (DOM) (**23**), and 1-(2,5-dimethoxy-4-iodophenyl)-2-aminopropane (DOI) (**24**).<sup>83</sup>

After the almost simultaneous discovery of 5-HT and LSD, initial investigations found that LSD (**19**) interacted with 5-HT receptors to cause certain behavior changes, and the striking structural similarities between 5-HT and LSD warranted further examination when it was thought that 5-HT could be responsible for the actions mediated by LSD.<sup>76</sup>

It can be concluded from radioligand binding work and studies on animal models such as drug discrimination (with DOM), head-twitch behavior, startle reflex, conducted in the past by our laboratory and several others that 5-HT is indeed involved in the mechanism of action of both classes of hallucinogens with 5-HT<sub>2A</sub> receptors (referred to as 5-HT<sub>2</sub> at that time) being the key site of action.<sup>78-80</sup>

LSD (**19**) was found to be a non-selective low efficacy agonist (or a partial agonist) at 5-HT<sub>2A</sub> and 5-HT<sub>1</sub> receptors.<sup>84</sup> In fact, drug discrimination studies conducted by Glennon<sup>77</sup> have established that there is a correlation between the ED<sub>50</sub> values of the drugs and their affinity at the 5-HT<sub>2A</sub> receptor.<sup>85</sup> Additionally, studies with antagonists selective for 5-HT<sub>2A</sub> and 5-HT<sub>2C</sub>, revealed that this hallucinogenic property is due to 5-HT<sub>2A</sub> and not 5-HT<sub>2C</sub> receptors.<sup>86,87</sup> The effects of these serotonergic hallucinogens are dose-dependent and resemble the earliest phases of schizophrenia, which include changes in mood, thought, intuition, perception of self and euphoria.<sup>88,89</sup> The predominantly visual hallucinations brought about by these agents recreate those experienced in the acute stages of the disease, that become more auditory as the disease worsens. This is one of the tenets of the

‘serotonin hypothesis of schizophrenia’ and the effects of serotonin hallucinogens have been used to generate models of schizophrenia for research.<sup>89,90</sup>

Activation of the 5-HT<sub>2A</sub> receptor in the prefrontal cortex leads to an increase in the excitatory postsynaptic potentials (EPSP) in the apical dendritic region of layer V pyramidal cells which indicates a release of glutamate.<sup>91</sup> This has been supported with mGlu<sub>2/3</sub> agonists and AMPA/kainate glutamate receptor antagonists.<sup>91,92</sup> NMDA receptor antagonists such as PCP (**25**) and ketamine (**26**) (Figure 6) have been shown to recreate not only the positive symptoms of psychosis (such as those mediated by the serotonergic hallucinogens) but also the negative symptoms (depression, anhedonia, social withdrawal) and cognitive deficits of schizophrenia.<sup>93</sup> This has given rise to the ‘NMDA hypothesis of schizophrenia’ and these models are considered to better depict the overall symptoms of schizophrenia.<sup>92</sup>

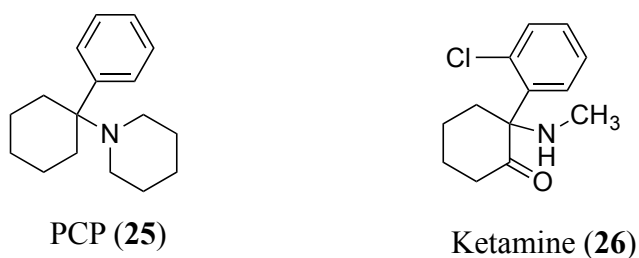


**Figure 6.** NMDA receptor antagonists capable of producing schizophrenia-like symptoms.<sup>81,92</sup>



## 2. Depression:

Depression is a chronic, persistent mood disorder characterized by anhedonia, feelings of emptiness, worthlessness, lack of concentration, fatigue, increased or decreased appetite and an inexplicable need to ‘escape’.<sup>94</sup> Depression can be life threatening and is responsible for an increasing number of suicides across the world.<sup>95</sup> Evidence has pointed towards genetic (40-50% risk) as well as non-genetic factors, such as childhood trauma, stress, bereavement, and major lifestyle changes, in the pathophysiology of the disease.<sup>94,95</sup>

Reserpine was found to mediate depletion of monoamine neurotransmitters and produce depression-like symptoms and is believed to be the foundation of the monoamine hypothesis of depression.<sup>96</sup> The first two drugs showing antidepressant-like activity (Figure 7) were discovered rather serendipitously. Iproniazid (**27**) and imipramine (**28**) (Figure 7) were obtained as a part of antituberculosis and antihistamine research, respectively, and were found to dramatically elevate the moods of hospitalized patients.<sup>96</sup>

These drugs, initially called as ‘psychic energizers’<sup>4</sup>, were seen to increase the synaptic levels of 5-HT and norepinephrine (NE) by two different mechanisms: Imipramine (**28**) inhibited the reuptake of 5-HT, while iproniazid (**27**) inhibited monoamine oxidase (MAO), the enzyme responsible for metabolizing 5-HT and NE.<sup>96,97</sup> Imipramine (**28**) has led to the development of several classes of marketed drugs inhibiting the reuptake of 5-HT and NE such as tricyclic antidepressants [amitriptyline (**29**)], ‘selective serotonin reuptake inhibitors’ (SSRIs) [fluoxetine (**30**)], ‘norepinephrine reuptake inhibitors’ (NRIs)

[nortryptiline (**31**)] and ‘dopamine reuptake inhibitors’ [bupropion (**32**)] (Figure 7).<sup>98-100</sup>

The discovery of iproniazid (**27**) delivered another class of antidepressants called the monoamine oxidase inhibitors (MAOIs) [isocarboxazid (**33**)] (Figure 7).<sup>101,102</sup>

These drugs were developed based on the monoamine hypothesis of depression – that depression is caused by a deficiency of 5-HT and/or NE (and possibly, DA).<sup>91</sup> However, this hypothesis could not explain why it took 2-4 weeks before activity of antidepressants was evident and research was extended to receptors and second messenger signaling pathways, mainly related to 5-HT.<sup>94,96</sup> Different regions of the brain such as the hippocampus and the prefrontal cortex, amygdala, nucleus accumbens and the hypothalamus have been postulated to be involved in the cognitive problems, the lack of pleasure and the loss of appetite, reminiscent of depression.<sup>103,104</sup>

Therapeutic strategies such as deep brain stimulation are practiced for certain treatment-resistant depressions.<sup>94</sup> Also, novel therapeutic targets such as the organic cation transporters (OCTs) are currently being explored to account for the fact that the available antidepressants, which mainly target the serotonin transporter (SERT), fail to provide relief to a considerable percentage of patients.<sup>105</sup>

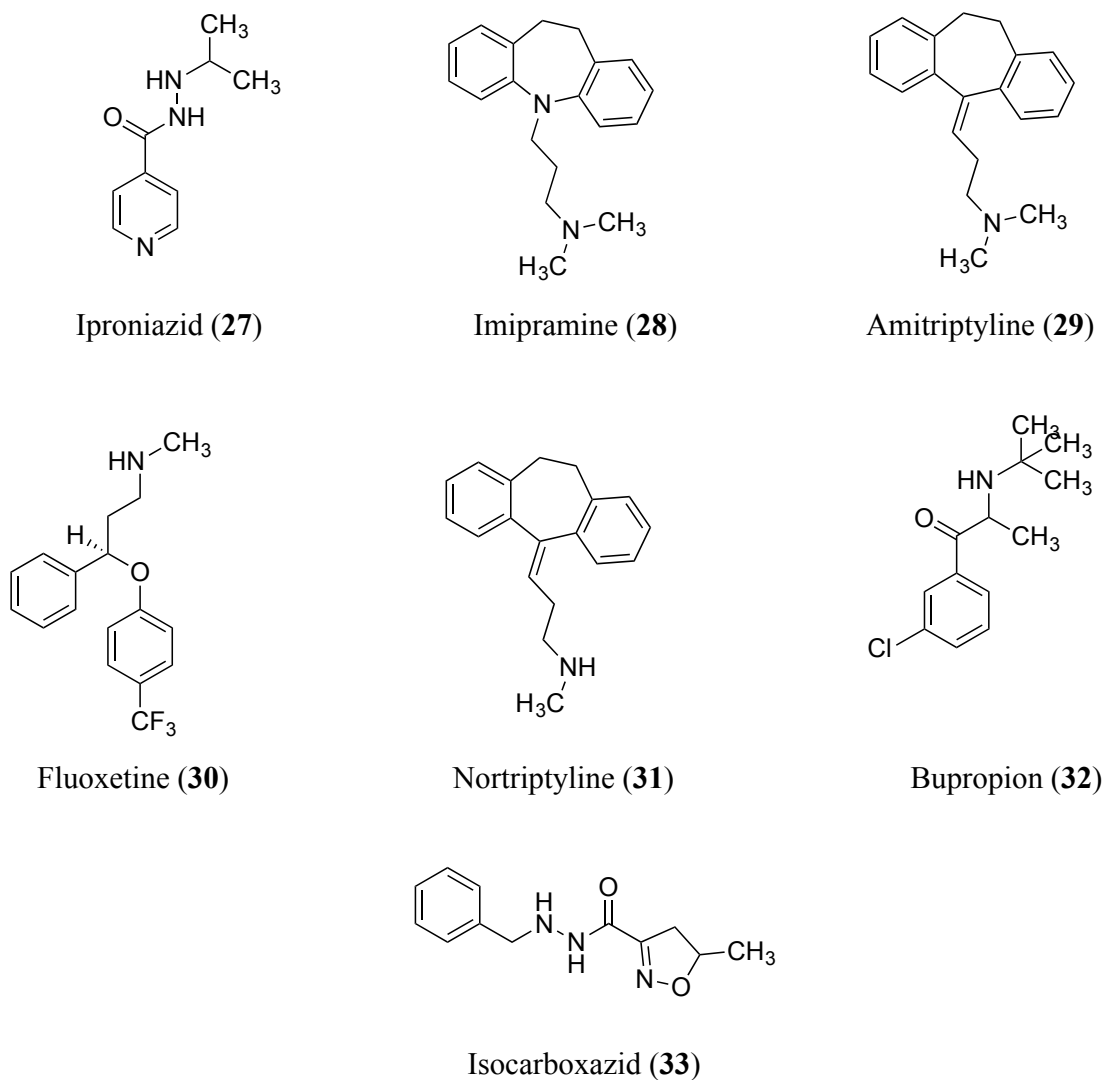
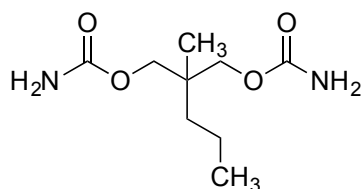


**Figure 7.** Antidepressants of the past and of the present.<sup>94,99,100,102,106</sup>

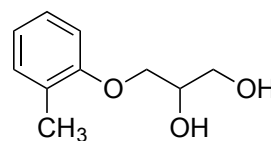
### 3. Anxiety disorders:

The first antianxiety agent was also discovered by chance during drug development for another therapeutic target.<sup>107</sup> The first antianxiety drug was meprobamate (Miltown®) (**34**), introduced by Wallace laboratories in 1955, and it was a descendent of mephesisin (**35**),

which was discovered for its tranquillizing and muscle relaxant properties, during antibiotic research (Figure 8).<sup>107</sup>



Meprobamate (34)



Mephenesin (35)

**Figure 8.** The first antianxiety agents.<sup>107,108</sup>

According to the Diagnostic and Statistical Manual of Mental Disorders, Fifth Edition (*DSM-5*), “anxiety disorders include disorders that share features of excessive fear and anxiety and related behavioral disturbances”.<sup>109</sup> The disorder is characterized by fear of certain future events and the anticipation of reacting to them.<sup>109,110</sup> Anxiety disorder is a class of disorders, each having its own specific trigger. The *DSM-5* further classifies anxiety disorders into the following: separation anxiety, selective mutism, specific phobia, social anxiety disorder, panic disorder, agoraphobia, generalized anxiety disorder and substance/medication induced anxiety.<sup>109</sup>

Recent neuroimaging studies have implicated a role of the amygdala, different regions of the orbitofrontal cortex, anterior cingulate, parietal and occipital cortices, in the pathophysiology of anxiety disorders.<sup>111</sup> There is evidence that 5-HT<sub>1A</sub> receptors are involved in the perception of fear-related cues from studies conducted on homozygote as well as heterozygote 5-HT<sub>1A</sub> knockout mice.<sup>112</sup> 5-HT<sub>1A</sub> receptors are located

presynaptically (on serotonergic neurons in the raphe nuclei) and postsynaptically (on glutamatergic and GABAergic pyramidal neurons in the limbic, frontal and entorhinal cortices).<sup>112,113</sup> Studies on transgenic mice have elicited a role of the postsynaptic 5-HT<sub>1A</sub> receptors located in the forebrain to modulate anxious behavior and 5-HT<sub>1A</sub> receptor knockout mice show resistance to benzodiazepine (common medications for anxiety) treatment.<sup>112,114</sup>

5-HT<sub>1A</sub> receptors also play a role in the effect of SSRIs (first line of treatment) in anxiety treatment.<sup>115,116</sup> In fact the 5-HT<sub>1A</sub> receptor antagonist pindolol hastens the action of SSRIs by preventing the inhibitory action of 5-HT<sub>1A</sub> autoreceptors that has been shown to delay the onset of action of SSRIs in humans.<sup>112,117</sup> To further bolster this observation, positron emission tomographic (PET) examination with a radiolabelled selective 5-HT<sub>1A</sub> antagonist WAY-100635 has shown that there is a negative correlation between 5-HT<sub>1A</sub> binding affinity and anxiety scores, and suggested a role of partial agonists at 5-HT<sub>1A</sub> (postsynaptic) receptors in the treatment of anxiety.<sup>118</sup>

The most commonly prescribed antianxiety agents for generalized anxiety disorder, panic disorder and social anxiety include the SSRIs and the SNRIs such as sertraline (**36**), escitalopram (**37**), paroxetine (**38**) (SSRIs), and venlafaxine (**39**) (SNRI), respectively (Figure 9).<sup>116</sup> Benzodiazepines such as alprazolam (**40**) (Figure 9) are still used, however, they are associated with side effects such as sedation, physical dependence and impaired concentration. They also carry a risk of withdrawal symptoms and rebound anxiety.<sup>116,119</sup>

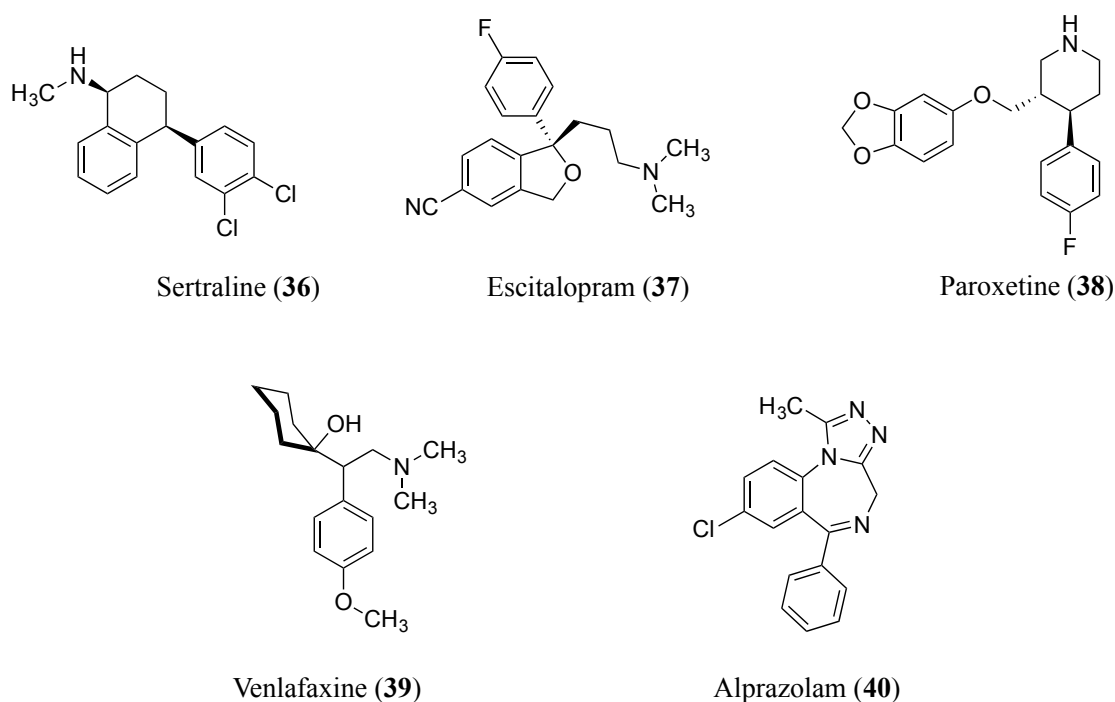


**Figure 9.** Antianxiety agents currently prescribed.<sup>116</sup>

#### 4. Schizophrenia:

The symptoms of schizophrenia become evident as hallucinations (initially visual and then progressing to auditory), delusions and thought disorders (these are called as positive symptoms), social withdrawal, apathy, lack of affect and catatonia (these are known as negative symptoms); and cognitive and decision-making impairments (see Figure 11).<sup>91,120,121</sup> The genetic risk of schizophrenia is quite high and it is known that there is a 50% chance for the identical twin of a schizophrenia patient to develop the disease. The type of household environment during childhood (abusive or emotionally distant parents) can also contribute.<sup>122</sup>

Schizophrenia is neurodevelopmental rather than neurodegenerative in nature, suggested by the absence of inclusion bodies or gliosis, reminiscent of neurodegenerative diseases.<sup>123</sup> It has a varied phenotype and is subjective; hence modeling schizophrenia as a whole in animal models has been difficult.<sup>124</sup> However, animal models of psychosis (e.g. LSD and PCP) have been successful to an extent, in recreating the positive and negative symptoms, and have been helpful in determining the brain regions affected.<sup>89,92</sup> Neuroimaging and pharmacological advances have supported this and although we are far from completely solving the mystery of schizophrenia, we now know that the dopaminergic, serotonergic, glutamatergic and the GABAergic systems are involved (Figure 10).<sup>120,125</sup>

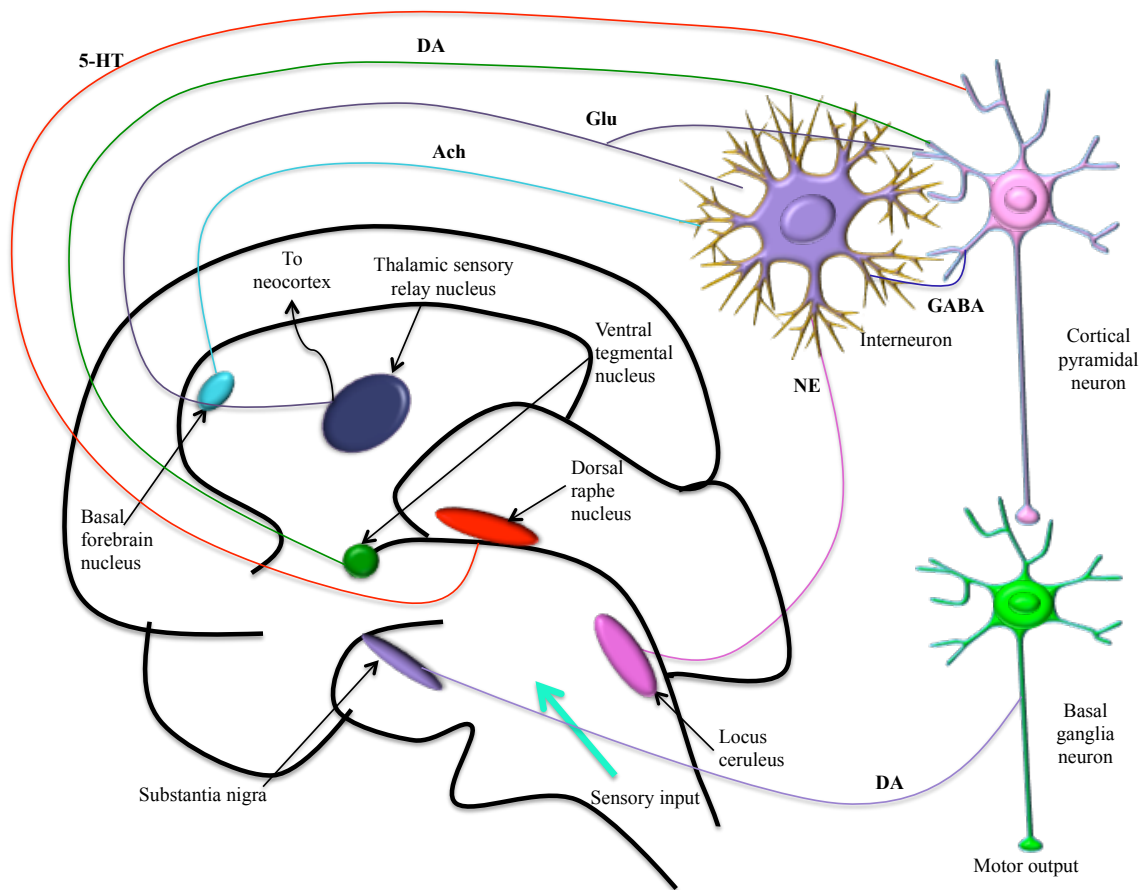


**Figure 10.** The neural circuits involved in schizophrenia, adapted from Freedman, R.<sup>120</sup>

#### **a. Symptoms and neuroanatomical changes:**

Schizophrenia as a disease can be divided into three stages: the prodromal stage, the acute/active stage and the residual stage.<sup>92</sup> The outward symptoms (Figure 11) that help in diagnosis generally appear in the mid-20s.<sup>120</sup> However, the actual onset of the disease (the prodromal stage), which can be as early as in the teens, often gets shrouded under the guise of the emotional and physical changes of adolescence and adjustment to early adulthood.<sup>122</sup>





One of the hypotheses to explain the perceptual abnormalities (hallucinations) and an inability to differentiate between the internal ‘voices’ and extraneous environmental stimuli (contributing to delusions) is hyperactivity of the thalamus.<sup>125</sup> The thalamus is responsible for filtering sensory input and is under an inhibitory influence of GABAergic neurons. This inhibition of the thalamus by GABAergic neurons is controlled by dopamine D<sub>2</sub> receptors.<sup>125,126</sup> An abnormally active dopaminergic system can lead to disinhibition of the thalamus, which is now unable to filter out information, rendering the patient incapable of discerning the ‘real’ from the ‘fabricated’.<sup>125,127</sup>

In schizophrenia, the Glu-GABA-Glu-DA pathway (Figure 10) is impaired leading to an overactive limbic dopaminergic system.<sup>128</sup> In the non-psychotic brain, the Glu neurons from the thalamic sensory relay nucleus (Figure 10) are connected to a smaller GABAergic interneuron that has an inhibitory influence on the glutamatergic cortical pyramidal neuron, leading to a lower firing rate. This regulates the dopaminergic output in the limbic system (Figure 10).<sup>120,125</sup> However, compromised NMDA receptors on the GABAergic interneuron prevent GABA from exerting its inhibitory action on the cortical pyramidal neuron. The result is an overdose of dopamine in the limbic system and this can lead to psychosis.<sup>128</sup> There is also a failure of the inhibitory interneurons and the inhibitory neurotransmitter GABA, leading to impaired synaptic connections between cortical and pyramidal neurons.<sup>125</sup>

There are certain striking neuroanatomical changes observed in the schizophrenic brain such as a marked decrease in the migration of neurons to the cortex from the underlying white matter, white matter disorganization in the prefrontal cortex and lower pyramidal cell density.<sup>123,125,129</sup> A hallmark of schizophrenia, which is also present in first-episode, non-medicated patients, is enlarged ventricles (especially third and lateral ventricles) and diminished volume of the hippocampus and the superior temporal cortex.<sup>123</sup> There is a distinct volume reduction in the frontal lobe, especially in the prefrontal and orbitofrontal regions.<sup>130</sup> Abnormalities in the basal ganglia and thalamus have also been reported. All these could contribute to the negative symptoms and the cognitive deficits of the disorder.<sup>125,130,131</sup>

Although all aspects are not hereditary, there is increasing evidence of a pre-developmental lesion in the brain, which can interact with certain environmental stressors and this in already predisposed people can precipitate the onset of the disease.<sup>122,123</sup>

#### **b. The dopamine hypothesis of schizophrenia:**

The dopamine hypothesis of schizophrenia initially stemmed from the discovery that antipsychotics such as CPZ (**1**) elicited their effects by decreasing DA concentration in the mesolimbic region of the brain, that is, they function as DA receptor antagonists.<sup>132</sup> In fact it has been shown that antipsychotic potency is related to the binding affinity of antipsychotic agents at DA receptors.<sup>131</sup>

This was followed by the observation that stimulants such as amphetamine could lead to effects quite similar to the positive symptoms of schizophrenia.<sup>131,133</sup> The dopamine hypothesis postulated that schizophrenia is caused by overstimulation of dopaminergic receptors in the mesolimbic region (leading to hallucinations and delusions) and a lack of dopamine at the nucleus accumbens leading to the anhedonia and lack of motivation.<sup>132</sup>

The dopamine hypothesis that gained ground during the 1960s led to a thorough investigation of the dopaminergic tracts in the brain. It was shown that stimulation of DA receptors in the nigrostriatal pathway by amphetamine led to stereotyped motor effects, and inhibition of these receptors by the antipsychotic agents led to the extrapyramidal side effects commonly experienced with these agents.<sup>132</sup> This further bolstered the hypothesis.

However, it soon came to light that antipsychotic agents were only effective against the positive symptoms and had little, if any, effect against the negative symptoms and cognitive deficits.<sup>92,133</sup> Atypical antipsychotic drugs, especially clozapine (**2**) and risperidone (**3**), had greater affinity towards 5-HT<sub>2A</sub> receptors over D<sub>2</sub> receptors, a faster dissociation rate at D<sub>2</sub> receptors, and could help against the positive as well as the negative symptoms of schizophrenia.<sup>134</sup> Additionally, they also had a lower tendency for causing extrapyramidal side effects.<sup>135</sup>

Thus, the dopaminergic system could not explain all the parameters of the disease and the serotonin hypothesis of schizophrenia came along.

### **c. The serotonin hypothesis of schizophrenia:**

5-HT and psychosis have been linked since the almost simultaneous discovery of LSD (**19**) and 5-HT (**18**) in the late 1940s.<sup>80</sup> As discussed earlier (section B), research on the serotonergic system has evolved hand-in-hand with studies on hallucinogens such as LSD (**19**), DMT (**20**), mescaline (**22**), and DOM (**23**), which are agonists and/or partial agonists at 5-HT receptors, 5-HT<sub>2A</sub> in particular.<sup>84</sup> The hallucinations and bizarre experiences created by these hallucinogens were very similar to the positive symptoms of the initial stages of schizophrenia.<sup>92</sup> The serotonin hypothesis postulated that hyperactivity of 5-HT in the cerebral cortex and the locus ceruleus (Figure 10) is responsible for schizophrenia.<sup>91</sup>

The first atypical antipsychotic, clozapine, further supported the serotonin hypothesis. Unlike typical antipsychotics such as CPZ (**1**) and haloperidol (**9**), it was effective against the positive, negative, as well as cognitive symptoms of schizophrenia and did not result in EPS that was a hallmark of classical antipsychotic treatment.<sup>30,134,135</sup> The atypical antipsychotics had a higher affinity at 5-HT<sub>2A</sub> receptors than at dopamine D<sub>2</sub> receptors, and acted as dual serotonin-dopamine antagonists.<sup>136</sup>

MRI and PET imaging studies of the cerebral cortex of schizophrenia patients revealed certain neuroanatomical changes in the serotonergic system.<sup>131</sup> Schizophrenia has been associated with a hyperactive dorsal raphe nucleus (DRN) (Figure 10) and overdriven serotonergic signaling to the cerebral cortex, especially in the anterior cingulate nucleus (ACC) and the dorsolateral frontal lobe.<sup>91</sup> Post mortem brain samples from schizophrenia

patients have shown an increase in 5-HT, especially in the putamen, globus pallidus, nucleus accumbens and the basal ganglia.<sup>131</sup> There was a decrease in 5-HT in the hypothalamus, medulla oblongata, and hippocampus.<sup>131,137</sup> This was accompanied by a loss of grey matter in the ACC, potentially explaining the decreased utilization of ATP in the frontal lobe.<sup>91</sup>

Although the atypical antipsychotics are certainly more sparing in their EPS-causing liability, they have only a modest efficacy over the typical antipsychotics, especially with regard to the negative symptoms, and a considerable number of patients did not respond to treatment.<sup>68,138</sup> The psychosis generated by NMDA antagonists such as PCP (**25**) and ketamine (**26**) produced the entire spectrum of symptoms and model the disease much better.<sup>92</sup> This focused attention on the role of glutamate in the pathophysiology of schizophrenia.

#### **d. The NMDA hypofunction/glutamate hypothesis of schizophrenia:**

The complete clinical syndrome of schizophrenia captured by NMDA receptor antagonists such as PCP and ketamine is the foundation of the glutamate hypothesis of schizophrenia that was put forward by Olney and Farber in 1995.<sup>68,92</sup>

Classical hallucinogens such as LSD and mescaline, enhance glutamatergic neurotransmission in the prefrontal cortex by increasing the frequency of the excitatory postsynaptic potentials (EPSPs) in the apical dendritic region of the layer V pyramidal cells.<sup>91,139</sup> As discussed earlier, malfunctioning NMDA receptors on the interneurons (Figure 10) could lead to loss of GABAergic control of the dopaminergic influence on the mesolimbic regions.<sup>68,91</sup> An increase in the glutamatergic neurotransmission and a lack of inhibition by GABA can perhaps explain the positive symptoms of schizophrenia.<sup>91</sup> A potential explanation for the negative symptoms and cognitive deficits is an overactivation of GABA interneurons by a hyperactive glutamate signaling and the resulting overinhibition of the dopaminergic pathway to the mesocortical region.<sup>68,91,131</sup>

Currently, the pharmacological treatment of schizophrenia entails one or more of the atypical antipsychotics (Figure 1).<sup>12,23</sup> However, since the DA and 5-HT hypotheses could not completely explain the behavioral or the neuropathological changes occurring in schizophrenia, glutamate receptors are now being explored as potential antipsychotic targets.<sup>23,68</sup> Additionally, a pharmacological agent targeting both the serotonergic and

glutamatergic aspects of schizophrenia (a heteromer of 5-HT<sub>2A</sub> and mGlu<sub>2</sub> receptors) could be more efficacious in treating the disorder.<sup>9</sup>

### C. THE 5-HT CLASS OF RECEPTORS:

5-HT receptors (5-HT<sub>1</sub>-5-HT<sub>7</sub>) can be divided into seven main classes that can further be divided into several subclasses.<sup>80</sup> With the exception of 5-HT<sub>3</sub>, which is a ligand-gated ion channel, all other 5-HT receptors belong to the class A GPCR superfamily of receptors.<sup>80,140</sup> They consist of seven transmembrane-spanning helices and have an extracellular N-terminus and an intracellular C-terminus.<sup>80</sup> Listed below in Table 2 is the current classification of 5-HT receptors into seven main classes and their respective subclasses.<sup>80</sup>

**Table 2.** Classification of 5-HT receptors adapted from Glennon and Dukat.<sup>80</sup>

| Populations and Subpopulations | Second messenger System | Currently Accepted Name | Comments  |
|--------------------------------|-------------------------|-------------------------|---|
| 5-HT <sub>1</sub>              |                         |                         |   |
| 5-HT <sub>1A</sub>             | AC (-)                  | 5-HT <sub>1A</sub>      | Cloned and pharmacologic 5-HT <sub>1A</sub> receptors |
| 5-HT <sub>1B</sub>             | AC (-)                  | 5-HT <sub>1B</sub>      | Rodent homolog of 5-HT <sub>1B</sub> receptors        |
| 5-HT <sub>1Bβ</sub>            |                         |                         | A mouse homolog of h5-HT <sub>1B</sub> receptors      |



|                     |        |                     |   |
|---------------------|--------|---------------------|---|
| 5-HT <sub>1D</sub>  |        |                     | Sites identified in binding studies using human and calf brain homogenates<br>A cloned 5-HT <sub>1D</sub> subpopulation |
| 5-HT <sub>1Dα</sub> | AC (-) | h5-HT <sub>1D</sub> | Human counterpart of rat 5-HT <sub>1B</sub>   |
| 5-HT <sub>1Dβ</sub> | AC (-) | h5-HT <sub>1B</sub> | Sites identified in binding studies using brain homogenates and cloned receptors  |
| 5-HT <sub>1E</sub>  | AC (-) | 5-HT <sub>1E</sub>  |   |
| 5-HT <sub>1Eα</sub> |        |                     | Cloned h5-HT <sub>1E</sub>  |
| 5-HT <sub>1Eβ</sub> | AC (-) | 5-HT <sub>1F</sub>  | Cloned mouse homolog of 5-HT <sub>1F</sub> receptors  |
| 5-HT <sub>1F</sub>  |        |                     | Cloned h5-HT <sub>1F</sub> receptors  |
| 5-HT <sub>2</sub>   |        |                     |   |
| 5-HT <sub>2</sub>   | PI     | 5-HT <sub>2A</sub>  | Originally known as 5-HT <sub>2</sub>   |
| 5-HT <sub>2F</sub>  | PI     | 5-HT <sub>2B</sub>  | 5-HT <sub>2</sub> -like, found in rat fundus  |

|                    |             |                    |  |
|--------------------|-------------|--------------------|--|
| 5-HT <sub>1C</sub> | PI          | 5-HT <sub>2C</sub> | Originally known as 5-HT <sub>2C</sub>             |
| 5-HT <sub>3</sub>  | Ion Channel | 5-HT <sub>3</sub>  | Ligand-gated ion channel                           |
| 5-HT <sub>4</sub>  | AC (+)      | 5-HT <sub>4</sub>  |  |
| 5-HT <sub>4S</sub> |             |                    | Short form of cloned 5-HT <sub>4</sub> receptors   |
| 5-HT <sub>4L</sub> |             |                    | Long form of cloned 5-HT <sub>4</sub> receptors    |
| 5-HT <sub>5</sub>  |             |                    |  |
| 5-HT <sub>5A</sub> | ?           | 5-HT <sub>5A</sub> | Cloned mouse, rat and h5-HT <sub>5</sub> receptors |
| 5-HT <sub>5B</sub> | ?           | 5-HT <sub>5B</sub> | Cloned mouse and rat 5-HT <sub>5</sub> receptors   |
| 5-HT <sub>6</sub>  | AC (+)      | 5-HT <sub>6</sub>  | Cloned rat and h5-HT receptor                      |
| 5-HT <sub>7</sub>  | AC (+)      | 5-HT <sub>7</sub>  | Cloned rat, guinea pig and h5-HT <sub>7</sub>      |

---

## 1. 5-HT<sub>2A</sub> RECEPTORS AND SOME LIGANDS TARGETING THEM:

5-HT<sub>2A</sub> receptors are a major target of atypical antipsychotics, antidepressants, hallucinogens and other psychoactive drugs, as well as some antihypertensive drugs.<sup>77,140</sup> They are GPCRs and are coupled to the G<sub>α/q</sub> subunit of the heterotrimeric G-proteins (Figure 12).<sup>141</sup>

Activation of 5-HT<sub>2A</sub> receptors leads to several downstream events such as the activation of phospholipase C (PLC), catalyzing hydrolysis of phosphatidylinositol 4,5-bisphosphate (PIP<sub>2</sub>) to inositol 1,4,5-triphosphate (IP<sub>3</sub>) and diacylglycerol (DAG). IP<sub>3</sub> then releases calcium ions (Ca<sup>2+</sup>) from the endoplasmic reticulum (ER) which then activates inwardly rectifying chloride channels (Figure 12).<sup>80,140,141</sup>

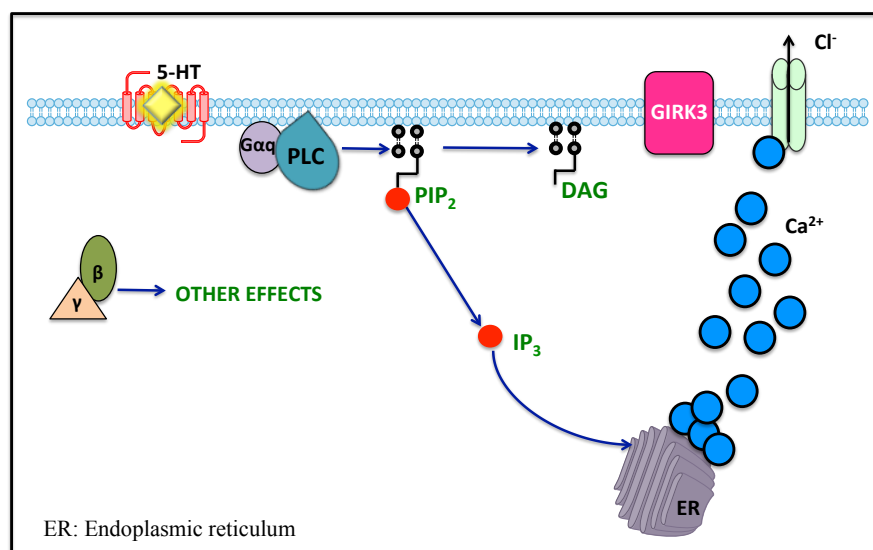


**Figure 12.** The second messenger signal transduction pathway of 5-HT<sub>2A</sub> receptors.<sup>80,141</sup>

Tools such as radioactively labeled ligands, in situ hybridization, RT-PCR and immunocytochemistry have revealed the CNS presence of 5-HT<sub>2A</sub> receptors in the cerebral cortex, basal forebrain, hippocampus, amygdala, hypothalamus, superior colliculus, latero dorsal tegmental nucleus, spinal cord motor neurons, sympathetic and sensory neurons and the peripheral presence in vascular, gastrointestinal smooth muscles, platelets and retina.<sup>141</sup>

Initially, 5-HT receptor binding sites were investigated using a number of radioactively labeled ligands such as [<sup>3</sup>H]-5-HT, [<sup>3</sup>H]-LSD, and [<sup>3</sup>H]-spiperone.<sup>141</sup> Spiperone (**41**) was selective for 5-HT<sub>2A</sub> over 5-HT<sub>2C</sub> (about 1000 fold) however; it had high affinity for dopamine D<sub>2</sub> receptors (Figure 13).<sup>142</sup> Ketanserin (**42**) was the first ligand to selectively label 5-HT<sub>2A</sub> receptors (referred to as 5-HT<sub>2</sub> receptors or S<sub>2</sub> receptors back then) (Figure 13).<sup>143</sup> It was devoid of activity at 5-HT<sub>1</sub> receptors and had minimal affinity for dopamine D<sub>2</sub> receptors. It became a prototypic 5-HT<sub>2</sub> antagonist with high binding affinity ( $K_i = 3.5$  nM at 5-HT<sub>2A</sub> and  $K_i = 50$  nM at 5-HT<sub>2C</sub> receptors in rat frontal cortex)<sup>143</sup> and has remained a radioligand of choice for investigations at 5-HT<sub>2</sub> receptors for over two decades.<sup>142–144</sup>

DOI is a 5-HT<sub>2A</sub> agonist (highly selective for 5-HT<sub>2</sub> sites) and is a hallucinogen.<sup>145</sup> Our laboratory had previously reported that the R(-) stereoisomer is more active.<sup>145,146</sup> Its radiolabeled form, [<sup>125</sup>I]-R(-)-DOI is used to label 5-HT<sub>2A</sub> receptors that were traditionally labeled with antagonists such as spiperone, ketanserin and partial agonists such as LSD. [<sup>125</sup>I]-R(-)-DOI led to the labeling of the low density, high affinity sites for 5-HT<sub>2A</sub> agonists.<sup>147</sup>

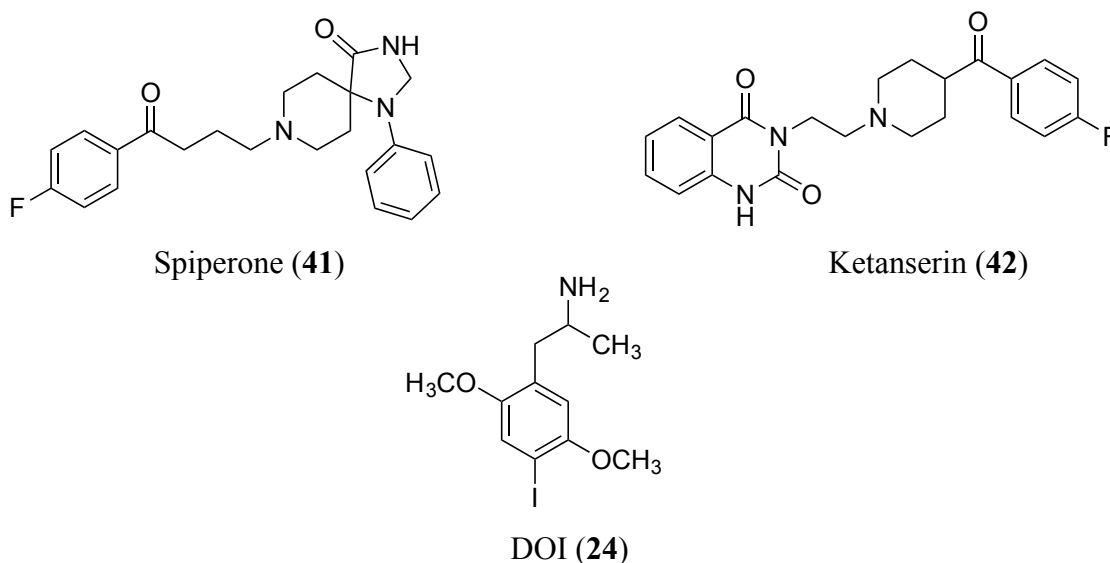


**Figure 13.** Radioligands commonly used to label 5-HT<sub>2A</sub> receptor sites.<sup>142,146</sup>

5-HT<sub>2A</sub> receptors have been a subject of great interest since atypical antipsychotic agents such as clozapine (2) and risperidone (3) were found to be dual serotonin-dopamine antagonists (SDAs) and having a higher binding affinity for 5-HT<sub>2A</sub> receptors over dopamine D<sub>2</sub> receptors.<sup>8,30</sup> In the late 1990s, it was observed that some atypical antipsychotic agents could inhibit the constitutive activity of 5-HT<sub>2A</sub> receptors and possessed inverse agonist activity.<sup>26</sup>

## 2. THE 5-HT<sub>2A</sub>-mGLU<sub>2</sub> HETEROMER:

The 5-HT<sub>2A</sub> receptor specifically forms a heterodimer with the mGlu<sub>2</sub> receptor.<sup>61</sup> The two receptors have been shown to co-localize in mouse cortical slices and neuronal primary

cultures in autoradiographic studies (Figure 14) and interact to downregulate the  $G_{\alpha/q}$  signaling of 5-HT<sub>2A</sub> receptors and upregulate the  $G_{i/o}$  signaling of mGlu<sub>2</sub> receptors.<sup>9,61</sup>

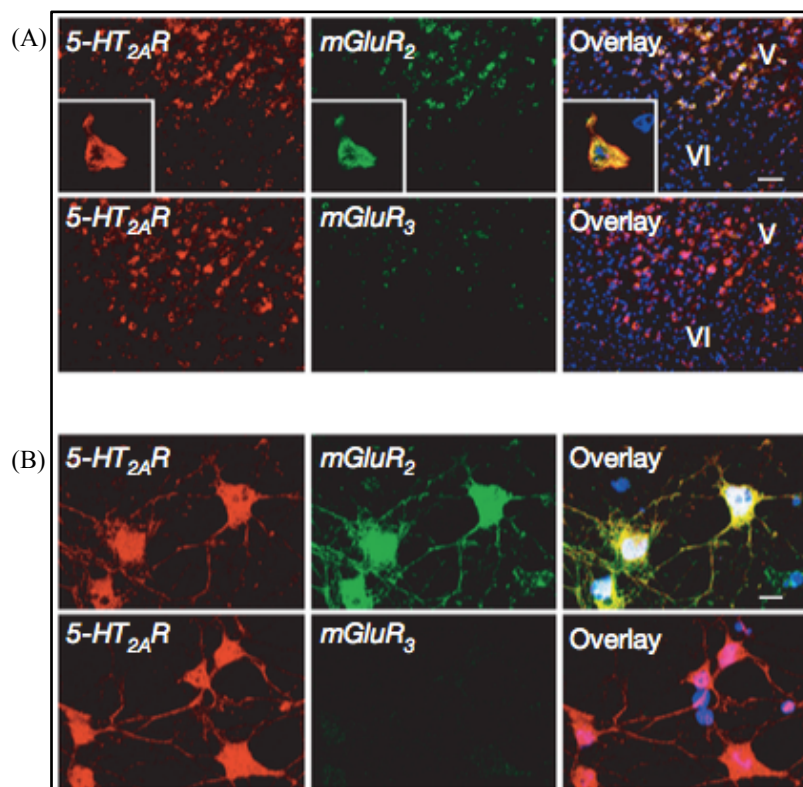


**Figure 14.** Overlay of 5-HT<sub>2A</sub> and mGlu<sub>2</sub> receptors in mouse somatosensory cortex (A), and mouse cortical primary culture (B).<sup>61</sup>

Clozapine (**2**) and risperidone (**3**) were found to crosstalk (downregulate the  $G_{\alpha/q}$  signaling of 5-HT<sub>2A</sub> receptors and upregulate the  $G_{i/o}$  signaling of mGlu<sub>2</sub> receptors when the two receptors are coexpressed) at the 5-HT<sub>2A</sub>-mGlu<sub>2</sub> heterodimer and this target is currently being explored with respect to the pathophysiology of schizophrenia and the mechanism of action of certain hallucinogens.<sup>9,61</sup>

### CHAPTER III: SPECIFIC AIMS

The pharmacological and biochemical profile of risperidone (**3**) was extensively explored in the mid-1980s – around the time it was realized that excessive DA might not be the only contributing factor in schizophrenia.<sup>131,148</sup> The serotonergic component of antipsychotic activity was gaining increasing importance with the discovery that several 5-HT receptor (specifically 5-HT<sub>2A</sub>, referred to as 5-HT<sub>2</sub> sites then) antagonists (Figure 15) such as spiperone (**41**) inhibited the pharmacological actions of the 5-HT receptor agonist tryptamine (TRY) as well as apomorphine (APO)-induced stereotypy with potency being directly related to binding affinity.<sup>149</sup> Ligands having a ‘mixed’ or dual serotonin-dopamine antagonism (SDA) profile, such as risperidone (**3**) (ED<sub>50</sub> = 0.028 mg/kg) and pirenperone (**43**) (ED<sub>50</sub> = 0.020 mg/kg) (Figure 15) dose-dependently attenuated the LSD-cue in drug discrimination studies, and differed from the selective 5-HT<sub>2A</sub> antagonist ritanserin (**44**) (ED<sub>50</sub> = 11.6 mg/kg), which was not a very potent blocker of the LSD-cue, and the classical D<sub>2</sub> receptor antagonist haloperidol, which did not block the LSD-cue.<sup>150–154</sup>

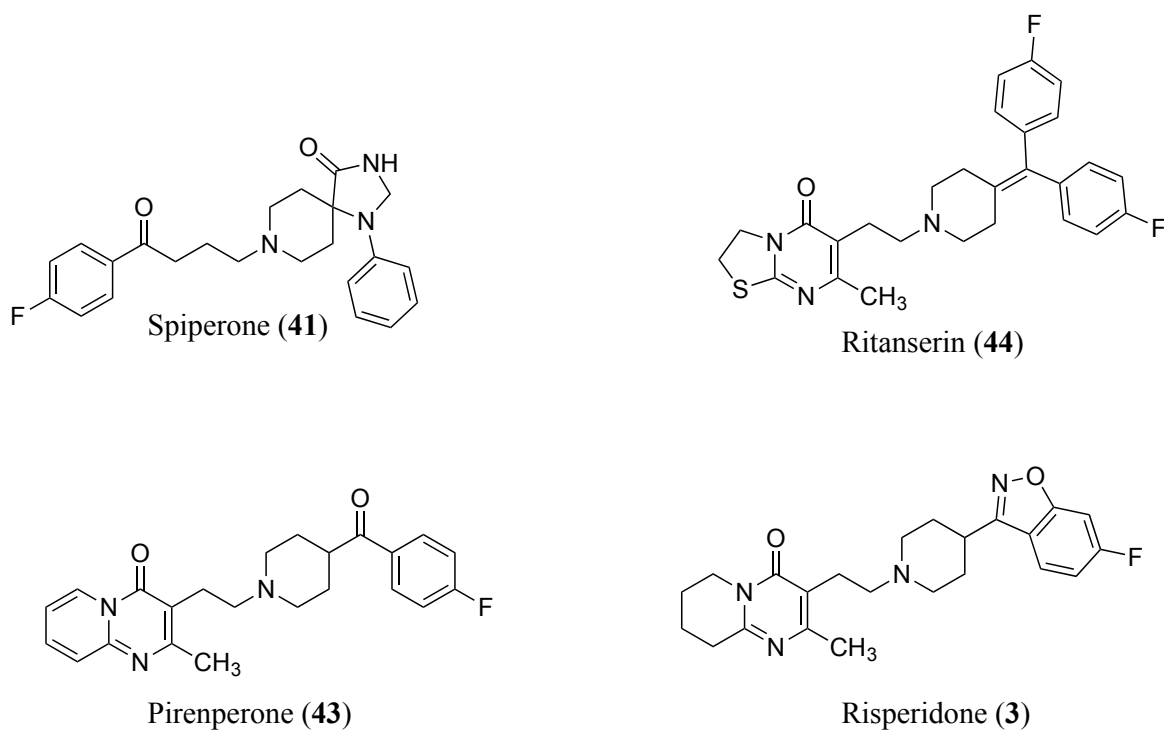


**Figure 15.** Representative structures of 5-HT<sub>2A</sub> antagonists.<sup>155,156</sup>

Risperidone (**3**) is said to be a prototype of centrally active ligands having optimum dopamine D<sub>2</sub> receptor and 5-HT<sub>2A</sub> receptor binding affinity and antagonist activity.<sup>24,148,155</sup> In fact, atypical antipsychotics have a greater affinity for 5-HT<sub>2A</sub> receptors, as compared to D<sub>2</sub> receptors and Meltzer had defined a ratio of D<sub>2</sub>/5-HT<sub>2A</sub> binding affinities, with a higher value being conducive for atypical antipsychotic-like activity.<sup>25</sup>

The development of risperidone (Figure 16), stemmed from the need to integrate antiapomorphine and anti-tryptamine activities in a single centrally active ligand with good bioavailability.<sup>149,157</sup>



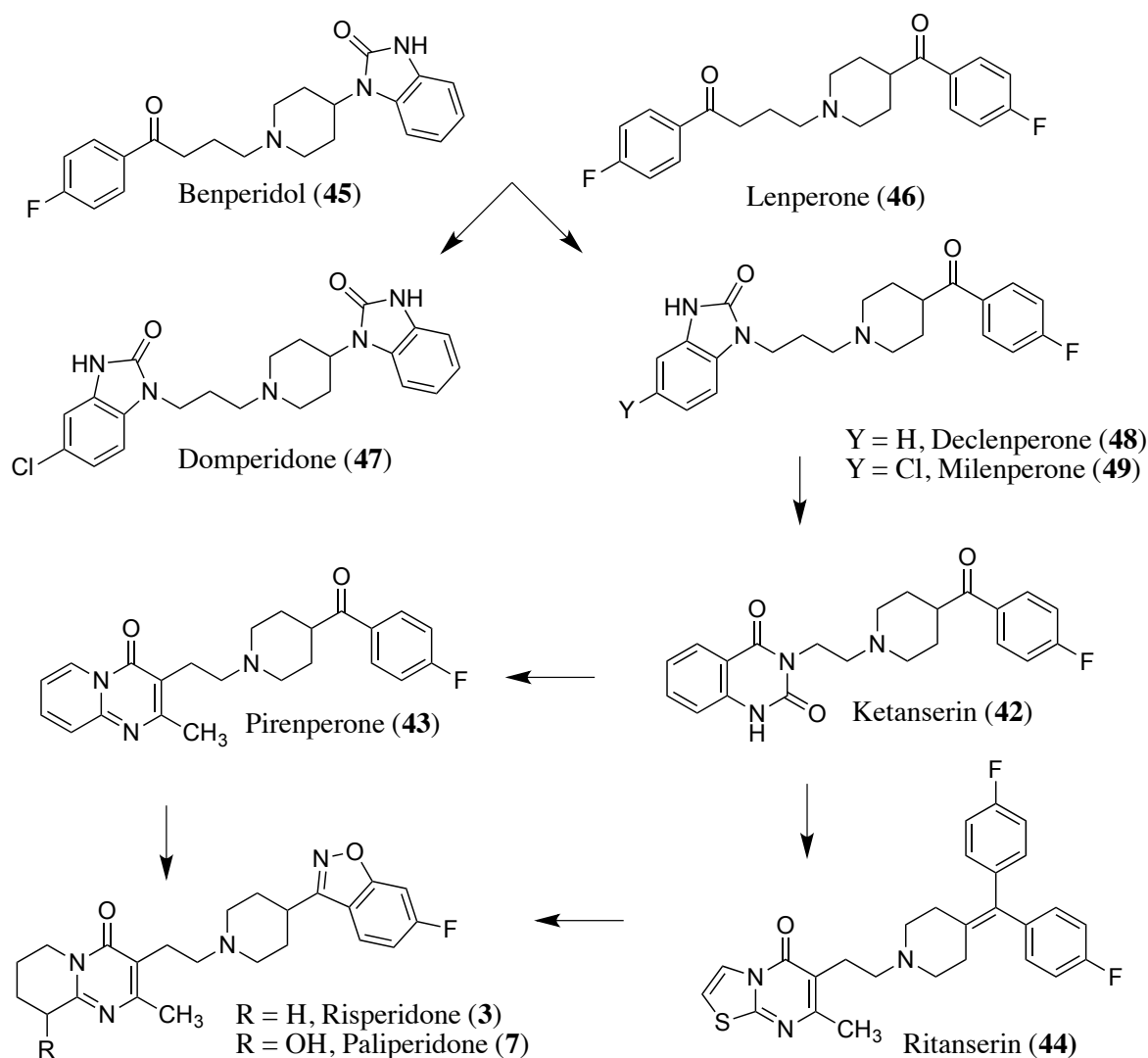


**Figure 16.** The development of risperidone from butyrophenones.<sup>157</sup>

The development of risperidone began with two structurally related butyrophenones – benperidol (also known as benzperidol) (**45**) and lenperone (**46**) having affinity for the dopamine D<sub>2</sub> receptor (Figure 16).<sup>157</sup> Benperidol and lenperone had two aromatic groups separated from the central nitrogen atom by 4 carbon atoms and their structures could be considered as two ‘halves’ or ‘fragments’ around the central nitrogen atom (Figure

17).<sup>142,157</sup> As both ligands bound to dopamine D<sub>2</sub> receptors (Table 3), it was believed that the benzoyl moiety of lenperone had pharmacophoric similarities with the benzimidazolone moiety of benperidol.<sup>157</sup>

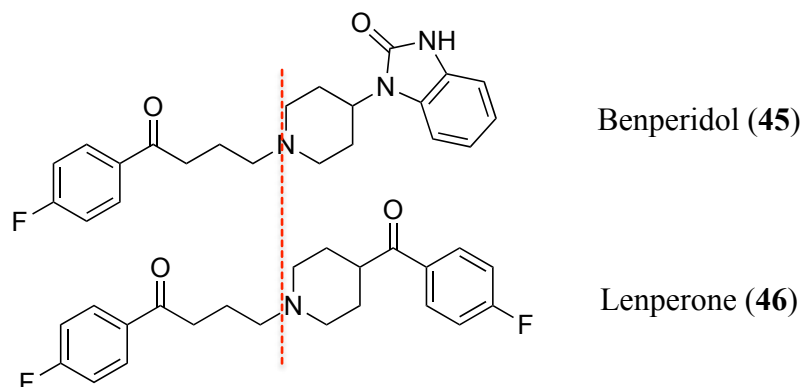


**Figure 17.** The ‘halves’ or ‘fragments’ of benperidol and lenperone.<sup>157</sup>

Structural combinations of the fragments of benperidol and lenperone were then synthesized and evaluated for binding affinity and activity. Combining the two benzimidazolone fragments led to domperidone (47), which had affinity for peripheral DA receptors and activity only in the APO-induced emesis test in dogs suggesting peripheral activity and limited or no central activity.<sup>157</sup> A combination of benzimidazolone with the benzoyl fragment led to declenperone (48) and milenperone (49), which were centrally active dopamine D<sub>2</sub> antagonists with weak 5-HT<sub>2A</sub> antagonist activity (Table 3).<sup>157</sup>

Further, several modifications to the benzimidazolone ring eventually led to the quinazolinedione ring system, represented by ketanserin (42).<sup>144,157</sup> This increased the 5-HT<sub>2A</sub> antagonist activity and imparted a 100-fold selectivity over D<sub>2</sub> receptors.

Ketanserin had high affinity and functional activity at 5-HT<sub>2A</sub> receptors and limited central and peripheral D<sub>2</sub> antagonist activity (Table 3).<sup>144,157,158</sup>

Replacement of the quinazolinedione ring with several different saturated and unsaturated heterocyclic ring systems led to the development of pirenperone (**43**), a potent 5-HT<sub>2A</sub> and D<sub>2</sub> receptor antagonist, having ~8-fold selectivity for 5-HT<sub>2A</sub> receptors over dopamine D<sub>2</sub> receptors.<sup>157</sup> However, it suffered from poor oral bioavailability. In a quest to develop metabolically stable molecules, changes were made on the right side of pirenperone and its analogs, giving rise to ritanserin (**44**), which had high selectivity for 5-HT<sub>2A</sub> receptors over D<sub>2</sub> receptors.<sup>155</sup>

Another approach to deter metabolism and increase bioavailability was based on the isosteric replacement of the benzoyl fragment with a benzisoxazole ring, giving rise to risperidone (**3**).<sup>148,157</sup> Risperidone was centrally active and had excellent oral bioavailability. It was a potent antagonist at both receptors with about 20-fold selectivity for 5-HT<sub>2A</sub> ( $K_i = 0.16$  nM) over D<sub>2</sub> ( $K_i = 3.1$  nM) and also had affinity for  $\alpha_1$ -adrenoceptors and histamine H<sub>1</sub> receptors in the nanomolar range.<sup>157,159</sup> Risperidone seemed to combine the favorable structural features of all its predecessors in terms of affinity and activity at D<sub>2</sub> and 5-HT<sub>2A</sub> receptors.

**Table 3.** Binding affinity and functional activity profile of risperidone and its predecessors adapted from Megens et al.<sup>157</sup>

| Agent        | Receptor binding $K_i$ (nM) |                | Activity against central 5-HT <sub>2A</sub> and D <sub>2</sub> receptors ED <sub>50</sub> (mg/kg, s.c.) |                       |
|--------------|-----------------------------|----------------|---|-----------------------|
|              | 5-HT <sub>2A</sub>          | D <sub>2</sub> | TRY (5-HT <sub>2A</sub> )   | APO (D <sub>2</sub> ) |
| Benperidol   | 6.60                        | 0.35           | 0.29  | 0.0093                |
| Lenperidol   | Not tested                  | 4.60           | 0.39  | 0.085                 |
| Declenperol  | 2.40                        | 9.30           | 2.40  | 0.44                  |
| Milenperone  | 9.20                        | 3.90           | 0.51  | 0.025                 |
| Domperidone  | 330                         | 0.90           | > 40  | > 40                  |
| Ketanserin   | 2.10                        | 220            | 2.40  | > 40                  |
| Pirenperone  | 2.10                        | 16.00          | 0.11  | 0.098                 |
| Ritanserin   | 1.20                        | 23.00          | 0.26  | >160                  |
| Risperidone  | 0.16                        | 3.10           | 0.13  | 0.15                  |
| Paliperidone | 0.22                        | 4.10           | 0.22  | 0.39                  |

\*Radioligand binding studies were performed in rat frontal cortex homogenates with [<sup>3</sup>H]-spiperone. TRY and APO-assays studied inhibition of bilateral clonic seizures and agitation induced by TRY and APO, respectively.<sup>157</sup>

In order to compare its serotonergic and dopaminergic activity components, risperidone (**3**) was explored for its in vitro and in vivo affinity and activity and was compared to

ritanserin (**44**) (a centrally acting selective 5-HT<sub>2A</sub> antagonist) and haloperidol (**9**) (a selective D<sub>2</sub> antagonist).<sup>148,150</sup>

Similar to ritanserin, risperidone showed antagonist activity in all tests related to central and peripheral 5-HT<sub>2A</sub> receptors, such as clonic seizures and tremors in rat forepaws induced by TRY, mescaline- and 5-hydroxytryptophan (5-HTP)-induced twitches with ED<sub>50</sub> values of 0.014 mg/kg, 0.019 mg/kg and 0.016 mg/kg, respectively, and was more potent than ritanserin.<sup>150</sup>

As regards activity against D<sub>2</sub> receptors, risperidone antagonized central and peripheral dopaminergic activities such as apomorphine-induced emesis in dogs, amphetamine- and cocaine-induced agitation and stereotypies (Table 3).<sup>150,157</sup> While haloperidol seemed to have a narrow dose range of 1:3.5 for all effects including locomotion, risperidone had a dose range of 1:10, excluding effects on locomotion, which were above this broad range.<sup>150</sup>

Risperidone was found to be 10 times more potent at central 5-HT<sub>2A</sub> receptors than at central dopamine D<sub>2</sub> receptors.<sup>160</sup>

That risperidone had an antipsychotic-like profile different from haloperidol and other typical antipsychotics, was evident from the fact that it was a very potent LSD antagonist (ED<sub>50</sub> = 0.028 mg/kg) in drug discrimination studies.<sup>153</sup> Haloperidol (selective D<sub>2</sub> antagonist) does not affect the discriminative stimulus and ritanserin (selective 5-HT<sub>2A</sub>

antagonist) is not a very potent blocker ( $ED_{50} = 11.6 \text{ mg/kg}$ ) of the discriminative stimulus.<sup>150,152</sup> In an open trial, risperidone (2-8 mg p.o. for 28 days) was effective in improving the condition of schizophrenia patients resistant to typical antipsychotics and having a major component of negative symptoms, without inducing EPS.<sup>161</sup>

It was believed that the 5-HT<sub>2A</sub> component of the activity could be responsible for the effect of risperidone on negative symptoms of schizophrenia, as selective 5-HT<sub>2A</sub> antagonists such as pipamperone and ritanserin had demonstrated antidepressant-like properties and reduced catalepsy in rats.<sup>162</sup> This hypothesis was further supported by electrophysiological studies that showed that a marked antagonism of 5-HT<sub>2A</sub> receptors (as shown by risperidone) could lead to a release of DA from the midbrain, which in turn could lead to release of DA in the nucleus accumbens and prefrontal cortex, thus circumventing the symptoms of lack of affect and concentration.<sup>8,160</sup>

Risperidone proved to be unique in its receptor occupancy profile when compared to haloperidol (**9**) and clozapine (**2**) (another atypical antipsychotic). Apart from binding primarily to 5-HT<sub>2A</sub> receptors (clozapine binds primarily to histamine H<sub>1</sub> receptors and haloperidol to D<sub>2</sub> receptors), risperidone had a shallow occupancy curve at D<sub>2</sub> receptors in the striatum and mesolimbic regions – suggesting a gradual increase in the occupancy of the receptor with increasing doses (Figure 18).<sup>159</sup> Risperidone occupied 50% of 5-HT<sub>2A</sub> and dopamine D<sub>2</sub> receptors at a dose of 0.0075 and 2.5 mg/kg s.c., respectively. At a dose at which 50% of D<sub>2</sub> receptors are occupied, there is full occupancy of 5-HT<sub>2A</sub> sites, which

as previously described, can be helpful against negative symptoms.<sup>8,160</sup> Also, the gradual occupation of D<sub>2</sub> receptors suggests that at a lower dose and with partial occupation, risperidone might be helpful against positive symptoms without inducing EPS.

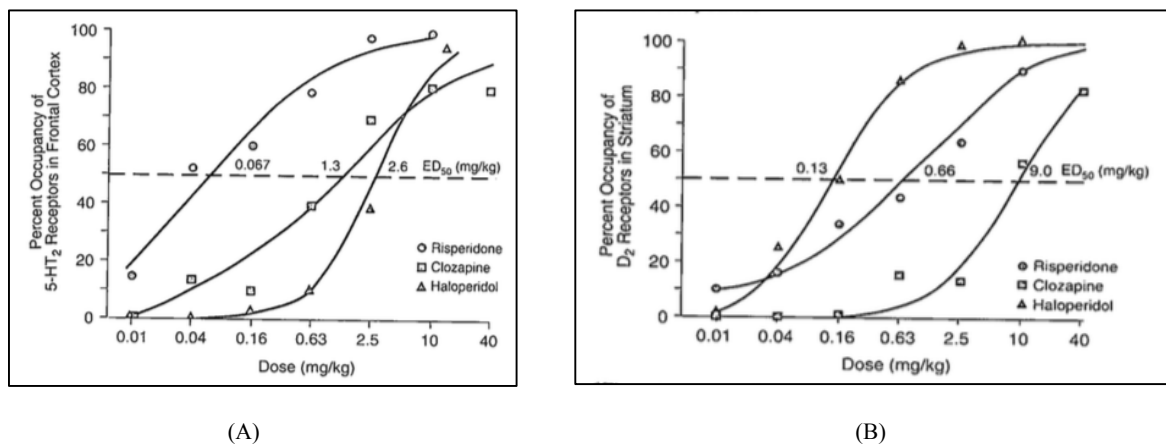


**Figure 18.** The receptor occupancy profile of risperidone (○), clozapine (□) and haloperidol (Δ) at 5-HT<sub>2A</sub> receptors (A), and dopamine D<sub>2</sub> receptors (B).<sup>8</sup>

Physiologically, risperidone is metabolized by three major pathways in humans, rats and dogs leading to active and inactive metabolites: alicyclic hydroxylation, oxidative *N*-dealkylation and cleavage of the benzisoxazole ring (Figure 19).<sup>163</sup> The major active metabolite is paliperidone (**7**), which is the product of hydroxylation at the 9-position.<sup>157</sup> 7-Hydroxylated (7-OH) **50**, dihydroxylated **51**, benzisoxazole ring cleavage products **52** and oxidative *N*-dealkylated **53** and **54** also form a small percentage of the metabolites.<sup>163</sup> One of the metabolites in dogs, which is also a putative metabolite in humans, is **55** and it is a part of the current as well as past investigations by our laboratory.<sup>164</sup>

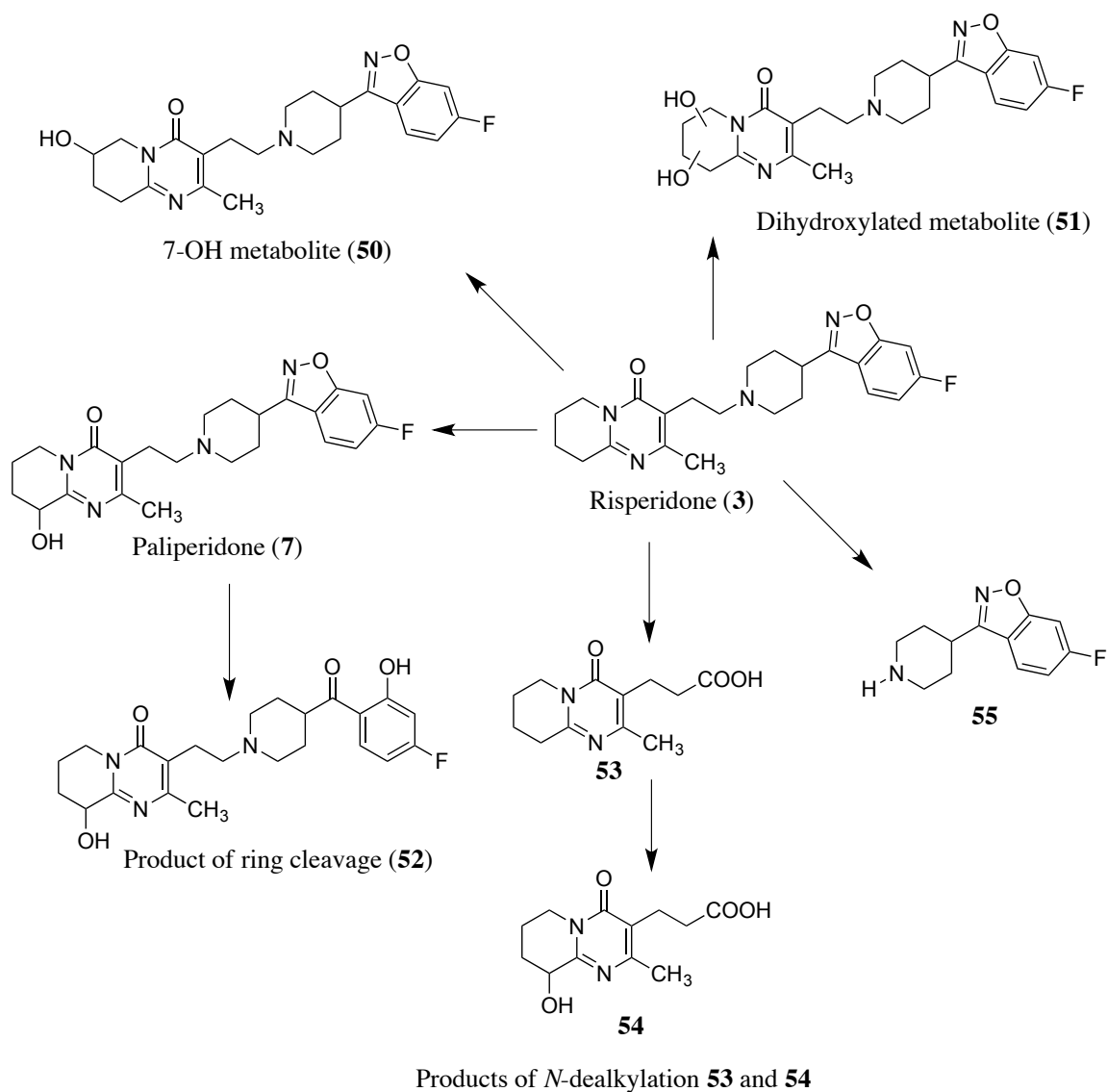


**Figure 19.** Metabolism of risperidone adapted from Mannens et al.<sup>163</sup>

Although paliperidone and risperidone differ by a hydroxyl group, they possess similar binding affinity for both 5-HT<sub>2A</sub> and D<sub>2</sub> receptors (risperidone possesses a slightly higher affinity for both receptors).<sup>45</sup> Several groups have attempted to explore the possible pharmacological and/or downstream signaling consequences of this structural difference



and have found differences at the mitochondrial, neuronal firing and synaptic plasticity level.<sup>45,165</sup> However, since the hydroxyl group could contribute in terms of additional interactions at the receptor and also change the physical and chemical properties, further studies are needed to validate the exact role of the hydroxyl group and that is a part of the current investigation.

Similar to several other GPCRs (e.g.  $\alpha_{1A}$ - and  $\beta_2$ -adrenergic and 5-HT<sub>2C</sub> receptors), 5-HT<sub>2A</sub> receptors possess constitutive activity and stimulate PIP<sub>2</sub> hydrolysis in the absence of agonist stimulation.<sup>166,167</sup> This phenomenon was shown in 5-HT<sub>2A</sub> receptors by a single amino acid mutation (C322K). Risperidone (and even paliperidone later on) was shown to inhibit the constitutively activated PIP<sub>2</sub> hydrolysis and to possess inverse agonist activity.<sup>166</sup>

The inverse agonist activity of risperidone was evident by another approach. Similar to clozapine (another atypical antipsychotic and inverse agonist at the 5-HT<sub>2A</sub> receptor), risperidone crosstalks in the 5-HT<sub>2A</sub>-mGlu<sub>2</sub> heteromer in such a way as to balance the G<sub>i</sub>-G<sub>αq</sub> signaling and possessing a high balance index (BI) [BI =  $\Delta G_i - \Delta G_q$ ].<sup>9</sup> Through the crosstalk, risperidone downregulates the unusually high G<sub>αq</sub> signaling back to basal level and maintains the balance between the G<sub>i</sub>-G<sub>q</sub> signaling, which is disrupted in schizophrenia.<sup>9</sup>

Risperidone possesses some structural features, which confer upon it a unique balance of receptor affinity and functional activity, quite different from structurally related predecessors.

The specific aims of the current investigation are:

**1. Determination of the minimal structural features responsible for the antagonist activity of risperidone/paliperidone at 5-HT<sub>2A</sub> receptors – Deconstruction of risperidone/paliperidone**

- 1a. Deconstruction of risperidone/paliperidone into smaller analogs and assessing their functional activity and binding affinity
- 1b. Investigating the role of the hydroxyl group of paliperidone

Deconstruction will involve the systematic removal of specific functional groups of risperidone to generate analogs lacking some features, which will be tested for functional activity and binding affinity by electrophysiological assays and radioligand binding studies, respectively.

**2. Investigation of the structural differences between risperidone and ketanserin and the role of the two halves of risperidone in its activity – Elaboration of risperidone**

- 2a. Examination of structural hybrids of risperidone and ketanserin
- 2b. Investigation of the role of the right half of risperidone in its functional activity

2c. Investigation of the role of the benzisoxazole ring in the functional activity and binding affinity of risperidone

2d. Investigating the role of Arien's hypothesis in the antagonist activity of risperidone

Elaboration will involve the substitution of the left and right halves of risperidone with the left and right halves of ketanserin. The potential role of the right half of risperidone in antagonist activity will be explored by making it as similar to 5-HT as possible. The analogs will be tested for binding affinity and functional activity by radioligand binding studies and electrophysiological assays, respectively.

### **3. Molecular modeling studies to understand the binding mode of risperidone and its analogs at 5-HT<sub>2A</sub> receptors**

Homology models of the 5-HT<sub>2A</sub> receptors will be constructed and the compounds will be analyzed for their binding poses and interactions with amino acids at the receptors by docking and scoring. The interactions will be validated by previous site-directed mutagenesis data and quantified by performing Hydropathic INTERaction (HINT) studies.

## CHAPTER IV: APPROACH, RESULTS AND DISCUSSION

### A. DECONSTRUCTION OF RISPERIDONE:

#### 1. Approach:

The medicinal chemistry principles of ‘deconstruction-reconstruction-elaboration’ were used to examine the structural features contributing to the antagonist activity of risperidone and paliperidone at 5-HT<sub>2A</sub> receptors.<sup>168</sup>

This approach basically helps to understand which functional groups making up the structure of a compound contribute to its activity and binding affinity. The study begins with deconstruction, which involves the systematic removal of functional groups of the parent compound, to generate analogs lacking some features. The smaller analogs lacking certain features of the parent compound are then tested for functional activity and/or binding affinity. The change in the activity and/or affinity compared to the parent compound reflects the role of the functional group that is removed.<sup>168</sup> For example, if removal of a carbonyl group leads to a 20-fold decrease in affinity, this indicates that the polar interactions that the carbonyl group is capable of making might be important for binding affinity. Similarly, if removal of a phenyl group leads to a negligible increase or decrease in activity, this suggests that the phenyl group does not contribute significantly to activity, and can be removed or replaced.

Deconstruction helps to simplify the structure to the minimum structural features responsible for activity and affinity. This is helpful in determining a pharmacophore for that particular activity.

The structure of risperidone/paliperidone was systematically deconstructed and its structural features were explored as shown in Figure 20.

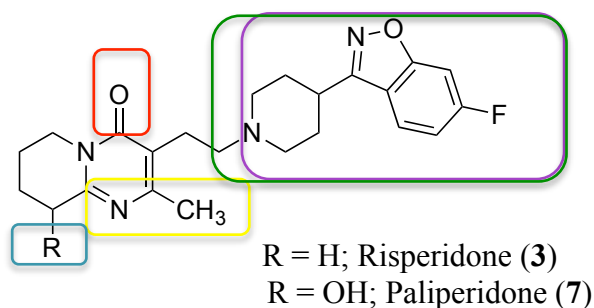


**Figure 20.** Approach to the deconstruction of risperidone/paliperidone. Circled regions represent structural features that were excised.

Risperidone can be divided into two halves: 6-fluoro-3-(4-piperidinyl)-1,2-benz[*d*]isoxazole (right half) and 2-methyl-6,7,8,9-tetrahydro-4*H*-pyrido[1,2-*a*]pyrimidin-4-one (left half) connected by an ethyl linker. The halves were explored further to determine their respective contribution towards activity and affinity (Figure 21).

Our laboratory had in the past explored the structure-activity relationships (SAR) of ketanserin (**42**) by deconstruction (tested on the frontal cortical homogenates of male Sprague-Dawley rats using [ $^3\text{H}$ ]-ketanserin).<sup>143</sup> We have used a similar approach in our

study of risperidone (Figure 20). Figure 21 shows all the deconstructed analogs of risperidone included in the present study.

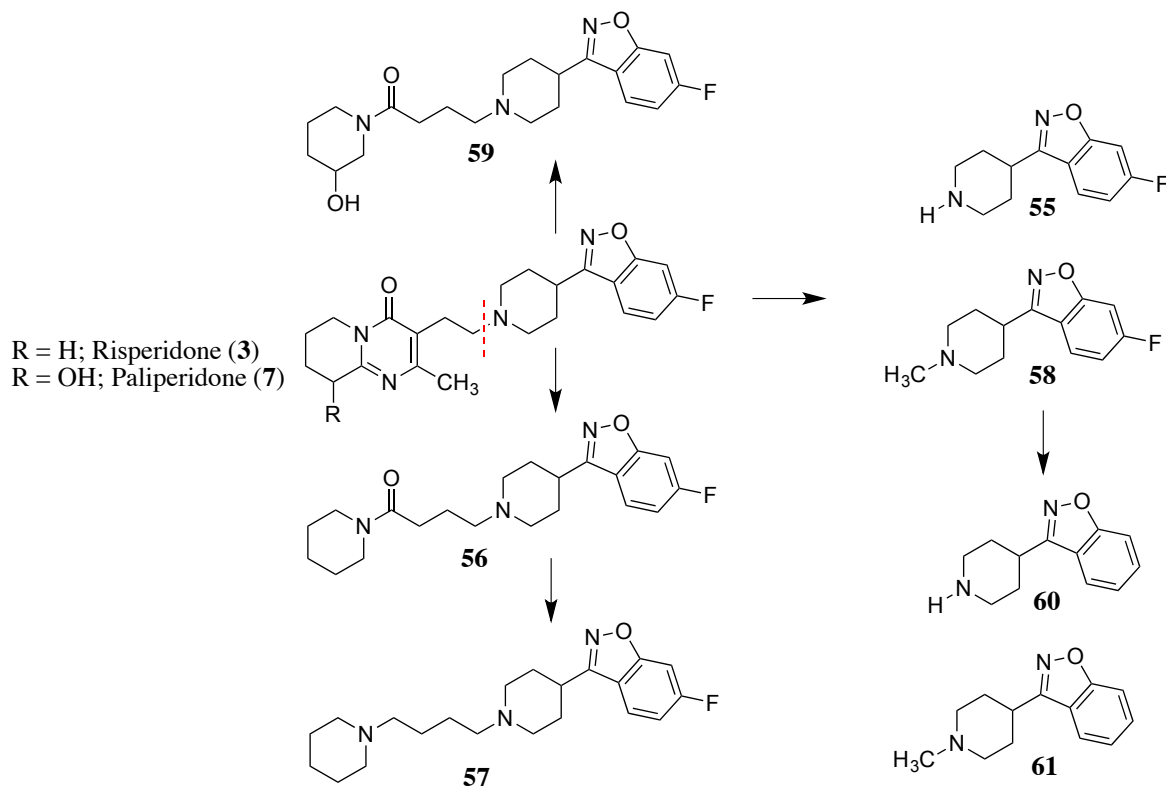


**Figure 21.** The halves of risperidone/paliperidone and the deconstructed analogs.

As a starting point for the current investigation, the 6,7,8,9-tetrahydro-4*H*-pyrido[1,2-*a*]pyrimidin-4-one ring system comprising the left half of risperidone was opened to give the tertiary amide, a compound retaining the carbonyl group, **56**. The carbonyl group of **56** was removed (reduced) to afford **57**. These analogs retain part of the hydrophobicity of the 6,7,8,9-tetrahydro-4*H*-pyrido[1,2-*a*]pyrimidin-4-one ring system. Herndon et al.<sup>143</sup> had previously reported similar modifications on the structure of ketanserin, and the analogs retained binding affinity for the receptor (Figure 22).

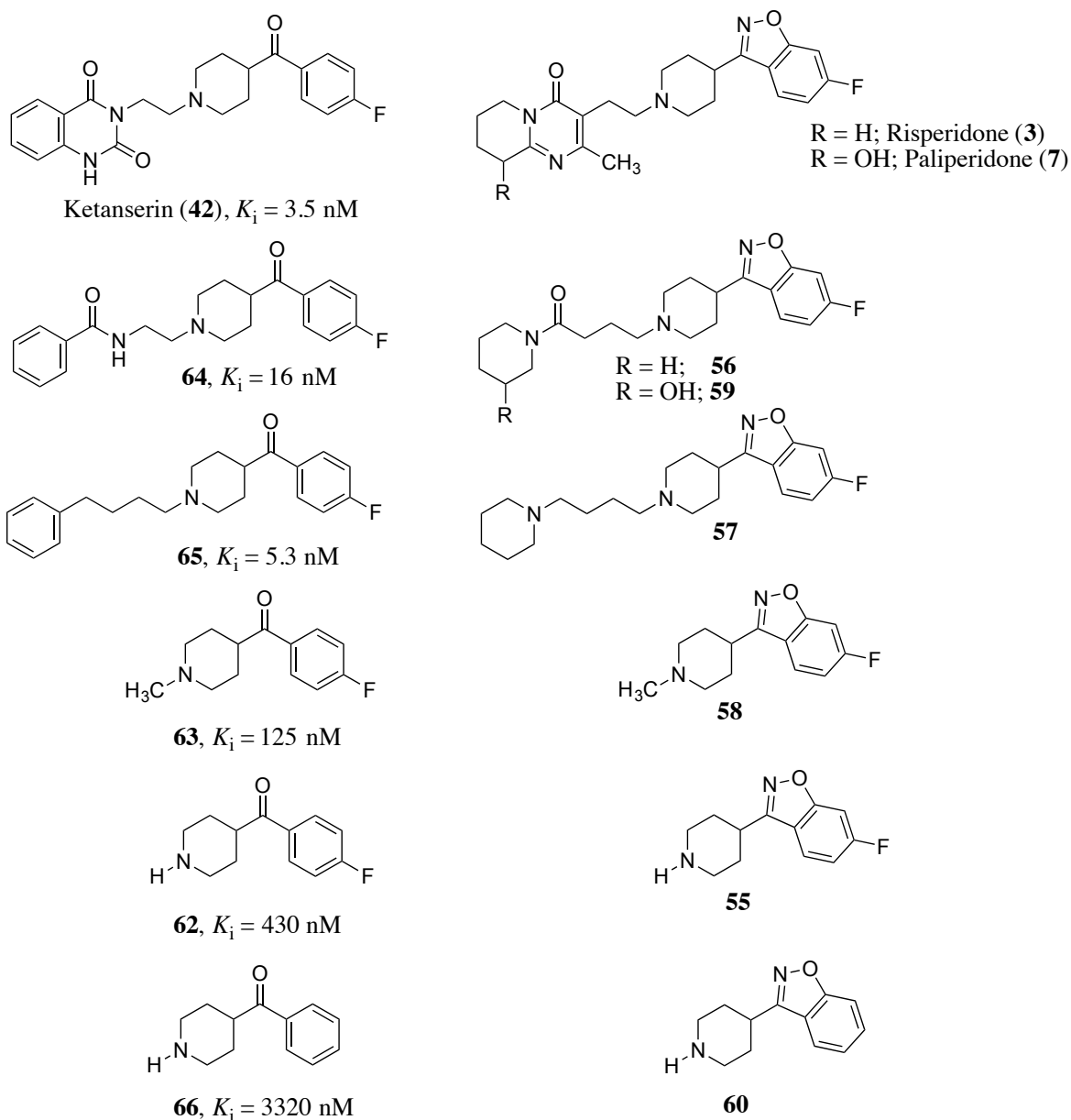


**Figure 22.** A comparison of the deconstruction of ketanserin and risperidone. Binding data are provided for ketanserin and its deconstructed analogs at 5-HT<sub>2A</sub> receptors.<sup>143</sup>

Similar deconstruction studies were also conducted with paliperidone (i.e., **59**). A comparison of the result of the two series will be informative regarding the role of the

hydroxyl group – whether it plays a role in binding affinity and/or activity, or whether it is merely tolerated.

Thereafter, the left portion of risperidone was removed to give the *N*-methyl analog **58** that retains a part of the alkyl bridge connecting the two halves of risperidone in the form of a methyl group. This methyl group was then removed to give analog **55**, which was reported previously by our laboratory.<sup>164</sup> Herndon et al.<sup>143</sup> had similarly deconstructed and tested the right half of ketanserin (**42**) (i.e., **62**) and reported that there is a dramatic loss of binding affinity (~120 fold) when compared to ketanserin (Figure 22).<sup>143</sup> Removal of the methyl group of **63** to afford the desmethyl analog **62** resulted in a ~3-fold lower binding affinity over the *N*-methyl analog **63**. (Figure 22).<sup>143</sup>

Based on the preliminary results of the functional activity of **55**, the precise role of the benzisoxazole ring system and its substituents was probed where the benzisoxazole ring was kept constant and the substituents were varied (Figure 21). Herndon et al.<sup>143</sup> had reported that the desfluoro analog (i.e., **66**) of **62** (Figure 22) displayed ~8-fold decreased affinity and more than 900-fold decreased affinity compared to ketanserin (**42**), suggesting a role of the fluoro group in binding.<sup>143</sup> Evaluation of desfluoro analogs **60** and **61** should reveal the importance of the fluoro group in the binding affinity of risperidone and its deconstructed analogs.

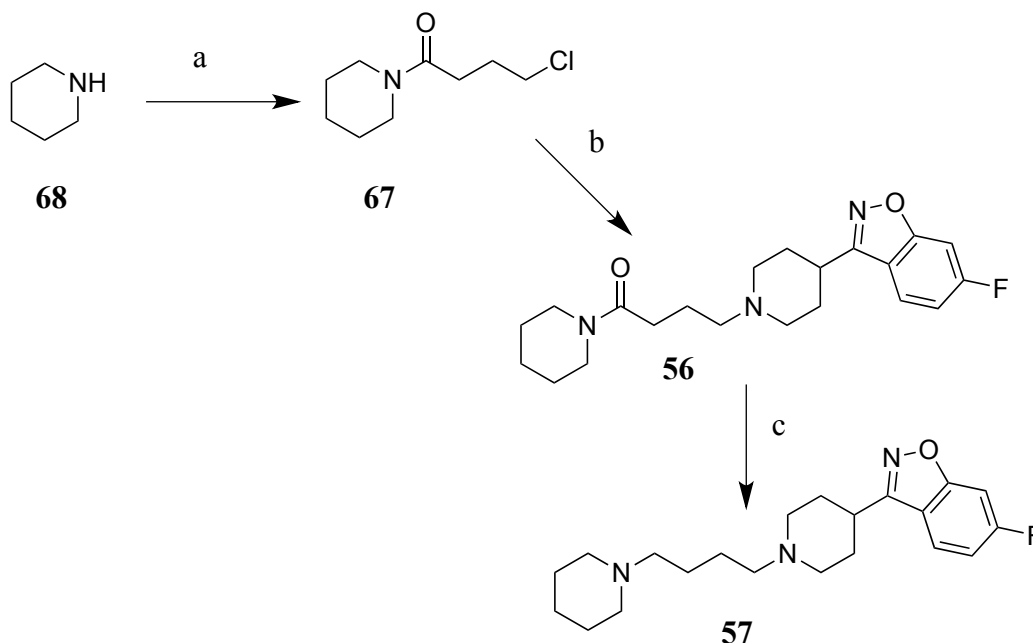


## 2. Results:

### a. Chemistry:

The synthesis of the deconstructed analogs of risperidone was carried out in collaboration with others in our laboratory. Rakesh Vekariya initially synthesized the compound without the carbonyl group **57** and the synthesis is outlined in Scheme 1. Compounds **56** and **57** were re-synthesized through a common intermediate **67**, which was synthesized by reacting freshly distilled piperidine (**68**) with the acid chloride 4-chlorobutyryl chloride (Scheme 1).<sup>169</sup> The synthesis of compound **56** was initially attempted by heating at reflux, however, the reaction did not go to completion and the yields were poor. Subsequently, a Finkelstein reaction was tried under pressure in a screw-cap vial that drove the reaction to completion and the yield was increased from 1% to 10%. The free base of **56** when subjected to reduction with  $\text{BH}_3$ -THF, followed by acidic hydrolysis, afforded **57** (Scheme 1).

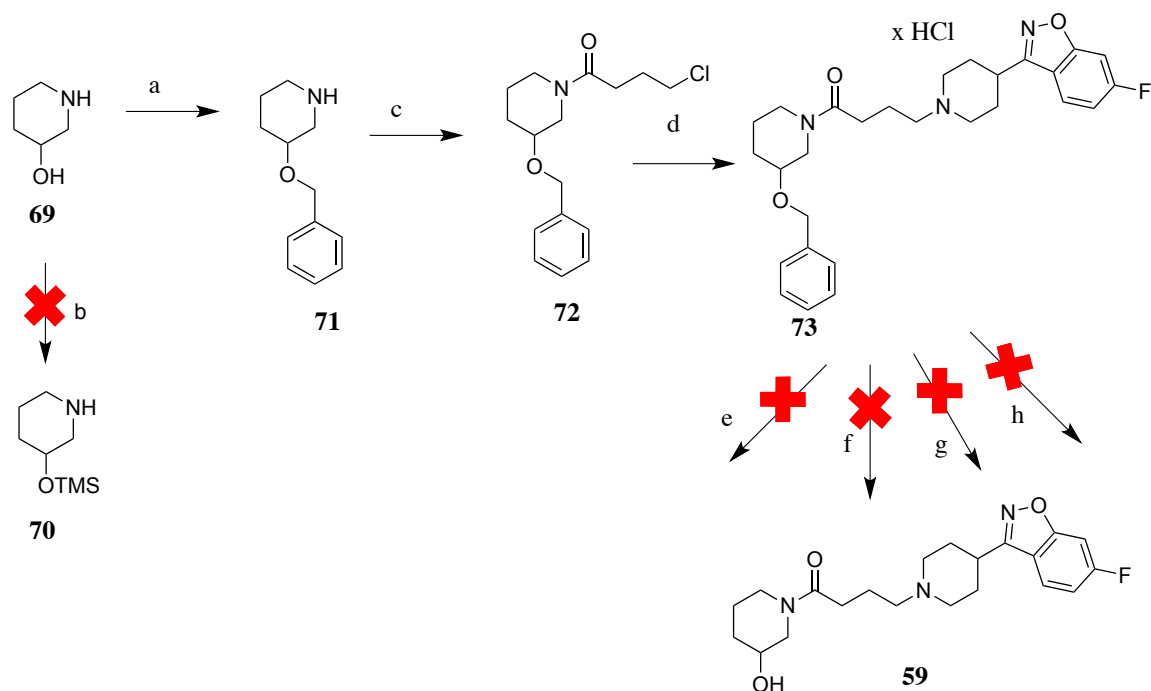
**Scheme 1.** Synthesis of compounds **56** and **57**<sup>a</sup>



<sup>a</sup>Reagent: (a) 4-Chlorobutyryl chloride,  $\text{Et}_3\text{N}$ ,  $\text{CH}_2\text{Cl}_2$ , room temperature, 75 h; (b) 6-fluoro-3-(piperidin-4-yl)benz[d]isoxazole,  $\text{K}_2\text{CO}_3$ , KI, MeCN, screw-cap vial, 88 °C, 16 h; (c) (1)  $\text{BH}_3\text{-THF}$ , THF, reflux, 2 h; (2) 6N HCl, reflux, 1 h.

The paliperidone counterpart **59** was synthesized similarly. However, the starting material, ( $\pm$ )-3-hydroxypiperidine (**69**), had a free hydroxyl group which could potentially interfere with the subsequent reactions that would be conducted at the amine group. Hence, attempts were made to protect this group using a trimethylsilyl ether (TMS), which was unsuccessful with starting material being recovered. Thereafter, the benzyl ether of ( $\pm$ )-3-hydroxypiperidine (**71**) was synthesized and the ensuing reactions gave good yields; however, subsequent efforts to remove the benzyl protecting group proved fruitless. Debenzylations with hydrogenolysis at atmospheric pressure and under pressure with various reaction conditions were attempted (Scheme 2).

**Scheme 2.** Initial attempts to synthesize compound **59**<sup>a</sup>



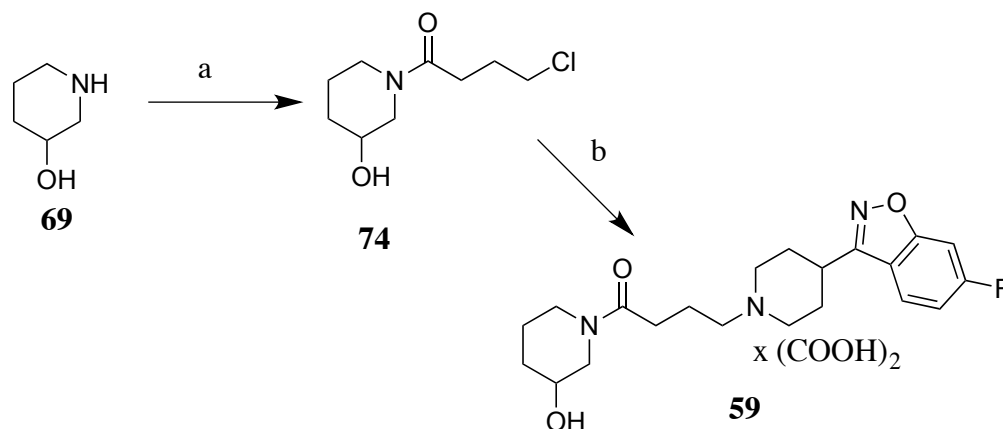
<sup>a</sup>Reagent: (a) Benzylchloride, tetraethylammonium bromide, CH<sub>2</sub>Cl<sub>2</sub>, room temperature; (b) TMSCl, imidazole, DMF, room temperature, 20 h; (c) 4-chlorobutyl chloroformate, Et<sub>3</sub>N, CH<sub>2</sub>Cl<sub>2</sub>, room temperature, 75 h; (d) 6-fluoro-3-(piperidin-4-yl)benz[d]isoxazole, K<sub>2</sub>CO<sub>3</sub>, KI, MeCN, screw-cap vial, 88 °C, 16 h; (e) HCl/EtOH, EtOH, Pd/C (5%), hydrogen balloon; (f) HCl/EtOH, EtOH, Pd/C (10%), hydrogen balloon; (g) HCl/EtOH, EtOH, Pd/C (10%), Parr hydrogenator, 15 psi; (h) HCl/EtOH, EtOH, Pd/C (10%), Parr hydrogenator, 55 psi.

A literature review provided information about the potential role of amines (a specific case of a tertiary amine was reported) in hindering *O*-debenzylation by hydrogenolysis.<sup>170</sup> Since our compound also contained a tertiary amine, it was speculated that the amine might be hampering the last step of *O*-debenzylation.

Eventually, the reaction was attempted without protecting the hydroxyl group of (±)3-hydroxypiperidine (**69**) and, although the yields were moderate (~30%), the reactions

proceeded to finally yield **59**. Compound **59** was synthesized through the intermediate **74**, (Scheme 3) and was obtained as an oxalate salt because its hydrochloride salt was hygroscopic and difficult to isolate.

**Scheme 3.** Synthesis of compound **59**<sup>a</sup>

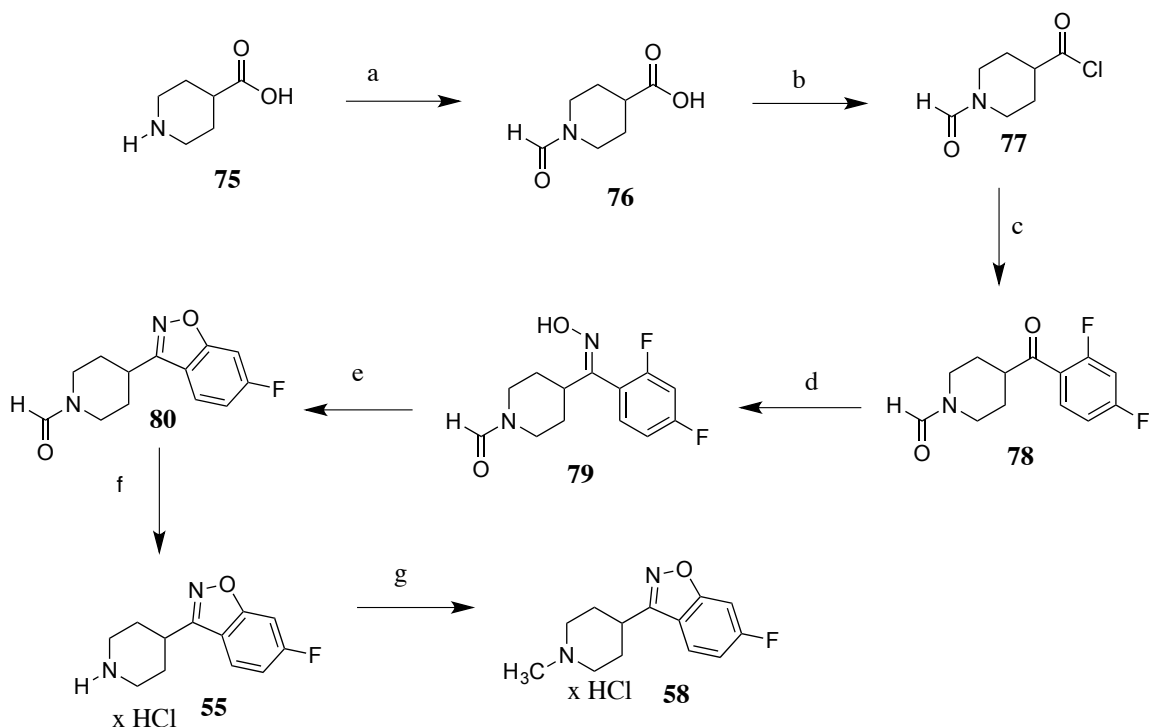


<sup>a</sup>Reagent: (a) 4-Chlorobutyryl chloride, Et<sub>3</sub>N, CH<sub>2</sub>Cl<sub>2</sub>, room temperature, 75 h; (b) (1) 6-fluoro-3-(piperidin-4-yl)benzo[*d*]isoxazole, K<sub>2</sub>CO<sub>3</sub>, KI, MeCN, screw-cap vial, 88 °C, 16 h; (2) oxalic acid, MeOH, Et<sub>2</sub>O.

The synthesis of compound **55** was reported by Strupczewski et al.,<sup>171</sup> and was replicated as outlined in Scheme 4. The amino group of isonipecotic acid (**75**) was protected by formylation. This was followed by conversion to *N*-formylisonipecotic acid chloride (**77**), which was generated *in situ* and was monitored by IR spectroscopy to denote the loss of the broad peak of the –OH group of the carboxylic acid of isonipecotic acid (**75**) at 3200 cm<sup>-1</sup>. The acid chloride was subjected to acylation by Friedel-Crafts acylation reaction with 1,3-difluorobenzene to afford **78**. This reaction was limited by the condition of AlCl<sub>3</sub>, which was used in the same equivalence as the starting materials. The reaction was highly

sensitive to moisture, and freshly sublimed  $\text{AlCl}_3$  was used for this step. The oxime **79** was synthesized for the intramolecular displacement of the 2-fluoro moiety to afford benzisoxazole **80**. TLC suggested formation of both *E* and *Z* isomers, of which only the *Z* isomer is believed to participate in the cyclization reaction. The formamide group was removed by acidic hydrolysis (Scheme 4). Compound **58** was synthesized by *N*-methylation of **55** using a Eschweiler-Clarke reaction.<sup>143</sup> The subsequent commercial availability of 6-fluoro-3-(piperidin-4-yl)benz[*d*]isoxazole (**55**) facilitated the preparation of additional product.

**Scheme 4.** Synthesis of compounds **55** and **58**<sup>a</sup>

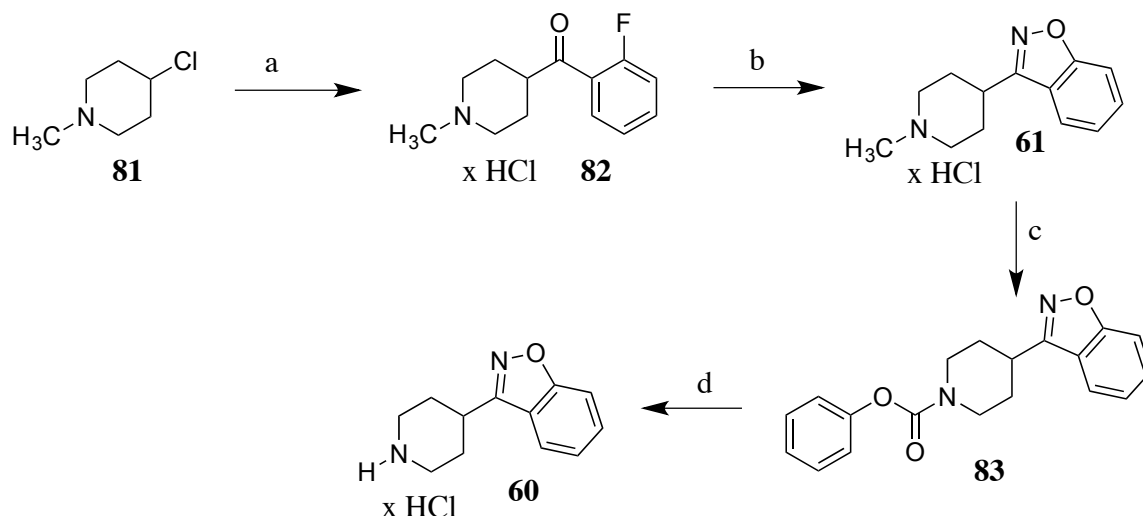


<sup>a</sup>Reagent: (a) (1) HCOOH, Ac<sub>2</sub>O, 65 °C, 1 h; (2) room temperature, 16 h; (3) vacuum distillation; (b) SOCl<sub>2</sub>, DMF, room temperature, 6 h; (c) 1,3-difluorobenzene, AlCl<sub>3</sub>, ClCH<sub>2</sub>CH<sub>2</sub>Cl, reflux, 45 h; (d) hydroxylamine hydrochloride, NaOH/H<sub>2</sub>O, EtOH, reflux, 96 h; (e) NaH (toluene washed), DMF, room temperature, 48 h; (f) (1) conc. HCl, EtOH, reflux, 3 h; (g) (1) HCOOH, HCHO, EtOH, reflux, 10 h; (2) HCl/Et<sub>2</sub>O.

The syntheses of compounds **60** and **61** followed the procedure reported by Strupczewski et al.<sup>171</sup> and are outlined in Scheme 5. Due to the unavailability of a commercial Grignard reagent, 4-chloro-*N*-methylpiperidine (**81**) was converted to a Grignard reagent *in situ* and reacted with the cyano compound 2-fluorobenzonitrile to give the acylated product **82**. This compound was cyclized by a one-pot conversion of the acylated product oxime and, which by intramolecular displacement of fluorine, afforded **61**. The *N*-methyl group was

removed by converting it to a phenyl carbamate **83**, followed by basic hydrolysis to yield **60** (Scheme 5).

**Scheme 5.** Synthesis of compounds **60** and **61**<sup>a</sup>



<sup>a</sup>Reagent: (a) (1) 4-Chloro-*N*-methylpiperidine, THF, Mg, bromoethane, reflux, 1 h; (2) room temperature, 2-fluorobenzonitrile, reflux, 3 h; (3) room temperature, 36 h; (4)  $\text{NH}_4\text{Cl}$ , 50 °C, 2 h; (5)  $\text{HCl}/\text{Et}_2\text{O}$ ; (b) (1) KOH (85%), hydroxylamine hydrochloride, ethoxyethanol, reflux, 6 h; (2)  $\text{HCl}/\text{Et}_2\text{O}$ ; (c) (1) NaOH, toluene, phenyl chloroformate, reflux, 24 h; (2) petroleum ether; (d) KOH (85%), EtOH, reflux, 48 h; (2)  $\text{HCl}/\text{Et}_2\text{O}$ .

## b. Functional activity studies:

The functional activity studies of risperidone (**3**) and compounds **55-58** were performed in Dr. Logothetis' laboratory by Jason Younkin, Amr Ellaithy, Dr. Lia Baki and Sneha Shah, and two biological assay systems were used: calcium imaging by an epifluorescence assay using the  $\text{Ca}^{2+}$  sensitive dye Fura2AM in HEK293 cells stably expressing 5-HT<sub>2A</sub> receptors, and the two-electrode voltage-clamp (TEVC) electrophysiological assay in a *Xenopus laevis* oocyte heterologous expression system.<sup>172,173</sup> Risperidone (**3**) and

preliminary studies with paliperidone (**7**) were carried out in the TEVC electrophysiological assay system.

The calcium imaging assay reflects the amount of calcium released from the endoplasmic reticulum (Figure 12) on activation of IP<sub>3</sub> receptors on the ER by IP<sub>3</sub> when the 5-HT<sub>2A</sub> receptor is stimulated. The potentiometric dye Fura2AM is sensitive to calcium and chelates the released calcium and fluoresces at two wavelengths: 340 nM and 380 nM. A ratio of the fluorescence at 340/380 nM is an indication of the concentration of calcium released. At a concentration of 100  $\mu$ M for compounds **55**, **57** and **58** and 32 mM for compound **56**, the compounds by themselves generated no calcium signal (Figure 23).



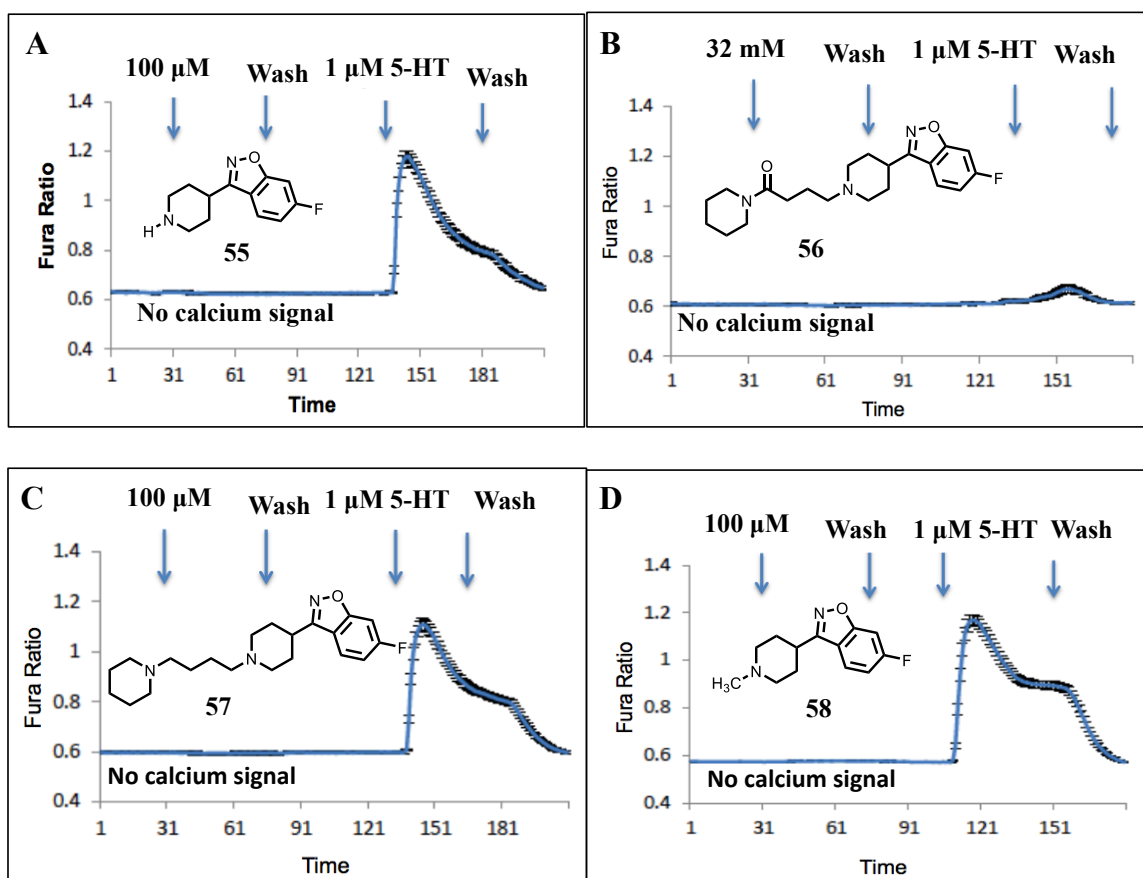


**Figure 23.** Compounds **55** (A), **56** (B), **57** (C), and **58** (D) did not generate the calcium signal indicating the intracellular release of calcium (figures provided by Dr. Lia Baki).

As seen from Figure 23, the carbonyl compound **56** was not only difficult to ‘wash-off’ from the receptor but also inhibited the agonist activity of 5-HT. Compounds **55**, **57** and **58**, on the other hand could be ‘washed off’ so that 5-HT could exert its full agonist activity at the receptor. However, when compounds **55-58** were applied in the presence of 5-HT, the compounds dose-dependently inhibited the activity of 1  $\mu$ M 5-HT. Risperidone was also included in this study. A typical dose-response curve (Figure 24) for the

compounds was generated and the half maximal inhibitory constants ( $IC_{50}$  values) for the compounds were calculated (Table 4).

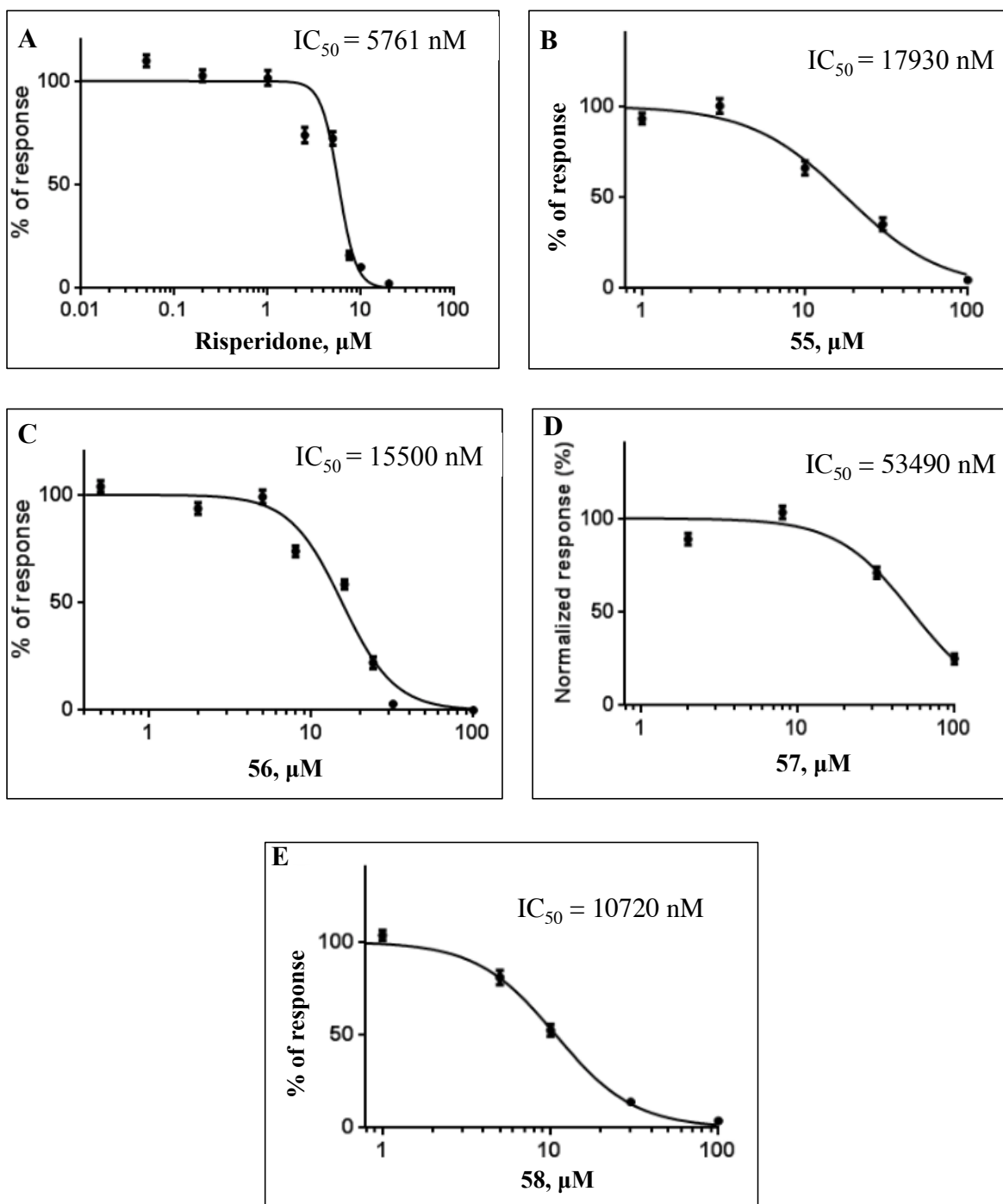


**Figure 24.** Dose-response curves for risperidone and compounds **55-58** by the calcium imaging assay. Results are from a single experiment (figures provided by Dr. Lia Baki).

The TEVC assay measures the inhibition of current from the inwardly-rectifying potassium channel GIRK4\* associated with the 5-HT<sub>2A</sub> receptor (Figure 25).<sup>172</sup> Here, the K<sup>+</sup> channel functions as a “reporter” of the ligand-mediated G<sub>αq</sub> activity. In the assay, the heterologous oocyte system co-expressing the 5-HT<sub>2A</sub> receptor and the GIRK4\* channel is perfused with a solution of high concentration of K<sup>+</sup> (HK), which sets a baseline current (sensitive to Ba<sup>2+</sup> ions). On stimulation of the receptor by the ligand, the G<sub>αq</sub> subunit activates PLC leading to the hydrolysis of PIP<sub>2</sub> and release of IP<sub>3</sub> and DAG. The activity of GIRK4\* is PIP<sub>2</sub>-dependent, and a decrease in PIP<sub>2</sub> concentration (due to its hydrolysis) leads to current inhibition through GIRK4\*. The IP<sub>3</sub>-mediated release of calcium from the ER leads to activation of chloride channels, (which is indicated by a spike at the onset of the inhibitory current due to 5-HT) and phosphorylation of GIRK4\* (Figure 25). The phosphorylation of GIRK4\*, also inhibits the potassium current, which is measured and gives an indication of G<sub>αq</sub>-mediated activity of the compound under study.<sup>174</sup>

The GTP-bound G<sub>αq</sub> subunit is then acted upon by RGS2, which is a GTPase-activating protein, converting GTP to GDP, and leading to the reassociation of G<sub>αq</sub> subunit with the βγ subunit, thereby stopping the current inhibition due to the ligand.<sup>174</sup>

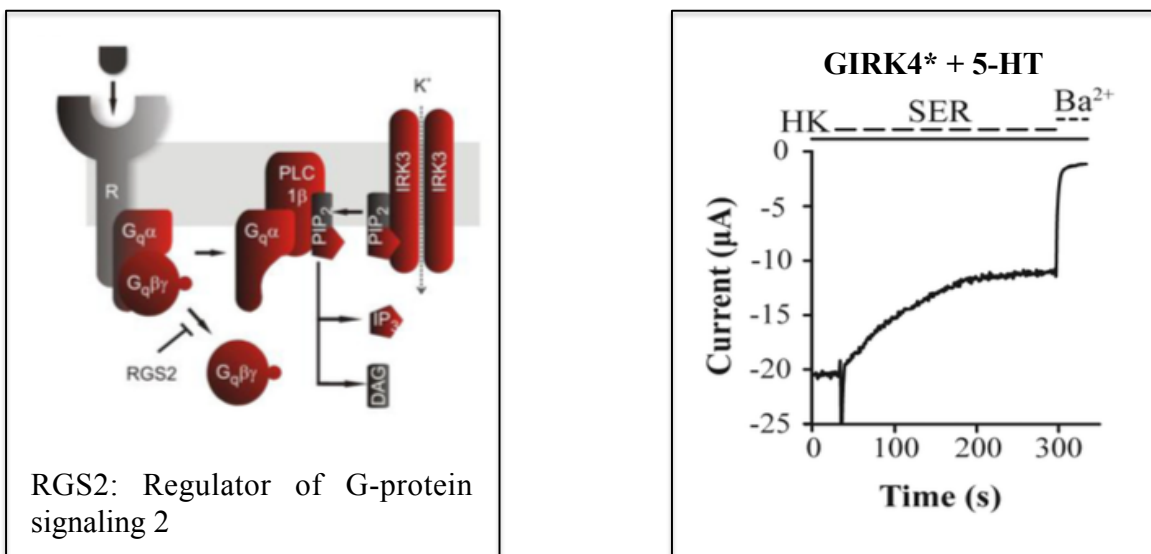


**Figure 25.** A schematic representation of the measurement of G $\alpha_q$ -mediated activity at 5-HT $_2A$  receptors by the TEVC assay.<sup>172</sup>

The TEVC assay is ~10-fold more sensitive than the calcium imaging epifluorescence assay. Preliminary studies with risperidone indicated an IC $_{50}$  value of 57 nM and in the presence of 5-HT, it brought the agonist activity of 5-HT (the normalized G $\alpha_q$  activity considered as 100%) down to ~20%. Compounds **55-58** inhibited the 5-HT-mediated G $\alpha_q$  activity with IC $_{50}$  values of 2800 nM, 199.7 nM, 16.8 nM and 101 nM, respectively (Figure 26).

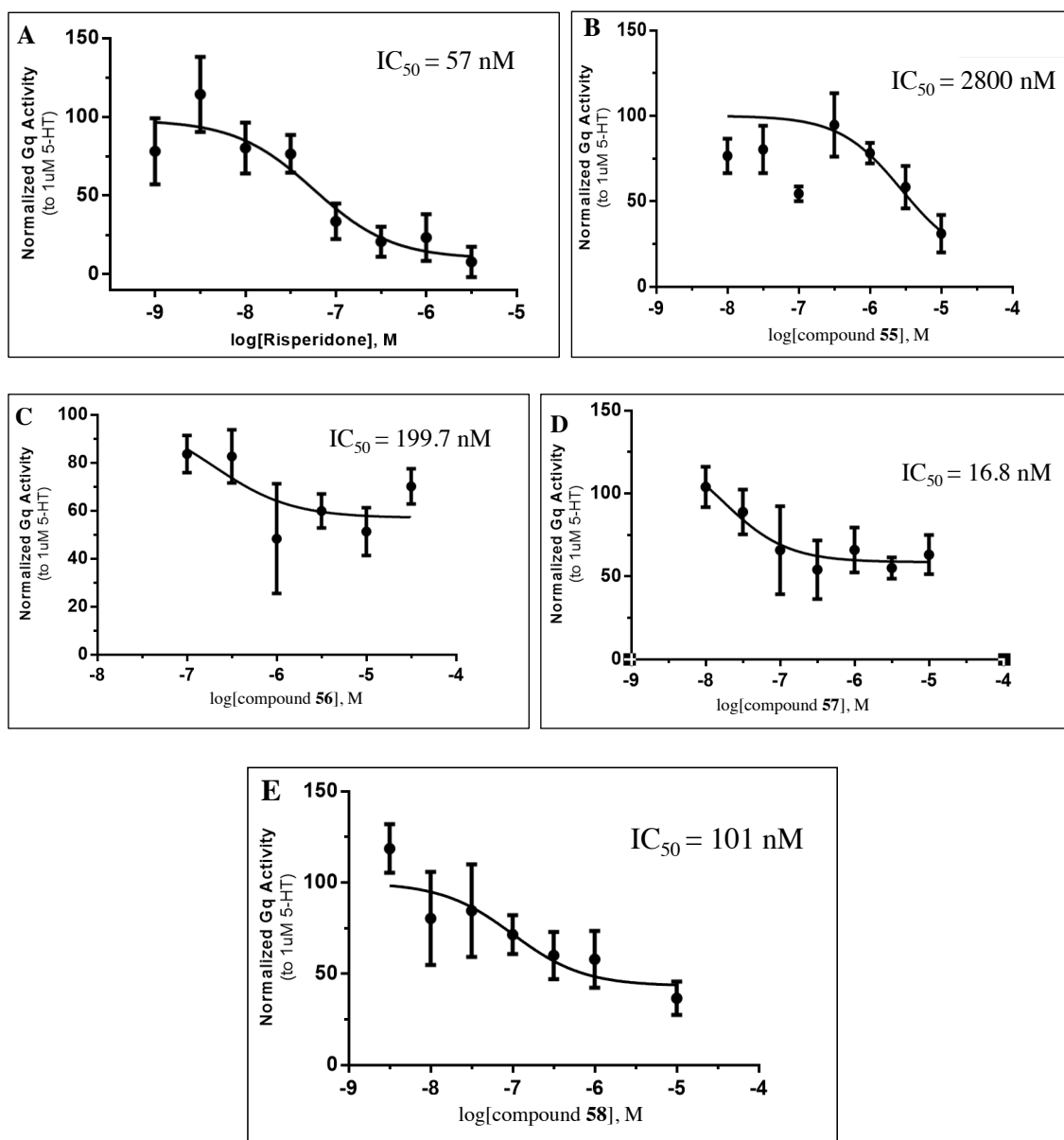


**Figure 26.** The dose-response curves for inhibitory activity exhibited by risperidone (A), compounds **55** (B), **56** (C), **57** (D), and **58** (E) (figures provided by Jason Younkin).

In the preliminary data, at a concentration of 10  $\mu$ M, compounds **55-58** demonstrated  $G_{\alpha q}$  activity by themselves (Figure 27) with about 25% (**55**), 45% (**56**), 70% (**57**) and 30% (**58**) of the activity of 5-HT (100%  $G_{\alpha q}$  activity). However, at a concentration of 50  $\mu$ M the compound lacking the carbonyl group, **57**, showed an agonist activity of ~150% (Figure 27B).

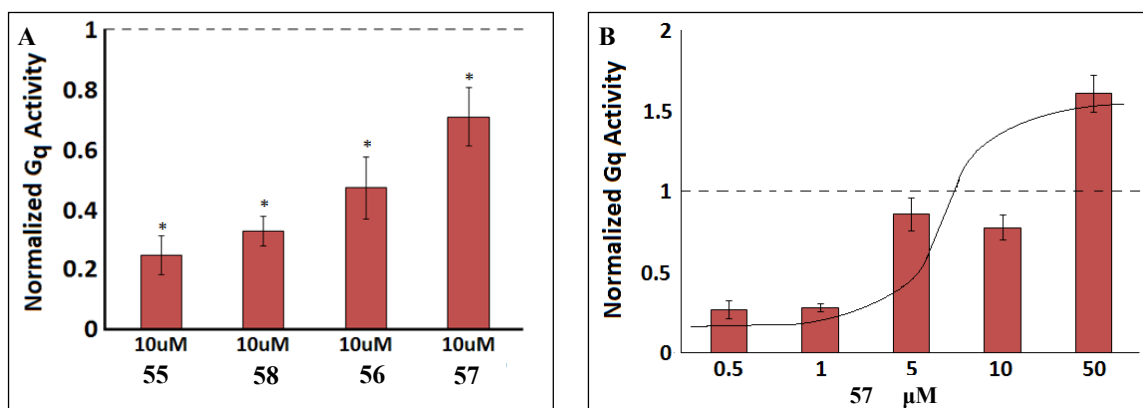


**Figure 27.** The positive efficacy of compounds **55-58** (A), and the potential 'superagonist' activity of compound **57** (B) (figures provided by Jason Younkin).

To ascertain whether the activity exhibited by the compounds is solely G-protein coupled or due to independent activity at the GIRK4\* channel, they were tested in an assay system expressing the channel alone. Compound **57** showed strong agonist activity at the channel. These studies have been continued and additional data generated (see Appendix A).

When the 5-HT<sub>2A</sub> receptor is activated by 5-HT, the release of calcium from the ER leads to an increase in the intracellular positive ion concentration. This produces an initial inward spike in the electrophysiological tracing after the application of the concentration of

5-HT under study (Figure 28). The sharp inward spike then continues upwards to show inhibition of the GIRK4\* channel current, which is measured by the assay. The intracellular calcium release simultaneously activates chloride channels (inward), producing a strong outward current (reflected as an outward spike in the electrophysiological tracing). This outward chloride spike was not observed with compounds **55-58** (data shown for **58** in Figure 28). Also, the compounds produced a rather broad inward peak instead of the sharp spike shown by the application of 1  $\mu$ M of 5-HT. This is similar to the lack of calcium signal observed with the calcium imaging assay.

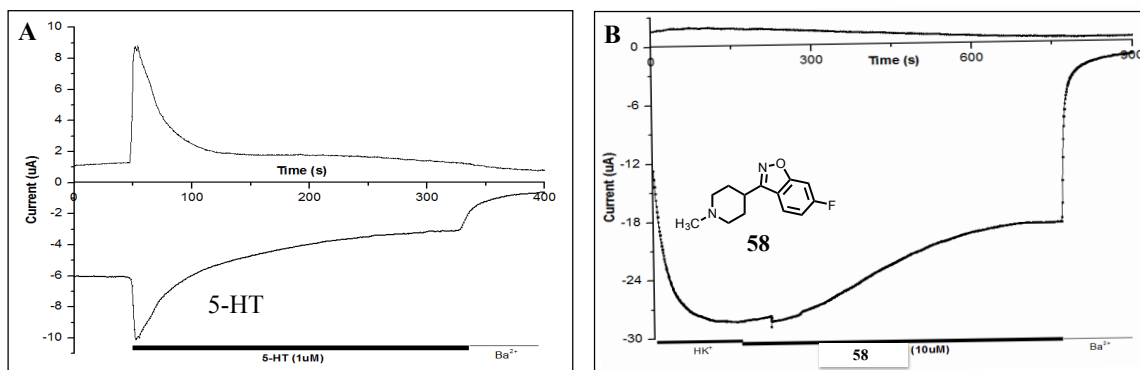


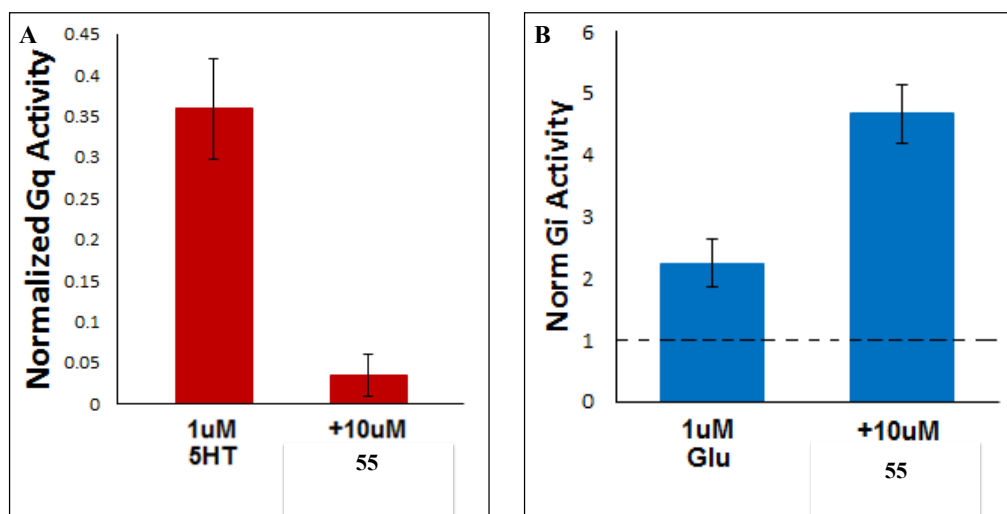
**Figure 28.** The outward current due to the inward movement of chloride ions and the inward current due to the intracellular release of calcium ions after application of 5-HT (A), and the lack of inward and outward current after the application of the compounds, represented by the *N*-methyl compound **58** (figures provided by Jason Younkin).

It was interesting to note that in the preliminary studies with paliperidone (**7**), a concentration of 5  $\mu$ M in the absence of 5-HT, led to a reversal of basal current, which is



reminiscent of inverse agonist activity. This study with paliperidone is currently under further investigation.

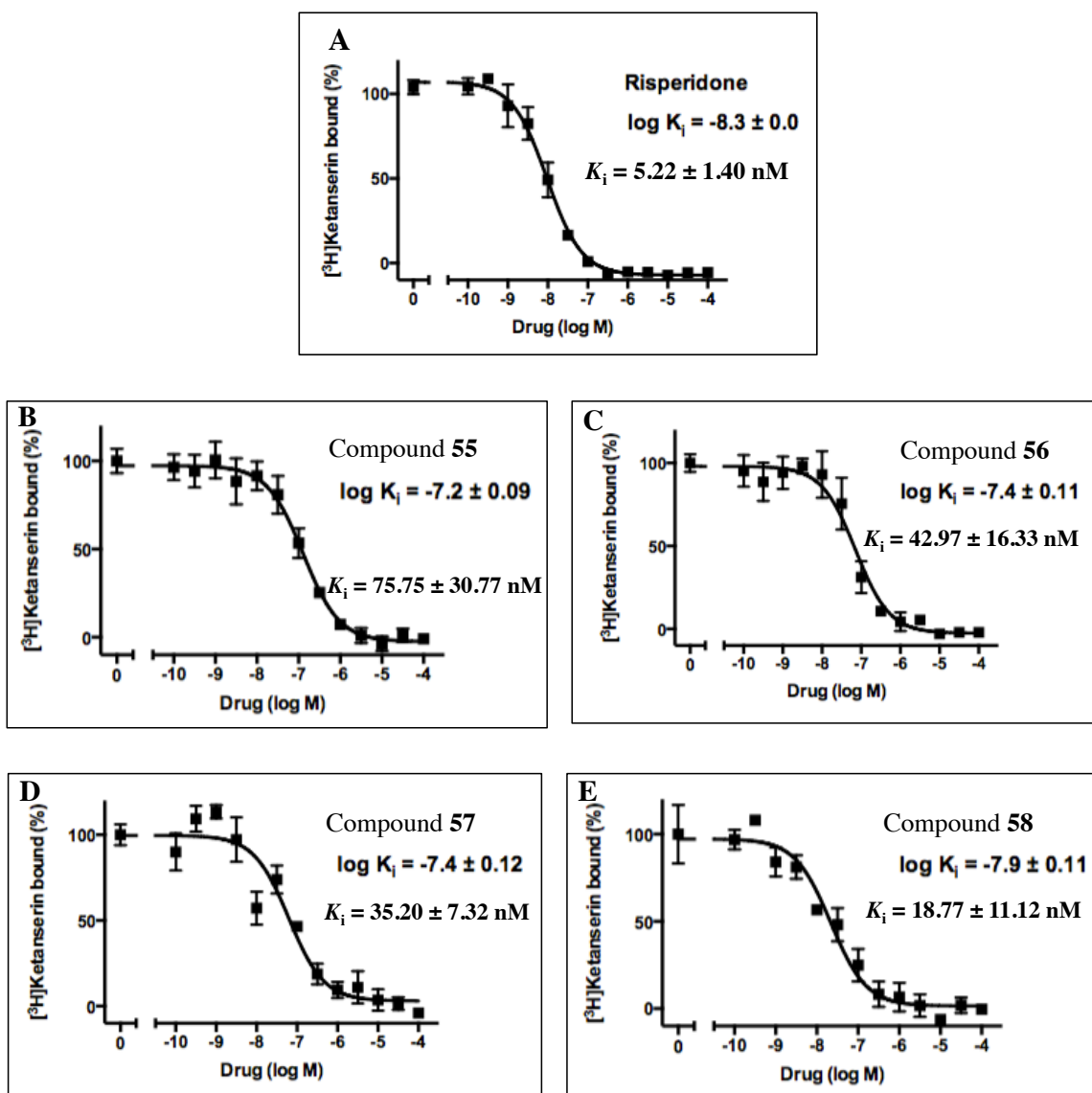
As discussed earlier, risperidone, similar to clozapine, crosstalks in the 5-HT<sub>2A</sub>-mGlu<sub>2</sub> heteromer and this is an indication of their inverse agonist activity. The crosstalk is evident from a decrease in 5-HT induced G<sub>αq</sub> activity of the 5-HT<sub>2A</sub> portion, and a simultaneous increase in glutamate-induced G<sub>i</sub> activity of the mGlu<sub>2</sub> portion of the heteromer.<sup>9</sup> Compounds **55-58** were tested in the heteromer expressed in the *Xenopus laevis* oocyte heterologous expression system, wherein the 5-HT<sub>2A</sub>-mediated G<sub>αq</sub> activity was measured by the inhibition of the GIRK3 channel and the glutamate-mediated G<sub>i</sub> activity was measured by the activation of the GIRK4\* channel. Compound **55** was able to crosstalk across the heteromer system (Figure 29), while compounds **56-58** were incapable of exerting this effect. This crosstalk effect is currently under further investigation.



**Figure 29.** The crosstalk in the 5-HT<sub>2A</sub>-mGlu<sub>2</sub> heteromer system exhibited by compound **55** (figures provided by Jason Younkin).

### c. Radioligand binding studies:

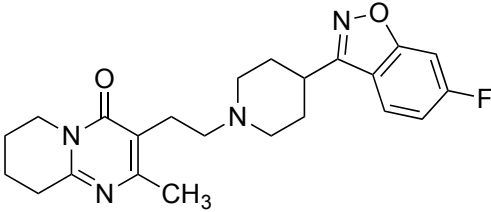
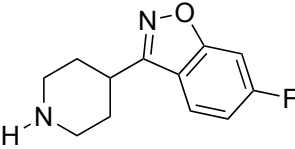
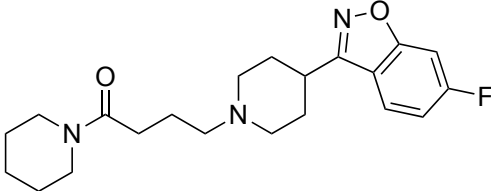
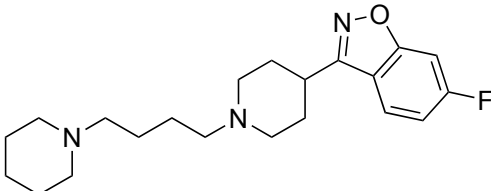
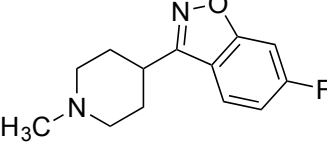
The radioligand binding assay was conducted in Dr. Javier González-Maeso's laboratory by Dr. José L. Moreno. These studies were performed in HEK293 cells expressing 5-HT<sub>2A</sub> receptors with [<sup>3</sup>H]-ketanserin ( $K_i = 2$  nM) as the radioligand. Non-specific binding was determined in the presence of 10  $\mu$ M methysergide and competition curves were generated and analyzed by nonlinear regression to derive the dissociation constants ( $K_i$  values) (Figure 30).



**Figure 30.** Radioligand binding affinity at 5-HT<sub>2A</sub> receptors expressed in HEK293 cells of risperidone (A), compounds **55-58** (B), (C), (D), (E), respectively (figures provided by Dr. José L. Moreno).

Binding affinities of risperidone and the deconstructed analogs **55-58** were determined in this assay system and resulted in  $K_i$  values of  $5.22 \pm 1.40$  and  $75.75 \pm 30.77$ ,  $42.97 \pm 16.33$ ,  $35.20 \pm 7.32$  and  $18.77 \pm 11.12$  nM, respectively (Table 4).

**Table 4.** Results from the functional and binding assays.

|   | Calcium<br>imaging<br>assay<br>(IC <sub>50</sub> , nM) | TEVC assay;<br>percent<br>reduction of<br>5-HT-induced<br>G <sub>αq</sub> activity* | Radioligand<br>binding assay,<br>K <sub>i</sub> ± SEM<br>values (nM) |
|---|--|---|--|
| <br>Risperidone ( <b>3</b> ) | 5,761  | ~20%<br>IC <sub>50</sub> = 57 nM  | 5.22 ± 1.40  |
| <br><b>55</b>                | 17,930   | ~25%<br>IC <sub>50</sub> = 2800 nM  | 75.75 ± 30.77  |
| <br><b>56</b>              | 15,500   | ~45%<br>IC <sub>50</sub> = 199.7 nM   | 42.97 ± 16.33  |
| <br><b>57</b>              | 53,490   | ~70%<br>IC <sub>50</sub> = 16.8 nM  | 35.20 ± 7.32   |
| <br><b>58</b>              | 10,720   | ~30%<br>IC <sub>50</sub> = 101 nM   | 18.77 ± 11.12  |

\*Preliminary data.

### 3. Discussion:

The calcium imaging epifluorescence assay showed that compounds **55-58** are capable of inhibiting the activity of 5-HT at the receptor. As the compounds do not produce any calcium signal (which is a reflection of activity in this assay) by themselves, it suggests antagonist activity.

The TEVC electrophysiological assay system, however, owing to its sensitivity, indicated a positive efficacy of compounds **55-58** that at the tested concentration of 10  $\mu$ M, was lower than the activity produced by 5-HT at 1  $\mu$ M. Compounds **55**, **56** and **58** inhibited the activity of 5-HT, essentially bringing it down to their respective efficacies. This is in agreement with the definition of a partial agonist, which is a ligand having positive efficacy lower than that of a full agonist, and antagonizes the activity of the full agonist by competing for the orthosteric site (the primary binding site of the endogenous ligand).<sup>175</sup>

The positive efficacy of compound **57** is considerably higher than the other compounds and at a concentration of 10  $\mu$ M, the activity of **57** when tested by itself, was close to that of 5-HT (1 $\mu$ M). At a concentration of 10  $\mu$ M, **57** inhibits the action of 5-HT to 70% (its own efficacy; Figure 27) fitting the profile of a high potency partial agonist. However, when compound **57** was tested at a concentration of 50  $\mu$ M, it produced an activity of ~150% (Figure 27), suggesting enhanced agonist activity or potential ago-allosteric activity (see Appendix A).

To examine this in greater detail, additional studies were performed. The agonist action of compound **57** could be due, in part, to its effect on the GIRK4\* channel. Indeed, when examined in cells lacking 5-HT<sub>2A</sub> receptors, **57** still produced an “agonist” effect (see Appendix A).

The action of **57** could also involve an allosteric effect. Hence, it was important to determine whether or not **57** binds at the 5-HT<sub>2A</sub> orthosteric site. Radioligand binding studies revealed that **57** binds at the orthosteric site with high affinity ( $K_i = 35$  nM) suggesting that it exerts at least part of its activity through the orthosteric binding site of the receptor.

The fact that the compound retaining the carbonyl group **56** and without the carbonyl group, **57**, show comparable binding affinity, suggests that the carbonyl group might not be essential for binding at the 5-HT<sub>2A</sub> receptors.

The high binding affinity of the *N*-methyl analog **58** (only ~3 fold lower than risperidone) suggests that the 6-fluoro-3-(1-methylpiperidin-4-yl)benz[*d*]isoxazole portion of risperidone is sufficient to maintain high binding affinity at the receptor. Similar to their ketanserin counterparts, the *N*-methyl analog **58** and the desmethyl analog **55** differ by ~4-fold in their binding affinity, suggesting additional interactions by the *N*-methyl group at the receptor.

The functional data shows that the analogs lacking certain features of risperidone have positive efficacy. As the structure of risperidone is deconstructed, the analogs **55-58** have some positive efficacy and reflect partial agonist activity (or potential superagonist activity in the case of **57**). However, when compared to the activity of risperidone (**3**), which could be due to noise and other factors, and which cannot be eliminated or accounted for at this moment, compounds **55-58** could actually be behaving as neutral antagonists (supported by the lack of the  $\text{Ca}^{2+}$  signal in both functional assays). This would be in agreement with the studies carried out by our laboratory in the past, reported by Iwamura et al. in which **55** showed antagonist activity.<sup>164</sup>

The TEVC functional assay system has shown that the smaller deconstructed analogs of risperidone, compounds **55** and **58** have a comparable inhibitory activity at 5-HT<sub>2A</sub> receptors (Table 4). The radioligand binding assay has shown that the *N*-methyl compound **58** is comparable in affinity to risperidone. These results suggest that the right half of risperidone, [(6-fluoro-(3-piperidinyl)benz[*d*]isoxazole] is important for its activity and/or affinity.

## **B. ELABORATION OF RISPERIDONE:**

### **1. Approach:**

The ‘elaboration’ approach of the medicinal chemistry principle of deconstruction-reconstruction-elaboration’ was utilized to determine the role of the two ‘halves’ of risperidone in imparting it with its inhibitory activity.

Elaboration involves replacing part of the molecule (which was thought to impart a particular effect) with new substituents. In the current investigation, the right and the left half of risperidone was replaced one at a time to investigate the role of that particular half in its activity at the receptor. Ketanserin (**42**) is a prototypical antagonist at the 5-HT<sub>2A</sub> receptor.<sup>144,158</sup> Structurally, ketanserin can also be divided into two halves (Figure 31). In fact, the right half of ketanserin, 4-(4-fluorobenzoyl)piperidine [bioisoteric with the right half of risperidone – 6-fluoro-3-(4-piperidinyl)-1,2-benz[*d*]isoxazole] is known to possess 5-HT<sub>2A</sub> receptor antagonist activity.<sup>176</sup> Our laboratory had reported in the past that the 6-fluoro-3-(4-piperidinyl)-1,2-benz[*d*]isoxazole portion of risperidone (i.e., compound **55**) possesses this antagonist activity.<sup>164</sup>



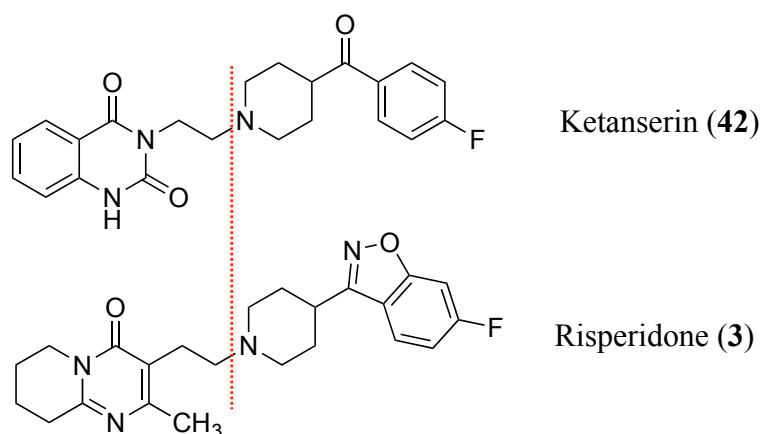


**Figure 31.** A comparison of the left and the right ‘halves’ of ketanserin and risperidone.

The present investigation aimed not only to determine what structural features of risperidone are responsible for its functional activity, but also what makes it different from ketanserin, which is structurally similar. Ketanserin and risperidone possess striking structural similarities (the right halves) and some structural differences (the left halves). We replaced the left and the right halves of risperidone and ketanserin and created two hybrid compounds **84** and **85** (Figure 32). The binding affinity and the functional activity of these structural hybrids should be informative about the effect that the structures of risperidone and ketanserin have on their functional activity and binding affinity.

The right hand portion of ketanserin (i.e., **63**) binds with >35-fold lower affinity than its parent<sup>143</sup> (Figure 22) whereas its benzisoxazole counterpart (i.e., **58**) binds only with 3-fold lower affinity than risperidone (Table 4). This suggests that the right half of risperidone contributes more towards binding affinity than the right half of ketanserin.

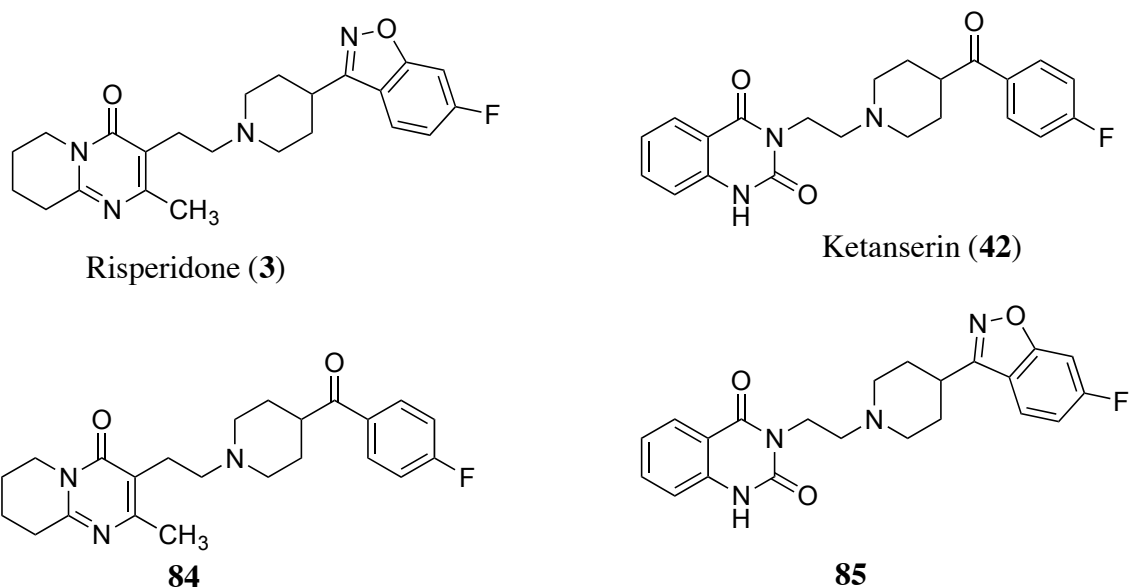


**Figure 32.** The structures of risperidone (**3**), ketanserin (**42**) and hybrids **84** and **85**.

If compound **84** loses inhibitory activity, it will tell us that the right half of risperidone is indeed playing a role in the activity. Similarly, if compound **85** is inactive, this will mean that the left half of risperidone contributes and is important for activity or the left half of ketanserin does not contribute to the antagonist activity.

As reported previously by Iwamura et al.,<sup>164</sup> the structure of the deconstructed analog of risperidone, compound **55**, is similar to that of structurally rigid tryptamines such as RU 28253 (**86**) and RU 24969 (**87**) (Figure 33) of the tetrahydropyridylindole class of compounds, which are potent 5-HT<sub>1</sub> and 5-HT<sub>2</sub> receptor agonists.<sup>164,177</sup> Yet, Iwamura et al.<sup>164</sup> reported **55** to be a potent 5-HT<sub>2A</sub> receptor antagonist. In the present investigation analogs **88** and **89**, which are structurally related to RU 28253 (**86**) and RU 24969 (**87**) but

still have the 6-fluoro group reminiscent of **55** (Figure 33), were synthesized to examine their binding affinity and functional activity at 5-HT<sub>2A</sub> receptors. The results should reveal the role of the benzisoxazole ring in maintaining binding affinity and activity at the 5-HT<sub>2A</sub> receptor. As discussed earlier, the role of the ring substituents (fluoro group) of compound **55** was probed by synthesizing analogs lacking the fluoro group (i.e., **60** and **61**). Similarly, in the present study, the role of the substituents was probed further by replacing the 6-fluoro group with a 5-methoxy group (i.e. **90**). Compound **90** is similar to RU 28253 (**86**) and RU 24969 (**87**), which are known to be agonists at 5-HT receptors. If compound **90** is an antagonist, it would suggest that the benzisoxazole ring system might play a role in converting an agonist (RU 24969) to an antagonist.

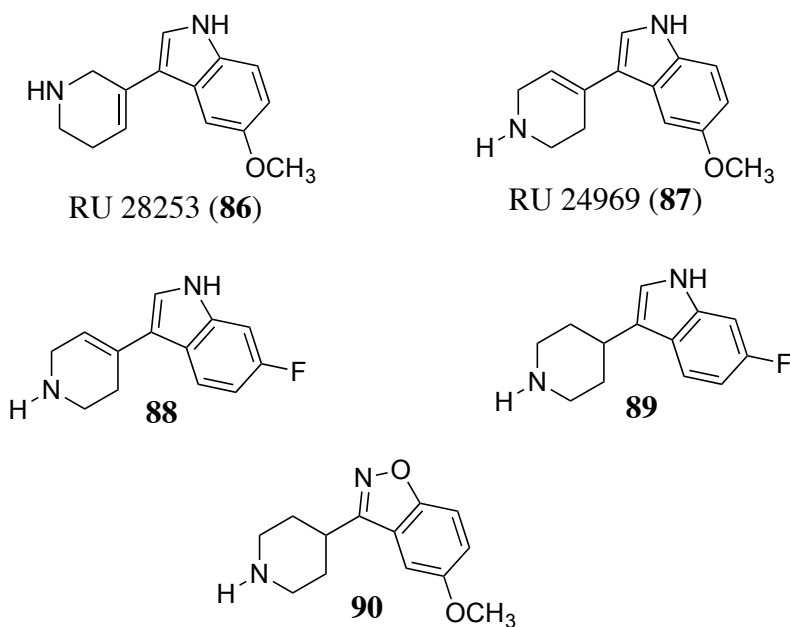


**Figure 33.** Comparison of the benzisoxazole ring with tetrahydropyridylindole ring.<sup>164,177</sup>

We replaced the right half of risperidone with one of the constrained tryptamines from our study to give compound **91** (Figure 34). The purpose of this replacement is dual. First, we will be investigating the role of the right half of risperidone by replacing it with another group. Second, by replacing the benzisoxazole ring with an indole ring, we are making the right half of risperidone more like 5-HT and other agonists at 5-HT receptors. If compound **91** retains antagonist activity it will support the Ariens hypothesis of conversion of agonists to antagonists on addition of bulky substituents on amines. However, if **91** does not exhibit antagonist activity, it could mean that either the left half of risperidone is not contributing to its antagonist activity, or the right half of risperidone is important for the activity.

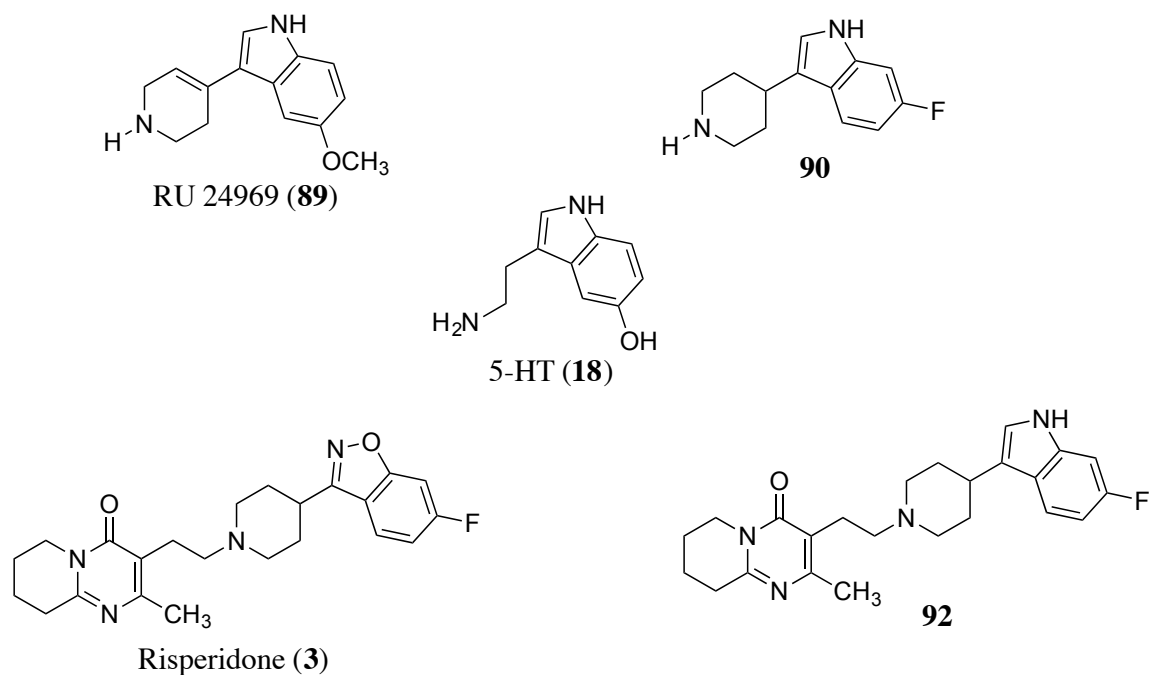


**Figure 34.** Elaboration of risperidone with constrained tryptamine analogs.

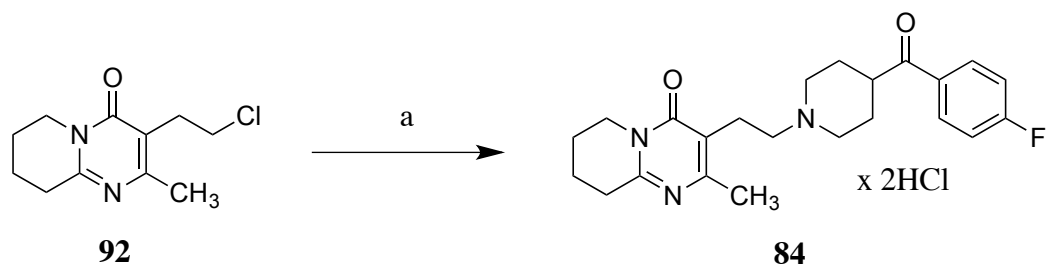
## 2. Results:

### a. Chemistry

The synthesis of the elaborated analogs of risperidone was carried out in collaboration with Urjita Shah from our laboratory, who synthesized compound **84**, the synthesis of which is outlined in Scheme 6.

Compound **84** was synthesized by a Finkelstein reaction between the heterocyclic alkyl chloride **92** with 4-fluorobenzoylpiperidine hydrochloride in the presence of 2 equivalents of  $K_2CO_3$ , because the amine is present as its hydrochloride salt, and KI as the catalyst. The solvent, acetonitrile (MeCN), was utilized because with *N,N*-dimethylformamide (DMF), the yields were poor. Also, the literature suggests that for reactions with compound **92**, solvents such as MeCN, *i*-PrOH and isobutanol work better than DMF.<sup>178</sup>

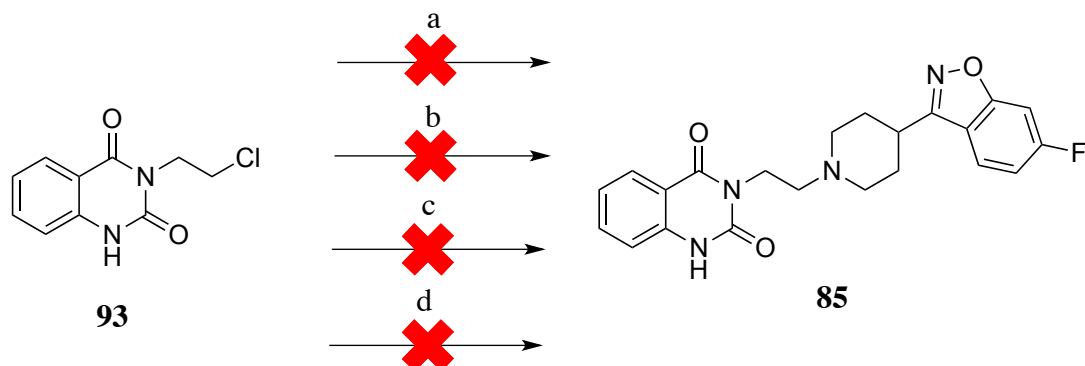
**Scheme 6.** Synthesis of compound **84**<sup>a</sup>



<sup>a</sup>Reagent: (a) 4-(4-fluorobenzoyl)piperidine hydrochloride, K<sub>2</sub>CO<sub>3</sub>, KI, MeCN, reflux, 16 h.

Multiple synthetic routes were attempted for the synthesis of compound **85**, and with different reaction conditions for a particular synthetic route (Scheme 7). The ketanserin-left half counterpart of the heterocyclic alkyl halide **93** was initially reacted with *N,N*-diisopropylethylamine (DIEA) or Hünig's base in the presence of MeCN. The reaction did not go to completion and neither the product, nor the starting material, could be isolated.

**Scheme 7.** Initial attempts to synthesize compound **85**<sup>a</sup>



<sup>a</sup>Reagent: (a) (1) 6-Fluoro-3-(piperidin-4-yl)benz[*d*]isoxazole, *N,N*-diisopropylethylamine (DIEA), MeCN, room temperature, 23 h (2) 50 °C, 2h (3) reflux, 18 h; (b) 6-fluoro-3-(piperidin-4-yl)benz[*d*]isoxazole, K<sub>2</sub>CO<sub>3</sub>, KI, DMF, reflux, 18 h; (c) 6-fluoro-3-(piperidin-4-yl)benz[*d*]isoxazole, K<sub>2</sub>CO<sub>3</sub>, KI, MeCN, 16 h; (d) 6-fluoro-3-(piperidin-4-yl)benz[*d*]isoxazole, screw-cap vial, 88 °C, 16 h.

Next, based on the procedure for similar analogs reported by our laboratory in the past,<sup>143</sup> a Finkelstein reaction was attempted, initially in the presence of DMF, which had a tendency of giving multiple products from which the desired product was difficult to isolate. Then MeCN was used as a solvent, however, it produced the same results as with DMF. Another method was reported by Herndon et al.,<sup>143</sup> which involved heating in a screw-cap vial (sealed tube) in the presence of toluene. However, since no base was added, the reaction did not go to completion.

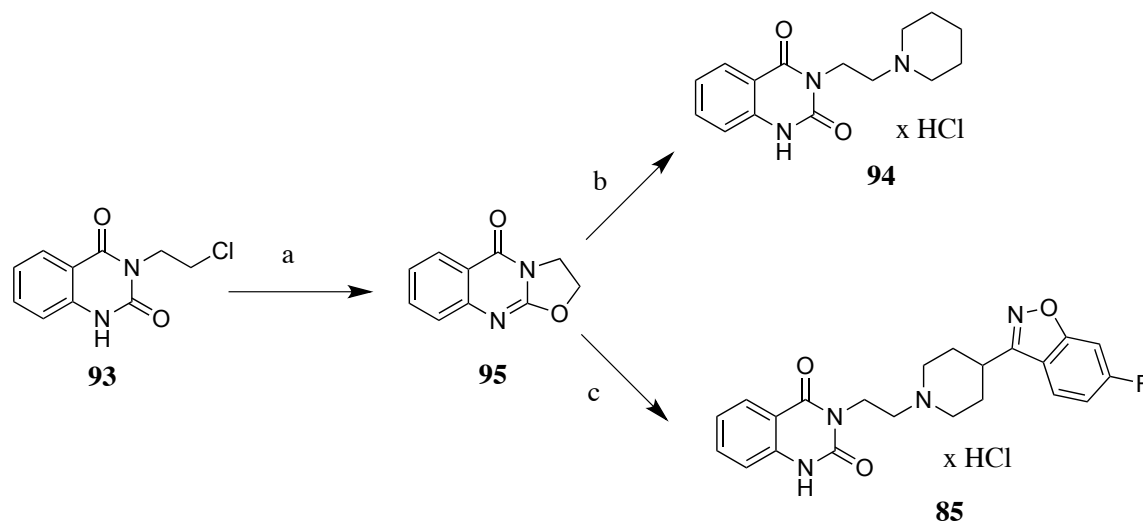
Model reactions were conducted for the structurally similar compound **94**, the starting materials for which were more economical. A series of similar reactions outlined in Scheme 7 were attempted for the synthesis of **94**, which brought us to the conclusion that

perhaps it was the synthetic routes and not the technique that was the undoing. Compound **94** was synthesized by yet another general procedure reported by Herndon et al.<sup>143</sup> and outlined in Scheme 8, which successfully resulted in compound **94**. The reaction seemed to work better with the tricyclic compound **95**.<sup>179</sup> Nucleophilic attack of the amine seemed to occur best on the oxazoloquinazoline **95** with a minimum amount of solvent and when done neat.

Thereafter, compound **85** was synthesized under high-pressure in a screw-cap vial (Scheme 8), which gave better yields. It was difficult to dissolve the free base of **85** in an appropriate solvent for the preparation of its hydrochloride salt. A number of solvents such as EtOH, MeOH, MeCN, CHCl<sub>3</sub>, CH<sub>2</sub>Cl<sub>2</sub> and ethyl acetate (EtOAc) were attempted. Finally, the free base was treated directly with conc. HCl to form the hydrochloride salt.



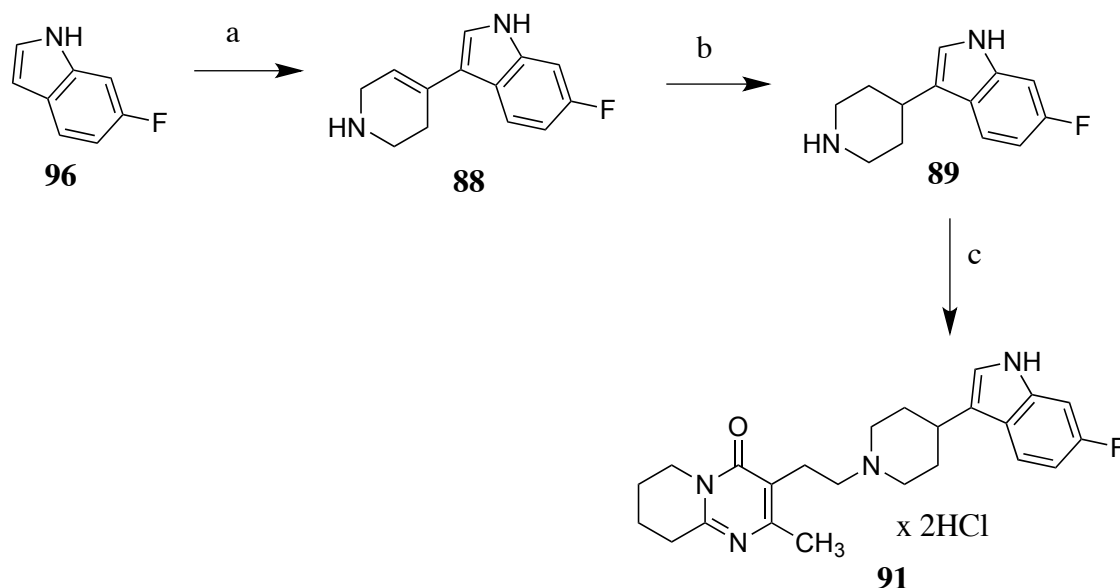
**Scheme 8.** Synthesis of compounds **85** and **94**<sup>a</sup>



<sup>a</sup>Reagent: (a) K<sub>2</sub>CO<sub>3</sub>, acetone, reflux, 2 h; (b) piperidine, screw-cap vial, 98 °C, 4 h; (c) 6-fluoro-3-(piperidin-4-yl)benz[d]isoxazole, toluene, screw-cap vial, 100 °C, 44 h.

Compounds **88** and **89** were synthesized from 6-fluoroindole (**96**) and compound **89** was synthesized from **88** by reduction of the double bond by hydrogenation with Pd/C (10%) under pressure and was submitted as a free base (Scheme 9). Compound **91** was synthesized from compounds **89** and **92**, and is outlined in Scheme 9. After the optimization of the solvent, MeCN, for the Finkelstein reaction for compound **84**, compound **91** was also synthesized by refluxing in MeCN. The yield, 9%, as for other Finkelstein reactions in this study, was low.

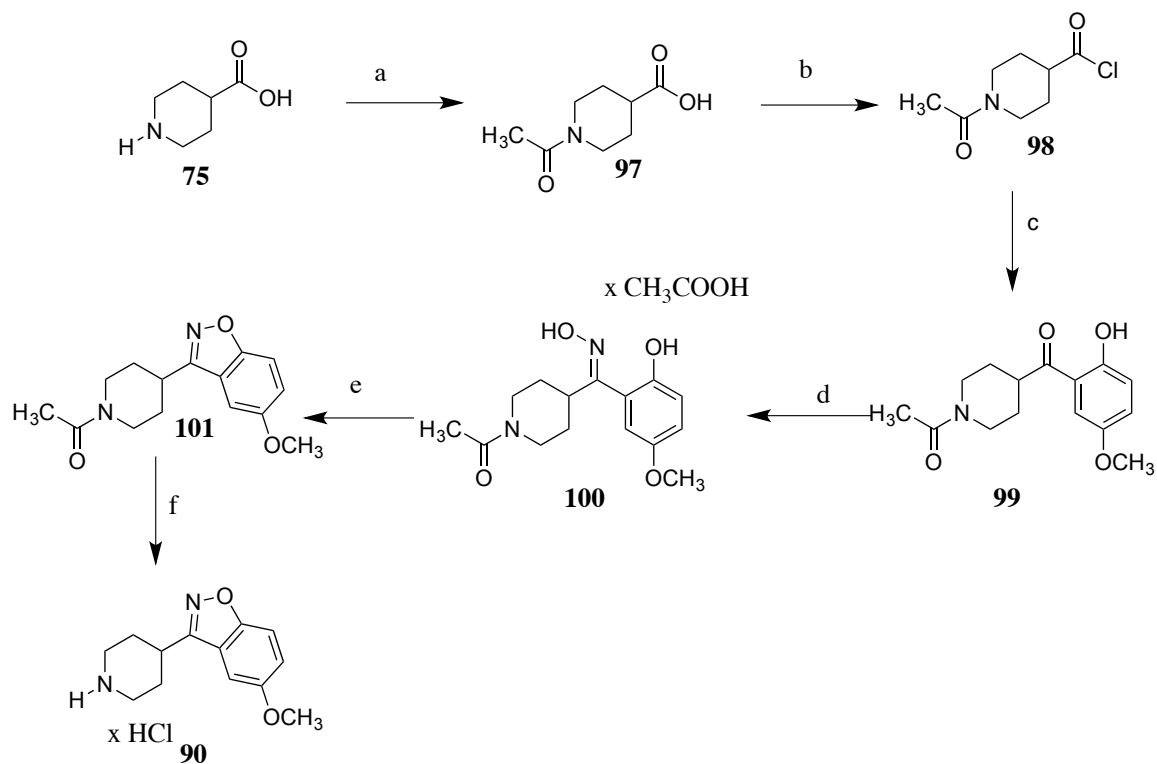
**Scheme 9.** Synthesis of compounds **88**, **89** and **91**<sup>a</sup>



<sup>a</sup>Reagent: (a) 4-piperidone monohydrate hydrochloride, KOH, MeOH, reflux, 5 h; (b) (1) HCl/EtOH, MeOH, Pd/C (10%), Parr hydrogenator, 43 psi; (2) NaOH; (c) (1) compound **92**, MeCN, reflux, 45 h; (2) HCl/Et<sub>2</sub>O.

A synthetic route for compound **90** has been reported<sup>171</sup> and it was synthesized in a manner similar to that of **55**, with the exception that the amino group of isonipecotic acid (**75**) was protected by converting it to the acetamide **97** (Scheme 10). Demethylation of a methoxy group in the Friedel-Crafts product **99** was due to excessive AlCl<sub>3</sub> and dichloroethane (ClCH<sub>2</sub>CH<sub>2</sub>Cl). The oxime was converted to its acetate salt **100** and then reacted further with NaH to give the cyclized product **101**. It has been suggested that the phenolic hydroxyl group of **100** effects a nucleophilic displacement reaction on the nitrogen of the oxime and the acetate salt makes the nitrogen of the oxime more conducive to this displacement reaction.<sup>171</sup> The acetamide-protecting group was eventually removed by acidic hydrolysis. The synthesis is outlined in Scheme 10.

**Scheme 10.** Synthesis of compound **90**<sup>a</sup>



<sup>a</sup>Reagent: (1)  $\text{Ac}_2\text{O}$ ,  $\text{EtOAc}$ ,  $60\text{ }^\circ\text{C}$ , 2 h; (2) room temperature, 24 h; (b)  $\text{SOCl}_2$ ,  $\text{CH}_2\text{Cl}_2$ , room temperature, 1.5 h; (c) 1,4-dimethoxybenzene,  $\text{AlCl}_3$ ,  $\text{ClCH}_2\text{CH}_2\text{Cl}$ , reflux, 20 h; (d) (1) hydroxylamine hydrochloride,  $\text{NH}_4\text{OAc}$ ,  $\text{EtOH}$ , reflux, 16 h; (2)  $\text{Ac}_2\text{O}$ , 2 h,  $60\text{ }^\circ\text{C}$ ; (e)  $\text{NaH}$  (toluene washed),  $\text{DMF}$ , room temperature, 48 h; (f) (1) conc.  $\text{HCl}$ ,  $\text{EtOH}$ , reflux, 3 h.

**b. Functional activity studies:**

The functional activity assays of risperidone (**3**), ketanserin (**42**) and the hybrid compounds **84** and **85** were performed in Dr. Logothetis' laboratory by Jason Younkin and Amr Ellaithy, and were tested in the TEVC electrophysiological assay in the *Xenopus laevis* oocyte heterologous expression system. As discussed earlier, the TEVC assay measures the current at the GIRK4\* channel associated with the 5-HT<sub>2A</sub> receptor (Figure 25).

In the preliminary studies, at a dose of 10  $\mu$ M, risperidone (**3**), ketanserin (**42**) and compound **84** antagonized the activity of 1  $\mu$ M 5-HT and brought the G<sub>αq</sub>-mediated activity of 5-HT down to about 20%, 15% and 21%, respectively. Paliperidone (10  $\mu$ M) was also tested in the same assay system and it had an activity similar to risperidone by bringing the activity of 5-HT (1  $\mu$ M) down to 20%. However, compound **85** had relatively little effect on the activity of 5-HT (Figure 35).

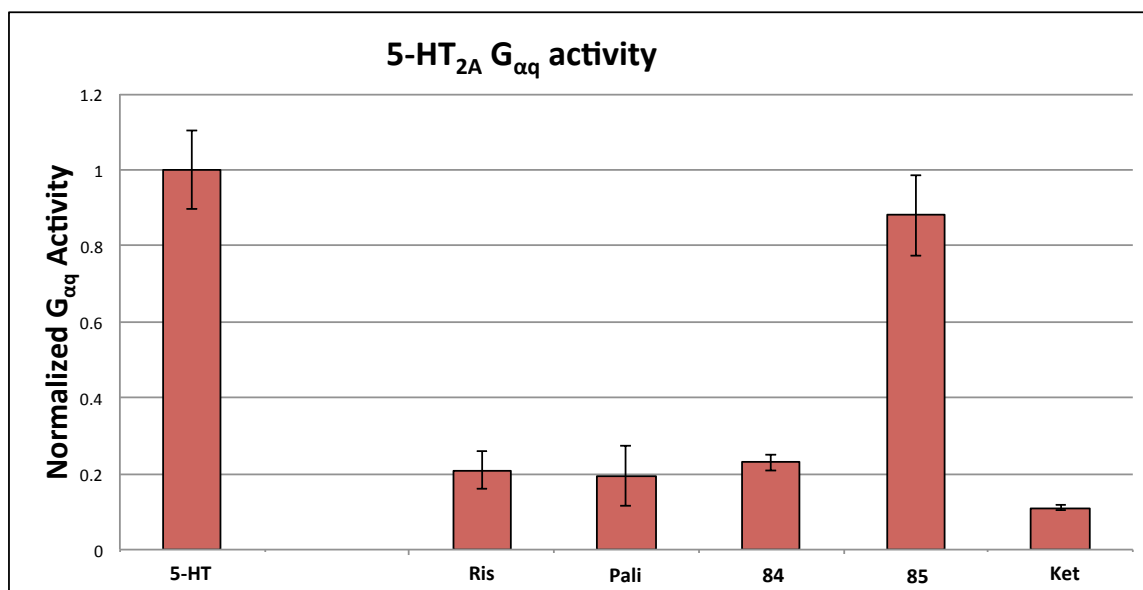


**Figure 35.** The activity of risperidone, paliperidone, compounds **84** and **85**, and ketanserin in the presence of 5-HT (figures provided by Jason Younkin and Amr Ellaithy).

Compound **85** was thereafter tested by itself (in the absence of 5-HT) for G<sub>αq</sub>-mediated activity and in the very preliminary studies showed an activity of around 20% compared to the activity of 5-HT (100%) (Figure 36).

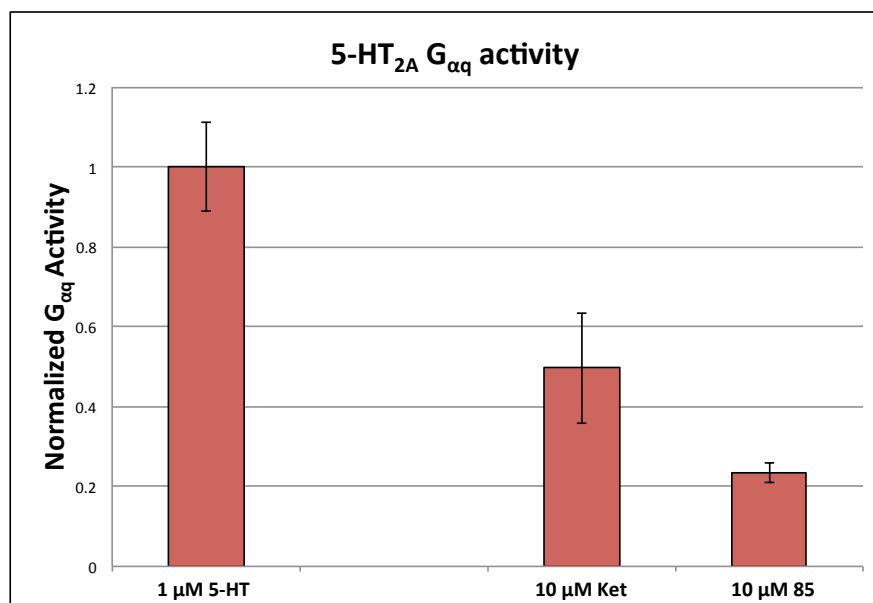


**Figure 36.** The positive efficacy shown by ketanserin and compound **85** (figures provided by Jason Younkin and Amr Ellaithy).

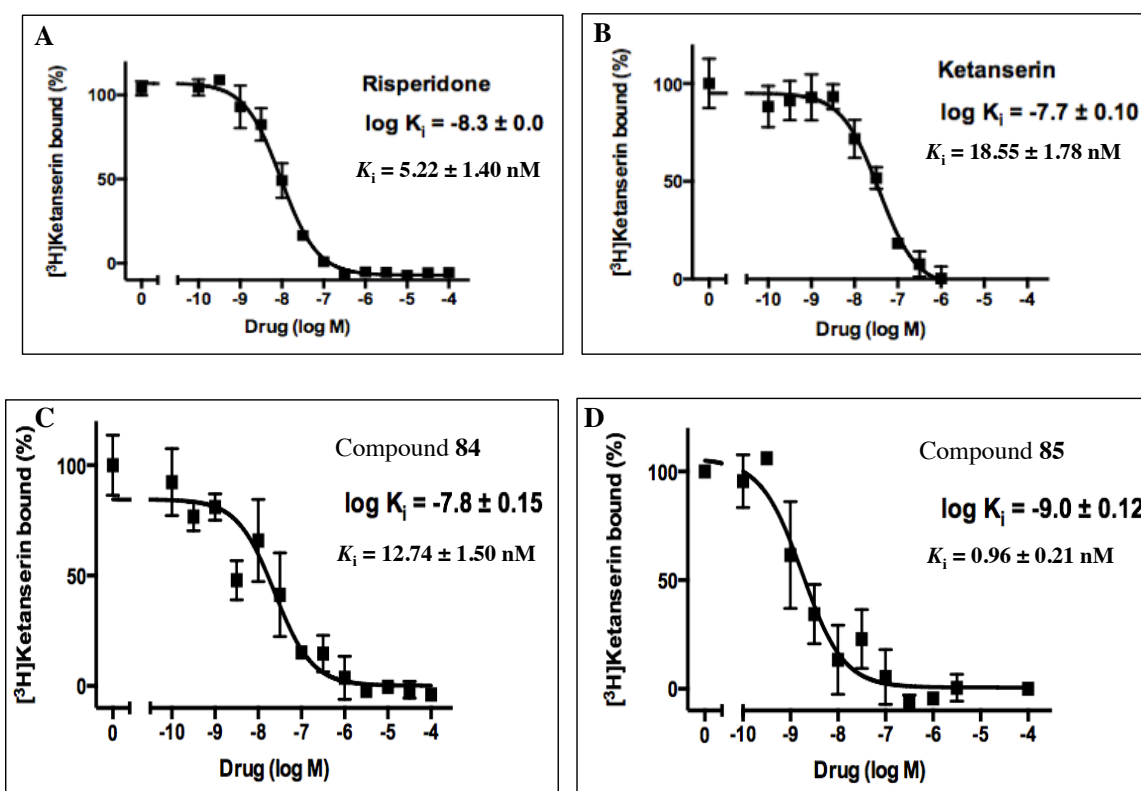
However, ketanserin, which is an established antagonist at 5-HT<sub>2A</sub> was shown to have a positive efficacy of 45% (Figure 36). This positive efficacy, as discussed previously for risperidone and its deconstructed analogs, could be due to the activity of the compound at the GIRK4\* channel independent of the  $G_{\alpha q}$ -mediated activity. This is under further investigation.

### **c. Radioligand binding studies:**

The radioligand binding assay was conducted in Dr. Javier González-Maeso's laboratory by Dr. José L. Moreno. As discussed earlier, these studies were performed in HEK293 cells with [<sup>3</sup>H]-ketanserin (2 nM) as the radioligand. Non-specific binding was determined

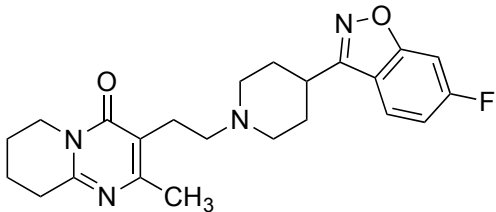
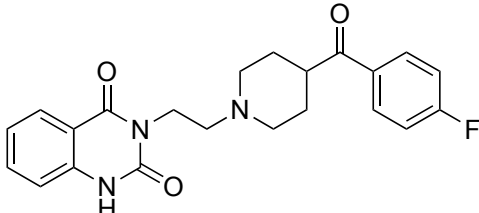
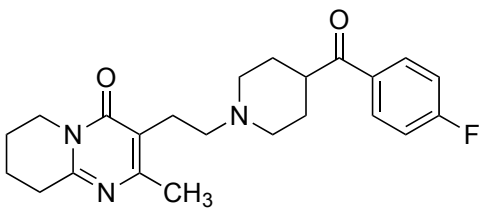
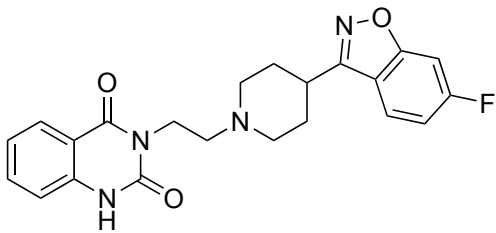
in the presence of 10  $\mu$ M methysergide and competition curves were generated and analyzed by nonlinear regression to derive the dissociation constants ( $K_i$  values).

Risperidone (**3**), ketanserin (**42**) and their structural hybrids, compounds **84** and **85** were tested in this assay system. They bound with high affinity with  $K_i$  values of  $5.22 \pm 1.40$ ,  $18.55 \pm 1.78$ ,  $12.74 \pm 1.50$  and  $0.96 \pm 0.21$  nM, respectively (Figure 37) (Table 5).



**Figure 37.** The binding affinity data for risperidone (A), ketanserin (B), compounds **84** (C), and **85** (D) (figures provided by Dr. José L. Moreno).

**Table 5.** Biological activity of risperidone, ketanserin and their two hybrids.

| Compounds  | TEVC<br>electrophysiology<br>assay<br>[% activity of 5-<br>HT in presence of<br>the compounds] | Radioligand<br>binding assay,<br>$K_i \pm \text{SEM}$<br>values (nM) |
|--|--|--|
| <br>Risperidone ( <b>3</b> )  | 20   | $5.22 \pm 1.40$  |
| <br>Ketanserin ( <b>42</b> ) | 15   | $18.55 \pm 1.78$   |
| <br><b>84</b>               | 21   | $12.74 \pm 1.50$   |
| <br><b>85</b>               | 85   | $0.96 \pm 0.21$  |

\*The biological assay data for **84** and **85** are from two experimental determinations.



### 3. Discussion:

The functional activity data suggests that the structural hybrids of risperidone and ketanserin, compounds **84** and **85** have different activities at the receptor. Similar to risperidone, paliperidone and ketanserin, compound **84** seems to antagonize the activity of 5-HT at the receptor, bringing it almost down to the baseline.

Compound **85** did not seem to affect the activity of 5-HT to a great extent. Also, when tested by itself at the receptor, it gave a positive efficacy of ~20% suggesting partial agonist activity. Also judging by its activity in the presence of 5-HT, it can be suggested that compound **85** shows potential to be a low potency partial agonist. However, dose response curves for both hybrids would be needed to confirm this. In the same study (Figure 36), ketanserin gives an activity of 45%, which as discussed earlier, could be due to its activity at the GIRK4\* channels. Although the same cannot be unequivocally said for the hybrid, testing compound **85** at the GIRK4\* channel as a negative control would tell us how much of the activity is actually mediated through the  $G_{\alpha q}$  pathway.

Radioligand binding affinity data suggests that the two hybrids bind with high affinity at the 5-HT<sub>2A</sub> receptor. Compound **85**, which has the left half of ketanserin and the right half of risperidone binds with the highest affinity, almost 5-, 13- and 19-fold higher than risperidone, **84** and ketanserin, respectively. The higher binding affinity of compound **85** suggests that the right half of risperidone (which is common to both, **85** and risperidone), might be important for the binding affinity of risperidone. As the binding affinity of **85** is

~5-fold higher than risperidone, the quinazolinedione moiety might be contributing towards enhancing the binding affinity.

Compound **85**, which contained the left half of ketanserin, binds with ~19 times higher binding affinity compared to ketanserin. This suggests that the right half made certain interactions that reinforce its binding activity at the receptor. Herndon et al. had reported that the right half of ketanserin (4-fluorobenzoyl piperidine) was sufficient for binding at the receptor, while the left half (quinazolinedione) enhances the binding.<sup>143</sup> The quinazolinedione could be strengthening the binding of compound **85** in a similar fashion, such that the binding affinity of 0.96 nM could be a combined effect of the left and the right halves of the compound.

Compound **84** binds at the receptor with ~2 times lower binding affinity than risperidone. As the binding affinity of the left half of risperidone has yet to be tested, we cannot make a strong argument regarding which structural half is responsible for its binding affinity. However, owing to its ~13 fold lower binding affinity than compound **85**, certain speculations can be made. First, it lacks certain structural features that contribute to the high binding affinity of **85** (0.96 nM). Second, the left half of **84** might not be contributing to its binding affinity, unlike the quinazolinedione moiety of compound **85**, which seems to be bolstering the affinity (Herndon et al.).<sup>143</sup> However, without the binding affinity of the left half of compound **84**, it is difficult to draw conclusions about the effect the two structural halves have on the binding affinity of compound **85**.

## C. MOLECULAR MODELING STUDIES:

### 1. Approach

Homology modeling and docking studies of risperidone and its deconstructed and elaborated analogs were conducted to examine their binding modes at the orthosteric binding site at the human 5-HT<sub>2A</sub> receptor. The different kinds of interactions with various amino acids at the receptor would give us an idea of the relative importance of the structural features making interactions. Moreover, we will gain a perspective into the relative binding modes of risperidone and ketanserin at the 5-HT<sub>2A</sub> receptor, and to identify any differences in their binding mode(s) (ligand receptor interactions), if they exist. Binding affinity and functional data will be compared with the results from the docking studies.

Furthermore, the possible role of the hydroxyl group of paliperidone was investigated, as was the role of the fluoro group of risperidone.

As discussed earlier, the 5-HT<sub>2A</sub> receptor consists of seven transmembrane (TM) spanning helices<sup>180</sup> with an extracellular N-terminus and an intracellular C-terminus (Figure 38). The human 5-HT<sub>2A</sub> protein subunit is about 52 kDa and is composed of 471 amino acids with 124 amino acids forming the extracellular domain (ECD), 159 amino acids forming the TM, and 188 amino acids forming the intracellular domain (ICD).<sup>80</sup> In addition, the protein also has a DRY motif (D172, R173, Y174), a NPxxY motif and a PDZ-motif along with two disulfide bridges formed by two sets of cysteine residues (i.e., C148 with C227 and C350 with C353).<sup>80,181,182</sup> There is evidence that the DRY-motif is important for

maintaining receptor conformation, G-protein coupling/recognition and mutations of this conserved sequence has led to agonist-independent constitutive activity in certain GPCRs (rhodopsin,  $\beta_2$ -adrenoceptors).<sup>183</sup> The NPxxY motif is involved in stabilizing the active conformation of the receptor after activation and the PDZ domain can bind to PDZ proteins, which can influence almost all aspects of GPCR signaling, from ligand binding and G-protein coupling to downstream signaling events.<sup>184,185</sup>

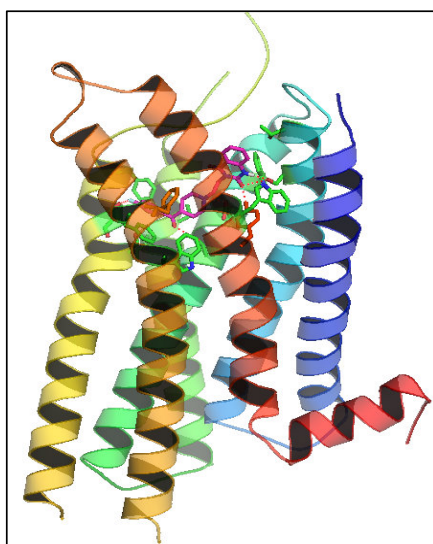


**Figure 38.** A model of the 5-HT<sub>2A</sub> receptor generated as a part of the current study.

As the crystal structure of the 5-HT<sub>2A</sub> receptor has not yet been solved, we had to rely on homology with appropriate template proteins for a 3-dimensional view of the receptor. Initially, before the 3-dimensional structures of the known neurotransmitter receptors were resolved, graphical models of 5-HT<sub>2A</sub> receptors were built and analyzed using the structure of bacteriorhodopsin, which is not a GPCR, but a light-dependent proton pump.<sup>180</sup> These models suffered from weak sequence homology and were highly dependent on

computationally intensive dynamics simulations.<sup>180</sup> Later on, bovine rhodopsin replaced bacteriorhodopsin as the template.<sup>182,186</sup> A breakthrough occurred in the field of homology modeling with the resolution of the crystal structure of the class A aminergic GPCR  $\beta_2$ -adrenoceptor in 2007. 5-HT<sub>2A</sub> receptors share a sequence homology of approximately 40% with  $\beta_2$ -adrenoceptors (Table 6).<sup>186</sup>

**Table 6.** Initial template choices for homology modeling of 5-HT receptors adapted from McRobb et al.<sup>186</sup>

| Receptor                 | %Homology |                         |                           |
|--------------------------|-----------|-------------------------|---------------------------|
|                          | Rhodopsin | $\beta_2$ adrenoceptors | Adenosine A <sub>2A</sub> |
| 5-HT <sub>1B</sub>       | 23        | 41                      | 35                        |
| <b>5-HT<sub>2A</sub></b> | <b>22</b> | <b>40</b>               | <b>30</b>                 |
| 5-HT <sub>2B</sub>       | 22        | 40                      | 30                        |
| 5-HT <sub>2C</sub>       | 23        | 42                      | 30                        |

The 5-HT<sub>2</sub> family of receptors shares a homology of about 70% with each other.<sup>80</sup> In 2013 the high-resolution crystal structure of the 5-HT<sub>2B</sub> receptor was solved (PDB ID: 4IB4, at 2.7 Å) in complex with the  $\beta$ -arrestin signaling-biased agonist ergotamine.<sup>187</sup> The P-I-F motif (located near the base of the ligand binding pocket, and involved in the conformational changes in GPCRs after activation),<sup>187</sup> undergoes a number of conformational changes in response to an agonist, and showed a conformation similar to that of the inactive  $\beta_2$ -adrenoceptor (PDB ID: 2RH1).<sup>187,188</sup> As our present investigation is

focused on risperidone (with negative efficacy at the 5-HT<sub>2A</sub> receptor), which possesses a high affinity for the inactive state of the 5-HT<sub>2A</sub> receptor, and because of the high sequence homology of 70% between the two receptors, we used the crystal structure of the 5-HT<sub>2B</sub> receptor as a template.

As a first step in building the homology models, the sequence of the target protein (5-HT<sub>2A</sub> receptor) was aligned with the corresponding residues from the template (5-HT<sub>2B</sub> receptor) using the CLUSTALX 2.1 program. As the sequence homology is quite high, most of the residues or the nature of the residues (such as hydrophobic or polar), matched (Figure 39).

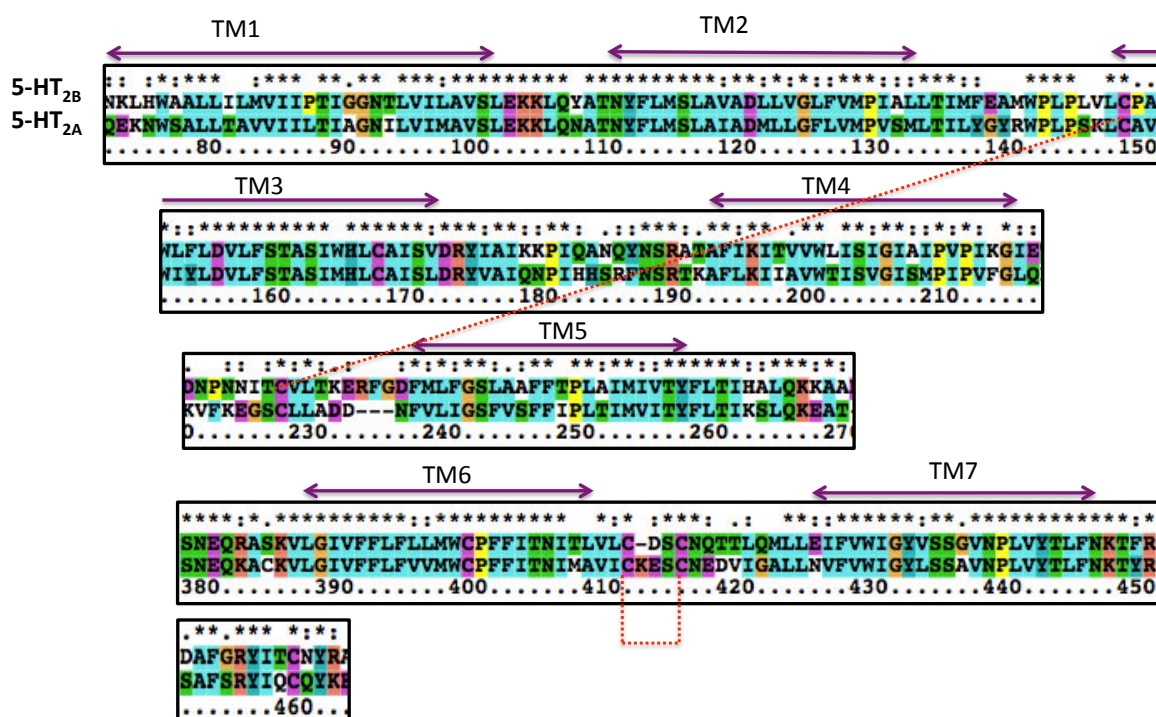


**Figure 39.** Multiple sequence alignment between 5-HT<sub>2A</sub> and 5-HT<sub>2B</sub> receptors generated by the software CLUSTALX 2.1.

One hundred homology models were generated using the MODELLER v9.1 program; these were further refined by adding hydrogens and bridging the disulfide connections on SYBYL-X2.1. Ligands were docked using the programs GOLD Suite 5.2 and 5.3 and the interactions of the solutions of ketanserin in the present study were compared with those reported in previously published homology models of 5-HT<sub>2A</sub> receptors and site-directed mutagenesis data by our laboratory as well as other groups.<sup>189–193</sup> The docked solutions were re-scored with the HINT (Hydropathic INteractions) program, which is based on the experimental free energy information derived from log P<sub>o/w</sub> (the solvent partition co-efficient for 1-octanol/water).<sup>194</sup> The HINT studies will quantify the different interactions each ligand makes with the receptor.

## **2. Results and discussion:**

As a first step, the binding pocket of models generated as a part of our study was compared to previously published 5-HT<sub>2A</sub> receptor homology models. The model with the highest DOPE (Discrete Optimized Protein Energy) score as calculated by MODELLER was chosen for this comparison. According to previously reported homology models,<sup>189–193</sup> the orthosteric binding pocket is located in the transmembrane region and is composed of residues belonging to TM3, TM5, TM6 and TM7, such as D155 and S159 (TM3), S239 (TM5), W336, F339 and F340 (TM6), Y370 (TM7) and L228 and L229 (ECL2). Our model conformed to these reported results (Figure 40).

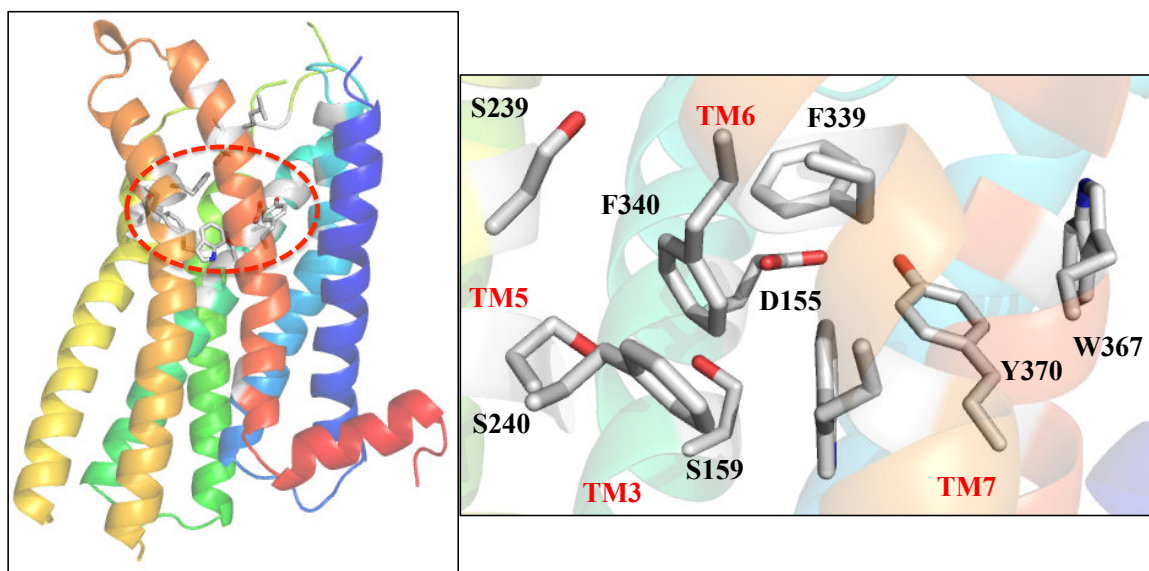


**Figure 40.** An energy minimized model from the current study with the binding pocket highlighted along with the residues constituting the binding pocket.

An energy-minimized complex of ketanserin with the 5-HT<sub>2A</sub> receptor is depicted in Figure 41. In addition to the ionic interaction of the ammonium ion in the piperidine ring of ketanserin with the conserved aspartate residue (D155) in TM5, there were three additional hydrogen bonds: S159 (TM3) with the *p*-fluorobenzoyl carbonyl oxygen, S131 (TM2) with the N1 quinazolinedione nitrogen atom and S242 (TM5) with the *p*-fluorobenzoyl fluorine atom (Figure 41). Additionally, ketanserin was surrounded with a bed of hydrophobic residues: W151, V156 (TM3), F339, F340 (TM6), L228, L229 (ECL).



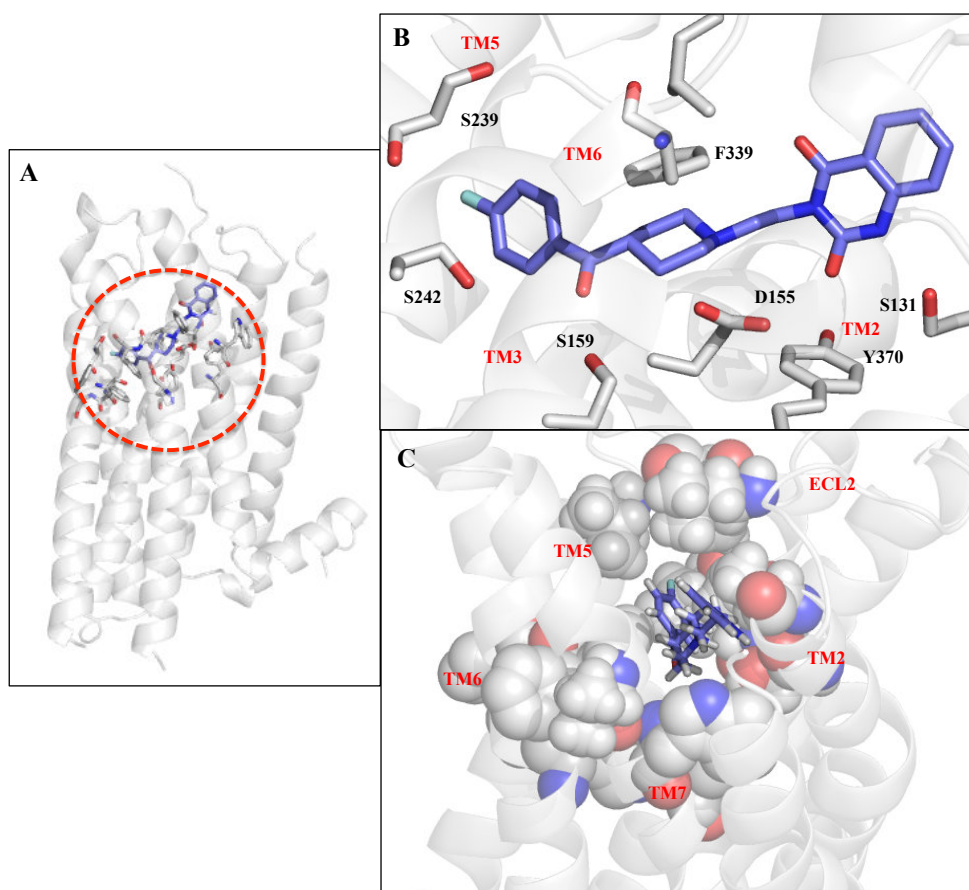


**Figure 41.** An energy-minimized ketanserin-receptor complex (A), interactions of ketanserin (purple) with amino acids forming the binding pocket (B), and hydrophobic residues, depicted as spheres, surrounding ketanserin (purple) in the binding pocket (C).

The interactions made by ketanserin in our models were compared to those considered important in the literature models. The importance of these residues in the binding of ketanserin was previously assessed by site-directed mutagenesis studies (Table 7). As depicted in Figure 41 and Table 7, our model showed all the interactions reported to be important, and more.

**Table 7.** Site-directed mutagenesis data reported in the literature for the binding affinity of ketanserin.<sup>191,192,195–198</sup>

| Mutation | TM domain | $K_d \pm \text{SEM}$<br>(nM) | $K_i \pm \text{SEM}$ (nM) | Mutant/WT<br>ratio | Reference |
|----------|-----------|------------------------------|---------------------------|--------------------|-----------|
| WT       | -         | -                            | $0.5 \pm 0.2$             | -                  | 191       |
| D155A    | III       | -                            | No binding                | -                  | 191       |
| D155N    | III       | -                            | No binding                | -                  | 191       |
| D155Q    | III       | -                            | No binding                | -                  | 191       |
| WT       | -         | -                            | $0.8 \pm 0.2$             | -                  | 192       |
| D155N    | III       | -                            | $60 \pm 1$                | 75                 | 192       |
| WT       | -         | 0.98                         | -                         | -                  | 195       |
| W336A    | -         | 899                          | -                         | 917.34             | 195       |
| W367L    | -         | No binding                   | -                         | -                  | 195       |
| Y370A    | VII       | 18.4                         | -                         | 18.77              | 195       |
| F365L    | -         | 3.9                          | -                         | 3.97               | 195       |
| WT       | -         | 0.4                          | -                         | -                  | 196       |
| F339A    | VI        | 4.6                          | -                         | 11                 | 196       |
| F339L    | VI        | 9.8                          | -                         | 24.5               | 196       |
| F339Y    | VI        | 2.8                          | -                         | 7                  | 196       |
| F340Y    | VI        | 29                           | -                         | 72.5               | 196       |
| F340A    | VI        | 0.9                          | -                         | 2.25               | 196       |
| F340L    | VI        | 0.3                          | -                         | 0.75               | 196       |
| WT       | -         | 0.84                         | -                         | -                  | 197       |
| S159A    | III       | 1.1                          | -                         | 1.30               | 197       |
| S159C    | III       | 0.66                         | -                         | 0.78               | 197       |
| WT       | -         | -                            | 2.3                       | -                  | 198       |
| F243A    | -         | -                            | 10.4                      | 4.52               | 198       |
| F244A    | -         | -                            | 6.7                       | 2.91               | 198       |
| S239A    | V         | -                            | 1.5                       | 0.65               | 198       |

Previously published models of the 5-HT<sub>2A</sub> receptor have described two possible binding modes for ketanserin: one with the *p*-fluorobenzoyl fluorine atom pointing towards TM5<sup>199</sup> and the second, with the fluorine atom pointing towards TM7<sup>182</sup> (Figure 42). We observed

both binding modes; however, the GOLD score of the model with the fluorine atom pointing towards TM7 was low (51.32) compared to the GOLD score of the model with the fluorine atom pointing towards TM5 (63.62), making this pose possible, but unlikely. Also, the models reported in the literature were built using the crystal structure of bovine rhodopsin (PDB ID: 4X1H) as the template (sequence homology: <22%).<sup>182,199</sup> A higher GOLD score coupled to a superior sequence homology of 70% with the template and adherence to interactions considered important by site-directed mutagenesis, validated our model (Figure 42).

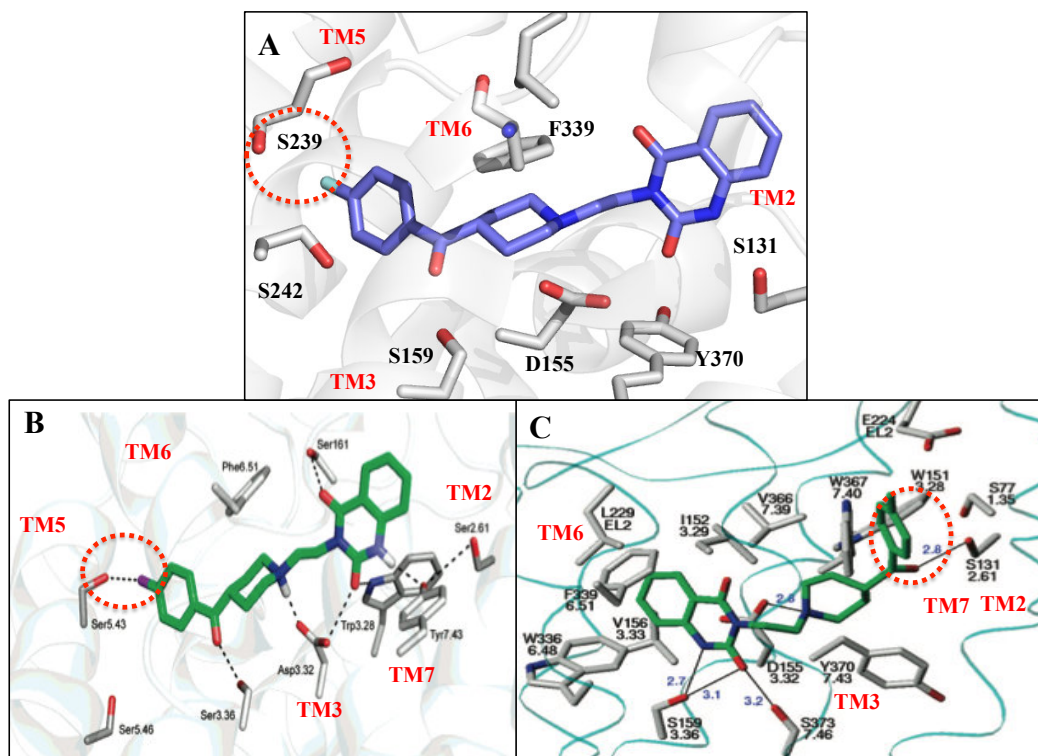


**Figure 42.** The two binding modes of ketanserin: our model (A), literature models with the fluorine atom pointing towards TM5 (B),<sup>199</sup> and pointing towards TM7 (C).<sup>182</sup>

Risperidone (**3**), paliperidone (**7**), ketanserin (**42**) and the analogs included in the deconstruction and elaboration of risperidone/paliperidone (i.e., compounds **55-58**, **60**, **84**, **85**, and **90**) were energy minimized before docking. Molecular docking was conducted using the scoring function within the docking program GOLD Suite 5.2 and the binding pocket was defined as being within a 10-Å radius surrounding the  $\alpha$ -carbon atom of the D155 residue in TM3. The docking solutions were divided into clusters (the cluster docking script was provided by Dr. Philip D. Mosier) based on the binding poses. The clusters were analyzed and the models were evaluated for each ligand, based on the GOLD fitness scores, and interaction of the ammonium ion of the ligands with D155. For models selected (~16 models for every ligand), based on the fitness score and the interactions, the solutions were merged with the models and energy-minimized using the Tripos Force field function in SYBYL-X2.1 to optimize the interactions. These models were further rescored by conducting HINT studies. The final model for each ligand was chosen based on the most optimal HINT score.

#### **a. Deconstruction of risperidone/paliperidone:**

The GOLD and HINT scores for the models chosen for risperidone, paliperidone and their deconstructed analogs (**55-58**) are summarized in Table 8. In the models chosen, risperidone (**3**), paliperidone (**7**) and all the deconstructed analogs had similar binding modes at the receptor, i.e., their 6-fluoro-3-(piperidin-4-yl)benz[*d*]isoxazole portion was oriented towards TM5 (see Figure 44).

**Table 8.** Risperidone and its deconstructed analogs: Ligands and the models chosen based on the GOLD and HINT scores.

| Ligand           | GOLD score | Polar | Hydrophobic | Total HINT score | D155 | S159 | S242       | N363       |
|------------------|------------|-------|-------------|------------------|------|------|------------|------------|
| Risperidone (3)  | 64.62      | 1523  | 1225        | 1204             | 737  | 374  | 82         | 22         |
| Paliperidone (7) | 58.19      | 1361  | 1026        | 873              | 732  | 368  | 67         | 210        |
| <b>55</b>        | 48.73      | 1593  | 430         | 1366             | 1370 | 28   | <b>115</b> | 0          |
| <b>56</b>        | 54.82      | 1250  | 1165        | 1093             | 740  | 379  | 87         | 6          |
| <b>57</b>        | 53.99      | 1464  | 792         | 1445             | 682  | 258  | 55         | <b>352</b> |
| <b>58</b>        | 46.56      | 1128  | 626         | 865              | 970  | 67   | 79         | 0          |

A previously published model of the 5-HT<sub>2A</sub> receptor had described another mode of binding for risperidone where the 6-fluoro-3-(piperidin-4-yl)benz[*d*]isoxazole portion was oriented towards TM7<sup>200</sup> (Figure 43) (similar to ketanserin, Figure 42).

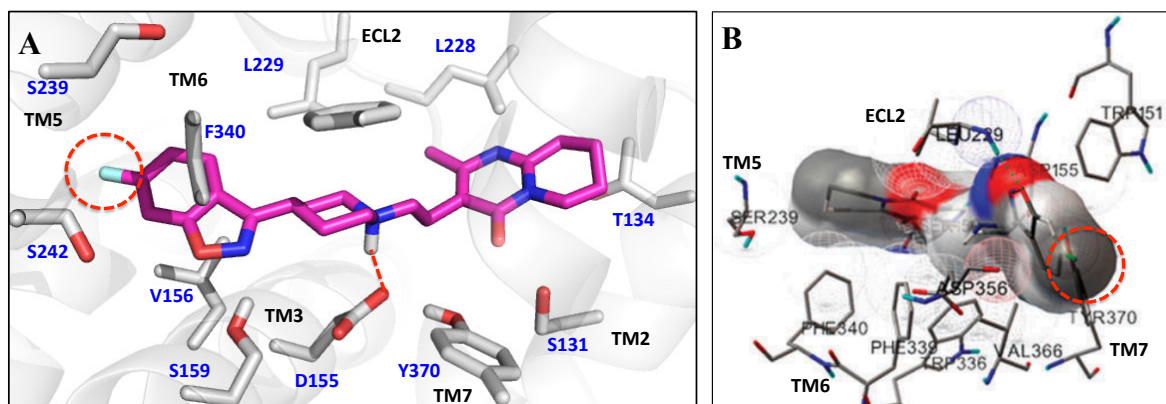


**Figure 43.** The binding modes of risperidone: our model with the fluorine atom pointing towards TM5 (A), and literature model with the fluorine atom pointing towards TM7 (B).<sup>200</sup>

Similar to ketanserin, we observed both binding modes, however, the GOLD score of the model with the fluorine atom pointing towards TM7 was low (51.55) compared to the GOLD score of the model with the fluorine atom pointing towards TM5 (64.02). Also, the model reported in the literature was built using the crystal structure of  $\beta_2$  adrenergic receptor (PDB ID: 2RH1) as the template (sequence homology: 40%), while our model was built using the crystal structure of the 5-HT<sub>2B</sub> structure as the template (sequence homology: 70%).

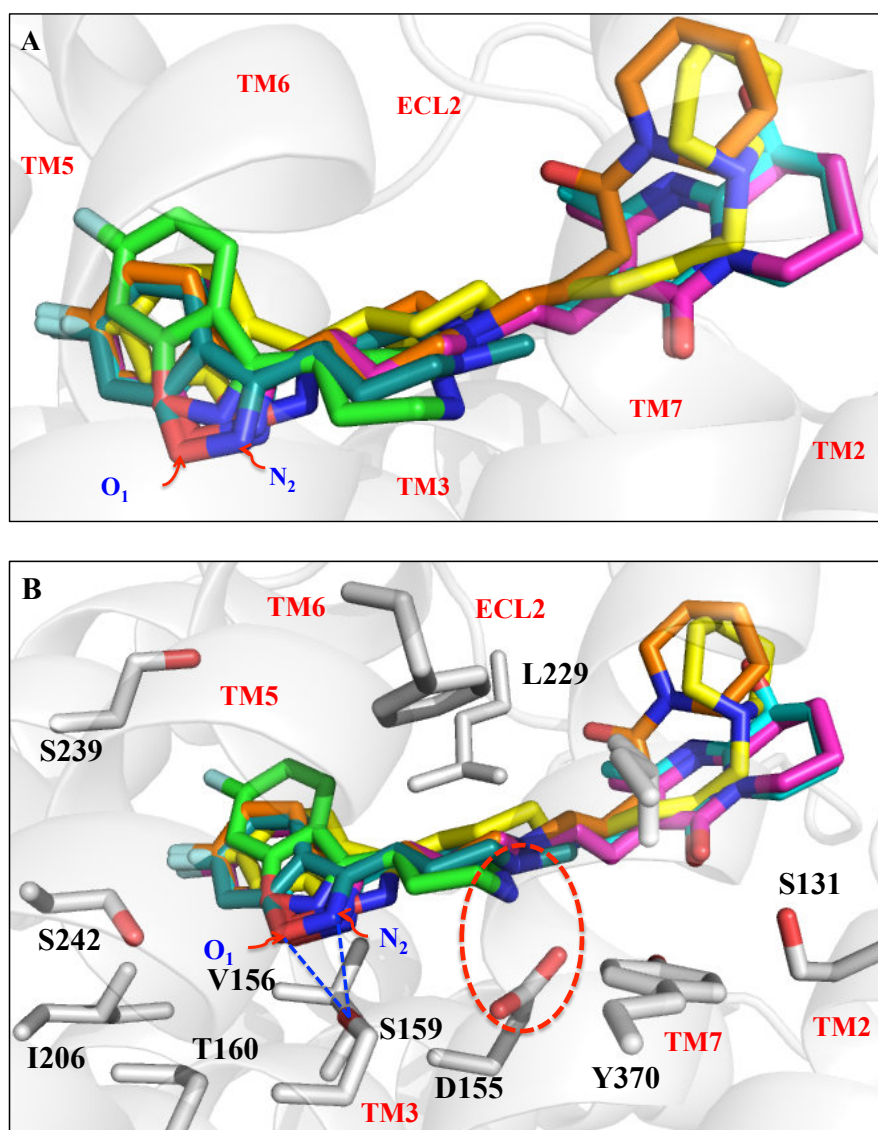


**Figure 44.** The binding orientation of risperidone (magenta), paliperidone (cyan) and their deconstructed analogs **55** (green), **56** (orange), **57** (yellow), and **58** (teal) at the 5-HT<sub>2A</sub> receptor (A), and their interactions with amino acids in the binding pocket (B).

Molecular modeling studies suggested that both halves of risperidone formed strong interactions at the receptor, while hydrophobic interactions predominated at the left half made up of the 6,7,8,9-tetrahydro-4*H*-pyrido[1,2-*a*]pyrimidin-4-one ring system; polar interactions seemed to dominate the front on the right half, consisting of the 6-fluoro-(3-piperidiny)benz[*d*]isoxazole moiety.

All ligands formed an ionic bond with the conserved D155 (TM3), which is involved in anchoring the terminal amine moiety of tryptamines at the receptor.<sup>195</sup> S159 (TM5) formed a bifurcated hydrogen bond with the 6-fluoro-(3-piperidiny)benz[*d*]isoxazole O<sub>1</sub> and N<sub>2</sub> atoms of all the deconstructed analogs (Figure 44). Bifurcated hydrogen bonds (H-bond) occur when one hydrogen atom simultaneously forms H-bonds to two other H-bond acceptors.<sup>201</sup> Compound **55** formed a second bifurcated H-bond interaction (O<sub>1</sub> and N<sub>2</sub> in 6-fluorobenzisoxazole) with S242 (TM5) (Figure 45). From the radioligand binding data at the 5-HT<sub>2A</sub> receptor for the deconstructed analogs of risperidone (**3**) (Table 4), we can conclude that there is ~15-fold difference in the binding affinity of risperidone and its smallest deconstructed analog **55**. This suggests that even after removing the entire left half of risperidone ( $K_i = 5.22$  nM), the compound **55** retained good binding affinity ( $K_i = 75.75$  nM). As seen from Figure 45, compound **55**, although devoid of certain hydrophobic interactions made by the left half of risperidone, formed two bifurcated H-bonds (S159 and S242) that this could be supported by its retention of affinity at the receptor.



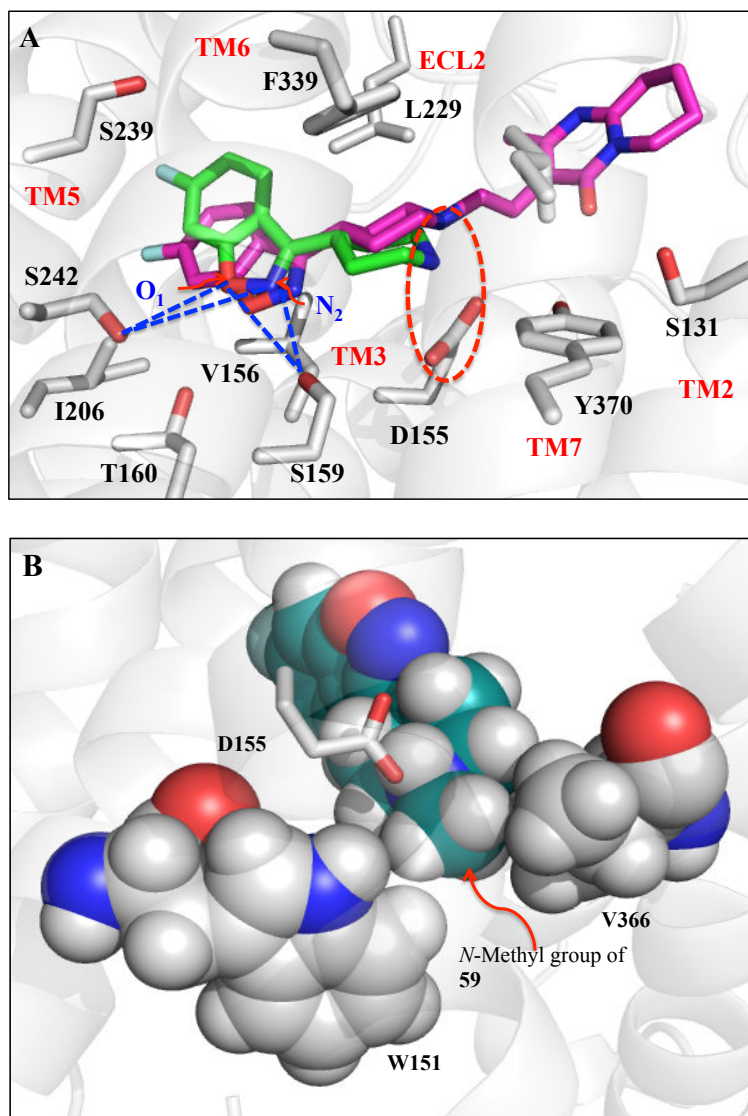


**Figure 45.** The bifurcated H-bonds by compound **55** with S242 (TM5) in comparison to risperidone (magenta) (A), and the additional hydrophobic interactions made by compound **58** (B).

Strong hydrophobic interactions were observed between compound **58** and W151 (TM3) and V366 (TM7) that were lacking with **55** and the other deconstructed analogs (Figure 45). Radioligand binding studies indicated that **58** has a high binding affinity ( $K_i = 18.77$  nM), and although it lacks certain structural features of risperidone, it binds with only ~3-fold lower affinity than risperidone. Compounds **55** and **58** differ only in a single *N*-methyl group, but compound **58** binds with ~4-fold higher affinity. The *N*-methyl group increased the binding affinity of **55** by ~4-fold and the extra hydrophobic interactions made by **58** might be contributing.

Functional data suggested that compound **57** enhanced the activity of 5-HT and could potentially behave as a superagonist or an ago-allosteric modulator. Its high binding affinity ( $K_i = 35.20$  nM) indicated that it might exert at least part of its activity at the orthosteric site of the 5-HT<sub>2A</sub> receptor. Modeling studies showed that the compound lacking the carbonyl group **57** formed a strong hydrogen bond with N363 (TM7) (Table 8 and Figure 46) with the ammonium ion in its second piperidine ring (risperidone has this nitrogen atom as a part of the 6,7,8,9-tetrahydro-4*H*-pyrido[1,2-*a*]pyrimidin-4-one ring system). This suggests that **57** is capable of forming additional interactions at the receptor close to the binding pocket. Although it cannot be said with certainty at this moment, compound **57** might potentially be binding at two sites (orthosteric as well as a potential allosteric site) simultaneously.

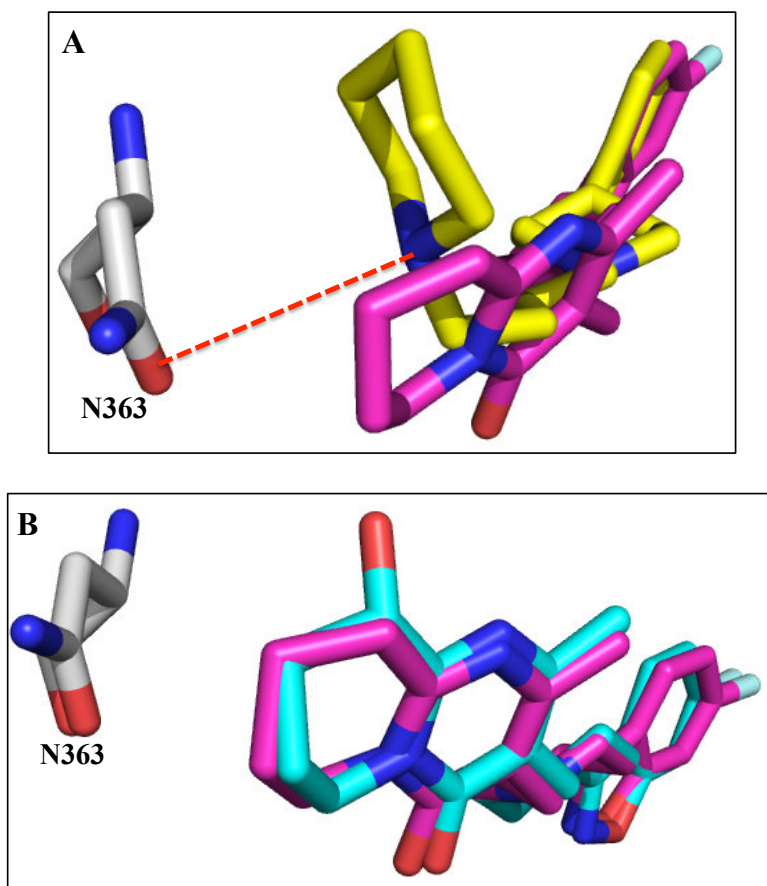


**Figure 46.** The interaction of compound **57** (yellow) with N363 (TM7) compared to risperidone (magenta) (A), and a comparison of the binding pose of risperidone (magenta) and paliperidone (cyan) (B).

Molecular modeling studies showed that the hydroxyl group of paliperidone (the only point of difference between risperidone and paliperidone) did not directly participate in hydrogen bonding (Figure 46). This could explain why the two compounds have almost identical binding affinities at the receptor as shown by literature (risperidone:  $K_i = 0.16$  nM and paliperidone:  $K_i = 0.25$  nM).<sup>202</sup>

## **b. Elaboration of risperidone/paliperidone:**

### **i. Comparison of the binding modes of risperidone and ketanserin:**

In order to gain insight into the functional and binding differences observed with risperidone (**3**) and ketanserin (**42**), we conducted a comparative study of their binding modes at the receptor and their respective molecular interactions with specific amino acids lining the binding pocket. Furthermore, we docked their structural hybrids, compounds **84** and **85** to get a better insight into the two structural halves of risperidone and ketanserin. The GOLD scores and the HINT scores for the chosen models for risperidone, ketanserin and **84** and **85** are summarized in Table 9.

**Table 9.** Risperidone, ketanserin and their structural hybrids: Ligands and the models chosen based on the GOLD and HINT scores

| Ligand                   | GOLD score | Polar | Hydrophobic | Total HINT score | D155 | S159 | S242       |
|--------------------------|------------|-------|-------------|------------------|------|------|------------|
| Risperidone ( <b>3</b> ) | 64.62      | 1523  | 1225        | 1204             | 737  | 374  | 82         |
| Ketanserin ( <b>42</b> ) | 63.62      | 1658  | 900         | 1112             | 724  | 374  | <b>169</b> |
| <b>84</b>                | 61.16      | 1387  | 1054        | 1044             | 733  | 395  | 73         |
| <b>85</b>                | 63.09      | 1547  | 870         | 1121             | 745  | 369  | 12         |

All four ligands had a similar binding pose at the receptor and the hybrid compounds **84** and **85** made the ionic interaction with D155 as discussed earlier with ketanserin and risperidone (Figure 47).

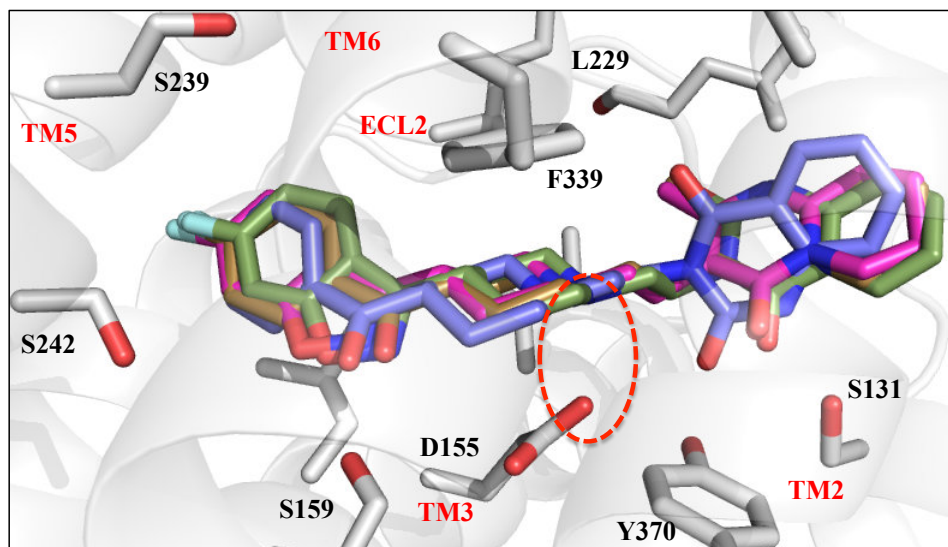


**Figure 47.** The similar binding pose of risperidone (magenta), ketanserin (purple), compounds **84** (gold) and **85** (dark green) at the receptor.

There was a difference in the manner in which ketanserin (**42**) docked at the receptor compared to risperidone (**3**) and compounds **84** and **85**. The right half of ketanserin (*p*-fluorobenzoyl) was oriented upwards compared to the other ligands to form a stronger interaction with S242 from TM5 (Table 9) (Figure 48).

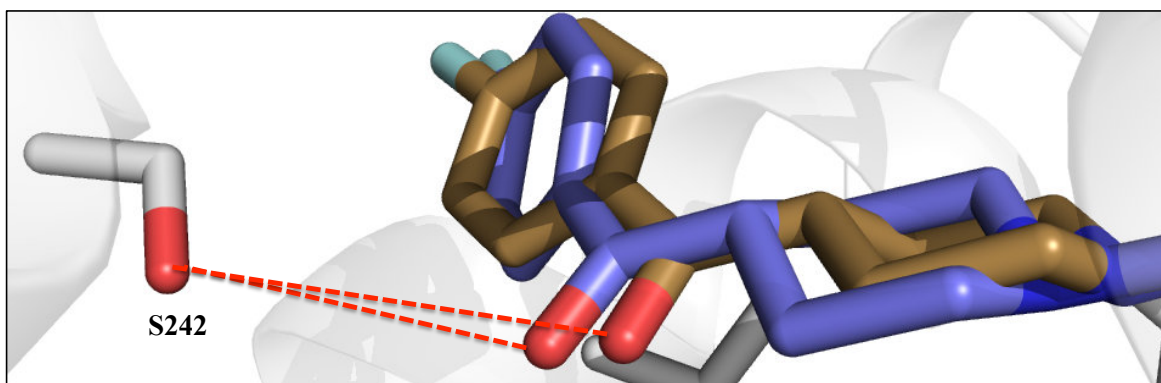


**Figure 48.** A snapshot of the differences in the orientation of the common *p*-fluorobenzoyl moiety of ketanserin (purple) and compound **84** (gold) at the receptor.

Both the hybrid compounds have certain structural remnants of ketanserin – compound **84** has the right half of ketanserin and compound **85** has the left half of ketanserin (Figure 32); however, both had a better overlap with risperidone in their docking solutions (Figure 49). In fact, the common quinazolinedione portion of ketanserin and compound **85** seemed to bind differently. The quinazolinedione ring of **85** seemed to rotate by 180° around the horizontal axis to overlap completely with the 6,7,8,9-tetrahydropyrido[1,2-*a*]pyrimidin-4-one ring system of risperidone (Figure 49). Radioligand binding bolstered this observation, with compound **85** ( $K_i = 0.96$  nM) having an almost identical binding affinity with risperidone ( $K_i = 5.22$  nM).

Additional hydrophobic interactions were observed between risperidone and the residues I135, I152, L229 (ECL2) and V366 on the receptor. These interactions, though absent in

ketanserin, were present in both hybrid compounds, suggesting a preference of binding similar to risperidone rather than ketanserin.

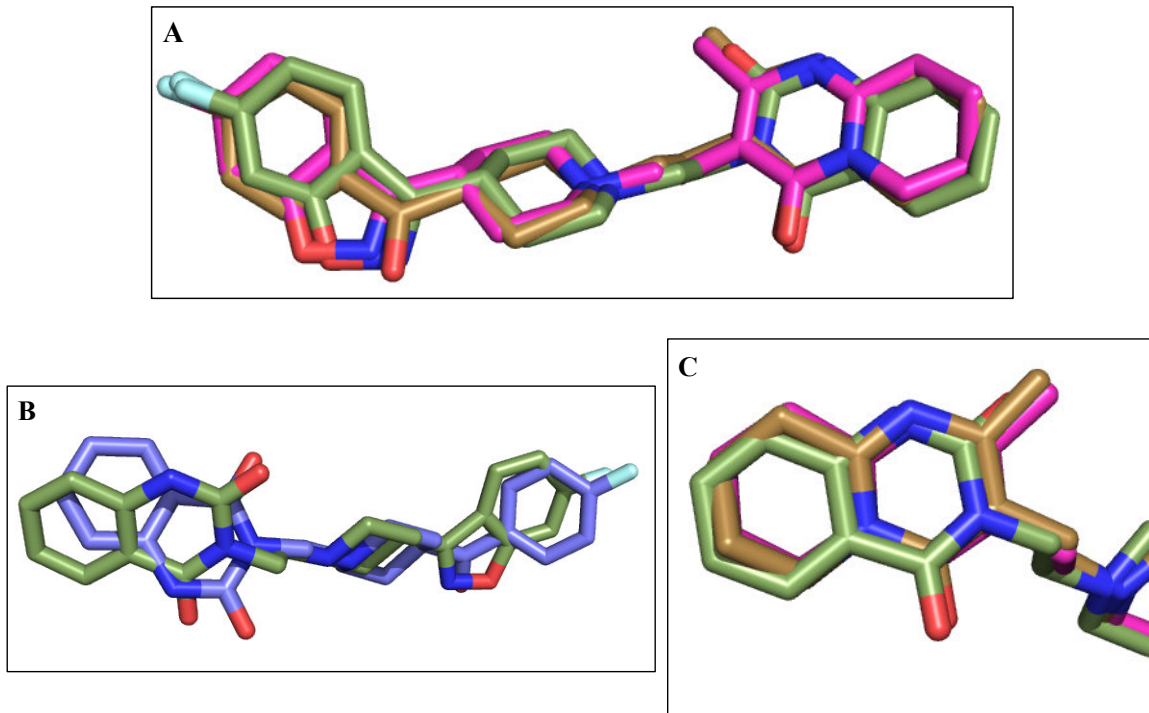


**Figure 49.** The alignment of the hybrid compounds **84** (gold) and **85** (dark green) with risperidone (magenta) (A), differences in the orientation of the common quinazolinedione moiety of ketanserin (purple) and compound **85** (dark green) at the receptor (B), and the perfect alignment of the left halves of risperidone (magenta) and compounds **84** (gold) and **85** (dark green) (C).

## ii. Effect of substituents on the benzisoxazole ring:

As discussed earlier, removal of the *p*-fluorobenzoyl fluorine atom decreased the binding affinity of certain deconstructed analogs of ketanserin (Figure 22).<sup>143</sup> In our molecular modeling studies all the ligands seemed to dock orienting their fluoro substituent towards S242 (TM5). Furthermore, the HINT studies suggested the formation of a potential hydrogen bond between the fluorine atom and S242 for all compounds.

Hence, we conducted molecular modeling studies on compounds **60** (lacking the fluoro group) and **90** (bearing a 5-OCH<sub>3</sub> group) and compared their binding modes and molecular interactions with the fluoro substituent of compound **55** (Figure 50) to determine the importance of the fluoro substituent to examine the effect of substituents (or the absence of them) and the position of the substituents on the benzisoxazole ring, on the polar and hydrophobic interactions of the benzisoxazole ring system.

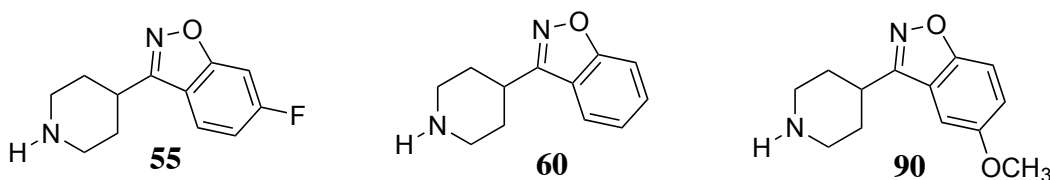


**Figure 50.** Structural comparison for the study of the effect of substituents on the three benzisoxazoles.

The three compounds **55**, **60**, and **90** had a similar binding mode at the receptor (Figure 51). Despite being structurally indistinguishable other than for the substituents, they did not align perfectly at the receptor and the source of the misalignment seemed to stem from



the interactions made by the substituents on the benzisoxazole ring or the lack of substituents (Figure 51).

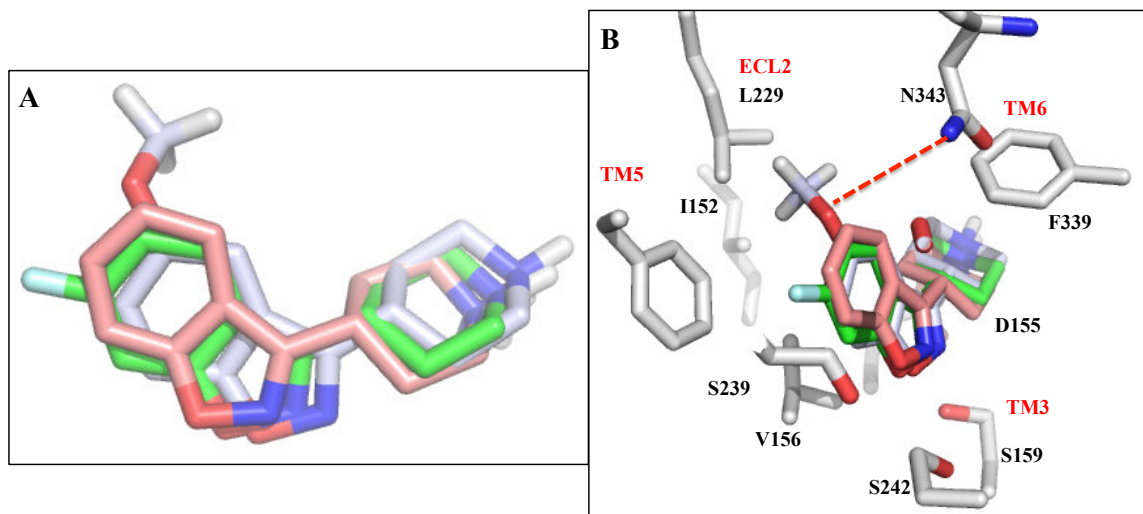


**Figure 51.** The binding modes of the three benzisoxazoles, **55** (green), **60** (pink) and **90** (gray) (A), and their molecular interactions with the orthosteric site amino acids (B).

All three ligands formed the indispensable ionic interaction with D155 from TM3 and the bifurcated H-bond with S159 (with their 6-fluoro-(3-piperidinyl)benz[*d*]isoxazole O<sub>1</sub> and N<sub>2</sub> atoms). As discussed earlier for compound **55**, S242 seemed to form a bifurcated H-bond with compounds **60** and **90** as well. The desfluoro compound **60** seemed to be closer to S242 and made a stronger interaction with S242 (Table 10).

**Table 10.** Role of substituents and their position on the binding interaction of benzisoxazole ring: Ligands and the models chosen based on the GOLD and HINT scores

| Ligand    | GOLD score | Polar | Hydrophobic | Total HINT score | D155 | L229       | S239     | S242       |
|-----------|------------|-------|-------------|------------------|------|------------|----------|------------|
| <b>55</b> | 48.73      | 1593  | 430         | 1366             | 1370 | 26         | 33       | 115        |
| <b>60</b> | 46.76      | 1862  | 342         | 1463             | 1548 | 18         | <b>1</b> | <b>199</b> |
| <b>90</b> | 46.74      | 2022  | 638         | 1654             | 1300 | <b>121</b> | <b>0</b> | 113        |

The difference in substituents was reflected in the interactions made by the three compounds and these were quantified by HINT studies (Table 10). Compound **55** formed a weak hydrogen bond with S239 from TM5, whereas compounds **60** and **90** did not form this interaction. The methoxy group of **90** made a strong hydrophobic interaction with L229 from ECL2, which was marginal for **55** and **60**. The O atom of the methoxy group of **90** also formed a weak hydrogen bond with N343 (TM6) and this interaction was lacking by both, **55** and **60**.

Radioligand binding data would be more conclusive regarding the role played by the presence (or absence) of substituents and on the position of the substituents on the benzisoxazole ring. Molecular modeling and HINT studies suggested some differences in their specific interactions. Although 5-methoxy compound **90** utilized more hydrophobic and hydrogen bonds than **55** and **60**, the lack of substituents seemed to orient compound **60** more towards S242 (TM5), compared to **55** and **90** (Figure 51).

## CHAPTER V: CONCLUSION

The primary intent of the current investigation was to study the structure of risperidone with respect to its inhibitory action at 5-HT<sub>2A</sub> receptors and to determine the minimum structural features of risperidone responsible for its antagonist activity. This was probed by the medicinal chemistry principles of deconstruction and elaboration. The current investigation also focused on the deconstruction of paliperidone (9-OH risperidone). Structurally, risperidone is a deconstructed analog of paliperidone.

The systematically deconstructed analogs of risperidone (**55-58**) were tested for their functional activity in two assays, which gave differing results. Although the calcium imaging assay suggested that the compounds have antagonist activity, the more sensitive TEVC assay indicated that the compounds were low-efficacy partial agonists – with the exception of compound **57**, which at a higher concentration of 50  $\mu$ M seemed to possess activity greater than the endogenous ligand 5-HT. Compound **57** could either be a potential superagonist, an allosteric modulator or the compound might be activating the GIRK4\* channels independent of the 5-HT<sub>2A</sub> receptor, or a combination of two or more of these actions. These results were subjected to further investigation by testing compound **57** at the GIRK4\* channel in the presence and absence of the 5-HT<sub>2A</sub> receptor (see Appendix A).

The most striking feature of the functional activity data was the fact that in the TEVC assay compounds **55** and **58** had inhibitory activity comparable to that of risperidone, implying that the entire structure of risperidone might not be required for its antagonist activity. As such, this (coupled with our previously published data on **55**<sup>164</sup>) suggest that the benzisoxazolylopyrrolidine moiety represents a pharmacophore for the 5-HT<sub>2A</sub> antagonist action (and binding) of risperidone-type agents.

With speculation about the functional activity data in hand and speculations about the potential ‘superagonist’ or ‘ago-allosteric’ properties of compound **57** the compounds were tested in a radioligand binding assay to determine if the functional activity observed was due to their effect at 5-HT<sub>2A</sub> receptors. Risperidone and its deconstructed analogs bind with high affinity at the receptor, which suggested that compound **57** exerts at least part of its activity by binding at the orthosteric site of the receptor.

The radioligand binding data of the deconstructed analogs suggested that the *N*-methyl compound **58** ( $K_i = 18.77$  nM), which has the highest binding affinity among all the deconstructed analogs of risperidone (**55-58**), was comparable to risperidone ( $K_i = 5.22$  nM). This means that the entire structure of risperidone is not important for its affinity at the receptor, and that the 2-methyl-6,7,8,9-tetrahydro-4*H*-pyrido[1,2-*a*]pyrimidin-4-one ring system can be removed (along with the hydrophobic interactions it makes) and the hydrophobic interactions made by the free *N*-methyl group can substitute for those interactions. Molecular modeling studies showed that the *N*-methyl group of compound **58**

forms certain hydrophobic interactions (V366 and W151) (Figure 45). These interactions were not exhibited by even the longer deconstructed analogs **56** and **57**.

The comparative study between risperidone ( $K_i = 5.22$  nM) and ketanserin ( $K_i = 18.55$  nM) brought out certain differences in the way risperidone and ketanserin bind at the receptor. Compound **85**, which has the left half of ketanserin and the right half of risperidone had the highest affinity at the 5-HT<sub>2A</sub> receptor, almost 5-, 13-, and 19-fold higher than risperidone, **84** and ketanserin, respectively. This suggested that the interactions formed by **85** are optimal for high binding affinity. One conclusion that can be drawn from the higher binding affinity of compound **85** is that the right half of risperidone might be important for its binding affinity at the 5-HT<sub>2A</sub> receptor. As **85** and risperidone differ in their left halves (**85** has the quinazolinedione moiety), the quinazolinedione moiety of **85** might be contributing towards the binding affinity and enhancing it.

Herndon et al.<sup>143</sup> had previously reported that the left half of ketanserin, 2,4-quinazolinedione, contributed to or enhanced the affinity of ketanserin and the 2,4-quinazolinedione moiety by itself bound poorly at the receptor ( $K_i = 10,000$  nM). It can be speculated from this information that the right half of compound **85** might be sufficient to maintain affinity at the receptor and the left half (the 2,4-quinazolinedione moiety) could be reinforcing the affinity. A comparison of the binding affinities of compounds **55** ( $K_i = 75.75$  nM), **85** ( $K_i = 0.96$  nM) and risperidone ( $K_i = 5.22$  nM) indicates that the quinazolinedione moiety might be a better contributor towards high binding affinity at

5-HT<sub>2A</sub> receptors than the 2-methyl-6,7,8,9-tetrahydro-4*H*-pyrido[1,2-*a*]pyrimidin-4-one ring system of risperidone.

The functional activity data of the hybrid compounds suggested that compound **85** is a partial agonist at the 5-HT<sub>2A</sub> receptor. The observed efficacy could be due to its activity at GIRK4\* entirely that masks the potential antagonist activity of the compound (thus making it a potential partial agonist; Figure 27) or a combination of the two (making it a low-efficacy partial agonist). However, with the binding affinity data in hand, if we consider the current efficacy as the G<sub>αq</sub>-mediated activity at 5-HT<sub>2A</sub> receptors, compound **85** shows potential to be a low-efficacy partial agonist. However, both its structural halves are composed of ligands (left half: ketanserin and right half: risperidone), which are known to be antagonists at the 5-HT<sub>2A</sub> receptor.

According to previously published reports the quinazolinedione moiety can be a part of agonists, partial agonists or antagonists, depending upon the moiety attached to the other end (Figure 52). In fact, RH-34 (**103**) is known as a selective, potent partial agonist at 5-HT<sub>2A</sub> receptors (Figure 52).

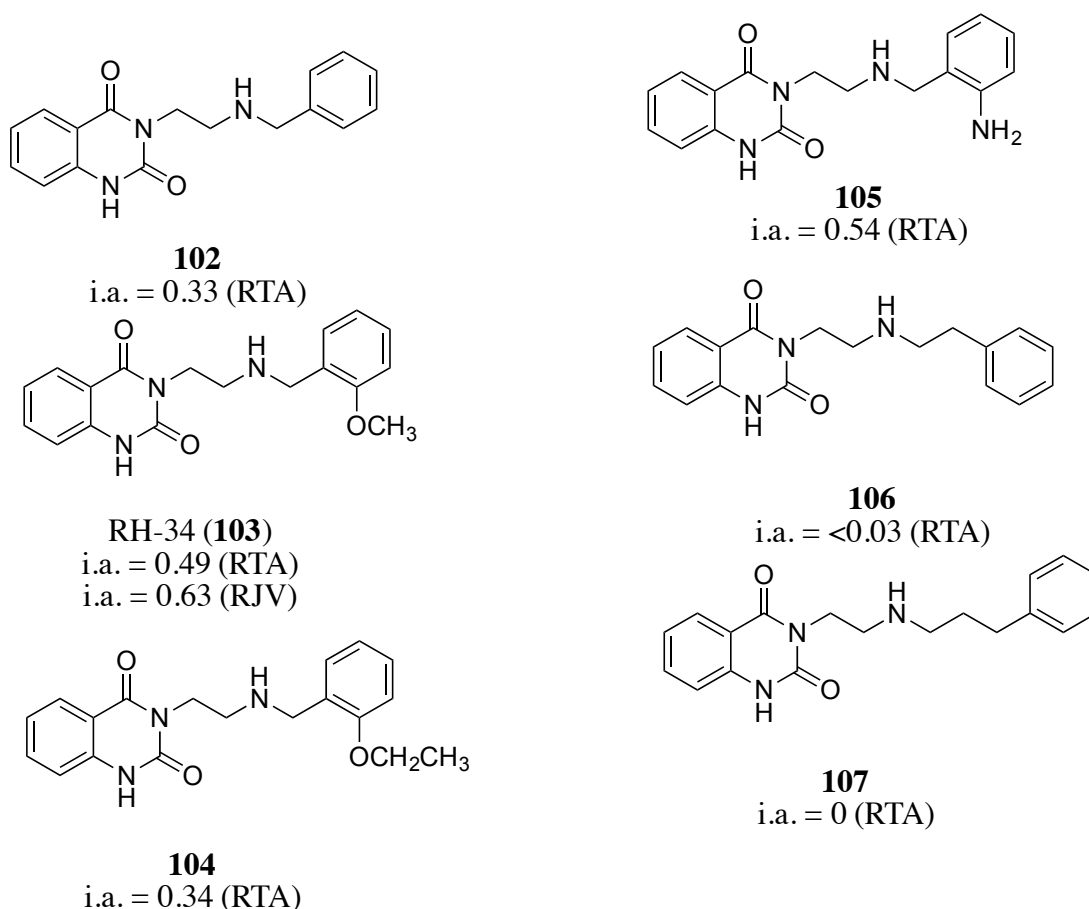


**Figure 52.** The range of efficacies (intrinsic activities) that the quinazolinedione moiety can be a part of. The intrinsic activity (i.a.) was measured using either rat tail artery (RTA) or rat jugular vein (RJV).<sup>203,204</sup>

Thus the quinazolinedione moiety does not seem to influence the action of the compounds (Figure 52) and the action is likely determined by the moiety linked to it or the functional group on those moieties. The functional activity of compound **85**, (which has the 2,4-quinazolinedione moiety as its left half) could be influenced by its right half, which is 6-fluoro-(3-piperidiny)benz[*d*]isoxazole or compound **55**. The functional activity data as it

currently stands, could imply that **85** is a low-efficacy partial agonist or it is an antagonist (if the efficacy shown is due to activity at GIRK4\*). We can speculate the same about compound **55**. If **85** and **55** are antagonists (Iwamura et al.<sup>164</sup> had reported **55** to be an antagonist), it suggests that the quinazolinedione moiety in **85**, as portrayed for other quinazolinedione-containing compounds (Figure 52), might not influence its action and the activity could be due to the 6-fluoro-(3-piperidinyl)benz[*d*]isoxazole moiety attached to it.

Compound **84** shows a functional activity similar to risperidone in the TEVC assay system (Figure 35). However, as the binding affinity and functional activity of 2-methyl-6,7,8,9-tetrahydro-4*H*-pyrido[1,2-*a*]pyrimidin-4-one ring system is forthcoming, we cannot conclude on the structural half contributing to its activity. However, there is literature evidence that the 6-fluoro-(3-piperidinyl)benz[*d*]isoxazole moiety is a more potent antagonist at 5-HT<sub>2A</sub> receptors than the 4-fluorobenzoylpiperidine moiety. As the current functional data (Figure 35) indicates that **84** antagonizes the 5-HT mediated activity more potently than **85**, this suggests that perhaps the left half of **84** (2-methyl-6,7,8,9-tetrahydro-4*H*-pyrido[1,2-*a*]pyrimidin-4-one ring system) could be influencing the activity of this compound.

Forthcoming binding affinity data and functional activity studies will guide us as regards making a conclusive argument about the precise role of various structural elements of risperidone in its activity at the receptor. However, with the biological data currently in



hand, it does seem that the entire intact structure of risperidone might not be required for its activity and its affinity at 5-HT<sub>2A</sub> receptors.

The ability of compound **55** to crosstalk in a system co-expressing 5-HT<sub>2A</sub> receptors and mGlu<sub>2</sub> receptors is promising in terms of the fact that established inverse agonists at 5-HT<sub>2A</sub> receptors such as clozapine and risperidone also exhibit this crosstalk. It would mean that this portion of risperidone, could be sufficient for its inverse agonist activity at 5-HT<sub>2A</sub> receptors.

## CHAPTER VI: EXPERIMENTALS

### A. Synthesis:

Melting points (mp) were measured on the Thomas Hoover melting point apparatus and are uncorrected. Proton NMR ( $^1\text{H}$  NMR) spectra were recorded with a Bruker ARX 400 MHz spectrometer using trimethylsilane (TMS) as an internal standard, with peak positions indicated by parts per million ( $\delta$ ). Infrared spectroscopy was conducted on a Thermo Nicolet iS10 FT-IR. Electrospray ionization-mass spectrometry studies were conducted using a Waters Acquity TDQ (tandem quadrupole) spectrometer in positive ion mode. Elemental analyses (CHN) determined the purity of the compounds and was performed by Altantic Microlab Inc. and the obtained values were within 0.4% of theoretical values. Reactions were monitored by thin-layer chromatography (TLC) on silica gel GHLF plates (250  $\mu\text{m}$ , 2.5 x 10 cm; Analtech Inc. Newark, DE), and flash chromatography was performed on a CombiFlash Companion/TS (Teledyne Isco Inc. Lincoln, NE) using packed silica gel (Silica Gel 230-400 mesh) columns (RediSep Rf Normal-phase Silica Flash Column, Teledyne Isco Inc., Lincoln, NE).

**6-Fluoro-3-(piperidin-4-yl)benz[*d*]isoxazole hydrochloride (55).**

Compound **80** (0.10 g, 0.40 mmol) was added to a stirred solution of HCl (12 N, 0.14 mL) and EtOH (7.0 mL) under an N<sub>2</sub> atmosphere. The reaction mixture was heated at reflux for 3 h and allowed to stand at room temperature for 48 h to afford a buff-colored solid that was recrystallized from EtOH/H<sub>2</sub>O to yield 0.02 g (18%) of compound **55** as a white solid: mp 302-304 °C (lit.<sup>171</sup> 302-306 °C) <sup>1</sup>H (DMSO-*d*<sub>6</sub>): 2.07-2.52 (m, 6H, CH<sub>2</sub>), 3.09 (s, 2H, CH<sub>2</sub>), 3.34-3.58 (m, 1H, CH), 7.33 -7.39 (m, 1H, ArH), 7.73-7.76 (m, 1H, ArH), 8.11-8.14 (m, 1H, ArH), 9.03 (br s, 1H, NH<sup>+</sup>).

**4-(4-(6-Fluorobenz[*d*]isoxazol-3-yl)piperidin-1-yl)-1-(piperidin-1-yl)butan-1-one hydrochloride (56).**

Compound **67** (0.22 g, 1.14 mmol) and 6-fluoro-3-(piperidin-4-yl)benz[*d*]isoxazole (0.25 g, 1.14 mmol) were added to a stirred solution of K<sub>2</sub>CO<sub>3</sub> (0.31 g, 2.26 mmol) and KI (few crystals) in anhydrous MeCN (5 mL). The reaction mixture was allowed to stir in a screw-cap vial at 88 °C for 16 h. The solvent was evaporated under reduced pressure; the residue was suspended in H<sub>2</sub>O and extracted with CHCl<sub>3</sub> (3 x 15 mL). The combined organic portions were washed with H<sub>2</sub>O (3 x 10 mL), dried (Na<sub>2</sub>SO<sub>4</sub>) and evaporated under reduced pressure to yield a buff-colored solid. The solid was dissolved in EtOH (5 mL) and the solution was cooled to 0 °C. A saturated solution of gaseous HCl in Et<sub>2</sub>O (2 mL) was added and the mixture was allowed to stand at room temperature for 3 h. The solvent was evaporated to yield a white solid that was recrystallized from EtOH to yield 0.01 g (3%) of compound **56** as a tan-colored solid: mp 216-218 °C (This compound was

previously prepared in our laboratory as RHV-023 but has not been reported 207-210 °C)  
 $^1\text{H}$  (DMSO- $d_6$ ): 1.43-1.69 (m, 4H, CH<sub>2</sub>), 1.82-2.10 (m, 6H, CH<sub>2</sub>), 2.21-2.24 (m, 2H, CH<sub>2</sub>), 2.82-2.88 (m, 2H, CH<sub>2</sub>), 2.82-2.88 (m, 1H, CH), 3.23-3.26 (m, 2H, CH<sub>2</sub>), 3.40-3.52 (m, 2H, CH<sub>2</sub>), 3.63-3.66 (m, 2H, CH<sub>2</sub>), 3.98-4.02 (m, 2H, CH<sub>2</sub>), 4.48-4.51 (m, 2H, CH<sub>2</sub>), 7.29-7.38 (m, 1H, ArH), 7.70-7.76 (m, 1H, ArH), 8.05-8.18 (m, 1H, ArH), 10.17 (br s, 1H, NH<sup>+</sup>) Anal Calcd for (C<sub>21</sub>H<sub>28</sub>FN<sub>3</sub>O<sub>2</sub>·HCl·0.5H<sub>2</sub>O) C, 60.21; H, 7.02; N, 9.77. Found: C, 60.32; H, 7.22; N, 10.03.

**6-Fluoro-3-(1-(4-(piperidin-1-yl)butyl)piperidin-4-yl)benz[*d*]isoxazole (57).**

A 1M solution of BH<sub>3</sub> in THF (1.41 mL) was added to a stirred solution of the free base of 4-(4-(6-fluorobenz[*d*]isoxazol-3-yl)piperidin-1-yl)-1-(piperidin-1-yl)butan-1-one (**56**) (0.13 g, 0.35 mmol) in anhydrous THF (4 mL) at 0 °C (ice-bath). The reaction mixture was allowed to warm to room temperature and stirring was continued for 10 h. The reaction mixture was carefully quenched with 6 M aqueous HCl (0.40 mL, vigorous bubbling occurred) and heated at reflux for 1 h. The mixture was allowed to cool to room temperature and basified with 1N aqueous NaOH (2 mL). H<sub>2</sub>O (10 mL) was added and the aqueous layer was extracted with EtOAc (3 x 15 mL). The organic portion was combined, dried (Na<sub>2</sub>SO<sub>4</sub>), and solvent was removed under reduced pressure to give an oily residue. The oily residue was dissolved in absolute EtOH and HCl-anhydrous Et<sub>2</sub>O was added to afford a solid. Recrystallization from absolute EtOH/anhydrous Et<sub>2</sub>O gave 0.04 g (26%) of **57** as yellow crystals: mp 270-273 °C;  $^1\text{H}$ -NMR (DMSO- $d_6$ : salt)  $\delta$  1.37 (m, 1H, CH<sub>2</sub>), 1.68-1.78 (m, 10H, CH<sub>2</sub>), 2.17-2.20 (m, 2H, CH<sub>2</sub>), 2.38-2.53 (m, 2H, CH<sub>2</sub>), 2.83 (m, 2H,

CH<sub>2</sub>), 3.01-3.10 (m, 7H, CH, CH<sub>2</sub>), 3.36-3.46 (m, 1H, CH<sub>2</sub>), 3.58-3.61 (m, 2H, CH<sub>2</sub>), 7.32 (td,  $J = 9.1, 2.0$  Hz, 1H, ArH), 7.71 (dd,  $J = 9.0, 1.9$  Hz, 1H, ArH), 8.25 (dd,  $J = 8.6, 5.4$  Hz, 1H, ArH), 10.33 (br s, 1H, NH), 11.06 (br s, 1H, NH) Anal. Calcd (C<sub>21</sub>H<sub>30</sub>FN<sub>3</sub>O·2HCl·0.25H<sub>2</sub>O) C, 57.73; H, 7.50; N, 9.62. Found: C, 57.36; H, 7.21; N, 9.30.

**6-Fluoro-3-(1-methylpiperidin-4-yl)benz[*d*]isoxazole hydrochloride (58).**

6-Fluoro-3-(piperidin-4-yl)benz[*d*]isoxazole (the free base of compound **55**) (0.20 g, 0.90 mmol) was added to a stirred solution of HCOOH (0.2 mL, 5.45 mmol) and HCHO (0.2 mL, 5.45 mmol) in EtOH under an N<sub>2</sub> atmosphere. The reaction mixture was heated at reflux for 10 h and the solvent was evaporated to yield a white-colored solid. The solid was dissolved in EtOH (5 mL) and cooled to 0 °C. A saturated solution of gaseous HCl in Et<sub>2</sub>O (2 mL) was added and the mixture was allowed to stand at room temperature for 3 h. The solvent was evaporated to yield a white solid that was recrystallized from EtOH to yield 0.01 g (4%) of **58** as a white solid: mp 218-220 °C (This compound was previously prepared in our laboratory as RHV-008 but has not been reported 225-227 °C) <sup>1</sup>H (DMSO-*d*<sub>6</sub>): 2.20-2.25 (m, 4H, CH<sub>2</sub>), 2.20-2.23 (m, 1H, CH), 2.80 (s, 3H, CH<sub>3</sub>), 3.09-3.19 (m, 2H, CH<sub>2</sub>), 3.53-3.56 (m, 2H, CH<sub>2</sub>), 7.33-7.38 (m, 1H, ArH), 7.73-7.75 (dd,  $J = 2, 8$  Hz, 1H, ArH), 8.15-8.18 (m, 1H, ArH), 10.64 (br s, 1H, NH+) Anal Calcd for (C<sub>13</sub>H<sub>15</sub>FN<sub>2</sub>O·HCl·0.5H<sub>2</sub>O) C, 55.82; H, 6.13; N, 10.01. Found: C, 55.50; H, 6.08; N, 9.69.0

**(±)4-(4-(6-Fluorobenz[*d*]isoxazol-3-yl)piperidin-1-yl)-1-(3-hydroxypiperidin-1-yl)butan-1-one hydrogen oxalate (59).**

Compound **75** (0.37 g, 1.82 mmol) and 6-fluoro-3-(piperidin-4-yl)benz[*d*]isoxazole (the free base of compound **55**) (0.40 g, 1.82 mmol) were added to a stirred solution of K<sub>2</sub>CO<sub>3</sub> (0.50 g, 3.63 mmol) and KI (few crystals) in MeCN (4 mL). The reaction mixture was allowed to stir in a screw-cap vial for 45 h at 88 °C, cooled to room temperature and the excess solvent was evaporated under reduced pressure to afford a white solid. The residue was suspended in H<sub>2</sub>O (10 mL) and extracted with CHCl<sub>3</sub> (3 x 25 mL). The combined organic portion was washed with H<sub>2</sub>O (3 x 15 mL), brine (5 mL), dried (Na<sub>2</sub>SO<sub>4</sub>) and evaporated under reduced pressure to yield a pale yellow-colored oil, which was purified by flash chromatography (silica gel; CHCl<sub>3</sub>/MeOH; 9.5:0.5) to afford a colorless oil. The oil was dissolved in EtOAc (5 mL) and cooled to 0 °C. A saturated solution of oxalic acid (1.2 eq) in Et<sub>2</sub>O was added and the reaction mixture was allowed to stir at room temperature overnight. The precipitate was collected by filtration to yield a white solid, which upon recrystallization from EtOH/Et<sub>2</sub>O afforded 0.03 g (4%) of **59** as a white solid: mp 182-184 °C. <sup>1</sup>H NMR (DMSO-*d*<sub>6</sub>): 1.31-1.41 (m, 2H, CH<sub>2</sub>), 1.65-1.86 (m, 4H, CH<sub>2</sub>), 2.12-2.24 (m, 4H, CH<sub>2</sub>), 2.40-2.70 (m, 2H, CH<sub>2</sub>), 2.40-2.70 (m, 1H, CH), 3.00-3.18 (m, 6H, CH<sub>2</sub>), 3.33-3.49 (m, 6H, CH<sub>2</sub>), 7.30-7.33 (t, *J* = 12 Hz, 1H, ArH), 7.70-7.72 (d, *J* = 8 Hz, 1H, 1ArH), 7.89-8.19 (m, 1H, ArH) Anal Calcd for (C<sub>21</sub>H<sub>28</sub>FN<sub>3</sub>O<sub>3</sub>·C<sub>2</sub>H<sub>2</sub>O<sub>4</sub>) C, 57.61; H, 6.31; N, 8.76. Found: C, 57.57; H, 6.26; N, 8.58. MS calculated: [M+H]<sup>+</sup> = 390.2187, MS found: [M+H]<sup>+</sup> = 390.2195.

### **3-(Piperidin-4-yl)benz[*d*]isoxazole hydrochloride (60).**

A solution of KOH (85%) was added to a stirred solution of compound **83** (0.14 g, 0.45 mmol) in absolute EtOH (3 mL) under an N<sub>2</sub> atmosphere. The reaction mixture was heated at reflux for 48 h and cooled to room temperature. The solvent was removed under reduced pressure and the aqueous mixture was extracted with EtOAc (3 x 15 mL). The combined organic portion was dried (Na<sub>2</sub>SO<sub>4</sub>), and evaporated under reduced pressure to yield a brown-colored oil. The oil was dissolved in absolute EtOH (2 mL) and cooled to 0 °C. A saturated solution of gaseous HCl in Et<sub>2</sub>O (2 mL) was added and the reaction mixture was allowed to stir at room temperature overnight. The precipitate was collected by filtration to yield a buff-colored solid, which upon recrystallization from MeOH-Et<sub>2</sub>O afforded 0.02 g (20%) of **60** as a white solid: mp 304-306 °C (lit.<sup>171</sup> 313-315 °C) <sup>1</sup>H NMR (DMSO-*d*<sub>6</sub>): 2.18-2.19 (m, 4H, CH<sub>2</sub>), 2.18-2.19 (m, 1H, CH) 3.10-3.17 (m, 2H, CH<sub>2</sub>), 3.38-3.47 (m, 2H, CH<sub>2</sub>), 7.40-7.44 (t, *J* = 8 Hz, 1H, ArH), 7.67-7.69 (m, 1H, ArH), 7.74-7.76 (m, 1H, ArH), 8.07-8.09 (d, *J* = 8 Hz, 1H, ArH), 9.15 (s, 1H, NH, D<sub>2</sub>O ex).

### **3-(1-Methylpiperidin-4-yl)benz[*d*]isoxazole hydrochloride (61).**

A solution of KOH (85%) was added to a stirred solution of compound **82** (0.20 g, 0.78 mmol) and hydroxylamine hydrochloride (0.11 g, 1.67 mmol) in ethoxyethanol (3 mL)-H<sub>2</sub>O (2 mL) under an N<sub>2</sub> atmosphere. The reaction mixture was heated at reflux for 6 h, cooled to room temperature, quenched by addition of ice-H<sub>2</sub>O (50 mL) and extracted with Et<sub>2</sub>O (3 x 40 mL). The combined organic portion was washed with H<sub>2</sub>O (3 x 20 mL), brine (5 mL), dried (Na<sub>2</sub>SO<sub>4</sub>) and evaporated to yield an orange-colored oil. The oil was

dissolved in EtOH (2 mL) and cooled to 0 °C. A saturated solution of gaseous HCl in Et<sub>2</sub>O (2 mL) was added to yield a white solid, which upon recrystallization from EtOH/Et<sub>2</sub>O afforded 0.04 g (23%) of **61** as a white solid: mp 248-250 °C (lit.<sup>171</sup> 250-252 °C) <sup>1</sup>H NMR (DMSO-*d*<sub>6</sub>): 2.25-2.35 (m, 4H, CH<sub>2</sub>), 2.25-2.35 (m, 1H, CH) 2.73-2.88 (m, 3H, CH<sub>3</sub>), 3.09-3.25 (m, 2H, CH<sub>2</sub>), 3.43-3.62 (m, 2H, CH<sub>2</sub>), 7.40-7.44 (t, *J* = 8 Hz, 1H, ArH), 7.65-7.69 (m, 1H, ArH), 7.74-7.76 (m, 1H, ArH), 8.08-8.21 (m, 1H, ArH), 10.95 (s, 1H, NH, D<sub>2</sub>O ex).

#### **4-Chloro-1-(piperidin-1-yl)butan-1-one (67).**

Piperidine (**68**) (1.2 mL, 11.54 mmol) was added in a dropwise manner to a stirred solution of Et<sub>3</sub>N (1.2 mL, 11.54 mmol) in CH<sub>2</sub>Cl<sub>2</sub> (25 mL) and the reaction mixture was cooled to 0 °C under an N<sub>2</sub> atmosphere. A solution of 4-chlorobutyryl chloride (1.5 mL, 11.74 mmol) in CH<sub>2</sub>Cl<sub>2</sub> (5 mL) was added and the reaction mixture was allowed to stir at room temperature for 75 h and washed with H<sub>2</sub>O (2 x 25 mL). The organic portion was dried (Na<sub>2</sub>SO<sub>4</sub>) and evaporated under reduced pressure to yield a yellow-colored oil, which was purified by vacuum distillation to yield 1.00 g (45%) of **67** as a pale yellow-colored oil: bp 103 °C at 0.02 psi.

#### **(±)4-Chloro-1-(3-hydroxypiperidin-1-yl)butan-1-one (74).**

A solution of 4-chlorobutyryl chloride (1.39 g, 9.88 mmol) in CH<sub>2</sub>Cl<sub>2</sub> (20 mL) was added in a dropwise manner to a solution of (±)3-hydroxypiperidine (**69**) (1.00 g, 9.88 mmol) and Et<sub>3</sub>N (1.01 g, 9.98 mmol) in anhydrous CH<sub>2</sub>Cl<sub>2</sub> (25 mL). The reaction mixture was allowed



to stir at room temperature for 16 h, quenched by addition of H<sub>2</sub>O (20 mL), and extracted with CH<sub>2</sub>Cl<sub>2</sub> (3 x 15 mL). The combined organic portion was washed with H<sub>2</sub>O (3 x 20 mL), brine (5 mL), dried (Na<sub>2</sub>SO<sub>4</sub>) and evaporated under reduced pressure to yield a yellow-colored oil, which was purified by flash chromatography (silica gel; CHCl<sub>3</sub>/MeOH; 9.5:5) to afford 0.65 g (32%) of **74** as a colorless oil, which was used without further characterization in the preparation of compound **59**.

***N*-Formylpiperidine-4-carboxylic acid (**76**).**

A stirred solution of HCOOH (15 mL, 371.63 mmol) and Ac<sub>2</sub>O (35 mL, 371.63 mmol) was heated at 60 °C for 1 h and cooled to 0 °C (ice-bath). Isonipecotic acid (**75**) (8.00 g, 61.93 mmol) was added and the reaction mixture was allowed to stir at room temperature for 16 h. The solvent was removed by vacuum distillation to yield a white solid that was recrystallized from *i*-PrOH to yield 6.00 g of **76** (66%) as a white solid: mp 136-138 °C (lit.<sup>171</sup> 136-138 °C).

***N*-Formylpiperidine-4-carboxylic acid chloride (**77**).**

In a 3-neck flask, SOCl<sub>2</sub> (4.50 mL, 6.37 mmol) was added in a dropwise manner to a stirred solution of compound **76** (5.00 g, 3.18 mmol) in DMF (0.6 mL) under an N<sub>2</sub> atmosphere and cooled to 0 °C (ice-bath). The reaction mixture was allowed to stir at room temperature for 6 h. SOCl<sub>2</sub> was evaporated under reduced pressure to afford 5.00 g (90%) of 1-formylpiperidine-4-carboxylic acid chloride (**77**) as a yellow-colored oil, which was

verified spectrally and used without further characterization in the preparation of compound **78**.

***N*-Formyl-4-(2,4-difluorobenzoyl)piperidine (**78**).**

In a 3-neck flask, AlCl<sub>3</sub> (5.70 g, 4.27 mmol) was added to a stirred solution of compound **77** (5.00 g, 2.85 mmol) in 1,3-difluorobenzene (18 mL) and ClCH<sub>2</sub>CH<sub>2</sub>Cl (5 mL) under an N<sub>2</sub> atmosphere and the reaction mixture was heated at reflux for 45 h. The reaction mixture was cooled to room temperature, quenched by the careful addition of ice/H<sub>2</sub>O (50 mL) and extracted with CHCl<sub>3</sub> (3 x 50 mL). The combined organic portion was washed with H<sub>2</sub>O (3 x 50 mL), brine (5 mL), dried (Na<sub>2</sub>SO<sub>4</sub>), and evaporated under reduced pressure to yield 3.00 g of a brown-colored oil, which was purified by column chromatography (silica gel; hexanes/EtOAc; 0.4:0.6) to afford 0.75 g of a colorless oil which, when triturated with petroleum ether, afforded 0.75 g (8%) of **78** as a white solid: mp 60-62 °C (lit.<sup>171</sup> 64-66 °C).

***N*-Formyl-4-((2,4-difluorophenyl)(hydroxyimino)methyl)piperidine (**79**).**

In a 3-neck flask, compound **78** (0.50 g, 1.97 mmol) was added to a stirred solution of hydroxylamine hydrochloride (0.41 g, 5.91 mmol) in EtOH (10 mL) under an N<sub>2</sub> atmosphere. A solution of NaOH (0.24 g, 6.00 mmol) in H<sub>2</sub>O (1.5 mL) was added and the reaction mixture was heated at reflux for 96 h. The reaction mixture was allowed to cool to room temperature and filtered. The filtrate was evaporated under reduced pressure to yield

a yellow-colored solid that was recrystallized from H<sub>2</sub>O to yield 0.42 g of **79** (79%) as a white solid: mp 178-180 °C (lit.<sup>171</sup> 182-184 °C).

***N*-Formyl-4-(6-fluorobenz[*d*]isoxazol-3-yl)piperidine (**80**).**

Toluene washed NaH (0.06 g, 2.50 mmol) was added to a stirred solution of compound **79** (0.20 g, 0.75 mmol) in anhydrous DMF (10 mL) and the stirred reaction mixture was heated at 75 °C for 4 h. The reaction mixture was allowed to stir at room temperature for 48 h, quenched with H<sub>2</sub>O (25 mL) and extracted with EtOAc (3 x 20 mL). The combined organic portion was washed with H<sub>2</sub>O (3 x 20 mL), brine (5 mL), dried (Na<sub>2</sub>SO<sub>4</sub>), and evaporated under reduced pressure to yield 0.12 g of **80** (67%) as an orange oil. The structure was verified spectrally and used crude in the preparation of compound **55**. <sup>1</sup>H (CDCl<sub>3</sub>-*d*<sub>1</sub>): 1.80-1.89(m, 2H, CH<sub>2</sub>), 1.90-2.14(m, 2H, CH<sub>2</sub>), 2.45(s, 2H, CH<sub>2</sub>), 3.23-3.37(m, 2H, CH<sub>2</sub>), 3.74-3.77 (m, 1H, CH), 4.36-4.39(m, 1H, CHO), 6.99-7.02 (m, 1H, ArH), 7.54-7.57 (m, 1H, ArH), 7.99-8.08 (m, 1H, ArH).

**(2-Fluorophenyl)(1-methylpiperidin-4-yl)methanone (**82**).**

In a 3-neck flask, 4-chloro-*N*-methylpiperidine (**81**) (1 g, 7.48 mmol) in anhydrous THF (3 mL) was added in a dropwise manner to a stirred mixture of Mg (0.23 g, 9.51 mmol) in anhydrous THF (1 mL) and bromoethane (few drops) under an N<sub>2</sub> atmosphere and the reaction was initiated by a warm H<sub>2</sub>O bath. After complete addition of 4-chloro-*N*-methylpiperidine (**81**), the reaction mixture was heated at reflux for 1 h, cooled to room temperature and 2-fluorobenzonitrile (0.91 g, 7.48 mmol) in anhydrous THF (2 mL) was

added. The reaction was heated at reflux for 3 h, the reaction mixture was allowed to stir at room temperature for 36 h and quenched by addition of  $\text{NH}_4\text{Cl}$  (2.93 g in 10 mL  $\text{H}_2\text{O}$ ). The reaction mixture was heated on a  $\text{H}_2\text{O}$  bath for 2 h, cooled to room temperature and extracted with  $\text{Et}_2\text{O}$  (3 x 20 mL). The combined organic portion was washed with  $\text{H}_2\text{O}$  (3 x 15 mL), brine (5 mL), dried ( $\text{Na}_2\text{SO}_4$ ) and evaporated to yield a brown-colored oil, which was purified by column chromatography (silica gel;  $\text{CHCl}_3$ : $\text{MeOH}$ : 9.2:0.8) to yield a brown-colored oil. The oil was dissolved in  $\text{EtOH}$  (5 mL) and cooled to 0 °C. A saturated solution of gaseous  $\text{HCl}$  in  $\text{Et}_2\text{O}$  (2 mL) was added to yield a orange-colored solid, which was allowed to stir overnight with  $\text{Et}_2\text{O}$  to yield 0.22 g (12%) of **82** as an orange solid: mp 162-166 °C (lit.<sup>171</sup> 167-169 °C).

**Phenyl 4-(benz[*d*]isoxazol-3-yl)piperidine-1-carboxylate (83).**

An aqueous solution of compound **61** (0.23 g, 0.91 mmol) was basified with  $\text{NaOH}$  (1M, to pH 9) and extracted with toluene (4 mL). The organic portion was dried ( $\text{Na}_2\text{SO}_4$ ), filtered and added to a stirred solution of phenyl chloroformate under an  $\text{N}_2$  atmosphere. The stirred reaction mixture was heated at reflux for 22 h, cooled to room temperature and filtered. The filtrate was evaporated under reduced pressure to yield a yellow-colored oil. The oil was dissolved in  $\text{Et}_2\text{O}$  and petroleum ether was added to afford 0.15 g (52%) compound **83** as a buff solid: mp 91-92 °C (lit.<sup>171</sup> 96-98 °C).

**3-[2-[4-(6-Fluoro-1,2-benzisoxazol-3-yl)-1-piperidinyl]ethyl]-2,4(1*H*,3*H*)-quinazolinedione hydrochloride (85).**

Compound **95** (0.15 g, 0.79 mmol) was added to a stirred solution of 6-fluoro-3-(piperidin-4-yl)benz[*d*]isoxazole (the free base of compound **55**) (0.17 g, 0.79 mmol) in anhydrous toluene (3.6 mL). The reaction mixture was allowed to stir in a screw-cap vial for 44 h at 100 °C. The excess toluene was removed under reduced pressure to yield a white-colored solid. The solid was dissolved in HCl (12 N) and cooled to 0 °C. The solvent was removed under reduced pressure to yield a white solid that was recrystallized from EtOH/H<sub>2</sub>O to yield 0.05 g (27%) of **85** as a white solid: mp 268-270 °C. <sup>1</sup>H NMR (DMSO-*d*<sub>6</sub>): 2.15-2.22 (m, 2H, CH<sub>2</sub>), 2.30-2.34 (m, 3H, CH<sub>2</sub>), 3.17-3.23 (m, 2H, CH<sub>2</sub>), 3.46-3.50 (m, 3H, CH<sub>2</sub>), 3.87-3.90 (m, 2H, CH<sub>2</sub>), 4.32-4.33 (m, 2H, CH<sub>2</sub>), 7.23-7.25 (d, *J* = 8 Hz, 2H, ArH), 7.37-7.38 (d, *J* = 4 Hz, 1H, ArH), 7.69-7.74 (m, 2H, ArH), 7.97-7.99 (d, *J* = 8 Hz, 1H, ArH), 8.11-8.14 (dd, *J* = 4, 8 Hz, 1H, ArH), 9.81 (br, s, 1H, NH<sup>+</sup>, D<sub>2</sub>O ex) Anal Calcd for (C<sub>22</sub>H<sub>21</sub>FN<sub>4</sub>O<sub>3</sub>·HCl) C, 59.39; H, 4.98; N, 12.59. Found: C, 59.33; H, 5.14; N, 12.52.

**4-(6-Fluoro-[1*H*]-indol-3-yl)-1,2,3,6-tetrahydropyridine hydrogen oxalate (88).**

6-Fluoroindole (**96**) (0.25 g, 1.85 mmol) was added to a stirred solution of 4-piperidone monohydrate hydrochloride (0.72 g, 4.70 mmol) and KOH (0.55 g, 9.82 mmol) in anhydrous MeOH (6 mL) under an N<sub>2</sub> atmosphere. The stirred reaction mixture was heated at reflux for 5 h, quenched by addition of H<sub>2</sub>O (25 mL) and allowed to stir at room temperature overnight. The precipitate was collected by filtration, washed with H<sub>2</sub>O to yield 0.20 g of a yellow-colored solid. The solid was dissolved in anhydrous MeOH (3

mL) and the solution was cooled to 0 °C. A solution of oxalic acid (1 equivalent) in MeOH was added and the reaction mixture was allowed to stir at room temperature overnight to yield a yellow-colored solid, which upon recrystallization from EtOH/H<sub>2</sub>O afforded 0.03 g (43%) of **88** as a yellow solid: mp 224 °C. <sup>1</sup>H NMR (DMSO-*d*<sub>6</sub>): 2.61 (s, 2H, CH<sub>2</sub>), 3.20-3.23 (t, *J* = 4, 2H, CH<sub>2</sub>), 3.66 (s, 2H, CH<sub>2</sub>), 6.16 (s, 1H, CH), 6.89-6.94 (td, *J* = 4, 8, 1H, ArH), 7.16-7.19 (dd, *J* = 12 Hz, 1H, ArH), 7.46-7.47 (d, *J* = 4 Hz, 1H, ArH), 7.79-7.83 (m, 1H, ArH), 11.27 (s, 1H, NH<sup>+</sup>, D<sub>2</sub>O ex) Anal. Calcd for (C<sub>13</sub>H<sub>13</sub>N<sub>2</sub>F·0.5C<sub>2</sub>H<sub>2</sub>O<sub>4</sub>·0.25H<sub>2</sub>O) C, 63.26; H, 5.49; N, 10.54. Found: C, 63.05; H, 5.43; N, 10.16.

#### **6-Fluoro-3-(piperidin-4-yl)-1*H*-indole (89).**

A saturated solution of gaseous HCl in EtOH (12 mL) was added to a stirred solution of the free base of compound **88** (0.12 g, 2.312 mmol) in MeOH (12 mL). 10% Pd/C (0.018 g) was added and the reaction mixture was reduced in a Parr hydrogenator at 44 psi for 20 h. The reaction mixture was filtered and the filtrate was evaporated under reduced pressure. The residue was dissolved in H<sub>2</sub>O (10 mL), the solution was basified with NaOH (1N, to pH 8) and extracted with EtOAc (3 x 20 mL). The combined organic portion was washed with H<sub>2</sub>O (3 x 10 mL), dried (Na<sub>2</sub>SO<sub>4</sub>) and evaporated under reduced pressure to give a yellow-colored solid, which upon recrystallization from EtOH afforded 0.02 g (15%) of **89** as a pale yellow-colored solid: mp 216-218 °C (lit.<sup>205</sup> mp 214-216 °C) <sup>1</sup>H NMR (DMSO-*d*<sub>6</sub>): 1.54-1.65 (m, 2H, CH<sub>2</sub>), 1.87-1.89 (m, 2H, CH<sub>2</sub>), 2.66-2.73 (m, 2H, CH<sub>2</sub>), 2.81-2.89 (m, 1H, CH), 3.07 (m, 2H, CH<sub>2</sub>), 6.79-6.84 (m, 1H, ArH), 7.06-7.12 (m, 2H, ArH), 7.53-7.57 (m, 1H, ArH), 10.90 (s, 1H, NH<sup>+</sup>, D<sub>2</sub>O ex).

**5-Methoxy-3-(piperidin-4-yl)benz[d]isoxazole hydrochloride (90).**

Compound **101** (0.089 g, 0.55 mmol) was added to a stirred solution of HCl (12 N, 0.10 mL) and EtOH (5.0 mL) under an N<sub>2</sub> atmosphere. The reaction mixture was heated at reflux for 3 h and allowed to stand at room temperature for 48 h to afford a brown-color oil. The oil was dissolved in EtOAc (2 mL) and the solution was cooled to 0 °C. A saturated solution of HCl/Et<sub>2</sub>O was added and the reaction mixture was allowed to stir at room temperature overnight. The precipitate was collected by filtration to yield a pale yellow solid, which upon recrystallization from acetone afforded 0.012 g (13%) of **90** as an off-white solid: mp 265-270 °C (lit.<sup>171</sup> 270-274 °C, MeOH/Et<sub>2</sub>O) <sup>1</sup>H (DMSO-*d*<sub>6</sub>): 1.39-1.58 (m, 2H, CH<sub>2</sub>), 1.79-1.97 (m, 2H, CH<sub>2</sub>), 2.03 (s, 3H, OCH<sub>3</sub>), 2.70-2.76 (m, 1H, CH), 3.17-3.24 (m, 1H, CH<sub>2</sub>), 3.65-3.67 (m, 1H, CH<sub>2</sub>), 3.88-3.91 (m, 1H, CH<sub>2</sub>), 4.41-4.44 (m, 1H, CH<sub>2</sub>), 6.84 -6.86 (m, 1H, ArH), 7.01-7.03 (m, 1H, ArH), 7.26 (s, 1H, ArH), 9.20 (br s, 1H, NH<sup>+</sup>).

**3-[2-[4-(6-Fluoro[1H]indol-3-yl)-1-piperidinyl]ethyl]-6,7,8,9-tetrahydro-2-methyl-4H-pyrido[1,2-*a*]pyrimidin-4-one hydrochloride (91).**

In a 2-neck flask, 3-(2-chloroethyl)-2-methyl-6,7,8,9-tetrahydro-4H-pyrido[1,2-*a*]pyrimidin-4-one (**92**) (0.20 g, 0.88 mmol) and compound **89** (0.19 g, 0.88 mmol) were added to a stirred solution of K<sub>2</sub>CO<sub>3</sub> (0.12 g, 0.882 mmol) and KI (few crystals) in anhydrous MeCN (18 mL) under an N<sub>2</sub> atmosphere. The stirred reaction mixture was heated at reflux for 45 h, cooled to room temperature and the solvent was evaporated under reduced pressure. The residue was suspended in H<sub>2</sub>O and extracted with CHCl<sub>3</sub> (3 x 50

mL). The combined organic portion was washed with H<sub>2</sub>O (3 x 50 mL), dried (Na<sub>2</sub>SO<sub>4</sub>) and evaporated under reduced pressure to yield a yellow-colored solid. The solid was dissolved in anhydrous Et<sub>2</sub>O (2 mL) and cooled to 0 °C. A saturated solution of gaseous HCl in Et<sub>2</sub>O (2 mL) was added and the reaction mixture was allowed to stir at room temperature overnight. The precipitate was collected by filtration to yield a yellow-colored solid, which upon recrystallization from EtOH/H<sub>2</sub>O afforded 0.05 g (37%) of **91** as a yellow solid: mp 279-281 °C. <sup>1</sup>H (DMSO-*d*<sub>6</sub>): 1.62-1.68 (m, 2H, CH<sub>2</sub>), 1.68-1.79 (m, 2H, CH<sub>2</sub>), 1.83-1.94 (m, 4H, CH<sub>2</sub>), 2.11-2.16 (m, 2H, CH<sub>2</sub>), 2.21(s, 3H, CH<sub>2</sub>), 2.36-2.40 (m, 2H, CH<sub>2</sub>), 2.59-2.63 (m, 2H, CH<sub>2</sub>), 2.74-2.78 (m, 3H, CH<sub>2</sub>), 3.01-3.04 (m, 2H, CH<sub>2</sub>), 3.77-3.80 (t, *J* = 4 Hz, 2H, CH<sub>2</sub>), 6.78-6.84 (m, 1H, ArH), 7.08-7.11(m, 2H, ArH), 7.51-7.54 (dd, *J* = 4 Hz, 1H, ArH), 10.37 (br, s, 1H, NH<sup>+</sup>, D<sub>2</sub>O ex), 10.98 (s, 1H, NH, D<sub>2</sub>O ex) Anal. Calcd. for (C<sub>24</sub>H<sub>29</sub>N<sub>4</sub>OF·2HCl·0.5H<sub>2</sub>O) C, 58.77; H, 6.57; N, 11.42 Found: C, 58.78; H, 6.61; N, 11.22.

**3-(2-(1-Piperidinyl)ethyl)-2,4(1*H*,3*H*)-quinazolinedione hydrochloride (94).**

Compound **95** (0.10 g, 0.54 mmol) was added to piperidine (**68**) (3 mL) and the stirred reaction mixture was heated at reflux for 4 h. The excess piperidine was removed under reduced pressure to yield a tan-colored solid. The solid was dissolved in anhydrous Et<sub>2</sub>O (5 mL) and cooled to 0 °C. A saturated solution of gaseous HCl in Et<sub>2</sub>O (2 mL) was added and the reaction mixture was allowed to stir at room temperature overnight. The precipitate was collected by filtration to yield a white solid that was recrystallized from absolute EtOH to yield 0.06 g (75%) of **94** as a white solid: mp 274-276 °C (lit.<sup>143</sup> 276-278 °C). <sup>1</sup>H



NMR (DMSO-*d*<sub>6</sub>): 1.38-1.44 (m, 1H, CH<sub>2</sub>), 1.62-1.85 (m, 3H, CH<sub>2</sub>), 1.82-1.85 (m, 2H, CH<sub>2</sub>), 2.90-2.98 (m, 2H, CH<sub>2</sub>), 3.34-3.35 (m, 2H, CH<sub>2</sub>), 3.62-3.65 (m, 2H, CH<sub>2</sub>), 4.25- 4.28 (m, 2H, CH<sub>2</sub>), 7.22-7.26 (m, 2H, ArH), 7.68-7.72 (t, *J* = 8 Hz, 1H, ArH), 7.95-7.97 (d, *J* = 8 Hz, 1H, ArH), 9.38 (br s, 1H, NH<sup>+</sup>, D<sub>2</sub>O ex), 11.60 (s, 1H, NH<sup>+</sup>, D<sub>2</sub>O ex).

### **2,3-Dihydro-5*H*-oxazolo[2,3-*b*]quinazolin-5-one (95).**

3-(2-Chloroethyl)-2,4(1*H*,3*H*)quinazolinedione (**93**) (0.30 g, 1.33 mmol) was added to a stirred solution of K<sub>2</sub>CO<sub>3</sub> (0.18 g, 1.33 mmol) in anhydrous acetone (9 mL). The stirred reaction mixture was heated at reflux for 2 h, cooled to room temperature and evaporated under reduced pressure. The residue was suspended in H<sub>2</sub>O and extracted with CH<sub>2</sub>Cl<sub>2</sub> (3 x 10 mL). The combined organic portion was washed with H<sub>2</sub>O (3 x 10 mL), dried (Na<sub>2</sub>SO<sub>4</sub>) and evaporated to dryness under reduced pressure to yield 0.19 g (77 %) of **95** as a white solid: mp 159-162 °C (lit.<sup>143</sup> 160-162 °C), which was used without further purification in the preparation of compounds **85** and **94**.

### **1-Acetylpiperidine-4-carboxylic acid (97).**

A stirred solution of isonipecotic acid (**75**) (8.0 g, 61.93 mmol) and EtOAc (24 mL) was cooled to 0 °C (ice-bath). Then Ac<sub>2</sub>O (8.7 mL, 92.89 mmol) was added and the reaction mixture was allowed to stir at 5 °C for 0.16 h. The stirred reaction solution was heated at 60 °C for 2 h and cooled to room temperature. The precipitate was collected by filtration, washed with diisopropyl ether to yield 10.2 g of **97** (96%) as a white solid: mp 182-184 °C (lit.<sup>171</sup> 180-182 °C), which was used crude in the preparation of compound **98**.

### **1-Acetylpiperidine-4-carboxylic acid chloride (98).**

In a 3-neck flask,  $\text{SOCl}_2$  (61 mL, 6.37 mmol) was added to a stirred solution of **97** (10.0 g, 58.41 mmol) in  $\text{ClCH}_2\text{CH}_2\text{Cl}$  (24 mL) under an  $\text{N}_2$  atmosphere and the reaction mixture was allowed to stir at room temperature for 6 h. The precipitate was collected by filtration to yield 10.50 g of **98** (95%) as a white solid: mp 138-140 °C (lit.<sup>171</sup> 133-138 °C), which was used crude in the preparation of compound **99**.

### **1-Acetyl-4-(2-hydroxy-5-methoxybenzoyl)piperidine (99).**

In a 3-neck flask,  $\text{AlCl}_3$  (14.06 g, 105.46 mmol) was added to a stirred solution of compound **98** (1.00 g, 52.73 mmol), 1,3-dimethoxybenzene (7.28 g, 52.73 mmol) and  $\text{ClCH}_2\text{CH}_2\text{Cl}$  (5 mL) under an  $\text{N}_2$  atmosphere and the reaction mixture was heated at reflux for 45 h. The reaction mixture was cooled to room temperature, quenched by the careful addition of ice/ $\text{H}_2\text{O}$  (50 mL) and the aqueous portion was extracted with  $\text{CHCl}_3$  (3 x 50 mL). The combined organic portion was washed with  $\text{H}_2\text{O}$  (3 x 50 mL), brine (5 mL), dried ( $\text{Na}_2\text{SO}_4$ ), and evaporated under reduced pressure to yield a pale yellow-colored oil which, when triturated with petroleum ether, afforded a pale yellow solid, which upon recrystallization with EtOH yielded 0.20 g (13%) of **99** as a yellow solid: mp 93-95 °C (lit.<sup>171</sup> 93-94 °C).

**1-Acetyl-4-((2-hydroxy-5-methoxyphenyl)(hydroxyimino)methyl)piperidine (100).**

In a 3-neck flask, **99** (0.20 g, 3.61 mmol) was added to a stirred solution of hydroxylamine hydrochloride (0.29 g, 4.26 mmol) in EtOH (16 mL) under an N<sub>2</sub> atmosphere. A solution of NH<sub>4</sub>OAc (0.61 g, 7.94 mmol) in H<sub>2</sub>O (4.80 mL) was added and the reaction mixture was heated at reflux for 36 h. The reaction mixture was allowed to cool to room temperature and filtered. The filtrate was evaporated under reduced pressure to yield a yellow-colored solid that was recrystallized from H<sub>2</sub>O to yield 0.12 g of **100** (54%) as a yellow solid: mp 196-200 °C (lit.<sup>171</sup> 193-196 °C), which was converted to the acetate salt: mp 208-210, and used crude in the preparation of compound **101**.

**1-Acetyl-4-(5-methoxybenz[*d*]isoxazol-3-yl)piperidine (101).**

Toluene-washed NaH (0.011 g, 0.463 mmol) was added to a stirred solution of the acetate salt of compound **100** (0.15 g, 0.42 mmol) in anhydrous DMF (2 mL) and the stirred reaction mixture was heated at reflux for 6 h. The reaction mixture was allowed to stir at room temperature for 24 h, quenched by pouring in H<sub>2</sub>O (25 mL) and the reaction mixture was extracted with EtOAc (3 x 20 mL). The combined organic portion was washed with H<sub>2</sub>O (3 x 20 mL), brine (5 mL), dried (Na<sub>2</sub>SO<sub>4</sub>), and evaporated under reduced pressure to yield 0.09 g of **101** (81%) as a brown oil, which was verified spectrally and used crude in the preparation of compound **90**.

## **B. Molecular modeling studies:**

The primary sequence of the human 5-HT<sub>2A</sub> receptor was obtained from the Universal Protein Resource (UniProt) (entry code: P28223; *Homo sapiens*) in the FASTA format. The amino acid sequence of the crystal structure of the 5-HT<sub>2B</sub> receptor (PDB ID: 4IB4) was retrieved from the Protein Data Base (PDB). During crystallization, residues Y249-V313 (ICL3) of the 5-HT<sub>2B</sub> receptor were replaced with A1-L106 of BRIL.<sup>187,206</sup> These residues were deleted from the amino acid sequence file of the crystal structure of the 5-HT<sub>2B</sub> receptor prior to sequence alignment. Multiple sequence alignment of the 5-HT<sub>2B</sub> receptor amino acid sequence with the 5-HT<sub>2A</sub> receptor sequence was performed with the software ClustalX2.0, which provided output in the form of .ps, .aln and .dnd files. One hundred homology models of the 5-HT<sub>2A</sub> receptor were generated using the software package Modeller 9.12<sup>207</sup> (version 9.12; University of California San Francisco, San Francisco, CA). Modeller processes the sequence alignment in the form of the .ali format, which, along with the sequence alignment also includes details about the template, and the protein of interest.

The model for comparing the binding pocket of the receptor to previously published 5-HT<sub>2A</sub> homology models was chosen based on the discrete optimized protein energy (DOPE) scores and the models were further examined by docking studies of ketanserin.

The ligands were built using the sketch feature within SYBYL-X 2.1 (Tripos International, St. Louis, MO, USA), and were energetically minimized using the Tripos Force Field

[Gasteiger-Hückel charges, the dielectric constant ( $\epsilon$ ) = 4, the non bonded interaction cutoff = 8 Å and was terminated at an energy gradient of 0.05 kcal/(mol\*Å)] feature within SYBYL-X 2.1.

Molecular docking was performed using the GOLD scoring function within the genetic algorithm docking program GOLD<sup>208</sup> (Version 5.3; Cambridge Crystallographic Data Centre, Cambridge, UK). The binding pocket was defined to include all atoms within 10-Å of the  $\alpha$ -carbon atom of the highly conserved D155 (TM3). The docking solutions were sorted by cluster docking (the script was provided by Dr. Philip D. Mosier) and examined on SYBYL-X 2.1) The models chosen (based on binding interactions and their GOLD scores) were merged with the ligands and energetically minimized using the Tripos Force Field (Gasteiger Hückel charges, distance-dependent dielectric constant = 4.0). The models were further evaluated by HINT analysis<sup>194</sup> (as implemented within SYBYL 8.1) to quantify the ligand-receptor interactions and the model with the highest HINT scores was chosen for every ligand under the study. PyMOL was used to generate images.<sup>209</sup>

### **C. Functional activity studies:**

#### **a. Calcium imaging epifluorescence assay:**

##### **Measurements of Intracellular $\text{Ca}^{2+}$**

Cells (HEK293 cells) were plated on 96-well dishes the day before the experiment. The next day cells were switched to serum-free medium for about 3-4 hours, before being loaded with 5  $\mu\text{M}$  Fura2-AM (Molecular Probes, OR) in Imaging Solution (125 mM NaCl,

5 mM KCl, 2 mM CaCl<sub>2</sub>, 1 mM MgSO<sub>4</sub>, 6 mM glucose, and 25 mM Hepes/Tris, pH 7.4). Following incubation for 30 min at 37°C, cells were washed with imaging solution and kept at room temperature for about 15 min before being placed on the stage of an epifluorescence microscope, coupled to an automatic perfusion system.

The Fura-2 signal was acquired at 510 nm by switching the excitation wavelength between 340 nm and 380 nm. Intracellular calcium concentration was expressed as a 340/380 nm ratio and values were normalized to the basal 340/380 nm ratio level before perfusion of the drug. Results were expressed as mean  $\pm$  SEM. Statistical significance was determined by two-tailed Student's *t* test. IC<sub>50</sub> values are obtained by analysis in GraphPad PRISM (version 6.00 for Mac OS X, GraphPad Software, La Jolla California, US).<sup>210</sup>

#### **b. Electrophysiology studies:**

The electrophysiological functional assay studies were conducted in the *Xenopus laevis* heterologous oocyte system expressing the 5-HT<sub>2A</sub> and the GIRK4\* channels. After they were enzymatically isolated, the oocytes were microinjected with 1-2 ng cRNA constructs. The oocytes were then incubated for 2 days at 18 °C for expression. Responses were recorded by conventional two-electrode voltage clamp (TEVC) assay with a GeneClamp500 amplifier (Axon Instruments) 3-5 days after cRNA injection. A high potassium concentration solution containing 96 KCl, 1NaCl, MgCl<sub>2</sub>, 5 KOH/HEPES, in mM) was used to record basal channel expression levels and a 3mM BaCl<sub>2</sub> was used to block the GIRK4\* currents.<sup>173</sup>

#### **D. Radioligand binding studies:**

The radioligand binding studies were performed in HEK293 cells transiently transfected with the N-terminally c-Myc-tagged form of wild type human 5-HT<sub>2A</sub> receptor (pcDNA3.1-c-Myc-5HT2A) using Lipofectamine 2000 reagent (Invitrogen). The cell pellets were homogenized using a Teflon-glass grinder (10 up-and-down strokes at 1500 rpm) after 48 hours in 1 mL of binding buffer (50 mM Tris-HCl, pH 7.4), supplemented with 0.25 M sucrose. The crude homogenate was centrifuged at 1000 g for 5 min at 4 °C, and the supernatant was centrifuged at 40,000 g for 15 min at 4 °C. The resultant pellet (P<sub>2</sub> fraction) was washed twice in homogenization buffer and re-centrifuged in similar conditions. Aliquots were stored at 80 °C until assay. Curves were carried out by incubating each drug ( $10^{-10}$ – $10^{-4}$  M; 13 concentrations) in binding buffer containing 2 nM [<sup>3</sup>H]-ketanserin. Nonspecific binding was determined in the presence of 10 μM methylsergide (Tocris). Competition curves were analyzed by nonlinear regression by GraphPad PRISM (version 6.00 for Mac OS X, GraphPad Software, La Jolla California, US) to derive dissociation constants for high ( $K_{i-high}$ ) and low ( $K_{i-low}$ ) affinity states of the receptor<sup>211</sup> that were reported only as a single  $K_i$  value in Tables/Figures. The equation for the curve fitting:  $\log EC_{50} = \log (10^{\log K_i} * (1 + \text{Radioligand NM} / \text{Hot} K_d \text{ NM}))$

$$Y = \text{Bottom} + (\text{Top} - \text{Bottom}) / (1 + 10^{-(X - \log EC_{50})}).$$

## **Bibliography**



## Bibliography

1. Millier, A.; Schmidt, U.; Angermeyer, M. C.; Chauhan, D.; Murthy, V.; Toumi, M.; Cadi-Soussi, N. Humanistic burden in schizophrenia: A literature review. *J. Psychiatr. Res.* **2014**, *54*, 85-93.
2. Heinrichs, R. W. Historical origins of schizophrenia: Two early madmen and their illness. *J. Hist. Behav. Sci.* **2003**, *39*, 349-363.
3. Insel, T. R. Rethinking schizophrenia. *Nature* **2010**, *468*, 187-193.
4. Whitaker, R. *Anatomy of an epidemic: Magic bullets, psychiatric drugs, and the astonishing rise of mental illness in America*; Broadway Books: New York, 2010.
5. Miyamoto, S.; Duncan, G. E.; Marx, C. E.; Lieberman, J. A. Treatments for schizophrenia: A critical review of pharmacology and mechanisms of action of antipsychotic drugs. *Mol. Psychiatry* **2005**, *10*, 79-104.
6. Meert, T. F.; Awouters, F. Central 5-HT<sub>2</sub> antagonists: A preclinical evaluation of a therapeutic potential. *Acta Neuropsychiatr.* **1990**, *2*, 101-109.
7. Meltzer, H. Y. What's atypical about atypical antipsychotic drugs? *Curr. Opin. Pharmacol.* **2004**, *4*, 53-57.

8. Leysen, J. E.; Janssen, P. M. F.; Megens, A. A.; Schotte, A. Risperidone: A novel antipsychotic with balanced serotonin-dopamine antagonism, receptor occupancy profile and pharmacological activity. *J. Clin. Psychiatry* **1994**, *55*, 5-12.
9. Fribourg, M.; Moreno, J. L.; Holloway, T.; Provasi, D.; Baki, L.; Mahajan, R.; Park, G.; Adney, S. K.; Hatcher, C.; Eltit, J. M.; Ruta, J. D.; Albizu, L.; Li, Z.; Umali, A.; Shim, J.; Fabiato, A.; MacKerell, A. D., Jr.; Brezina, V.; Sealfon, S. C.; Filizola, M.; González-Maeso, J.; Logothetis, D. E. Decoding the signaling of a GPCR heteromeric complex reveals a unifying mechanism of action of antipsychotic drugs. *Cell* **2010**, *147*, 1011-1023.
10. Geller, J. L. The last half-century of psychiatric services as reflected in psychiatric services. *Psychiatr. Serv.* **2000**, *51*, 41-67.
11. De Jong, G. A. The use of psychic energizers in general practice. *J. Neuropsychiatry* **1961**, *2*, 55-57.
12. McDonagh, M.; Peterson, K.; Carson, S.; Fu, R.; Thakurta, S. *Drug class review: Atypical antipsychotic drugs: Final update 3 report*; Oregon Health & Science University: Portland, OR, 2010.
13. World Health Organization. *Mental Health Action Plan 2013-2020*.  
[http://apps.who.int/iris/bitstream/10665/89966/1/9789241506021\\_eng.pdf](http://apps.who.int/iris/bitstream/10665/89966/1/9789241506021_eng.pdf) (accessed Oct 24, 2015).
14. Kessler, R. C.; Aguilar-Gaxiola, S.; Alonso, J.; Chatterji, S.; Lee, S.; Ormel, J.; Ustun, T. B.; Wang, P. S. The global burden of mental disorders: An update from the WHO World Mental Health (WMH) surveys. *Epidemiol. Psychiatr. Soc.* **2009**, *18*, 23-33.

15. Bassuk, E. L.; Gerson, S. Deinstitutionalization and mental health services. *AMHC Forum* **1978**, *31*, 39-46.
16. Corrigan, P.; Gelb, B. Three programs that use mass approaches to challenge the stigma of mental illness. *Psychiatr. Serv.* **2006**, *57*, 393-398.
17. Takahashi, H.; Ideno, T.; Okubo, S.; Matsui, H.; Takemura, K.; Matsuura, M.; Kato, M.; Okubo, Y. Impact of changing the Japanese term for “schizophrenia” for reasons of stereotypical beliefs of schizophrenia in Japanese youth. *Schizophr. Res.* **2009**, *112*, 149-152.
18. National Alliance of Mental Illness. *Mental illness facts and numbers*.  
[http://www2.nami.org/factsheets/mentalillness\\_factsheet.pdf](http://www2.nami.org/factsheets/mentalillness_factsheet.pdf) (accessed Oct 22, 2015).
19. Drake, R. E.; Skinner, J. S.; Bond, G. R.; Goldman, H. H. Social security and mental illness: Reducing disability with supported employment. *Health Aff. (Millwood)*. **2009**, *28*, 761-770.
20. Reynolds, C. F., III.; Lewis, D. A.; Detre, T.; Schatzberg, A. F.; Kupfer, D. J. The future of psychiatry as clinical neuroscience. *Acad. Med.* **2009**, *84*, 446-450.
21. Ross, D. A.; Travis, M. J.; Arbuckle, M. R. The future of psychiatry as a clinical neuroscience. Why not now? *JAMA Psychiatry* **2015**, *72*, 413-414.
22. Elixhauser, A.; Steiner, C. Readmissions to U.S. hospitals by diagnosis, 2010: Statistical brief #153. In *Healthcare cost and utilization project (HCUP) statistical briefs*; Agency for health care policy and research (US): Rockville, MD, 2006.
23. MacDonald, G. J.; Bartolome, J. M. A decade of progress in the discovery and development of “atypical” antipsychotics. *Prog. Med. Chem.* **2010**, *49*, 37-80.

24. Awouters, F. H. L.; Lewi, P. J. Forty years of antipsychotic drug research - From haloperidol to paliperidone with Dr. Paul Janssen. *Arzneimittelforschung* **2007**, *57*, 625-632.
25. Meltzer, H. Y.; Huang, M. In vivo actions of atypical antipsychotic drug action on serotonergic and dopaminergic systems. *Prog. Brain Res.* **2008**, *172*, 177-197.
26. Weiner, D. M.; Burstein, E. S.; Nash, N.; Croston, G. E.; Currier, E. A.; Vanover, K. E.; Harvey, S. C.; Donohue, E.; Hansen, H. C.; Andersson, C. M.; Spalding, T. A.; Gibson, D. F.; Krebs-Thomson, K.; Powell, S. B.; Geyer, M. A.; Hacksell, U.; Brann, M. R. 5-Hydroxytryptamine<sub>2A</sub> receptor inverse agonists as antipsychotics. *J. Pharmacol. Exp. Ther.* **2001**, *299*, 268-276.
27. Divac, N.; Prostran, M.; Jakovcevski, I.; Cerovac, N. Second-generation antipsychotics and extrapyramidal adverse effects. *BioMed Res. Int.* **2014**, *2014*, 1-6.
28. Jafari, S.; Fernandez-Enright, F.; Huang, X.-F. Structural contributions of antipsychotic drugs to their therapeutic profiles and metabolic side effects. *J. Neurochem.* **2012**, *120*, 371-384.
29. Costa, A. M.; de Lima, M. S.; Mari, J. D. J. A systematic review on clinical management of antipsychotic-induced sexual dysfunction in schizophrenia. *Sao Paulo Med. J.* **2006**, *124*, 291-297.
30. Baldessarini, R. J.; Frankenburg, F. R. Clozapine: A novel antipsychotic agent. *N. Engl. J. Med.* **1991**, *324*, 746-754.
31. McIntyre, R.; Katzman, M. The role of atypical antipsychotics in bipolar depression and anxiety disorders. *Bipolar Disord.* **2003**, *5*, 20-35.

32. Nemeroff, C. B. Use of atypical antipsychotics in refractory depression and anxiety. *J. Clin. Psychiatry* **2005**, *66*, 13-21.
33. Alvir, J. M.; Lieberman, J. A.; Safferman, A. Z.; Schwimmer, J. L.; Schaff, J. A. Clozapine-induced agranulocytosis - Incidence and risk factors in the United States. *N. Engl. J. Med.* **1993**, *329*, 162-179.
34. Lally, J.; MacCabe, J. H. Antipsychotic medication in schizophrenia: A review. *Br. Med. Bull.* **2015**, *114*, 169-179.
35. Meltzer, H. Y. Treatment-resistant schizophrenia - The role of clozapine. *Curr. Med. Res. Opin.* **1997**, *14*, 1-20.
36. Henderson, D. C.; Goff, D. C. Risperidone as an adjunct to clozapine therapy in chronic schizophrenics. *J. Clin. Psychiatry* **1996**, *57*, 395-397.
37. Hasnain, M.; Vieweg, W. V. R.; Hollett, B. Weight gain and glucose dysregulation with second-generation antipsychotics and antidepressants: A review for primary care physicians. *Postgrad. Med.* **2012**, *124*, 154-167.
38. Fulton, B.; Goa, K. L. Olanzapine. A review of its pharmacological properties and therapeutic efficacy in the management of schizophrenia and related psychoses. *Drugs* **1997**, *53*, 281-298.
39. Kirk, S. L.; Glazebrook, J.; Grayson, B.; Neill, J. C.; Reynolds, G. P. Olanzapine-induced weight gain in the rat: Role of 5-HT<sub>2C</sub> and histamine H<sub>1</sub> receptors. *Psychopharmacology* **2009**, *207*, 119-125.

40. Manceaux, P.; Constant, E.; Zdanowicz, N.; Jacques, D.; Reynaert, C. Management of marked liver enzyme increase during olanzapine treatment: A case report and review of the literature. *Psychiatr. Danubina* **2011**, *23*, S15-S17.
41. Dodd, S.; Berk, M. Olanzapine/fluoxetine combination for treatment-resistant depression: Efficacy and clinical utility. *Expert Rev. Neurother.* **2008**, *8*, 1299-1306.
42. Shelton, R. C. Olanzapine/fluoxetine combination for bipolar depression. *Expert Rev. Neurother.* **2006**, *6*, 33-39.
43. Daly, E. J.; Trivedi, M. H. A review of quetiapine in combination with antidepressant therapy in patients with depression. *Neuropsychiatr. Dis. Treat.* **2007**, *3*, 855-867.
44. Kreys, T.-J.; Phan, S. V. A literature review of quetiapine for generalized anxiety disorder. *Pharmacotherapy* **2015**, *35*, 175-188.
45. Corena-McLeod, M. Comparative pharmacology of risperidone and paliperidone. *Drugs R&D* **2015**, *15*, 163-174.
46. Kim, S.-W.; Chung, Y.-C.; Lee, Y.-H.; Lee, J.-H.; Kim, S.-Y.; Bae, K.-Y.; Kim, J.-M.; Shin, I.-S.; Yoon, J.-S. Paliperidone ER versus risperidone for neurocognitive function in patients with schizophrenia: A randomized, open-label, controlled trial. *Int. Clin. Psychopharmacol.* **2012**, *27*, 267-274.
47. Keltner, N. L.; Johnson, V. Aripiprazole: A third generation of antipsychotics begins? *Perspect. Psychiatr. Care* **2002**, *38*, 157-159.
48. Leonhauser, M. Antipsychotics: Multiple indications help drive growth. *PM360*, January 2012, 22-24.

49. Fejgin, K.; Safionov, S.; Palsson, E.; Wass, C.; Engel, J. A.; Svensson, L.; Klammer, D. The atypical antipsychotic aripiprazole, blocks phencyclidine-induced disruption of prepulse inhibition in mice. *Psychopharmacology* **2007**, *191*, 377-385.
50. Nguyen, C. T.; Rosen, J. A.; Bota, R. G. Aripiprazole partial agonism at 5-HT<sub>2C</sub>: A comparison of weight gain associated with aripiprazole adjunctive to antidepressants with high versus low serotonergic activities. *Prim. Care Companion CNS Disord.* **2012**, *14*, 1-48.
51. Citrome, L. A review of aripiprazole in the treatment of patients with schizophrenia or bipolar I disorder. *Neuropsychiatr. Dis. Treat.* **2006**, *2*, 427-443.
52. Harrow, M.; Jobe, T. H. Does long-term treatment of schizophrenia with antipsychotic medications facilitate recovery? *Schizophr. Bull.* **2013**, *39*, 962-965.
53. Tandon, R.; Nasrallah, H. A.; Keshavan, M. S. Schizophrenia, 'just the facts' 5. Treatment and prevention. Past, present and future. *Schizophr. Res.* **2010**, *122*, 1-23.
54. McGorry, P.; Alvarez-Jimenez, M.; Killackey, E. Antipsychotic medication during the critical period following remission from first-episode psychosis: Less is more. *JAMA Psychiatry* **2013**, *70*, 898-900.
55. Tranter, R.; Healy, D. Neuroleptic discontinuation syndromes. *J. Psychopharmacol.* **1998**, *12*, 401-406.
56. Harrow, M.; Jobe, T. H.; Faull, R. N. Do all schizophrenia patients need antipsychotic treatment continuously throughout their lifetime? A 20-year longitudinal study. *Psychol. Med.* **2012**, *42*, 2145-2155.

57. Harrow, M.; Jobe, T. H. Factors involved in outcome and recovery in schizophrenia patients not on antipsychotic medications: A 15-year multifollow-up study. *J. Nerv. Ment. Dis.* **2007**, *195*, 406-414.
58. Zhang, J.-P.; Malhotra, A. K. Pharmacogenetics and antipsychotics: Therapeutic efficacy and side effects prediction. *Expert Opin. Drug Metab. Toxicol.* **2011**, *7*, 9-37.
59. Sawa, A.; Snyder, S. H. Schizophrenia: Diverse approaches to a complex disease. *Science* **2002**, *296*, 692-695.
60. Sanger, D. J. The search for novel antipsychotics: Pharmacological and molecular targets. *Expert Opin. Ther. Targets* **2004**, *8*, 631-641.
61. González-Maeso, J.; Ang, R. L.; Yuen, T.; Chan, P.; Weisstaub, N. V.; López-Giménez, J. F.; Zhou, M.; Okawa, Y.; Callado, L. F.; Milligan, G.; Gingrich, J. A.; Filizola, M.; Meana, J. J.; Sealfon, S. C. Identification of a serotonin/glutamate receptor complex implicated in psychosis. *Nature* **2008**, *452*, 93-97.
62. Scott, L. J. Iloperidone: In schizophrenia. *CNS Drugs* **2009**, *23*, 867-880.
63. Ishibashi, T.; Horisawa, T.; Tokuda, K.; Ishiyama, T.; Ogasa, M.; Tagashira, R.; Matsumoto, K.; Nishikawa, M.; Ueda, Y.; Toma, S.; Oki, H.; Tanno, N.; Saji, I.; Ito, A.; Ohno, Y.; Nakamura, M. Pharmacological profile of lurasidone, a novel antipsychotic agent with potent 5-hydroxytryptamine<sub>7</sub> (5-HT<sub>7</sub>) and 5-HT<sub>1A</sub> receptor activity. *J. Pharmacol. Exp. Ther.* **2010**, *334*, 171-181.
64. Carlsson, M. L.; Carlsson, A.; Nilsson, M. Schizophrenia: From dopamine to glutamate and back. *Curr. Med. Chem.* **2004**, *11*, 267-277.



65. Scarff, J. R.; Casey, D. A. Newer oral atypical antipsychotic agents: A review. *P T.* **2011**, *36*, 832-838.
66. Leucht, S.; Corves, C.; Arbter, D.; Engel, R. R.; Li, C.; Davis, J. M. Second-generation versus first-generation antipsychotic drugs for schizophrenia: A meta-analysis. *Lancet* **2009**, *373*, 31-41.
67. Morris, B. J.; Cochran, S. M.; Pratt, J. A. PCP: From pharmacology to modeling schizophrenia. *Curr. Opin. Pharmacol.* **2005**, *5*, 101-106.
68. Ellaithy, A.; Younkin, J.; González-Maeso, J.; Logothetis, D. E. Positive allosteric modulators of metabotropic glutamate<sub>2</sub> receptors in schizophrenia treatment. *Trends Neurosci.* **2015**, *38*, 506-516.
69. Swanson, C. J.; Bures, M.; Johnson, M. P.; Linden, A.-M.; Monn, J. A.; Schoepp, D. D. Metabotropic glutamate receptors as novel targets for anxiety and stress disorders. *Nat. Rev. Drug Discov.* **2005**, *4*, 131-144.
70. Lavreysen, H.; Ahnaou, A.; Drinkenburg, W.; Langlois, X.; Mackie, C.; Pype, S.; Lutjens, R.; Le Poul, E.; Trabanco, A. A.; Nunez, J. M. C. Pharmacological and pharmacokinetic properties of JNJ-40411813, a positive allosteric modulator of the mGlu<sub>2</sub> receptor. *Pharmacol. Res. Perspect.* **2015**, *3*, 1-15.
71. Verhoest, P. R.; Chapin, D. S.; Corman, M.; Fonseca, K.; Harms, J. F.; Hou, X.; Marr, E. S.; Menniti, F. S.; Nelson, F.; O'Connor, R.; Pandit, J.; Proulx-Lafrance, C.; Schmidt, A. W.; Schmidt, C. J.; Suiciak, J. A.; Liras, S. Discovery of a novel class of phosphodiesterase 10A inhibitors and identification of clinical candidate. *J. Med. Chem.* **2009**, *52*, 5188-5196.

72. Hashimoto, K. Glycine transport inhibitors for the treatment of schizophrenia. *Open Med. Chem. J.* **2010**, *4*, 10-19.
73. Woolley, D. W.; Shaw, E. Some neurophysiological aspects of serotonin. *Br. Med. J.* **1954**, *2*, 122-126.
74. Rapport, M. M. Serum vasoconstrictor (serotonin) the presence of creatinine in the complex; a proposed structure of the vasoconstrictor principle. *J. Biol. Chem.* **1949**, *180*, 961-969.
75. Freyburger, W. A.; Graham, B. E.; Rapport, M. M.; Seay, P. H.; Govier, W. M.; Swoap, O. F.; Vander Brook, M. J. The pharmacology of 5-hydroxytryptamine (serotonin). *J. Pharmacol. Exp. Ther.* **1952**, *105*, 80-86.
76. Glennon, R. A.; Rosecrans, J. A. Speculation on the mechanism of action of hallucinogenic indolealkylamines. *Neurosci. Behav. Rev.* **1981**, *5*, 197-207.
77. Glennon, R. A. Central serotonin receptors as targets for drug research. *J. Med. Chem.* **1987**, *30*, 1-12.
78. Jonnakuty, C.; Gragnoli, C. What do we know about serotonin? *J. Cell Physiol.* **2008**, *217*, 301-306.
79. Nordquist, N.; Orelund, L. Serotonin, genetic variability, behavior and psychiatric disorders - A review. *Upsala. J. Med. Sci.* **2010**, *115*, 2-10.
80. Glennon, R. A.; Dukat, M. Serotonin receptors and drugs affecting serotonergic neurotransmission. In *Foye's Textbook of Medicinal Chemistry*; 7<sup>th</sup> ed.; Williams, D. A. and Lemke, T., Eds.; Lippincot Williams and Wilkins: Baltimore, MD, 2013; pp 365-396.
81. Nichols, D. E. Hallucinogens. *Pharmacol. Ther.* **2004**, *101*, 131-181.

82. Hofmann, A. Psychotomimetic drugs. Chemical and pharmacological aspects. *Acta Physiol. Pharmacol. Neerl.* **1959**, 8, 240-258.
83. Glennon, R. A. Classical hallucinogens: An introductory overview. In *Hallucinogens: An update*. Lin, G. and Glennon, R. A., Eds.; U.S. Government Printing Office: Washington, D. C., 1994; pp 4-32.
84. Glennon, R. A. Do classical hallucinogens act as 5-HT<sub>2</sub> agonists or antagonists? *Neuropsychopharmacology* **1990**, 3, 509-517.
85. Glennon, R. A.; Teitler, M.; McKenney, J. D. Evidence for 5-HT<sub>2</sub> involvement in the mechanism of action of hallucinogenic agents. *Life Sci.* **1984**, 35, 2505-2511.
86. Schreiber, R.; Brocco, M.; Millan, M. J. Blockade of the discriminative stimulus effects of DOI by MDL 100,907 and the “atypical” antipsychotics, clozapine and risperidone. *Eur. J. Pharmacol.* **1994**, 264, 99-102.
87. Kennett, G. A.; Wood, M. D.; Glen, A.; Grewal, S.; Forbes, I.; Gadre, A.; Blackburn, T. P. In vivo properties of SB 200646A, a 5-HT<sub>2C/2B</sub> receptor antagonist. *Br. J. Pharmacol.* **1994**, 111, 797-802.
88. Aghajanian, G. K.; Marek, G. J. Serotonin and hallucinogens. *Neuropsychopharmacology* **1999**, 21, 16S-23S.
89. Geyer, M. A.; Vollenweider, F. X. Serotonin research: Contributions to understanding psychoses. *Trends Pharmacol. Sci.* **2008**, 29, 445-453.
90. Steeds, H.; Carhart-Harris, R. L.; Stone, J. M. Drug models of schizophrenia. *Ther. Adv. Psychopharmacol.* **2015**, 5, 43-58.

91. Aghajanian, G. K.; Marek, G. J. Serotonin model of schizophrenia: Emerging role of glutamate mechanisms. *Brain Res. Rev.* **2000**, *31*, 302-312.
92. González-Maeso, J.; Sealfon, S. C. Psychedelics and schizophrenia. *Trends Neurosci.* **2009**, *32*, 225-232.
93. Coyle, J. T. NMDA receptor and schizophrenia: A brief history. *Schizophr. Bull.* **2012**, *38*, 920-926.
94. Berton, O.; Nestler, E. J. New approaches to antidepressant drug discovery: Beyond monoamines. *Nat. Rev. Neurosci.* **2006**, *7*, 137-151.
95. Isacson, G.; Reutfors, J.; Papadopoulos, F. C.; Osby, U.; Ahlner, J. Antidepressant medication prevents suicide in depression. *Acta Psychiatr. Scand.* **2010**, *122*, 454-460.
96. Castren, E. Is mood chemistry? *Nat. Rev. Neurosci.* **2005**, *6*, 241-246.
97. Charney, D. S. Monoamine dysfunction and the pathophysiology and treatment of depression. *J. Clin. Psychiatry* **1998**, *59*, 11-14.
98. Vaswani, M.; Linda, F. K.; Ramesh, S. Role of selective serotonin reuptake inhibitors in psychiatric disorders: A comprehensive review. *Prog. Neuropsychopharmacol. Biol. Psychiatry* **2003**, *27*, 85-102.
99. Stahl, S. M.; Pradko, J. F.; Haight, B. R.; Modell, J. G.; Rockett, C. B. Learned-Coughlin, S. A. A review of the neuropharmacology of bupropion, a dual norepinephrine and dopamine reuptake inhibitor. *Prim. Care Companion J. Clin. Psychiatry* **2004**, *6*, 159-166.

100. Brunello, N.; Mendlewicz, J.; Kasper, S.; Leonard, B.; Montgomery, S.; Nelson, J.; Paykel, E.; Versiani, M.; Racagni, G. The role of noradrenaline and selective noradrenaline reuptake inhibition in depression. *Eur. Neuropsychopharmacol.* **2002**, *12*, 461-475.
101. Goldberg, J. F.; Thase, M. E. Monoamine oxidase inhibitors revisited: What you should know. *J. Clin. Psychiatry* **2013**, *74*, 189-191.
102. Thase, M. E.; Trivedi, M. H.; Rush, A. J. MAOIs in the contemporary treatment of depression. *Neuropsychopharmacology* **1995**, *12*, 185-219.
103. Nestler, E. J.; Barrot, M.; DiLeone, R. J.; Eisch, A. J.; Gold, S. J.; Monteggia, L. M. Neurobiology of depression. *Neuron* **2002**, *34*, 13-25.
104. Manji, H. K.; Drevets, W. C.; Charney, D. S. The cellular neurobiology of depression. *Nat. Med.* **2001**, *7*, 541-547.
105. Daws, L. C.; Koek, W.; Mitchell, N. C. Revisiting serotonin reuptake inhibitors and the therapeutic potential of “uptake-2” in psychiatric disorders. *ACS Chem. Neurosci.* **2013**, *4*, 16-21.
106. Ramachandriah, C. T.; Subramanyam, N.; Bar, K. J.; Baker, G.; Yeragani, V. K. Antidepressants: From MAOIs to SSRIs and more. *Indian J. Psychiatry* **2011**, *53*, 180-182.
107. Ban, T. A. The role of serendipity in drug discovery. *Dialogues Clin. Neurosci.* **2006**, *8*, 335-344.
108. Jacobsen, E. The early history of psychotherapeutic drugs. *Psychopharmacology* **1986**, *89*, 335-344.
109. American Psychiatric Association. (2013). Diagnostic and statistical manual of mental disorders (5<sup>th</sup> ed.).

110. Etkin, A. Neurobiology of anxiety: From neural circuits to novel solutions? *Depress. Anxiety* **2012**, *29*, 355-358.
111. Milad, M. R.; Rauch, S. L. The role of the orbitofrontal cortex in anxiety disorders. *Ann. N. Y. Acad. Sci.* **2007**, *1121*, 546-561.
112. Akimova, E.; Lanzenberger, R.; Kasper, S. The serotonin<sub>1A</sub> receptor in anxiety disorders. *Biol. Psychiatry* **2009**, *66*, 627-635.
113. Ramboz, S.; Oosting, R.; Amara, D. A.; Kung, H. F.; Blier, P.; Mendelsohn, M.; Mann, J. J.; Brunner, D.; Hen, R. Serotonin receptor<sub>1A</sub> knockout: An animal model of anxiety-related disorder. *Proc. Natl. Acad. Sci. U.S.A.* **1998**, *95*, 14476-14481.
114. Gross, C.; Zhuang, X.; Stark, K.; Ramboz, S.; Oosting, R.; Kirby, L.; Santarelli, L.; Beck, S.; Hen, R. Serotonin<sub>1A</sub> receptor acts during development to establish normal anxiety-like behavior in the adult. *Nature* **2002**, *416*, 396-400.
115. Parsons, L. H.; Kerr, T. M.; Tecott, L. H. 5-HT<sub>1A</sub> receptor mutant mice exhibit enhanced tonic, stress-induced and fluoxetine-induced serotonergic neurotransmission. *J. Neurochem.* **2001**, *77*, 607-617.
116. Koen, N.; Stein, D. J. Pharmacotherapy of anxiety disorders: A critical review. *Dialogues Clin. Neurosci.* **2011**, *13*, 423-437.
117. Artigas, F.; Perez, V.; Alvarez, E. Pindolol induces a rapid improvement of depressed patients treated with serotonin reuptake inhibitors. *Arch. Gen. Psychiatry* **1994**, *51*, 248-251.
118. Tauscher, J.; Bagby, R. M.; Javanmard, M.; Christensen, B. K.; Kasper, S.; Kapur, S. Inverse relationship between serotonin 5-HT<sub>1A</sub> receptor binding and anxiety: A

[<sup>11</sup>C]WAY-100635 PET investigation in healthy volunteers. *Am. J. Psychiatry* **2001**, *158*, 1326-1328.

119. Kessler, R. C.; Ruscio, A. M.; Shear, K.; Wittchen, H.-C. Epidemiology of anxiety disorders. *Curr. Top. Behav. Neurosci.* **2010**, *2*, 21-35.

120. Freedman, R. Schizophrenia. *N. Engl. J. Med.* **2003**, *349*, 1738-1749.

121. Jablensky, A. The diagnostic concept of schizophrenia: Its history, evolution and future prospects. *Dialogues Clin. Neurosci.* **2010**, *12*, 271-287.

122. Tamminga, C. A.; Holcomb, H. H. Phenotype of schizophrenia: A review and formulation. *Mol. Psychiatry* **2005**, *10*, 27-39.

123. Ross, C. A.; Margolis, R. L.; Reading, S. A. J.; Pletnikov, M.; Coyle, J. T. Neurobiology of schizophrenia. *Neuron* **2006**, *52*, 139-153.

124. Arguello, P. A.; Gogos, J. A. Modeling madness in mice: One piece at a time. *Neuron* **2006**, *52*, 179-196.

125. Carlsson, A. The neurochemical circuitry of schizophrenia. *Pharmacopsychiatry* **2006**, *39*, S10-S14.

126. Fletcher, P. C.; Frith, C. D. Perceiving is believing: A Bayesian approach to explaining the positive symptoms of schizophrenia. *Nat. Rev. Neurosci.* **2009**, *10*, 48-58.

127. Carlsson, A.; Waters, N.; Holm-Waters, S.; Tedroff, J.; Nollson, M.; Carlsson, M. L. Interactions between monoamines, glutamate, and GABA in schizophrenia: New evidence. *Annu. Rev. Pharmacol. Toxicol.* **2001**, *41*, 237-260.

128. Schwartz, T. L.; Sachdeva, S.; Stahl, S. M. Glutamate neurocircuitry: Theoretical underpinnings in schizophrenia. *Front. Pharmacol.* **2012**, *3*, 1-11.

129. Akbarian, S.; Kim, J. J.; Potkin, S. G.; Hetrick, W. P.; Bunney, W. E. J.; Jones, E. G. Maldistribution of interstitial neurons in prefrontal white matter of the brains of schizophrenic patients. *Arch. Gen. Psychiatry* **1996**, *53*, 425-436.
130. Harrison, P. J. The neuropathology of schizophrenia. A critical review of the data and their interpretation. *Brain* **1999**, *122*, 593-624.
131. Bleich, A.; Brown, S. L.; Kahn, R.; van Praag, H. M. The role of serotonin in schizophrenia. *Schizophr. Bull.* **1988**, *14*, 297-315.
132. Meltzer, H. Y.; Stahl, S. M. The dopamine hypothesis of schizophrenia: A review. *Schizophr. Bull.* **1976**, *2*, 19-76.
133. Moncrieff, J. A. A critique of the dopamine hypothesis of schizophrenia and psychosis. *Harvard Rev. Psychiatry* **2009**, *17*, 214-225.
134. Meltzer, H. Y.; Matsubara, S.; Lee, J. C. Classification of typical and atypical antipsychotic drugs on the basis of dopamine D<sub>1</sub> and D<sub>2</sub> and serotonin<sub>2</sub> pK<sub>i</sub> values. *J. Pharmacol. Exp. Ther.* **1989**, *251*, 238-246.
135. Grunder, G.; Hippus, H.; Carlsson, A. The “atypicality” of antipsychotics: A concept re-examined and re-defined. *Nat. Rev. Drug Discov.* **2009**, *8*, 197-202.
136. Richtand, N. M.; Welge, J. A.; Logue, A. D.; Keck, P. E. J.; Strakowski, S. M.; McNamara, R. K. Dopamine and serotonin receptor binding and antipsychotic efficacy. *Neuropsychopharmacology* **2007**, *32*, 1715-1726.
137. Baumeister, A. A.; Hawkins, M. F. The serotonin hypothesis of schizophrenia: A historical case study on the heuristic value of theory in clinical neuroscience. *J. Hist. Neurosci.* **2004**, *13*, 277-291.



138. Keefe, R. S. E.; Bilder, R. M.; Davis, S. M.; Harvey, P. D.; Palmer, B. W.; Gold, J. M.; Meltzer, H. Y.; Green, M. F.; Capuano, G.; Stroup, T. S.; McEvoy, J. P.; Lieberman, J. A. Neurocognitive effects of antipsychotic medications in patients with chronic schizophrenia in the CATIE trial. *Arch. Gen. Psychiatry* **2007**, *64*, 633-647.
139. Aghajanian, G. K.; Marek, G. J. Serotonin, via 5-HT<sub>2A</sub> receptors, increases EPSCs in layer V pyramidal cells of prefrontal cortex by an asynchronous mode of glutamate release. *Brain Res.* **1999**, *825*, 161-171.
140. Nichols, D. E.; Nichols, C. D. Serotonin receptors. *Chem. Rev.* **2008**, *108*, 1614-1641.
141. Leysen, J. E. 5-HT<sub>2A</sub> receptors. *Curr. Drug Targets: CNS Neurol. Disord.* **2004**, *3*, 11-26.
142. Glennon, R. A. Metwally, K.; Dukat, M.; Ismaiel, A. M.; De los Angeles, J.; Herndon, J.; Teitler, M.; Khorana, N. Ketanserin and spiperone as templates for novel serotonin 5-HT<sub>2A</sub> antagonists. *Curr. Top. Med. Chem.* **2001**, *2*, 539-558.
143. Herndon, J. L.; Ismaiel, A. M.; Ingher, S. P.; Teitler, M.; Glennon, R. A. Ketanserin analogues: Structure-affinity relationships for 5-HT<sub>2</sub> and 5-HT<sub>1C</sub> serotonin receptor binding. *J. Med. Chem.* **1992**, *35*, 4903-4910.
144. Awouters, F. The pharmacology of ketanserin, the first selective serotonin S<sub>2</sub> antagonist. *Drug Dev. Res.* **1985**, *6*, 263-300.
145. Glennon, R. A. Discriminative stimulus properties of the serotonergic agent. *Life Sci.* **1986**, *39*, 825-830.

146. Shannon, M.; Battaglia, G.; Glennon, R. A.; Tietler, M. 5-HT<sub>1</sub> and 5-HT<sub>2</sub> binding properties of the derivatives of the hallucinogen 1-(2,5-dimethoxyphenyl)-2-aminopropane (2,5-DMA). *Eur. J. Pharmacol.* **1984**, *102*, 23-29.
147. Appel, N. M.; Mitchell, W. M.; Garlick, R. K.; Glennon, R. A.; Teitler, M.; De Souza, E. B. Autoradiographic characterization of (±)-1-(2,5-dimethoxy-4-[<sup>125</sup>I]iodophenyl)-2-aminopropane ([<sup>125</sup>I]DOI) binding to 5-HT<sub>2</sub> and 5-HT<sub>1C</sub> receptors in rat brain. *J. Pharmacol. Exp. Ther.* **1990**, *255*, 843-857.
148. Leysen, J. E.; Gommeran, W.; Eens, A.; de Chaffoy de Courcelles, D.; Stoof, J. C.; Janssen, P. A. Biochemical profile of risperidone, a new antipsychotic. *J. Pharmacol. Exp. Ther.* **1988**, *247*, 661-670.
149. Leysen, J. E.; Niemegeers, C. J.; Tollenaere, J. P.; Laduron, P. M. Serotonergic component of neuroleptic receptors. *Nature* **1978**, *272*, 168-171.
150. Janssen, P. A.; Niemegeers, C. J.; Awouters, F.; Schellekens, K. H.; Megens, A. A.; Meert, T. F. Pharmacology of risperidone (R 64 766), a new antipsychotic with serotonin S<sub>2</sub> and dopamine D<sub>2</sub> antagonistic properties. *J. Pharmacol. Exp. Ther.* **1988**, *244*, 658-693.
151. Colpaert, F. C.; Janssen, P. A. A. Characterization of LSD-antagonist effects of pirenperone in the rat. *Neuropharmacology* **1983**, *22*, 1001-1005.
152. Colpaert, F. C.; Niemegeers, C. J.; Janssen, P. A. J. A drug discrimination analysis of lysergic acid diethylamide (LSD): In vivo agonist and antagonist effects of purported 5-hydroxytryptamine antagonists and of pirenperone, a LSD antagonist. *J. Pharmacol. Exp. Ther.* **1982**, *221*, 206-214.

153. Meert, T. F.; de Haes, P.; Janssen, P. A. Risperidone (R 64 766), a potent and complete LSD antagonist in drug discrimination by rats. *Psychopharmacology* **1989**, *97*, 206-212.
154. Holohean, A. M.; White, F. J.; Appel, J. B. Dopaminergic and serotonergic mediation of the discriminable effects of ergot alkaloids. *Eur. J. Pharmacol.* **1982**, *81*, 595-602.
155. Leysen, D.; Linders, J. M.; Ottenheijm, H. C. 5-HT<sub>2</sub> antagonists: A concept for the treatment of schizophrenia. *Curr. Pharm. Des.* **1997**, *3*, 367-390.
156. Anderson, K.; Liljefors, T.; Gendertofte, K.; Perregaard, J.; Bogeso, K. P. Development of a receptor-interaction model for serotonin 5-HT<sub>2</sub> receptor antagonists. Predicting selectivity with respect to dopamine D<sub>2</sub> receptors. *J. Med. Chem.* **1994**, *37*, 950-962.
157. Megens, A. A. H. P.; Kennis, L. E. J. Risperidone and related 5-HT<sub>2</sub>/D<sub>2</sub> antagonists: A new type of antipsychotic agent? *Prog. Med. Chem.* **1996**, *33*, 185-232.
158. Leysen, J. E.; Niemegeers, C. J.; Van Nueten, J. M.; Laduron, P. M. [<sup>3</sup>H]Ketanserin (R 41 468), a selective <sup>3</sup>H-ligand for serotonin<sub>2</sub> receptor binding sites. Binding properties, brain distribution, and functional role. *Mol. Pharmacol.* **1982**, *21*, 301-314.
159. Leysen, J. E.; Janssen, P. M. F.; Gommeren, W.; Wynants, J.; Pauwels, P. J.; Janssen, P. A. J. In vitro and in vivo receptor binding and effects on monoamine turnover in rat brain regions of the novel antipsychotics risperidone and ocaperidone. *Mol. Pharmacol.* **1992**, *41*, 494-508.

160. Schotte, A.; de Bruyckere, K.; Janssen, P. F.; Leysen J. E. Receptor occupancy by ritanserine and risperidone measured using ex vivo autoradiography. *Brain Res.* **1989**, *500*, 295-301.
161. Bersani, G.; Bressa, G. M.; Meco, G.; Marini, S.; Pozzi, F. Combined serotonin-5-HT<sub>2</sub> and dopamine-D<sub>2</sub> antagonism in schizophrenia: Clinical, extrapyramidal and neuroendocrine response in a preliminary study with risperidone (R 64 766). *Hum. Psychopharmacol.* **1990**, *5*, 225-231.
162. Gelders, Y. G. Thymosthenic agents, a novel approach in the treatment of schizophrenia. *Br. J. Psychiatry* **1989**, *5*, 33-36.
163. Mannens, G.; Huang, M. L.; Meuldermans, W.; Hendrickx, J.; Woestenborghs, R.; Heykants, J. Absorption, metabolism, and excretion of risperidone in human. *Drug Metab. Dispos.* **1993**, *21*, 1134-1141.
164. Iwamura, I.; Casey, T. C.; Young, R.; Dukat, M.; Teitler, M.; Fadden, J. S. P.; Glennon, R. A. 4-(6-Fluorobenzisoxazol-3-yl)piperidine, a risperidone metabolite with serotonergic activity of potential clinical significance. *Med. Chem. Res.* **1996**, *6*, 593-601.
165. Clarke, W. P.; Chavera, T. A.; Silva, M.; Sullivan, L. C.; Berg, K. A. Signalling profile differences: Paliperidone versus risperidone. *Br. J. Pharmacol.* **2013**, *170*, 532-545.
166. Egan, C. T.; Herrick-Davis, K.; Teitler, M. Creation of a constitutively activated state of the 5-hydroxytryptamine<sub>2A</sub> receptor by site-directed mutagenesis: Inverse agonist activity of antipsychotic drugs. *J. Pharmacol. Exp. Ther.* **1998**, *286*, 85-90.

167. Seifert, R.; Wenzel-Seifert, K. Constitutive activity of G-protein coupled receptors: Cause of disease and common property of wild-type receptors. *Naunyn-Schmeidebergs Arch. Pharmacol.* **2002**, *366*, 381-416.
168. Glennon, R. A.; Young, R. *Drug discrimination: Applications to medicinal chemistry and drug studies*; Wiley: Hoboken, NJ, 2011.
169. Robertson, R. D.; Robert, J. D. Diphenylmethylenepiperidine derivatives. US Patent 5935974, January 30, 1997.
170. Czech, B. P.; Bartsch, R. A. Effect of amines on *O*-benzyl group hydrogenolysis. *J. Org. Chem.* **1984**, *49*, 4076-4078.
171. Strupczewski, J. T.; Alen, R. C.; Gardner, B. A.; Schmid, B. L.; Stache, U.; Glamkowski, E. J.; Jones, M. C.; Ellis, D. B.; Huger, F. P.; Dunn, R. W. Synthesis and neuroleptic activity of 3-(1-substituted-4-piperidiny)-1,2-benzisoxazoles. *J. Med. Chem.* **1985**, *28*, 761-769.
172. Hatcher-Solis, C.; Fribourg, M.; Spyridaki, K.; Younkin, J.; Ellaithy, A.; Xiang, G.; Liapakis, G.; González-Maeso, J.; Zhang, H.; Cui, M.; Logothetis, D. E. G-protein coupled receptor signaling to Kir channels in *Xenopus* oocytes. *Curr. Pharm. Biotechnol.* **2014**, *15*, 987-995.
173. Shah, S. Risperidone and its deconstructed analogs: Functional effects on the 5-HT<sub>2A</sub>R. Masters thesis, Thesis, Virginia Commonwealth University, Richmond, VA, 2015.
174. Keselman, I.; Fribourg, M.; Felsenfeld, D. P.; Logothetis, D. E. Mechanism of PLC-mediated Kir3 current inhibition. *Channels* **2007**, *1*, 113-123.

175. Ariens, E. J. Intrinsic activity: Partial agonists and partial antagonists. *J. Cardiovasc. Pharmacol.* **1983**, *5*, S8-S15.
176. Shutske, G. M.; Setescak, L. L.; Allen, R. C.; Davis, L.; Effland, R. C.; Ranbom, K.; Kitzen, J. M.; Wilker, J. C.; Novick, W. J. J. [(3-Aryl-1,2-benzisoxazol-6-yl)oxy]acetic acids. A new diuretic series. *J. Med. Chem.* **1982**, *25*, 36-44.
177. Taylor, E. W.; Nikam, S.; Weck, B.; Martic, A.; Nelson, D. Relative selectivity of some conformationally constrained tryptamine analogs at 5-HT<sub>1</sub>, 5-HT<sub>1A</sub> and 5-HT<sub>2</sub> recognition sites. *Life Sci.* **1987**, *41*, 1961-1969.
178. Slanina, P.; Bartl, J. Process for making risperidone and intermediates thereof. US Patent 7,405,298 B2, July 29, 2008.
179. Papadopoulos, P. E. Reactions of *O*-aminonitriles with isocyanates. 1. A two-step synthesis of [1,2-*C*]quinazolin-5-(3*H*)one. *J. Heterocycl. Chem.* **1980**, *17*, 1553-1558.
180. Westkaemper, R. B.; Glennon, R. A. Molecular graphics models of members of the 5-HT<sub>2A</sub>, 5-HT<sub>2B</sub> and 5-HT<sub>2C</sub> receptors. *Med. Chem. Res.* **1993**, *3*, 317-334.
181. Universal Protein Research Home Page. <http://www.uniprot.org/> (accessed Dec 24, 2015).
182. Runyon, S. P.; Mosier, P. D.; Roth, B. L.; Glennon, R. A.; Westkaemper, R. W. Potential modes of interaction of 9-aminomethyl-9,10-dihydroanthracene (AMDA) derivatives with the 5-HT<sub>2A</sub> receptor: A ligand structure-affinity relationship, receptor mutagenesis and receptor modeling investigation. *J. Med. Chem.* **2008**, *51*, 6808-6828.

183. Rovati, G. E.; Capra, V.; Neubig, R. R. The highly conserved DRY motif of class A G-protein coupled receptors: Beyond the ground state. *Mol. Pharmacol.* **2007**, *71*, 959-964.
184. Audet, M.; Bouvier, M. Restructuring G-protein coupled receptor activation. *Cell* **2012**, *151*, 14-23.
185. Romero, G.; von Zastrow, M.; Friedman, P. A. Role of PDZ proteins in regulating trafficking, signaling, and function of GPCRs: Means, motif, and opportunity. *Adv. Pharmacol.* **2011**, *62*, 279-314.
186. McRobb, F. M.; Capuano, B.; Crosby, I. T.; Chalmers, D. K.; Yuriev, E. Homology modeling and docking evaluation of aminergic G-protein coupled receptors. *J. Med. Chem.* **2010**, *50*, 626-637.
187. Wacker, D.; Wang, C.; Katritch, V.; Han, G. W.; Huang, X.-P.; Vardy, E.; McCorvy, J. D.; Gao, X.; Zhou, X. E.; Melcher, K.; Zhang, C.; Bai, F.; Yang, L.; Jiang, H.; Roth, B. L.; Cherezov, V.; Stevens, R. C.; Xu, H. E. Structural basis for functional selectivity at serotonin receptors. *Science* **2013**, *340*, 615-619.
188. Wang, C.; Jiang, Y.; Ma, J.; Wu, H.; Wacker, D.; Katritch, V.; Han, G. W.; Liu, W.; Huang, X.-P.; Vardy, E.; McCorvy, J. D.; Gao, X.; Zhou, X. E.; Melcher, K.; Zhang, C.; Bai, F.; Yang, H.; Yang, L.; Jiang, H.; Roth, B. L.; Cherezov, V.; Stevens, R. C.; Xu, H. E. Structural basis for molecular recognition at serotonin human 5-hydroxytryptamine<sub>2A</sub> receptor. *Science* **2013**, *340*, 610-614.

189. Muntasir, H. A.; Rashid, M.; Komiyama, T.; Kawakami, J.; Nagatomo, T. Identification of amino acid residues important for saprogrelate binding to the human 5-hydroxytryptamine<sub>2A</sub> serotonin receptor. *J. Pharmacol. Sci.* **2006**, *102*, 55-63.
190. Wang, C. D.; Gallaher, T. K.; Shih, J. C. Site-directed mutagenesis of the serotonin 5-hydroxytryptamine<sub>2</sub> receptor: Identification of amino acids necessary for ligand binding and receptor activation. *Mol. Pharmacol.* **1993**, *43*, 931-940.
191. Choudhary, M. S.; Craigo, S.; Roth, B. L. Single point mutation (Phe340→Leu340) of a conserved phenylalanine abolishes 4-[<sup>125</sup>I]iodo-(2,5-dimethoxy)phenylisopropylamine and [<sup>3</sup>H]ketanserin binding to 5-hydroxytryptamine<sub>2</sub> receptors. *Mol. Pharmacol.* **1993**, *43*, 755-761.
192. Choudhary, M. S.; Sachs, N.; Uluer, A.; Glennon, R. A.; Westkaemper, R. W.; Roth, B. L. Differential ergoline and ergopeptine binding to 5-hydroxytryptamine<sub>2A</sub> receptors: Ergolines require an aromatic residue at position 340 for high affinity binding. *Mol. Pharmacol.* **1995**, *47*, 450-457.
193. Braden, M. R.; Nichols, D. E. Assessment of the roles of serines 5.43(239) and 5.46(242) for binding and potency of agonist ligands at the human serotonin 5-HT<sub>2A</sub> receptor. *Mol. Pharmacol.* **2007**, *72*, 1200-1209.
194. Kellogg, G. E.; Abraham, D. J. Hydrophobicity: Is Log P (o/w) more than the sum of its parts? *Eur. J. Med. Chem.* **2000**, *35*, 651-661.
195. Kristiansen, K.; Kroeze, W. K.; Willins, D. L.; Gelber, E. I.; Savage, J. E.; Glennon, R. A.; Roth, B. L. A highly conserved aspartic acid (Asp-155) anchors the terminal amine moiety of tryptamines and is involved in membrane targeting of the 5-HT<sub>2A</sub> serotonin



- receptor but does not participate in activation via a “salt-bridge disruption” mechanism. *J. Pharmacol. Exp. Ther.* **2000**, *293*, 735-746.
196. Roth, B. L.; Shoham, M.; Choudhary, M. S.; Khan, N. Identification of conserved aromatic residues essential for agonist binding and second messenger production at 5-hydroxytryptamine<sub>2A</sub> receptors. *Mol. Pharmacol.* **1997**, *52*, 259-266.
197. Almaula, N.; Ebersole, B. J.; Zhang, D.; Weinstein, H.; Sealfon, S. C. Mapping the binding pocket of the serotonin 5-hydroxytryptamine<sub>2A</sub> receptor. Ser3.36 (159) provides a second interaction site for the protonated amine of serotonin but not of lysergic acid diethylamide or bufotenin. *J. Biol. Chem.* **1996**, *271*, 14672-14675.
198. Shapiro, D. A.; Kristiansen, K.; Kroeze, W. K.; Roth, B. L. Differential modes of agonist binding to 5-hydroxytryptamine<sub>2A</sub> serotonin receptors revealed by mutation and molecular modeling of conserved residues in transmembrane region 5. *Mol. Pharmacol.* **2000**, *58*, 877-886.
199. Dezi, C.; Brea, J.; Alvarado, M.; Ravina, E.; Masaguer, C. F.; Loza, M. I.; Sanz, F.; Pastor, M. Multistructure 3D-QSAR studies on a series of conformationally constrained butyrophenones docked into a new homology model of 5-HT<sub>2A</sub> receptor. *J. Med. Chem.* **2007**, *50*, 3242-3255.
200. Kanagarajadurai, K.; Malini, M.; Bhattacharya, A.; Panicker, M. M.; Sowdhamini, R. Molecular modeling and docking studies of human 2-hydroxytryptamine<sub>2A</sub> (5-HT<sub>2A</sub>) receptor for identification of hotspots for ligand binding. *Mol. Biosyst.* **2009**, *5*, 1877-1888.
201. Rozas, I.; Alkorta, I.; Elguero, J. Bifurcated hydrogen bonds: Three-centered interactions. *J. Phys. Chem. A* **1998**, *102*, 9925-9932.

202. Schotte, A.; Janssen, P. F.; Gommeren, W.; Luyten, W. H.; Van Gompel, P.; Lesage, A. S.; De Loore, K.; Leysen, J. E. Risperidone compared to new and reference antipsychotic drugs: In vitro and in vivo receptor binding. *Psychopharmacology* **1996**, *124*, 57-73.
203. Heim, R.; Pertz, H.; Walther, I.; Elz, S. Congeners of 3-(2-benzylaminoethyl)-2,4-quinazolinedione: Partial agonists for rat vascular 5-HT<sub>2A</sub> receptors. *Naunyn-Schmiedebergs Arch. Pharmacol.* **1998**, *358*, R105.
204. Silva, M. E.; Heim, R.; Strasser, A.; Elz, S.; Dove, S. Theoretical studies on the interaction of partial agonists with the 5-HT<sub>2A</sub> receptor. *J. Comp. Aided Mol. Des.* **2011**, *25*, 51-66.
205. Hayashi, R.; Ohmori, E.; Isogaya, M.; Moriwaki, M.; Kumagai, H. Alpha<sub>1B</sub> adrenergic receptor antagonists. US Patent 6,642,228, April 11, 2003.
206. Palczewski, K.; Kiser, P. D. Biochemistry. As good as chocolate. *Science* **2013**, *340*, 562-563.
207. Eswar, N.; Webb, B.; Marti-Ramon, M. A.; Madhusudhan, M. S.; Eramian, D.; Shen, M.; Pieper, U.; Sali, A. Comparative protein structure modeling using MODELLER. *Curr. Protoc. Protein Sci.* **2007**, 2.9.1-2.9.31.
208. Jones, G.; Willett, P.; Glen, R. C.; Leach, A. R.; Taylor, R. Development and validation of a genetic algorithm for flexible docking. *J. Mol. Biol.* **1997**, *267*, 727-748.
209. The PyMOL Molecular Graphics System, Version 1.7.4 Schrödinger, LLC.
210. Baki, L.; Fribourg, M.; Younkin, J.; Eltit, J. M.; Moreno, J. L.; Park, G.; Vysotskaya, Z.; Narahari, A.; Sealfon, S. C.; González-Maeso, J.; Logothetis, D. E. Cross-signaling in

metabotropic glutamate<sub>2</sub> and serotonin<sub>2A</sub> receptor heteromers in mammalian cells. *Pflugers Arch.* **2016** [Online early access] DOI: 10.1007/s00424-015-1780-7. Published online: January 16, 2016.

211. Moreno, J. L.; Muguruza, C.; Umali, A.; Mortillo, S.; Holloway, T.; Pilar-Ceullar, F.; Mocci, G.; Seto, J.; Callado, L. F.; Neve, R. L.; Milligan, G.; Sealfon, S. C. López-Giménez, J. F.; Meana, J. J.; Benson, D. L.; González-Maeso, J. Identification of three residues essential for 5-hydroxytryptamine<sub>2A</sub>-metabotropic glutamate<sub>2</sub> (5-HT<sub>2A</sub>-mGlu<sub>2</sub>) receptor heteromerization and its psychoactive behavioral function. *J. Biol. Chem.* **2012**, *287*, 44301-44319.

## Appendix A

After the dissertation had been written, additional data on the activity of risperidone and compounds **56** and **57** at the GIRK4\* channel in the presence and the absence of the 5-HT<sub>2A</sub> receptor in the TEVC assay system were obtained.

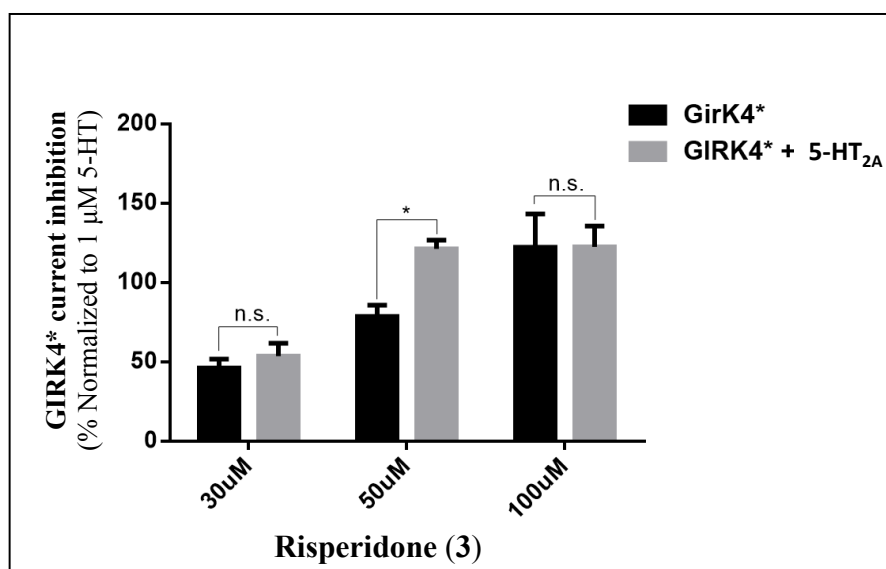


**Figure A1.** Inhibitory action of risperidone (**3**) at the GIRK4\* channel in the presence and the absence of the 5-HT<sub>2A</sub> receptor in the TEVC assay. (N = 4/condition). Data are mean ± SEM, \**p* < 0.05, experiments were replicated in a second batch of oocytes.

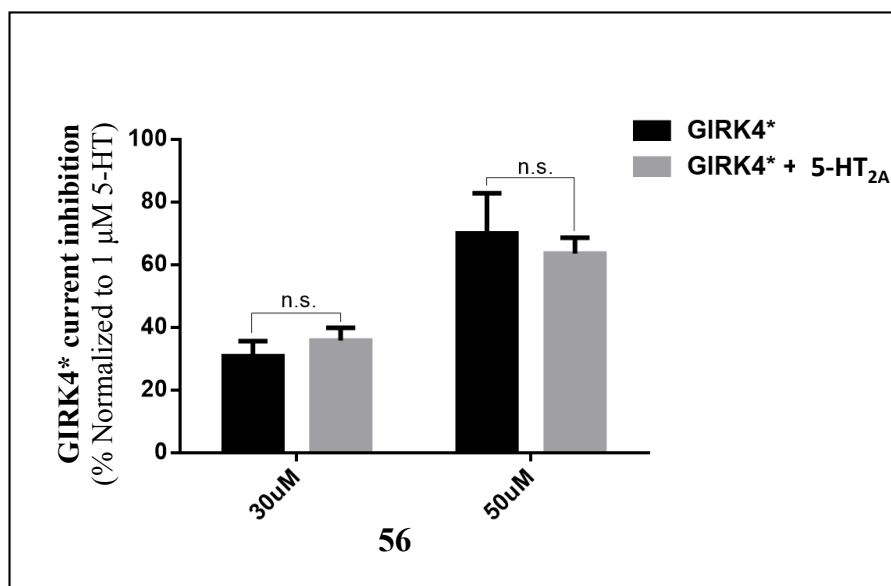


**Figure A2.** Inhibitory action of compound **56** at the GIRK4\* channel in the presence and the absence of the 5-HT<sub>2A</sub> receptor in the TEVC assay. (N = 4/condition). Data are mean ± SEM, \* $p < 0.05$ , experiments were replicated in a second batch of oocytes.

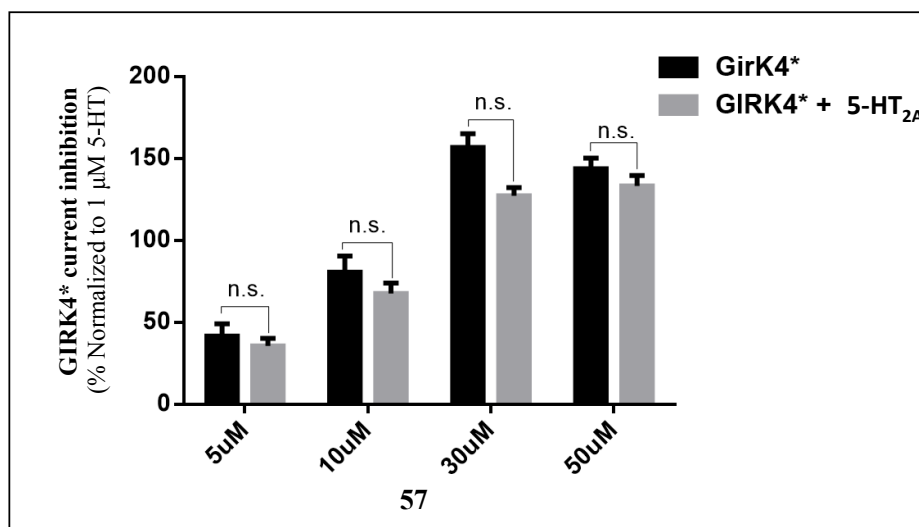


**Figure A3.** Inhibitory action of compound **57** at the GIRK4\* channel in the presence and the absence of the 5-HT<sub>2A</sub> receptor in the TEVC assay. (N = 4/condition). Data are mean ± SEM, \**p* < 0.05, experiments were replicated in a second batch of oocytes.

Risperidone (**3**) was tested at concentrations of 30, 50 and 100 μM (Figure A1), compound **56** was studied at 30 and 50 μM (Figure A2), and compound **57** was tested at 5, 10, 30 and 50 μM (Figure A3). All three compounds showed comparable agonist activity at the GIRK4\* channel in the presence and absence of the 5-HT<sub>2A</sub> receptor. This suggests that the positive efficacy shown by compounds **56** and **57** in the TEVC assay (Figure 27A) could be due to their activity at the GIRK4\* channel instead of G<sub>αq</sub>-mediated activity at the 5-HT<sub>2A</sub> receptor.

The activity seen with compound **57** at 50 μM in Figure 27B was comparable to its activity at GIRK4\* in the absence of the 5-HT<sub>2A</sub> receptor when studied at 50 μM (Figure A3). The

above information coupled with the high binding affinity of compound **57** at the receptor (Figure 30 and Table 4) imply that compound **57** might not be a superagonist or an allosteric modulator as speculated earlier, and that the 5-HT- potentiating activity seen at the concentration of 50  $\mu$ M (Figure 27B) could be solely due to its activity at the GIRK4\* channel. As a consequence, the IC<sub>50</sub> values shown in Table 4 for the TEVC assay might not be valid.

## VITA

Supriya Ajit Gaitonde was born on September 11, 1989 in Mumbai, India to the parents Shyamala and Ajit Gaitonde, and is an Indian citizen. She received a Bachelor of Pharmaceutical Science degree from the University of Mumbai, India in July 2011. Subsequently, she was enrolled in Virginia Commonwealth University's School of Pharmacy, Pharmaceutical Sciences doctoral program with a concentration in Medicinal Chemistry in August 2011.